

An introduction to polymer-matrix composites

Mustafa Akay



Download free books at

bookboon.com

Mustafa Akay

An introduction to polymer-matrix composites

An introduction to polymer-matrix composites

1st edition

© 2015 Mustafa Akay & bookboon.com

ISBN 978-87-403-0980-5

Contents

Preface	8
Acknowledgements	11
1 Introduction	12
1.1 Case for composites	12
1.2 History of the development of composites	15
1.3 Classification of composites	19
1.4 Composite constituents	25
1.5 Self-assessment questions	62
2 Processing and forming methods	66
2.1 Open-mould processes (Contact moulding)	66
2.2 Closed-mould processes	78
2.3 Wood-plastic composites	91
2.4 Other processing considerations	100
2.5 Self-assessment questions	112

**YOU THINK.
YOU CAN WORK
AT RMB**

 **RAND
MERCHANT
BANK**
A division of FirstRand Bank Limited
Traditional values. Innovative ideas.

Rand Merchant Bank uses good business to create a better world, which is one of the reasons that the country's top talent chooses to work at RMB. For more information visit us at www.rmb.co.za

Thinking that can change your world

Rand Merchant Bank is an Authorised Financial Services Provider



Click on the ad to read more

3	Estimation of mechanical properties	114
3.1	Continuous fibre composites	114
3.2	Short (discontinuous) fibre composites	122
3.3	Failure mechanisms that result in composite toughness	126
3.4	Self-assessment questions	137
4	Mechanical and thermal properties	142
4.1	Introduction	142
4.2	Tensile properties	144
4.3	Compressive properties	146
4.4	Flexural properties	148
4.5	Shear properties	150
4.6	Impact and fracture toughness properties	152
4.7	Bearing strength	164
4.8	Fatigue and wear	168
4.9	Differential scanning calorimetry	188
4.10	Dynamic mechanical thermal analysis	191
4.11	Environmental effects on properties	199
4.12	Non destructive evaluation	209
4.13	Self-assessment questions	213



Discover the truth at www.deloitte.ca/careers

Deloitte.

© Deloitte & Touche LLP and affiliated entities.



Click on the ad to read more

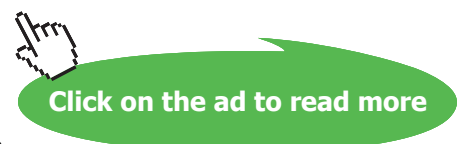
5	Applications and materials selection	215
5.1	Applications	215
5.2	Materials selection	255
5.3	Self-assessment questions	272
	References	274

**I WANT TO CHANGE DIRECTION,
AND THE WORLD.**

GOT-THE-ENERGY-TO-LEAD.COM

We believe that energy suppliers should be renewable, too. We are therefore looking for enthusiastic new colleagues with plenty of ideas who want to join RWE in changing the world. Visit us online to find out what we are offering and how we are working together to ensure the energy of the future.

RWE
The energy to lead



*To my parents (Rahmatullahi Aleyhima),
to my wife, and to Mevlüde, Latifa and Melek, the apples of my eye*

Preface

Learning involves acquiring knowledge, which is encouraged in all traditions. For example, the Quran urges people to seek knowledge and to use it for the well being of society:

“My Lord, increase me in knowledge”, Al-Quran 20:114.

“Ignorance is the curse of God; knowledge is the wing wherewith we fly to heaven”, William Shakespeare.

Knowledge should be applied in a safe, responsible and ethical manner not only to benefit us personally but also to improve the lot of the people we live with. It is also a duty to ensure that our surrounding habitat is not endangered. This sometimes requires knowledge of the local culture to help achieve a desirable outcome. Martin Palmer’s presentation on BBC Thought for the Day programme, 17/06/2006, on the subject of the protection of the oceans included:

“To many around the world the environmental movement and its proffered solutions – usually economic – are alien ways of thinking and seeing the world, and can be interpreted as telling people what is best for them whether they like it or not. Let me tell you a story. Dynamite-fishing off the East African coast is a major problem. Environmental organisations have been addressing it for years, from working with Governments, to sending armed boats to threaten those illegally fishing. None of this worked because it had no relationship to the actual lives or values of the local fishermen all of whom are Muslims. What has worked off one island, Misali, is the Qur’an. In the Qur’an, waste of natural resources is denounced as a sin. Once local imams had discovered this, they set about preaching that dynamite fishing was anti-Islamic, non-sustainable and sinful. This ended the dynamite fishing of the Misali fishermen because it made sense to them spiritually.”

The perception/foresight of Canadian scholar, Wilfred Cantwell Smith, is also relevant in this context, particularly these days when there is so much misunderstanding and misrepresentation about peoples of different religions and cultures. Regarding Muslims, Wilfred Cantwell Smith in his book *Islam in Modern History* (Princeton and London, 1957. p. 304) says, “the Muslim segment of human society can only flourish if Islam is strong and vital, is pure and creative and sound”. Practice of pure, creative and sound Islam by its followers will be for the good of all.

The contribution of materials science to society now and in the future is highlighted by many eminent scientists in the Japan Society for the Promotion of Science publication of “Science and Society”. Sir Colin Humphreys of Cambridge University (1997, p. 34) in his article indicates how material science is really enabling the lame to walk, saving lives, transforming the world energy scene and generating wealth and employment, and states that materials science is a key for our future health and our future wealth. Examples he gives include medical implants, shape-memory metals and the potential use of carbon fibre-based light tethers to facilitate deep sea exploration/extraction of oil or gas beyond depths of 1,500 metres (in deeper waters, longer lengths of steel ropes are needed to tether the rigs, which necessitates more and more buoyancy to prevent the rigs from sinking).

His article also alludes to the famous science fiction writer Arthur C. Clarke, who envisaged a situation where there is a satellite above the earth, in a geostationary orbit, tethered to the earth by a carbon fibre rope, with a lift on the rope (the Space Elevator) which would ferry people up and down to the satellite. That was thirty years ago and his predictions might be coming true! Back on earth, however, and across the seas, another application of carbon fibre ropes is suspension bridges. Seventy per cent of the weight of a suspension bridge is in the steel cables. As bridges get longer and longer, they can no longer hold up their own suspension cables. The maximum length or span, of a conventional suspension bridge is 5,000 metres. If the steel ropes are to be replaced with carbon fibre ropes however, then one can calculate that the maximum span goes up by a factor of three. In principle, one could have a suspension bridge which is 15,000 metres long.

The story of carbon-based materials continues to unravel: in his recent book, Miodownik (2014, p 198) introduces the story of graphene and describes his visit to Manchester University to see Andre Geim, a joint discoverer of graphene. Andre’s team received the Nobel Prize for demonstrating that single layers of graphite had properties that were extraordinary even by nanotechnology standards – so extraordinary that they merited their own name as a new material: graphene. Miodownik states, “this material and its rolled-up version in the form of nanotubes are going to be an important part of our future world, from the smallest scale to the very largest, from electronics, to cars, to aeroplanes, rockets and even – who knows? – to space elevators. Although it appears likely that graphene will usher in a new age of engineering, and indeed scientists and engineers are in love with this material already, this may not give it high status in the world at large. Diamonds may not be the hardest, strongest material any more, and we know that they will not last for ever, but they still represent those qualities to most people.”

The subject of this book reflects the strong relationship between material structure, properties and applications. Changing one affects the others and this has enabled scientists/engineers to tailor materials to suit purposes. The dependence of properties on the structural arrangement of material is so obvious in composites as demonstrated by the ancient Egyptians, who invented the process of cross-grain laminating veneers of wood.

Chapter 1 is a broad introductory chapter and includes a history of the development of composites; classification of composites; constituents of polymer-matrix composites; the fibre-matrix interface, and fibre arrangement. The subsequent two chapters deal with processing and forming methods, and estimation of mechanical properties for PMCs. Chapter 4 covers mechanical and thermal properties, including those that are specific to laminated structures such as, inter-laminar shear strength and residual compressive strength following barely-visible surface impact damage. The last chapter covers various areas of applications and methods of materials selection.

Mustafa Akay, January 2015

Acknowledgements

The book emerges from my work at the Ulster Polytechnic/University of Ulster, where I met and worked with various characters and personalities and I would like to mention Lesley Hawe, the late Archie Holmes, Myrtle Young who epitomise for me the constant kindness, help and support I received from the academic, technical and secretarial staff over the years.

The book incorporates material taken from various sources, including my lecture notes, research outcomes of my postgraduate students, some of them have become friends for life, and some excellent text books, research papers/news, industry/company/organisation literature and web material that we are so fortunate to have access to. The sources of the materials used are gratefully acknowledged and are listed as references, however, over the years material permeates into teaching notes that is not always possible to trace the references for. I apologise, therefore, for any such material that has no accompanying reference and I express my thanks and gratitude to the people concerned.

A special thank you goes to my wife for her proof reading, for the offers of regular walks to blow away the cobwebs and visits to “Waterstones” for coffee and book browsing.

bookboon.com

Corporate eLibrary

See our Business Solutions for employee learning

[Click here](#)

- Management
- Time Management
- Problem solving
- Self-Confidence
- Effectiveness
- Project Management
- Goal setting
- Motivation
- Coaching

[Click on the ad to read more](#)

1 Introduction

1.1 Case for composites

Polymers, which are a source of a wide variety of low-priced raw materials, offer many advantages. These include low specific weight, enhanced stability against corrosion, improved electrical and thermal insulation, ease of shaping and economic mass production, and attractive optical properties, e.g. fibre optics, glazing applications, etc. However, they suffer from some serious shortcomings:

- exhibiting, quite often, poor mechanical stiffness and strength, and poor resistance against heat
- being sensitive to aging i.e. change of the physical, chemical and mechanical properties by light, heat, oxygen and moisture
- being combustible
- exhibiting large values of coefficient of thermal expansion, which can generate high levels of internal frozen-in stresses.

Table 1.1 provides guidance concerning limited resistance of polymers to heat. The polymer abbreviations are defined in Table 1.2.

Polymers		Long-term working temperature, °C
Semi-crystalline	Amorphous	
PEEK, PPS, PTFE, LCP	PES, PSU, PEI, EP	150–250
PET, PBT, POM, PA 66, PA46, PP	PC, UP	90–120
HDPE, LDPE, LLDPE	PS, HIPS, PVC, PMMA, ABS, SAN	< 90

Table 1.1 Long-term temperature limit for some polymers

ABS	acrylonitrile-butadiene-styrene
EP	epoxy resin
HDPE	high-density polyethylene
HIPS	high-impact polystyrene
LCP	liquid crystalline polymer
LDPE	low-density polyethylene
LLDPE	linear low-density polyethylene
PA 46	polyamide 46
PA 66	polyamide 66
PMIA	poly (m-phenylene isophthalamide)
PBT	polybutylene terephthalate
PC	polycarbonate
PEEK	polyetherether ketone
PI	Polyimide (e.g. "Kapton", "Vespel")
PI	Thermosetting polyimide
BMI	bismaleimide
PAI	Polyamide imide (e.g. "Torlon")
PEI	polyetherimide
PES	polyethersulphone
PET	polyethylene terephthalate
PAR	polyarylate
PMMA	polymethyl methacrylate
POM	polyoxymethylene (acetal)
PP	polypropylene
PPO	Polyphenylene oxide and/or poly (2,6-dimethyl-1,4-phenylene oxide)
PPS	polyphenylene sulphide
PS	polystyrene
PSU	polysulphone
PPSS	polyphenylene sulfide sulfone
PTFE	polytetrafluoroethylene
PVC	polyvinyl chloride
SAN	styrene-acrylonitrile
UP	polyester (unsaturated) resin

Table 1.2 Abbreviations used in Table 1.1 and Table 1.6

Some of the shortcomings of polymers as engineering materials, particularly poor strength and stiffness, can be improved by combining them with other materials to form composites. Composite materials are defined as a mixture of two or more relatively homogeneous materials which have been bonded together to produce a material with properties that are superior to the ones exhibited by the individual component materials. This synergistic outcome, obviously, is the driving force for the development of composites.

Hull (1981, p. 3) outlines that in fibre reinforced plastics, fibres and plastics with some excellent physical and mechanical properties, are combined to give a material with new and superior properties. Fibres have very high strength and elastic modulus but this is only developed in very fine fibres, with diameter in the range 7–15 μm , and they are usually very brittle. Plastics may be ductile or brittle but they usually have considerable resistance to chemical environments. By combining fibres and resin a bulk material is produced with strength and stiffness close to that of the fibres and with the chemical resistance of plastic. In addition, it is possible to achieve some resistance to crack propagation and an ability to absorb energy during deformation.



Brain power

By 2020, wind could provide one-tenth of our planet's electricity needs. Already today, SKF's innovative know-how is crucial to running a large proportion of the world's wind turbines.

Up to 25 % of the generating costs relate to maintenance. These can be reduced dramatically thanks to our systems for on-line condition monitoring and automatic lubrication. We help make it more economical to create cleaner, cheaper energy out of thin air.

By sharing our experience, expertise, and creativity, industries can boost performance beyond expectations. Therefore we need the best employees who can meet this challenge!

The Power of Knowledge Engineering

Plug into The Power of Knowledge Engineering.
Visit us at www.skf.com/knowledge

SKF

Therefore, compared with conventional materials, composites offer:

- lightweight
- high specific strength and stiffness
- high toughness (impact strength)
- damping ability (attenuates noise and vibrations/shocks)
- high fatigue resistance (improves fatigue life)
- corrosion resistance
- low and controllable coefficient of thermal expansion (CTE) (i.e. good dimensional stability)
- ablative shielding
- non or low conductivity
- thermal insulation
- visual attractiveness
- reduced machining
- part consolidation: allows reduced number of assemblies and fasteners
- ability to manufacture complex shapes and one offs from low cost tooling
- damaged structures can be easily repaired
- potential to tailor mechanical and thermal properties, particularly by suitable fibre orientation/arrangement.

1.2 History of the development of composites

The history of composites is covered in various sources, including Strong (2006) and Palucka & Bernadette-Vincent (2002). Composites date back to the 1500 BC when early Egyptians and Mesopotamian settlers used a mixture of mud and straw to create strong and durable buildings. Straw provided reinforcement to ancient composite products including pottery and boats.

The subsequent recorded use of natural fibres include paper making. The first 'paper' was invented in ancient China sometime around 200 BC. However, the forerunner of modern paper was also first made in China from rags and plant fibres in 105 AD. The development of paper increasingly made it into a composite material. First, the Chinese used starch as a size for paper as early as 768 to reduce surface [porosity](#) and [fuzzing](#) with the goal of allowing inks and paints to remain on the surface of the paper and to dry there, rather than be absorbed into the paper. Mineral fillers were also added to improve gloss, whiteness, ink reception and weight. Arabian and Turkestan rag papers dating from the 8th century contained large quantities of talc, chalk or gypsum (hydrated calcium sulphate, $\text{CaSO}_4 \cdot 2\text{H}_2\text{O}$).

In 1200, the Mongols invented the composite archery bow, using a combination of wood/bamboo, bone/cattle horn, cattle tendons and animal glue or pine resin wrapped in birch bark or silk. These extremely powerful and extremely accurate bows were the main weapon of Genghis Khan's military might, and the most powerful weapon on earth until the invention of gunpowder.

The onset of modern composite materials began with the development of synthetic polymers, particularly those of thermosetting resins, such as phenolics and polyesters, and further strides were made with the advent of high performance fibres:

- 1850s Plywood: put into commercial production by John Henry Belter, a German emigré to the US.
- 1900s Reinforced rubber tyres.
- 1907 Leo Baekeland produced **phenol-formaldehyde**, the first truly synthetic plastic, Bakelite. Cast with pigments to resemble onyx, jade, marble and amber it has come to be known as phenolic resin.
- 1928 Otto Rohm in Germany stuck two sheets of glass together using an acrylic ester and accidentally discovered **safety glass**, and production of some articles began in 1933.
- 1933 **Melamine formaldehyde** resins were developed through the 1930s and 1940s in companies such as American Cyanamid, Ciba and Henkel.
- 1935 Owens Corning introduced the first **glass fibre**.
- 1936 Unsaturated **polyesters** were patented.
- 1938 **Epoxy resin** was discovered by Pierre Castan, a chemist in Switzerland.
- 1940 **Low pressure allyl polyester resins** were developed.
- 1940s The earliest applications for glass-fibre reinforced plastics (**GFRP**) products were in the marine industry. Fibreglass continues to be a major component of boats and ships today.
- 1942 The U.S. Navy replaced all the electrical terminal boards on their ships with fibreglass-melamine or asbestos-melamine composite boards with improved electrical insulation properties. Many other composite improvements were developed during WWII including some innovative manufacturing methods such as **prepreg** production and **filament winding**.
- 1943 At the Wright-Patterson Air Force Base in 1943, exploratory projects were launched to build structural aircraft parts from composite materials. This resulted in the first plane with a **GFRP fuselage** being flown at the base a year later (Palucka & Bernadette-Vincent, 2002).
- 1948 Introduction of sheet moulding compound (**SMC**) and dough moulding compound (**DMC**).

- 1940/1950s Development of innovative **manufacturing methods**, including pultrusion, vacuum bag moulding, and large-scale filament winding.
- 1956 Cincinnati Developmental laboratories added asbestos fibre to a phenolic resin for use as a possible re-entry nosecone material (the heat generated during re-entry of a spacecraft into the Earth's atmosphere could exceed 1500°C). Scientists also began looking at metal matrix composites (**MMCs**) for a solution.
- 1958 Roger Bacon of Union Carbide developed high-performance **carbon fibres** using rayon as the starting material. The resulting fibres contained only about 20% carbon and had low strength and stiffness properties.
- 1960 High-strength and high modulus **S-glass and boron fibres** were developed.
- 1961 Akio Shindo of the Government Industrial Research Institute in Osaka, Japan made high strength **carbon/graphite fibers** that contained about 55% carbon using polyacrylonitrile (PAN) as the precursor, replacing the rayon and pitch precursors used previously.

With us you can
shape the future.
Every single day.

For more information go to:
www.eon-career.com

Your energy shapes the future.

e-on



- 1963 William Watt et al. of the Royal Aircraft Establishment in Farnborough, England invented a still **higher-modulus fibre from PAN**. The carbon fibres were rapidly put into commercial production by companies such as Rolls-Royce.
- 1964 Stephanie Louise Kwolek of DuPont developed Kevlar fibre from **polyaramide** (an aromatic polyamide).
- 1970/1980s The **composites industry** began to mature, developing better plastic resins and improved reinforcing fibres, however, composites made with expensive fibres had to find civil applications when space and military demands declined. Sectors such as sports and leisure, transportation and construction industries became increasingly important markets.
- 1978 The development of the first fully **filament wound aircraft fuselage**, the Beech Starship, by Larry Ashton, an engineer at Hercules.
- 1979 **Dyneema fibre** was invented by DSM (the Netherlands) and has been in commercial production since 1990 at a plant in Heerlen, the Netherlands and Toyobo Co. in Japan. It is produced by means of a gel-spinning process and its properties combine extreme strength with incredible softness, and have been successfully used in bullet-resistant products (vests and panels, including those used in the doors of aeroplane cockpits), ropes, fishing nets, cut-resistant gloves, sails, sailing ropes and fishing lines. In the United States, Honeywell developed a chemically identical fibre of brand name **Spectra**.
- 1990s Miniaturisation has led to mixing organic and inorganic components at the molecular scale and to **nanocomposite** materials.
- 2000s **Smart materials** and intelligent structures.

Henry Ford exhibited his prototype car made from hemp and flax fibre reinforced resin composite body panels in 1941. The body consisted of fourteen plastic panels fixed to a welded tubular frame (instead of the customary parallel I-beam frame). The panels and frame each weighed about 250 pounds. The total weight of the automobile was 2,300 pounds, roughly two-thirds the weight of a steel model of comparable size. Figure 1.1 shows Henry Ford testing the body work: “the axe bounced, and there was no dent...”



Figure 1.1 Henry Ford tries out his first car (source: www.hempplastic.com)

1.3 Classification of composites

A Classification of Composites is listed in the text box below:

1. Polymer-polymer blends;
2. Particulates/whiskers/flakes filled materials – a continuous matrix phase and a dispersion of filler phase;
3. Fibre reinforced composites:
Classification based on fibre phase:
 - a) continuous fibres, (b) discontinuous fibres (chopped or short fibres).Classification based on matrix type:
 - a) polymer-matrix composites (PMCs) or fibre-reinforced plastics (FRPs),
 - b) metal-matrix composites (MMCs),
 - c) ceramic-matrix composites (CMCs);
4. Sandwich composites with solid skins (e.g. PMC laminate) and foam (e.g. PU, Rohacell) and/or honeycomb (nomex, aluminum) cores;
5. Nanocomposites;
6. Foams; 7. Ceramic-metal mixtures (i.e. cermets); 8. Timber; 9. Concrete; 10. Asphalt.

Composites enable the generation of a variety of materials: from low cost plastics (by the addition of low-cost fillers to polymers) to expensive high performance engineering materials, such as continuous carbon-fibre reinforced epoxy resins. Composites increasingly successfully compete with and replace conventional materials for various applications, particularly, in leisure/sports, engineering, transportation and construction sectors. Some of the attractive features/properties of composites are highlighted in the examples given below.

Weight reduction using composites has created a huge market demand in automotive, industrial, aerospace and other industries. Particularly, in the commercial airline industry due to the high cost of aviation fuel and environmental legislation, aircraft manufacturers are now competing based upon their aircraft's fuel efficiency.

The demand for energy-efficient and low-maintenance vehicles has spurred composites use in advanced automobile, truck, bus, and train products. Production parts include everything from small linkage assemblies to very large exterior structural panels. Glass fibre (GF) composite materials are less costly than carbon fibre (CF) alternatives and are, ideally suited for road and rail transportation applications because they are light weight, strong, stiff, and provide good protection from the elements. They can be **moulded** in to any size and shape, and enable visually **attractive finishes**. Furthermore, GF composite is resistant to most acids, bases, oxidizing agents and metal salts, making it suitable for **corrosion resistant** applications.

On the marine side, the consumer use of fibreglass PMCs in low- to high-end boats is the norm. Military ships have seen several applications of PMCs, primarily topside structures and minesweepers. Carbon-fibre composites are used in high-performance engine-powered, sail-powered, and human-powered racing boats. Military armoured vehicles have also benefited greatly from the application of PMCs – they offer **ballistic protection** of their occupants in addition to light weight.

A potentially huge market exists for composite materials in the upgrading of infrastructure needs. For example, 31% of the highway bridges in the United States are categorized as structurally deficient. To address this, many activities are underway at national, state, and local levels to use composites to repair and, in some cases, replace deficient bridges. Some all-fibreglass bridges, e.g. Butler County, Ohio, are fully instrumented to detect structural performance loss (Miracle and Donaldson 2001, p. 13).

© 2013 Accenture. All rights reserved.

be > your degree

Bring your talent and passion to a global organization at the forefront of business, technology and innovation. Discover how great you can be.

Visit accenture.com/bookboon

Be greater than.
consulting | technology | outsourcing

accenture
High performance. Delivered.



Low CTE, in addition to low weight, is a major advantage of PMCs in the production of satellite structures.

The **high-temperature** (using resins such as polyimides and bismaleimide) PMCs are used in many engine applications for both air and space vehicles.

High **specific mechanical properties** coupled with **dielectric characteristics** that render the material radar transparent are required for radomes and antennas: glass or aramid fibre composites meet the requirement but not electrically conducting reinforcements, such as carbon or boron.

Fatigue life is critical in dynamic applications: rotor blades for helicopters such as Lynx and Sea King consist of PMC continuous fibre composite solid skins with honeycomb/foam core for **low weight** and **superior stiffness** and **improved fatigue life**.

Composite sandwich structures, increasingly based on carbon fibre, meet light weight, high stiffness and strength and **durability** requirements of the latest wind turbines are designed with rotors up to 110 m in diameter and are capable of generating up to 5 MW of power.

Composites enable the achievement of **direction-specific properties**. This is successfully exploited in applications such as bicycle frames. Appropriate carbon fibre orientation/placement allows designing for lateral stiffness, torsional stiffness, vertical compliance, toughness and shock-dampening properties in the manufacture of frames. Such frames exhibit maximum strength-to-weight ratio: bicycle frames can be made with carbon-fibre epoxy prepregs that weigh just over one kilogram, but are incredibly strong. Furthermore the material is durable: exhibiting good resistance to failure under fatigue and impact conditions and to corrosion or attack by the elements, and it can also lend itself to attractive finishing.

Composite materials have numerous advantages for medical and security applications. CF is **X-ray transparent, strong, stiff and lightweight**, which is ideal for making panels, covers, support structures and beds for radiology, security or inspection equipment. Other medical uses exploit desirable mechanical properties of PMCs, such as orthopaedic devices as was demonstrated in the 2012 London Olympics by 400 m runner Oscar Pistorious (the **first** double **amputee** athlete to compete in the able-bodied Olympics) with his famous CF-composite prosthetic legs and, hence, he is popularly known as the **blade runner**.

Specific strength and stiffness coupled with damping ability are reasons for composites to continue to be popularly employed in sports and recreation products: golf clubs, bicycles, snowboards, water skis, tennis racquets, hockey sticks, etc. Composite tennis racquets and golf clubs began to replace wooden racquets and steel club shafts in the late seventies and changed everything, in spite of increased prices. The lighter weight and higher strength of CF/graphite enabled tennis racquets with tighter strings to be swung at higher speeds and, hence, greatly increasing the speed of the tennis ball. The increased stiffness of a golf club shaft transferred more of the energy of the swing to the golf ball, making it go further. In addition to these performance-related improvements, there were also reductions in sports injuries such as wrist strain and tennis elbow due to damping ability/shock absorbance capacity of these composite sports equipment. At present, nearly all tennis racquets are of composite construction.

Some of these desirable features of composite materials are also demonstrated for an ordinary engineering part in a case study (Kurcz et al. 2004) that proposes the replacement of steel with fibre-reinforced thermoplastic. The component studied is a spare-wheel well (SWW) for a vehicle. SWW components are required to pass tests that evaluate impact performance after a crash and resistance to noise-vibration-harshness (NVH), hot and cold climates, flammability, common automotive chemicals, and long-term heat aging. Additional tests include drivability over rough roads and various standard mechanical tests conducted on complete parts for impact strength, tensile strength and elongation behaviour. The benefits of using composites are indicated to be:

- reduced weight and systems costs.
- smaller package space required for stowing the tyre (because the steel parts are generally not easy to radius as steeply as those in plastics).
- better sound and mechanical vibration damping compared with steel for a quieter vehicle.
- the ability to tailor stiffness based on fibre lay-up configuration.
- the ability to mould-in hand grips, pockets to stow tools, and other functionality at no additional cost.
- lower tooling costs – especially attractive for lower build vehicles.
- reduced assembly-line space and cost via eliminating some secondary-finishing operations.
- no corrosion issues.

Issues in terms of heat resistance and flammability have also been indicated.

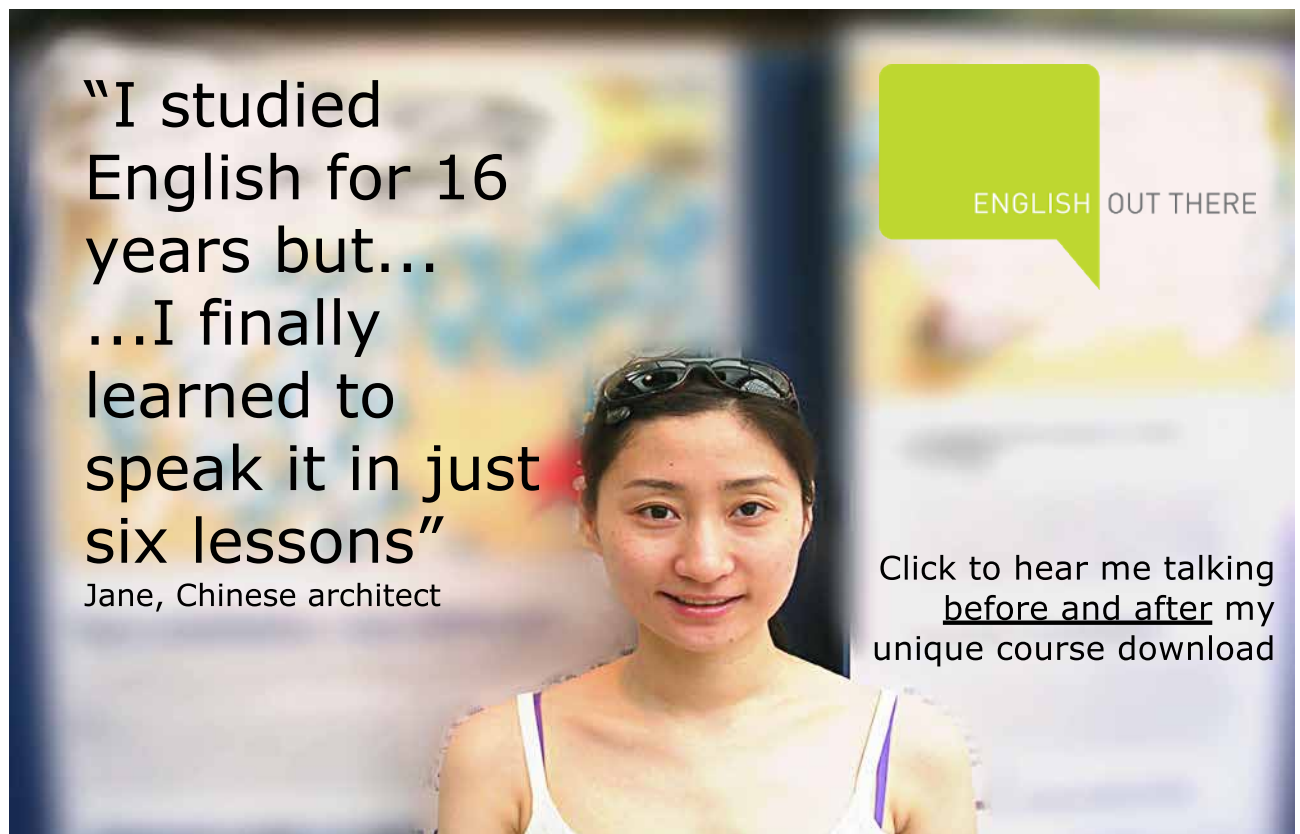
The study has considered glass-mat thermoplastic (GMT), long-fiber thermoplastic (LFT) and sheet-moulding compound (SMC): GMT and LFT are thermoplastic materials that can be melt-reprocessed, whereas SMC is a thermoset. LFT is processed by injection moulding whereas GMT is press formed, thermoformed or compression moulded and SMC is compression moulded, which influences the rate and volume of production – an important factor in the automotive industry.

Kurcz et al. have summarised that thermoplastic components facilitate recycling both in-plant scrap and postconsumer components – an important feature in Europe where all vehicle components must be able to be recycled. GMT and LFT have polypropylene matrices, offering lower specific gravity than polyester-based SMC, for lighter weight parts at comparable wall thicknesses. Additionally, SMC is known to be brittle, so is not well suited for applications subject to impact. SMC is also characterized by relatively long cycle times, on average 2–3 min for a part like a spare-wheel well.

Another important difference between these technologies is that GMT materials are able to achieve higher stiffness, impact, and strength values than LFT owing to greater preservation of glass fibre length after moulding. For the grades used in SWW applications, GMT tends to maintain fibre lengths of 30–50 mm vs. 5–20 mm for LFT after moulding. GMTs as-moulded cost tends to be lower than that of LFTs.

The study supports GMT composite technology for this application, concluding that it offers the same types of benefits as SMC – lower weight, lower systems costs, lower tooling costs, and design flexibility – while also providing faster cycle times, lighter weight parts, and avoiding brittle-failure problems.

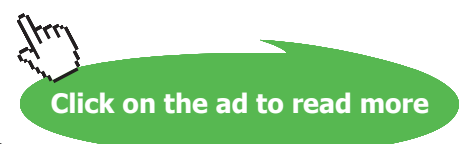
In most applications, specific strength (strength / specific gravity) and specific stiffness (stiffness / specific gravity) becomes an important factor and as can be seen in Figures 1.2 and 1.3 and Table 1.3 composites, particularly continuous-fibre composites, are much superior in this respect compared with other materials.



"I studied English for 16 years but...
...I finally learned to speak it in just six lessons"
Jane, Chinese architect

ENGLISH OUT THERE

Click to hear me talking before and after my unique course download



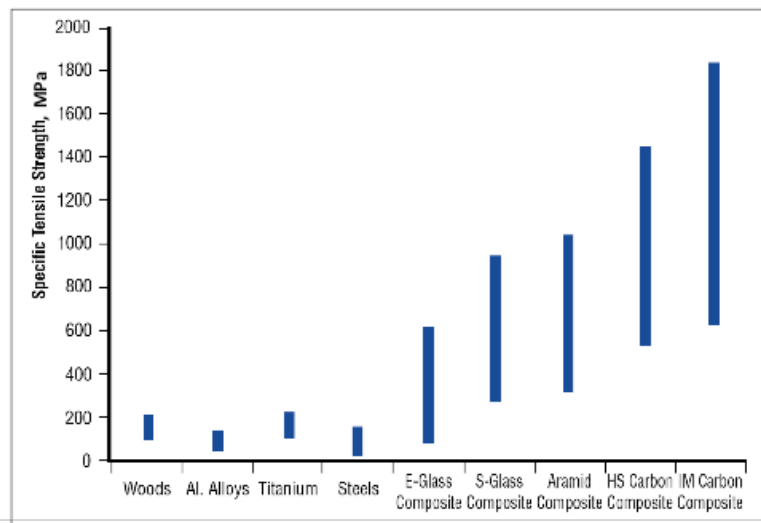


Figure 1.2 Specific tensile strength of various composites and other engineering materials (source: SP Systems 2005)

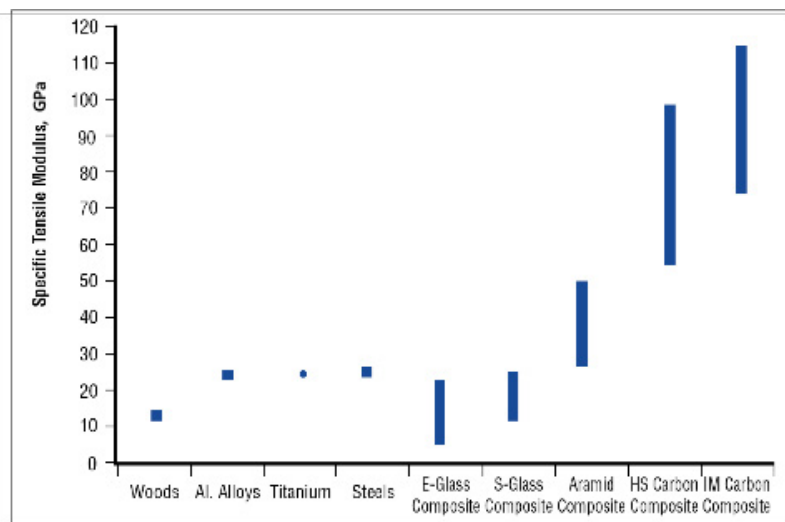


Figure 1.3 Specific tensile modulus of various composites and other engineering materials (source: SP Systems 2005)

Figures 1.2 and 1.3 show a wide range of values for composites: even when considering one fibre type on its own, the composite properties can vary considerably with the range of fibre contents and orientations that are commonly achieved. The comparisons that follow therefore show a range of mechanical properties for the composite materials. The lowest properties for each material are associated with simple manufacturing processes and material forms (e.g. spray lay-up glass fibre), and the higher properties are associated with higher technology manufacture (e.g. autoclave moulding of unidirectional glass fibre prepreg) as would be found in the aerospace industry.

Typically, with a common hand lay-up process as widely used in the boat-building industry, a limit for fibre-volume content (FVC) is approximately 30–40%. With the higher quality, more sophisticated and precise processes used in the aerospace industry, FVCs approaching 70% can be successfully obtained. The lay-up arrangement of the fibres in a composite is also important since fibres have their highest mechanical properties along their lengths, rather than across their widths.

For the other materials shown in the figures, a range of strength and stiffness (elastic modulus) values is also given to indicate the spread of properties associated with different alloy compositions.

Material	Tensile strength (MPa)	Young's modulus (GPa)	Specific gravity	Specific tensile-strength [#] (MPa)	Specific E [#] (GPa)
Carbon fibre (CF)/Epoxy composite*	1590	113	1.5	1060	75
High strength grade CF/Epoxy composite*	1900	128	1.5	1270	85
High modulus grade CF/Epoxy composite*	1400	210	1.6	875	131
S-glass fibre/Epoxy composite*	1790	55	2.0	900	27
Aramid ("Kevlar") fibre/Epoxy composite*	1800	77	1.4	1280	55
Steel	1000	210	7.8	130	27
Aluminium L65	470	75	2.8	170	26
Titanium DTD5173	960	110	4.5	210	25
Glass fibre/polyester composite ($v_f = 0.5$)	750	38	1.9	395	20
Short glass fibre/Nylon 6,6 ($v_f = 0.25$)	207	14	1.5	138	9
Nylon 6,6	70	2	1.1	61	1.8

Table 1.3 Comparison of material properties at 20°C

* Composites with fibre-volume fraction (v_f) of 0.6. The fibres are unidirectional in the composites and properties are measured parallel to fibres. The short glass fibre/nylon 6,6 is injection moulded.

Specific property = property / specific gravity

The highlighted rows in Table 1.3 demonstrate the superior strength and stiffness of the continuous unidirectional fibre reinforced composites, particularly on a weight basis. The reinforcement of the fibres is also very clear, when the properties of a typical engineering polymer nylon 6,6 is compared with any of the fibre reinforced polymers. Even the inclusion of the least expensive fibre, e.g. glass fibre, improves the properties of ordinary polymers/resins and renders them as an attractive alternative to some popular metals in usage.

1.4 Composite constituents

Properties of composites depend on the properties of the constituent components, i.e. matrix and fibres/fillers, the shape, size, amount, packing arrangement and stacking sequence of the fibre/filler phase and the nature of the interface between the components.

The function of the matrix:

- a) to hold the fibres together at a particular arrangement
- b) to protect the surface of the fibres from damage
- c) to transmit applied stress to the fibres
- d) to provide good finish to the product.

The function of the fibres/fillers:

- a) to provide strength
- b) to provide stiffness
- c) to inhibit crack propagation
- d) to reduce cost with some fillers.

The coverage here is mainly on fibre-reinforced composites.

DUKE
THE FUQUA
SCHOOL
OF BUSINESS

BUSINESS HAPPENS
HERE.

www.fuqua.duke.edu/globalmba

Learn More >



1.4.1 Fibres

Fibres are produced by a spinning/drawing process as continuous filaments, they are then coated with a suitable “sizing” chemical, which protects the surface of the filaments from damage during any subsequent processing and handling, and facilitates good interface bonding with the matrix in the composite. Filaments are normally bundled together into rovings (tens of filaments) for glass fibre or tows (thousands of filaments) for carbon fibre. These can be used either directly as unidirectional (UD) fibres or woven or stitched to produce a fabric or chopped into short fibres. A classification of fibres may be made in terms of fibre length and alignment: discontinuous fibre composite systems include short fibre (length < 7.5 mm), long fibre (length \geq 7.5 mm), and mat (chopped at 25–50 mm length); and continuous systems include unidirectionally aligned (UD), woven fabrics, mixtures of UD and fabrics (as in some pultruded profiles), 3-D arranged preforms/structures and swirled mat.

High performance synthetic fibres include:

- **Glass fibres** are produced by extrusion of molten glass through spinnerets at 1200 °C, followed by drawing, it is mostly lower in cost compared with other high-performance engineering fibres. Types of glass fibres include: E-glass (low alkali glass (alumino-borosilicate) exhibits excellent electrical insulation properties; S-glass (magnesium borosilicate glass) has excellent tensile strength; C-glass (sodium borosilicate glass) has excellent chemical resistance properties.
- **Quartz fibre** is very pure (99.95%) fused silica glass fibre. It exhibits the highest specific strength (strength-to-weight ratio) of all high temperature materials (tensile strength of 5.9 GPa).
- **Basalt fibre** fills in the gap between CF and GF in cost. It has a similar chemical composition to glass fibre but exhibits a higher density (2.7 g/cm³) and tensile strength. Compared with carbon and aramid fibre, it has higher compression strength and higher shear strength. It is highly resistant to alkaline, acidic and salt water attack, and has high temperature properties. It is suitable for manufacturing armours (e.g. ballistic resistant textiles), as well as being a good candidate for use in concrete, bridge and shoreline structures.

Basalt fibres typically have a filament diameter of between 9 and 13 μm , which is well above the respiratory limit of 5 μm to make basalt fibre a suitable replacement for asbestos, therefore, its high temperature resistance makes it suitable for fire-proof textile in the aerospace and automotive industries.

- **Carbon fibres** are produced from three types of precursor fibres, rayon, polyacrylo nitrile (PAN) or residue of petroleum refining (pitch). Precursor fibre is carbonized by heat treatment processes of oxidation (300°C) and thermal pyrolysis under tension in an inert (oxygen-free) atmosphere inside a series of furnaces with progressively increasing temperatures (700–3000°C) depending on the type of fibre produced in terms of tensile strength and modulus, and yielding 80 to 99% carbon content (carbon-carbon covalent bond is the strongest in nature). Figure 1.4 shows the formation of the ladder molecules from the stretched PAN molecules as a result of the reaction of the nitrile (cyano) functional groups ($-C\equiv N$) with heat. Following further heat processes, the final outcome is the transformation of white PAN fibre into black carbon fibre.

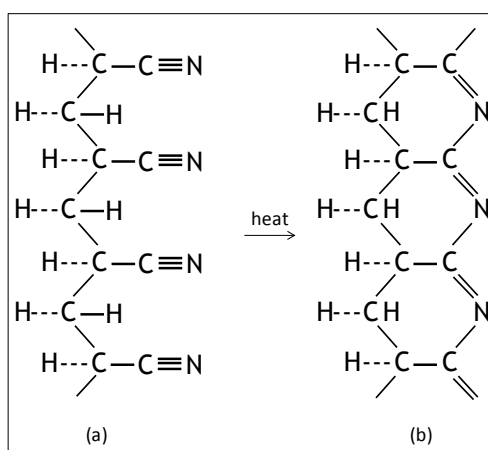


Figure 1.4 PAN (a) flexible stretched molecule, which converts into (b) rigid ladder-like molecule when heated

Fibre production finishes off with surface treatment and sizing (sizing is normally low-molecular weight epoxy resin since the fibres are mainly incorporated in epoxy matrices). Fibres are available in high strength (HS), standard modulus (SM), intermediate modulus (IM), high modulus (HM) and ultra high modulus grades.

Carbon fibre is anisotropic in its structure and hence in its properties. It is produced/supplied as tows (a tow is an untwisted bundle of continuous filaments of certain numbers in multiples of a thousand filaments (1 K)) of various weight: small tows (1000 (1K) to 24000 (24 K) filaments) and large tows on the order of 48 K-320 K filaments.

Historically, carbon fibre production focused around small tow products, however, companies interested in promoting non-aerospace industrial applications of carbon fibre, and therefore interested in higher productivity processes (laying down more carbon/unit time) and a lower price of fibre, have promoted the use of large tow products.

- Polymer fibres:
 - **Aramid** (trade names Kevlar, Twaron/Technora) is an aromatic polyamide (poly(p-phenylene terephthalamide) (see Figure 1.5) fibre and is produced by melt spinning from solution. Kevlar was developed by DuPont using poly(p-phenylene terephthalamide) with different grades based on elastic moduli and elongation to failure properties, and includes Kevlar-29, Kevlar-49 and Kevlar-149 with increasing moduli and decreasing elongation values. Aramid exhibits very good impact strength (the ability to absorb and dissipate energy) and has excellent abrasion resistance but suffers from poor compressive strength and modulus and absorbs moisture. Aramid fibres exhibit negative coefficient of thermal expansion (CTE).

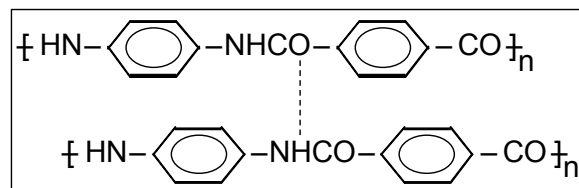


Figure 1.5 Aramid molecules with intermolecular H-bonding

Join American online LIGS University!

Interactive Online programs
BBA, MBA, MSc, DBA and PhD

Special Christmas offer:

- ▶ enroll **by December 18th, 2014**
- ▶ **start studying and paying only in 2015**
- ▶ **save up to \$ 1,200** on the tuition!
- ▶ Interactive Online education
- ▶ visit ligsuniversity.com to find out more!

Note: LIGS University is not accredited by any nationally recognized accrediting agency listed by the US Secretary of Education. More info [here](#).



- **Ultra-high molecular weight polyethylene fibres** (Dyneema of Honeywell and Spectra of Toyobo) are produced by dissolving UHMWPE in a solvent and then spinning through small orifices (spinneret) and then drawing into fibres of almost fully oriented molecular chains of almost 100% crystalline structure that yields the highest value of specific strength of any manmade fibre. It is mainly used for applications that require impact resistance. UHMWPE fibres have low dielectric properties that make them virtually invisible to radar. Hydrophobic character of these fibres makes them extremely resistant to moisture. However, they have poor temperature resistance and like, aramid, exhibit poor compression performance. Creep is also a problem. They bond poorly to most matrices (chemical inertness and low surface energy), and have low friction and excellent abrasion resistance properties.
- Poly(p-phenylene-2,6-benzobisoxazole) or **polybenzoxazole (PBO)**, which is an aromatic heterocyclic polymer (see Figure 1.6). Fibres are spun from liquid crystalline solution, and then heat stretched for improvement of mechanical properties. PBO is thermally and thermo-oxidatively stable; it chars rather than burns when exposed to fire. The fibres produced from PBO (Zylon developed by Toyobo) exhibit excellent impact resistance and tensile properties and high temperature stability. Their weaknesses include poor compressive strength and poor UV resistance.

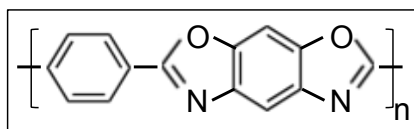


Figure 1.6 PBO molecule

Zylon, vaguely related to Kevlar and nylon in its chemistry, is used in various applications, including tennis racquets, table tennis blades, medical applications, bullet-proof vests, bomb containment vessels, also in roping and tethering systems, e.g. for Martian rovers. However, in 2003, it became controversial when two officers in the U.S. were mortally wounded while wearing Zylon based vests, leading to the re-assessment of Zylon for use in ballistic vests (<http://en.wikipedia.org/wiki/Zylon>).

- Thermoplastic liquid crystal polymer (LCP) or **aromatic polyester fibres**, e.g. Vectran, which is produced from copolymers poly(p-phenylene terephthalate). It is one of a family of naphthalene-based thermotropic liquid crystal polymers developed by the Celanese Corporation in the 1970s (see Beers et al. 2001, p. 93 for further details). It has the desirable feature that fibres are produced by melt spinning using conventional polyester extrusion practices. Melt spinning is cheaper than solution spinning, which requires the use of strong acids. The properties of Vectran are comparable to aramid fibres but exhibit better creep resistance. Uses include tow ropes and inflatables, such as the airbags used to cushion the Pathfinder's successful landing on the surface of Mars in 1997.

- **Boron fibre** is a composite fibre made by chemical vapour deposition (CVD) of boron on a substrate wire, which becomes the core of the composite fibre, at high temperatures (1000°C). Generally, a fine tungsten wire, 12 µm diameter, is used for this purpose. High cost of production is a big obstacle to the widespread use of boron fibre. The fibre is strong both in tension and compression.
- **Ceramic fibres** include alumina (Al₂O₃), silicon carbide (SiC) and nitride (e.g. boron nitride, BN, or silicon nitride, Si₃N₄) fibres. They retain strength at high temperatures and are used mainly in MMCs and CMCs in the form of whiskers or continuous filaments.

Property	Carbon	E-Glass	Aramid (Kevlar 49)	UHMWPE (Dyneema/Spectra)	Boron	PBO (Zylon AS)	LCP (Vectran HS)
Diameter, µm	6–10	8–14	12	9–38	≥100	12	23–27
Specific gravity	1.75–2.15	2.5–2.58	1.44–1.5	0.95–0.98	2.6	1.54	1.4
Young's modulus, GPa	228–550	69–81	120–135	65–175	400	180	65–80
Tensile strength, GPa	2–5.9	1.4–3.8	2.8–4.1	2.4–3.9	3.6	5.8	2.8–3.2
Elongation to failure, %	0.4–2.4	1.8–4.9	2.2–2.8	2.5–4	0.8	3.5	3–3.7
CTE (axial), 10 ⁻⁶ x°C ⁻¹	-0.1 to -1.2	4.9– 5.5	-2 to -2.7	-12	2.5–5	-6	-2.7 to -4.8

Table 1.4 Mechanical properties of various engineering fibres (sources: Joyce 2003, McDaniel et al. 2009)

As can be seen in Table 1.4, a range of values are exhibited by some of the fibres, which arises from the fact that some of these fibres are available in different grades/types, e.g. carbon fibres can be:

- Ultra-high-modulus, UHM (Young's modulus (E) > 440 GPa)
- High-modulus, HM (E of 325–440 GPa)
- Intermediate-modulus, IM (E of 270–325 GPa)
- Standard modulus, also known as high strength, HS, or high-tensile, HT (E of 160–270 GPa, tensile strength > 3.0 GPa)
- Super high-tensile, type SHT (tensile strength > 5 GPa).

A comparison of the properties for different fibres and the variation between the grades is also demonstrated in Figures 1.7 and 1.8.

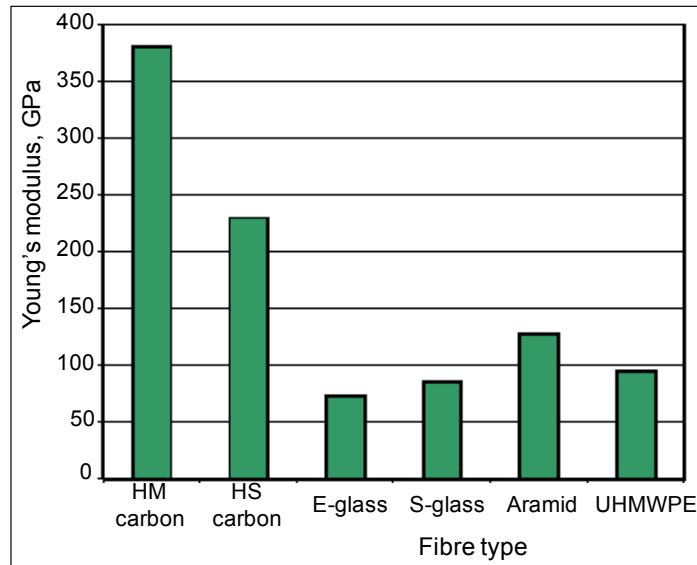


Figure 1.7 A comparison of Young's modulus values for various fibres (source: Umeco, p. 5)

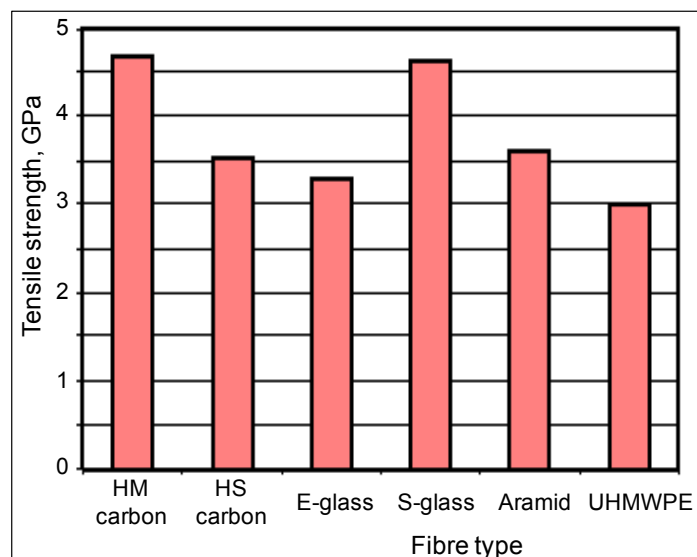


Figure 1.8 A comparison of tensile strength values for various fibres (source: Umeco, p. 6)

Natural fibres include:

- animal fibres: silk, wool, camel hair
- plant fibres: cotton, jute, kenaf, hemp, flax, bamboo, sisal, maze, sugarcane, banana, ramie, coir
- mineral fibres: asbestos, mineral wool, glass wool, basalt.

Table 1.5 shows the mechanical properties of fibres extracted from various plants.

Fibre type	Specific gravity	Tensile strength (MPa)	Specific tensile strength (MPa)	Young's modulus (GPa)	Specific Young's modulus (GPa)	Failure strain (%)
Abaca	1.5	12	8	41	27	3.4
Banana	1.3–1.35	529–914	392–677	27–32	20–24	1–3
Pineapple	1.52–1.56	413–1627	287–1130	60–82	42–57	0–1.6
Sisal	1.3–1.5	80–840	55–580	9–22	6–15	2–14
Bamboo	1.5	575	383	27	18	-
Flax	1.4–1.5	500–900	345–620	50–70	34–48	1.3–3.3
Hemp	1.4–1.5	310–750	210–510	30–60	20–41	2–4
Jute	1.3–1.5	200–450	140–320	20–55	14–39	2–3
Kenaf	1.22–1.4	295–1191	-	22–60	-	-
Ramie	1.55	915	590	23	15	3.7
Coir	1.15	106–175	92–152	6	5.2	15–40
Cotton	1.55	300–700	194–452	6–10	4–6.5	6–8
Kapok	0.31	93	300	4	12.9	1.2

Table 1.5 Mechanical properties of leaf and bast fibres (source: Mwaikambo 2006)

ie business school

#1 EUROPEAN BUSINESS SCHOOL
FINANCIAL TIMES 2013

#gobeyond

MASTER IN MANAGEMENT

Because achieving your dreams is your greatest challenge. IE Business School's Master in Management taught in English, Spanish or bilingually, trains young high performance professionals at the beginning of their career through an innovative and stimulating program that will help them reach their full potential.

- Choose your area of specialization.
- Customize your master through the different options offered.
- Global Immersion Weeks in locations such as Rio de Janeiro, Shanghai or San Francisco.

Because you change, we change with you.

www.ie.edu/master-management | mim.admissions@ie.edu | f t in YouTube



1.4.2 Matrices

Matrices for the production of polymer-matrix composites include a variety of thermoplastics (TPs), thermosets (TSs), metals, ceramics and carbon, e.g. carbonized phenol (carbon/carbon applications). Various aspects of TPs and TSs are covered elsewhere (Akay 2012). Thermosetting resins such as polyesters and phenolics are usually used in combination with glass fibre in producing economic-grade glass-fibre reinforced plastics (GRP), and epoxy resins and polyimides are employed with fibres such as carbon fibre and Kevlar in the manufacture of high-performance composites. Thermoplastics that are used in high-performance composites include polyetherether ketone (PEEK), polyetherimide (PEI), polyethersulphone (PES), polyphenylene sulphide (PPS), etc. Some of these polymers employed in the production of high-performance engineering composites are described below.

1.4.2.1 Thermoplastics

Both amorphous and crystalline thermoplastics (TPs) are employed in the production of high performance composites:

PEEK, is a semi-crystalline aromatic polymer (see Figure 1.9) and many of its properties depend on the degree of crystallinity in the final product (typically 35%).

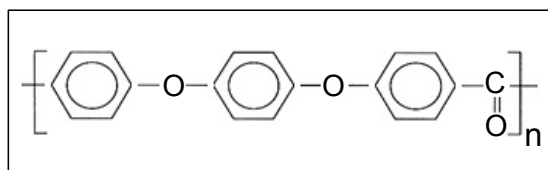


Figure 1.9 PEEK molecule

PEEK is used as biomaterial in medical implants, often in reinforced format with a biocompatible filler such as carbon fibre, and in aerospace applications as carbon fibre reinforced composite. The use of PEEK in advanced thermoplastic composites is well known since the advent of APC 2, initially sold as a unidirectional tape containing 60% by volume carbon fibre (Cogswell 1992). The appeal of PEEK is its high strength and high modulus-to-weight ratios, high impact strength, good fibre adhesion, excellent chemical resistance and non-flammability.

Other crystalline aromatic TPs used as a composite matrix include aromatic polyamides, aromatic polyesters, polyphenylene sulphide (PPS), polyphenylene oxide (PPO) and polyimide. Table 1.6 shows the chemical structure and some of the properties for these high-performance engineering thermoplastics.

Aromatic polyamides are either partially aromatic, e.g. polyhexamethyleneterephthalamide or nylon 6T (T for terephthalic acid) or fully aromatic as in poly(m-phenylene isophthalamide) or poly(p-phenylene isophthalamide). They have much higher glass-transition temperatures and melting points than their aliphatic versions. Nylon 6T exhibits mechanical properties similar to nylon 66, but with better retention of these properties at higher temperatures. It also suffers less creep.

Aromatic polyesters may also be either partially or fully aromatic. Examples of partially aromatic polyesters include polyethylene terephthalate (PET) and polybutylene terephthalate (PBT) and wholly aromatic ones include polyarylates (PAR) of hydroquinone and terephthalic acid monomers. The presence of aromatic rings increases thermal stability, especially when the rings are para-linked. These show thermotropic liquid crystalline behaviour with high melting points. Moulded liquid crystal polyesters (LCP) are highly oriented leading to high mechanical properties and a low CTE in the direction of flow.

In essence, LCP is a “self-reinforced” composite. The properties of different grades of polyarylates can vary significantly due to the variety of monomers that can be used. For example, in order to overcome processing difficulties associated with LCPs, copolymer formulations incorporating isophthalic acid and bisphenol A have been developed with properties between bisphenol A polycarbonate and polyethersulphones. These copolymers tend to be amorphous with T_g values of about 170–190°C.

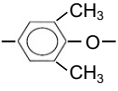
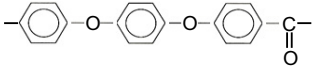
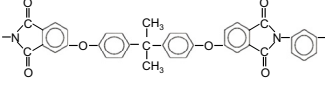
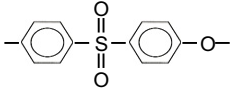
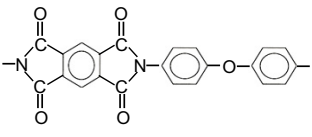
Polyphenylene sulphide, as poly p-phenylene sulphide, is highly crystalline and, therefore, thermally stable and may be used at temperatures above 200°C in air. It is insoluble in solvents below 200°C and is fire resistant. PPS has excellent chemical resistance, low moisture absorption and high strength and stiffness. Without modification, however, its impact strength is low.

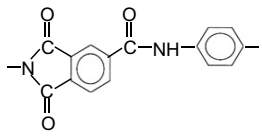
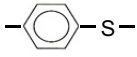
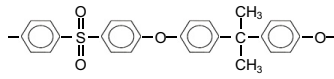
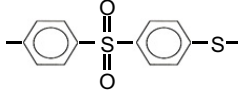
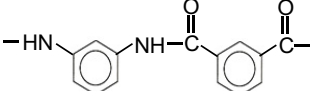
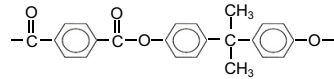
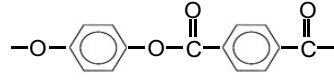
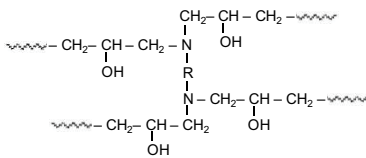
Polyphenylene oxide, in its unsubstituted form where the linking is through the para positions, is thermally very stable, but too unyielding and insoluble for fabrication purposes. An important commercial PPO uses substituted benzene to alleviate this difficulty. Alkyl groups or halogen atoms are usually substituted at the 2 and 6 positions on the benzene ring.

Amorphous and semi-crystalline **polyimides** are covered by Yang et al. (2012) and Zhuang (1998). Polyimides may have aliphatic or aromatic backbone chains. Aliphatic polyimides, as would be expected, exhibit low softening temperatures (< 150°C). Aromatic ones, however, with very high softening points and thermal stability have become popular as high temperature resistant polymers in many applications. However, they can be quite intractable and have to be processed from solution or converted into polymer from monomers in situ. Modified polyimides like polyamide imides (PAI), polyester imides, polyether imides (PEI) and heterocyclic polyimides have been developed over time to facilitate ease of processing.

Sulfur containing polymers in the form of sulphone links such as polysulfone, polyphenylenesulfone, poly (phenylene sulfide sulfone) (PPSS), polyethersulfone (PES) (or polyarylenesulphone), some of the copolymers of polyarylates, and polyetherimide (PEI) (due to its irregular structure) are examples of amorphous aromatic/cyclic TPs. The relatively large size of the sulfonyl group ($-\text{SO}_2-$) and the kink in the polymer backbone caused by the narrow C-S-C bond angle (close to 100°) are probably the reasons why the associated polymers tend to be amorphous in structure. Chemical formulae and properties for these polymers are also included in Table 1.6.

Sulfone ($\text{R-SO}_2\text{-R}'$) based polymers exhibit high glass transition temperatures. All have good strength and stiffness. **Polysulfone** has the lowest glass transition temperature of the three types and is the easiest to process. **Polyethersulfone** is fairly similar in performance. All these sulfone polymers are non-flammable. In comparison with PEEK, they can be processed at lower temperatures, but the materials produced are not as resistant to heat and chemicals.

Polymer type	Repeat unit	ρ	T_g , $^\circ\text{C}$	HDT (1.8 MPa), $^\circ\text{C}$	T_m , $^\circ\text{C}$	E, GPa	UTS, MPa	ϵ , %	Impact*, J/m
PPO		1.06; 1.04- 1.09; 1.08	117- 210; 110- 190; 210	123; 107- 149; 120	257- 305; 275	2.3- 2.6; 2.48- 2.65; 2.4;	55; 49- 66; 60	45; 50- 60; 25	190- 270
PEEK		1.31; 1.4; 1.3- 1.32; 1.32	145; 143; 142; 145; 145	155- 160; 160; 160	335- 340; 343; 335- 343; 335; 340	1.1- 3.5; 3.1- 3.8; 3.6; 3.6; 4	70- 103; 90- 100; 92; 70- 105; 100	75; 15- 30; 40	80- 90; 84
PEI		1.27; 1.26- 1.27; 1.27	215/ 230; 217; 215; 210	197- 200; 200; 193- 232; 200		3; 3; 2.72- 4; 3.4	97; 105; 62- 150; 115	60; 60; 5-90; 60	50- 60; 50; 60
PES		1.37; 1.37; 1.37	216- 218; 220; 225; 222; 223; 225; 220	205; 203; 234; 200; 195- 232; 200		2.45- 2.7; 2.6; 2.4; 2.44- 2.86; 2.5	84- 87; 80; 83; 86; 68- 101; 90	60; 40- 80; 40- 80; 70	90; 86
PI		1.4; 1.33- 1.43; 1.37	337- 364; 250- 365; 320; 260	319; 238- 360; 238- 360; 355	388; 388; 385	3.43- 3.58; 2.1- 2.8; 2.1-4; 3.7	118- 140; 72- 118; 72- 119; 120	6-90; 8-90; 4-10; 6	80-90

PAI		1.42; 1.38; 1.42; 1.41	275; 275; 275; 275	278; 252- 260; 275- 280; 280		4.83; 5.2; 2.5- 4.9; 4	76- 160; 117; 140	15; 10- 18; 2-15; 10	140; 109; 136
PPS		1.34; 1.35; 1.35; 1.34	90; 85; 90; 90	115; 115; 100- 135; 135	280; 285; 285; 290	4 (3.4- 4.2); 2.6- 3.9; 3.28- 3.42; 3.9	66 (33- 85); 65; 48- 87; 85	1.5; 1.6; 1-4; 20	30; 16
PSU		1.24; 1.24; 1.23; 1.24- 1.25; 1.24	185- 190; 186; 187; 190; 185	174; 174; 175; 175; 174; 175		2.6 (2.5- 2.75); 2.48; 2.6; 2.51- 2.72; 2.6	65 (50- 100); 70- 80; 69; 70; 60- 75; 70	25- 85; 50- 100; >50; 75; 50- 100; 75	70; 80;
PPSS		1.4	212- 217; 207; 217				99		10?;
Nylon 6T					370				
PMIA		1.17		120- 170	310	3.75	85- 105	3	
PAR		1.21- 1.26; 1.2	190; 190	110- 174; 175		2.1- 2.24; 2	69- 76; 66	8-100	
PAR (LCP)		1.35- 1.84; 1.79; 1.4		180- 355; 319; 243	400; 400; 280 see below	9.8- 19.6; 12; 11	110- 189; 86; 180	1-5; 2; 3	60
PAR (LCP)	Medium-melting point	1.35- 1.84		180- 355	280- 421	9.7- 19.3	110- 186	1-5	90- 530
EP		1.4; 1.1- 1.4; 1.15- 1.2; 1.2- 1.3;	180; 120	200; 50- 300;		4.5 (2.4- 6); 3- 5; 3-6; 2.8- 4.2;	40 (28- 100); 28- 90; 35- 100;	4; 1-2; 1-6; 4.5	10- 1000; 10-50

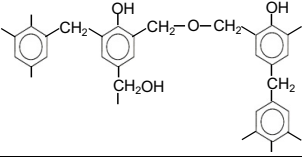
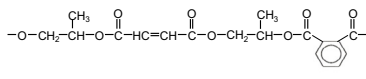
		1.3				2.4	55-130; 67		
MF	See Figure 1.12	1.5; 1.5	20-60	180		4.9-9.1; 7	30; 30	0.6-0.9; 1	10-20
PF		1.32; 1.3	80-120; 170?	79		2.76-4.83; 3.8	35-62; 48	1.5-2; 2	10-20
UP		1.5; 1.2-1.5; 1.04-1.46	0-150	80; 50-110		2.1 (2-4.5); 2-4.5	40-90; 40-90	2; 2; <2.6	10-20; 11-21
PI	See Figure 1.13	1.43; 1.41-1.9; 1.35	360	240-300; 300-302; 370		3.2; 3.2;	75-100; 86; 30-158; 115	4-9; 1; 10	40; 30-800; 75
BMI	See Figure 1.14 (the values for diphenylmethane linking group)	1.22-1.3	230-290; 205-320	230		4-5	41-83; 332-617?; 81	1.2-3.6	

Table 1.6 Various properties of polymers (sources: Efunda, Mark (1999) and MakeltFrom.com)

*These are notched Izod impact data

FREE
30 days trial!

SMS from your computer

...Sync'd with your Android phone & number

Go to
BrowserTexting.com

and start texting from your computer!

... **BrowserTexting**



1.4.2.2 Thermosets

Thermosetting polymers that are employed in polymer-matrix composites include polyesters, phenolics, aminoresins (mainly UF and MF), epoxy resin and polyimides.

Unsaturated polyesters are polymerised from a diol (e.g. 1,3-propylene glycol), saturated acids (e.g. phthalic anhydride/acid) and unsaturated acids (e.g. maleic acid/anhydride). The double bond containing linear polymer (prepolymer) chains are crosslinked using a suitable monomer, usually styrene. The inclusion of styrene also reduces the viscosity of the viscous resin. Other vinyl monomers, such as methyl methacrylate and diallyl phthalate are also used or halogenated monomers, e.g. chloromaleic acid, for fire resistancy may be used. Other ingredients include inhibitors (e.g. hydroquinone) in order to prevent premature cross-linking and to allow a suitable shelf life, initiators (catalysts), such as methyl ethyl ketone peroxides and benzoyl peroxides, and accelerators (e.g. cobalt naphthenate, and cobalt octanoate). Its attractive features include ease of mouldability, versatility and low cost.

Epoxy resins are prepared from low molecular weight oligomers containing two or more epoxy groups per molecule. The most common oligomers (prepolymers) are diglycidyl ethers, particularly the diglycidyl ether of bisphenol A (DGEBA). (Glycidyl is the prefix given to epoxy (a cyclic ether) containing groups.) DGEBA is a product of the condensation reaction between epichlorohydrin and bisphenol A, see Figure 1.10.

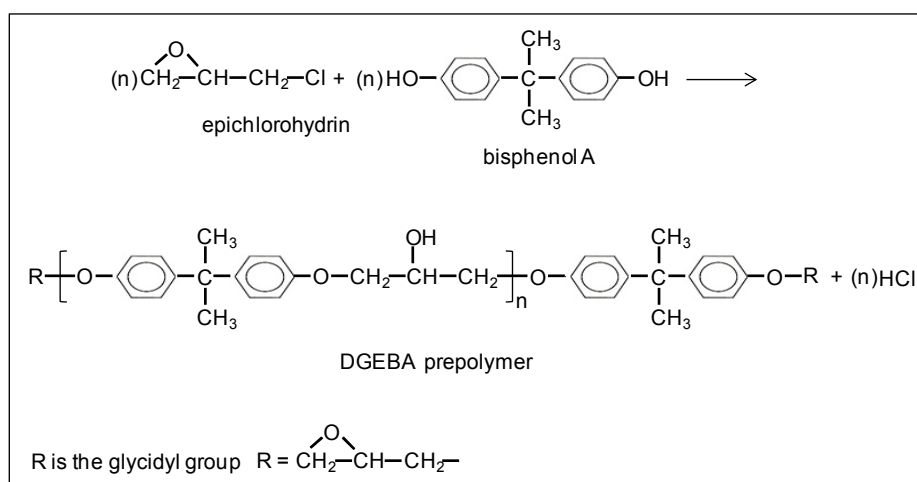


Figure 1.10 Formation of epoxy prepolymer

The linear epoxy prepolymers are crosslinked using curing agents, such as diamines and acid anhydrides that contain active hydrogen which react with the epoxy groups. For example the primary diamines offer a functionality of four so that network structure is formed, see Figure 1.11. Crosslinking may also be achieved by catalysing reaction between the epoxy oligomers by opening the epoxy rings. Depending on the curing system used, the material exhibits desirable properties such as toughness, low shrinkage, solvent and chemical resistance, hardness and good adhesion to substrates.

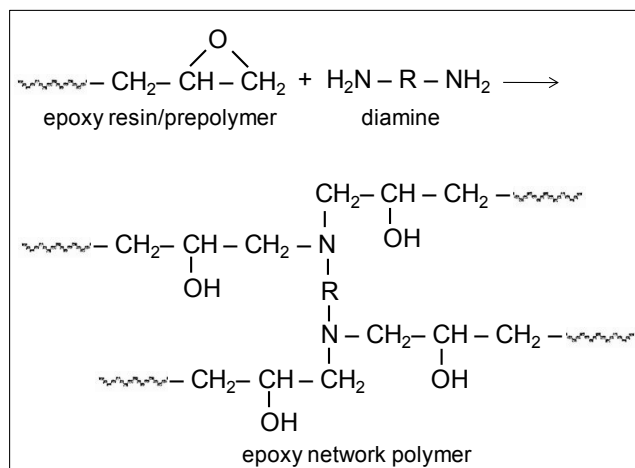


Figure 1.11 Crosslinking of epoxy resin (low molecular weight) with an amine curing agent (note that the term epoxy resin is used to describe both the network polymer and the oligomeric prepolymers)

Epoxy resins are presently used far more than any other matrices in advanced composite materials for structural aerospace applications. Some of the epoxy formulations are modified to produce toughened epoxies by, for instance, blending with high-temperature resistant thermoplastics or rubber additives. A study of such modification is presented by Akay and Cracknell (1994) for the blends of a series of amine-cured epoxy resins with polyethersulphone. This increases the elongation to failure for cured epoxies and reduces brittleness.

In comparison with polyesters, epoxy resins are not as sensitive to moisture absorption and exhibit superior mechanical and thermal performance, but the processing/curing of epoxies is slower and the cost of the resin is also higher than the polyesters.

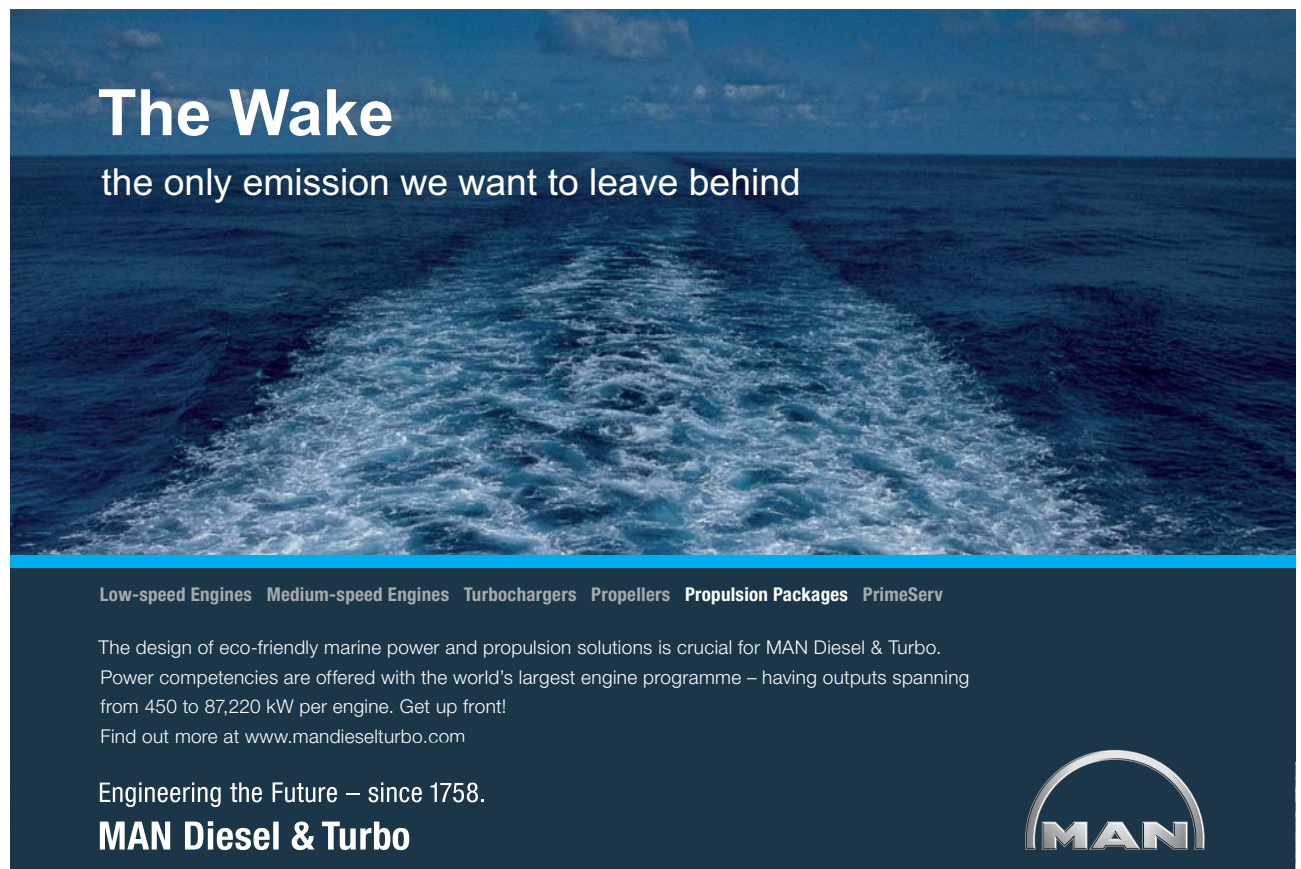
Vinyl ester resins, combining epoxy resin prepolymer with an unsaturated carboxylic acid, have properties intermediate between the epoxy and unsaturated polyester resins that may be crosslinked via unsaturated groups with a vinyl monomer, again often styrene.

Polyester and vinyl ester resins are used mainly in commercial, industrial, and transportation applications, including chemically resistant piping and reactors, truck cabs and bodies, and automobile bonnets, decks, and doors. The very large number of resin formulations, curing agents, fillers, and other components provides a tremendous range of possible properties.

Further information on the chemistry of epoxy, polyester and phenolic resin systems can be found in Nicholson (2006).

The phenolic polymers often called either phenolic resole or novolac resins are condensation polymers based upon either a reaction of excess formaldehyde with phenol under alkaline conditions with a base catalyst (yielding phenolic resole), or a reaction of excess phenol with formaldehyde under acidic conditions with an acidic catalyst (yielding phenolic novolac). The resoles route is what was used by Baekeland originally. Phenolic resins are particularly selected for use in applications requiring high heat resistance and excellent char and ablative performance. Accordingly applications include rocket nozzles and nose cones where the ablative nature of the phenolic resin is utilised. They also have good dielectric properties, combined with dimensional and thermal stability.

Melamine formaldehyde (MF), an amino resin, is formed by reaction of melamine with formaldehyde, see Figure 1.12. As a moulding material, it is usually filled with cellulosic filler, pigments and a crosslinking catalyst/accelerator and supplied as powder or in granular form. The moulding compounds are used in the production of durable objects such as kitchenware. MF is also used as laminating resin for the production of clear and decorative laminates (for worktops, flooring and furniture) and various other types of laminates and boards, adhesives, coatings and wet-strength agent in paper, e.g. banknotes and wallpaper.



The Wake
the only emission we want to leave behind

Low-speed Engines Medium-speed Engines Turbochargers Propellers Propulsion Packages PrimeServ

The design of eco-friendly marine power and propulsion solutions is crucial for MAN Diesel & Turbo. Power competencies are offered with the world's largest engine programme – having outputs spanning from 450 to 87,220 kW per engine. Get up front!
Find out more at www.mandieselturbo.com

Engineering the Future – since 1758.
MAN Diesel & Turbo



Click on the ad to read more

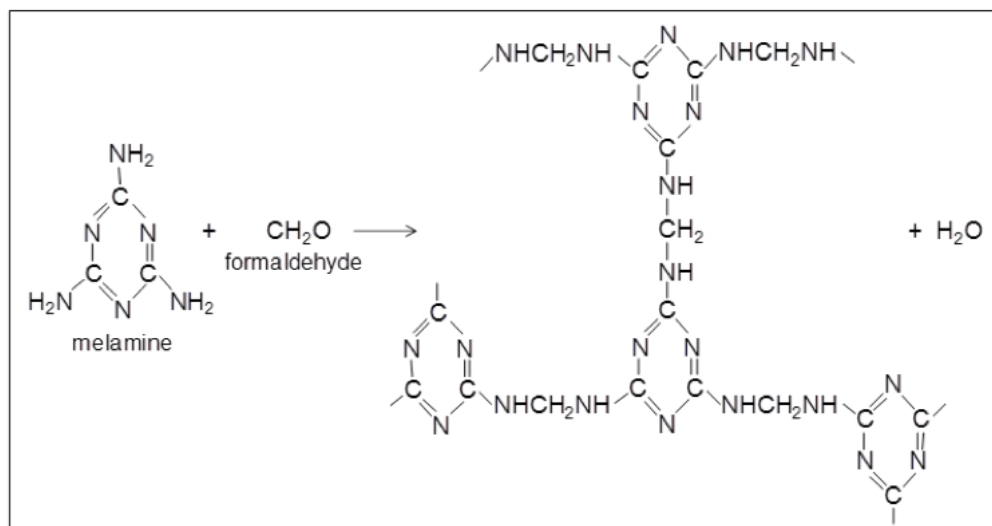


Figure 1.12 Formation of melamine-formaldehyde resin

Thermosetting **polyimides** are easier to process than their thermoplastic counterparts because they use low molecular weight, low viscosity monomers and/or prepolymers as starting materials. A great variety of structurally distinct thermosetting polyimides has been synthesized and characterized (Zhuang 1998). These polyimide oligomers, heterocyclic in structure, have been based on different aromatic diamines, carboxylic acids, as well as varying reactive end groups. Figure 1.13 shows the chemical structure of some of these end groups. The end group carries a functional group favourable to polymerization, copolymerization or crosslinking. Accordingly, thermosetting polyimides can be classified by the chemical nature of their reactive end groups.

Thermosetting polyimides possess desirable properties of high thermal resistance, oxidative stability, low coefficient of thermal expansion, good solvent resistance, and can be used in various applications, particularly aerospace structures and circuit boards.

Bismaleimides are a class of thermosetting resins available commercially in prepreg tapes, fabrics, rovings, and sheet moulding compounds. Bismaleimide resins, as the term implies, are the maleimide formed from the reaction of a diamine and maleic anhydride, Figure 1.14, in the presence of a catalyst.

The diamine is normally aromatic, mainly 4,4'-methylenedianiline (4,4'-diaminodiphenylmethane) is used because of its availability and relatively low cost. But almost any aromatic diamine can be converted into the corresponding maleimide, other examples of aromatic diamines are shown in Figure 1.15. Further details on the chemistry of bismaleimides can be found in Tan (1999, p. 306) and Spratt (1998).

Bismaleimides (BMIs) form useful polymers by homopolymerization or by polymerization with diamines, epoxies, or unsaturated compounds, singular or in mixtures. BMIs are versatile resins with many applications in the electronic and aerospace industries. In comparison with epoxy resins, their primary advantage is their high glass transition temperature, in the 260–320°C range. Thus, bismaleimide resins deliver higher temperature capability providing excellent performance at ambient and elevated temperatures. However like epoxies, BMI homopolymers are quite brittle and are usually copolymerised with another monomer/compound in order to improve toughness. Stenzenberger et al. (1986), in their investigation of the synthesis of comonomers and their use as co-reactants for bismaleimides, have stated that improved toughening agents should:

- render liquid or honey-like consistency at room temperature for improved processability.
- possess a totally aromatic backbone structure to provide high temperature capability.
- undergo a linear chain extension reaction with the bismaleimide to improve toughness and provide a network with low moisture absorption.

A widely used method of toughening a bismaleimide resin is by the addition of various engineering thermoplastics as a second phase material. The mechanical properties and in particular the toughness of a two component system is expected to depend upon the morphology of the blend. In some initial attempts, Stenzenberger et al. (1988) evaluated the use of various commercially available high-performance thermoplastics, such as polysulphone and polyetherimide as toughening agents.

Furthermore, because of the relatively high cure temperature (210°C), the resin is further modified using elastomers and reactive diluents to formulate the resin into a prepreg system with improved cure characteristics e.g. reduced cure temperature during autoclave moulding.

The processing of bismaleimide resins are essentially like that of epoxy resins. BMIs are suitable for standard autoclave processing, injection moulding, resin transfer moulding and SMC. The processing time of BMIs is similar to epoxies, except that for the additional higher service temperature, a free-standing post-cure is required. Primarily used in aircraft composites where operation at higher temperatures (230°C wet/250°C dry) is required. e.g. engine inlets, high speed aircraft flight surfaces.

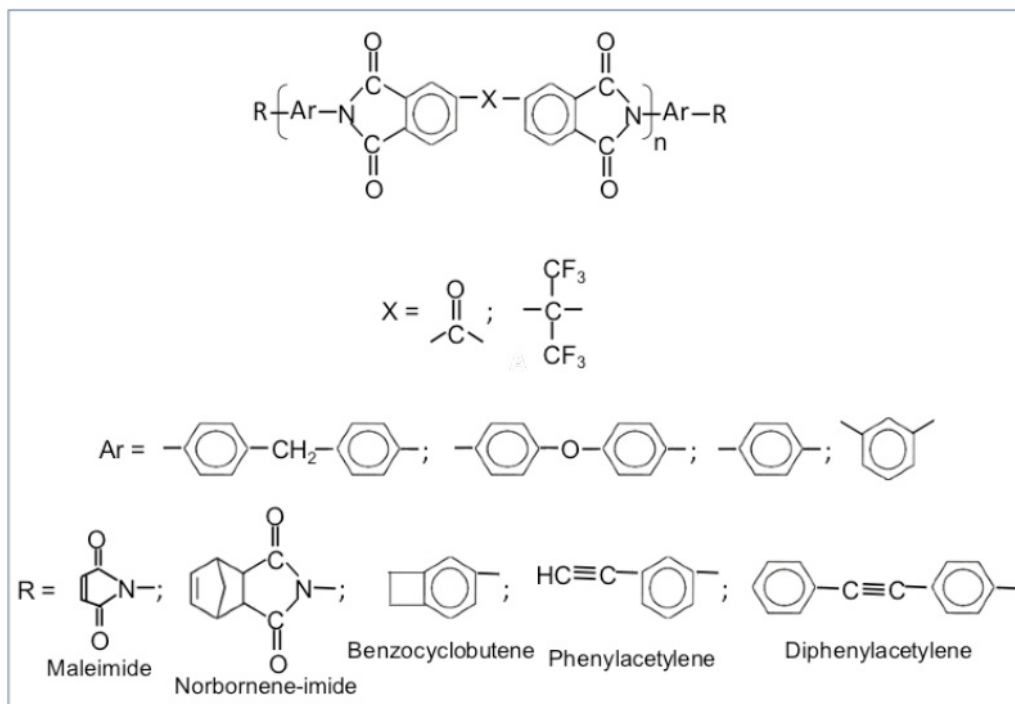


Figure 1.13 Chemical composition of thermosetting polyimides

TURN TO THE EXPERTS FOR SUBSCRIPTION CONSULTANCY

Subscribe is one of the leading companies in Europe when it comes to innovation and business development within subscription businesses.

We innovate new subscription business models or improve existing ones. We do business reviews of existing subscription businesses and we develop acquisition and retention strategies.

Learn more at [linkedin.com/company/subscribe](https://www.linkedin.com/company/subscribe) or contact
Managing Director Morten Suhr Hansen at mha@subscribe.dk

SUBSCR✓**IBE** - to the future

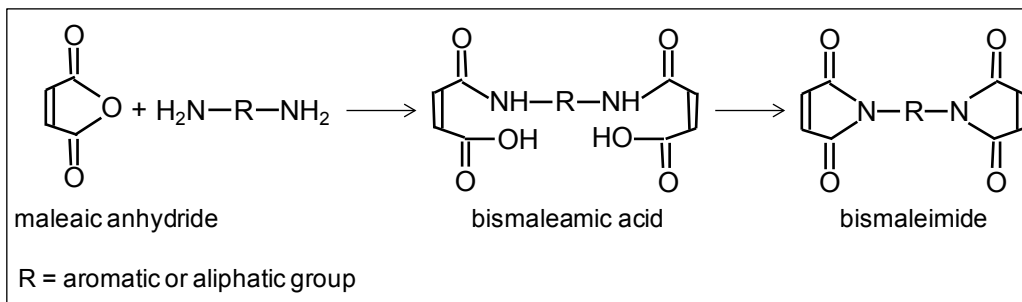


Figure 1.14 Formation of bismaleimides

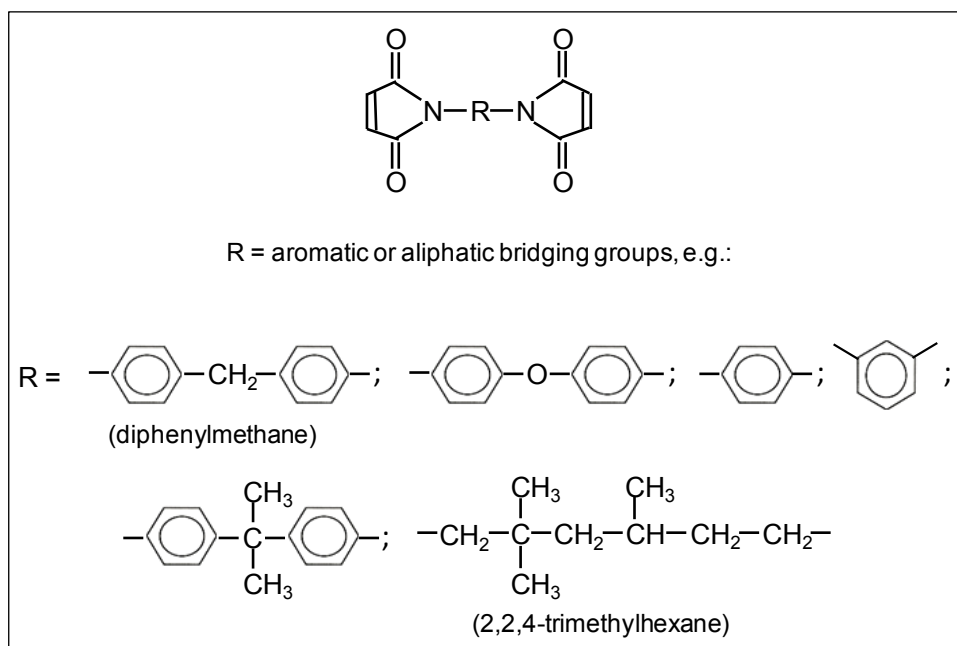


Figure 1.15 Bridging groups in bismaleimides

1.4.3 Fibre-matrix interface

The fibre-matrix interface is where the very important function of load transfer from matrix to the fibres occurs and, therefore, it has a major influence on the properties of composite materials, for instance, the material strength and stiffness falls as the interface weakens, but fracture toughness improves. These are controlled by the processes of fibre-matrix debonding and fibre pull-out from the matrix, which depend on the strength of adhesion between the fibres and matrix. The subject of adhesion in terms of fibre surface wetting and inter diffusion, electrostatic attraction, mechanical interlocking and chemical bonding between the component-materials is covered in general as well as for specific fibre-matrix combinations in (Hull 1981, p. 38).

With a given resin, the surface treatment of the fibre is the critical factor in determining the nature and the level of adhesion that can be achieved between the fibre and matrix. As a result, at material fracture, the fibres will either separate from the matrix cleanly (described as adhesive failure of the interface) or the surface of the extracted fibres will be covered with a layer of plastic (cohesive failure).

There are various ways of treating fibres, and the method selected depends on the type of fibre and matrix to be employed:

The **sizing** coating is applied to the fibres, mainly, to protect the surface of the fibres from damage and act as a lubricant during processing and handling, and act as a coupling agent to facilitate good adhesion, therefore, interface strength between the fibre surface and the matrix. An organosilane compound with suitable functional groups, to form links with the fibre surface and cured resin, is used as sizing/coupling-agent for glass fibres. The silane coupling agents, RSiX_3 , are particularly successful with thermosetting resins where the organo-functional groups (R) react chemically with the resin during the curing process of the resin. The hydrolysable groups (X) are intermediates during the chemical process that bonds the polysiloxane layer to the fibre surface. X is, typically, alkoxy, acyloxy (R-COO^-), amine, or chlorine. The most common alkoxy groups are methoxy (CH_3O^-) and ethoxy ($\text{CH}_3\text{CH}_2\text{O}^-$), which give methanol and ethanol as byproducts during coupling reactions. Since chlorosilanes generate hydrogen chloride as a byproduct during coupling reactions, they are generally utilized less than alkoxy-silanes.

Surface treatment of carbon fibres includes oxidative treatment as well as sizing. The production of carbon fibres from a precursor includes the process of pulling the fibres through a bath of some **oxidizing agents** such as nitric acid, potassium permanganate, or sodium hypochlorite, or through an electrochemical or electrolytic bath (**electrolysis**) that contains solutions, such as sodium hypochlorite or nitric acid. The process removes weak surface layers, etches/roughens the fibre surface, which increases the surface area available for interfacial fibre-matrix bonding and generates reactive or polar groups. Parameters such as current, voltage, electrolyte type or concentration can be varied to preferentially develop the functional groups (carboxyl, $-\text{COOH}$, carbonyl, $-\text{CO}$ and hydroxyl, $-\text{OH}$).

The next step is the application of sizing to the carbon fibre. Sizing protects the carbon fibre during handling and processing (e.g., weaving) into intermediate forms, such as dry fabric and prepregs (*Pre-impregnated fibre*). Sizing also holds filaments together in individual tows to reduce fuzz, improve processability and increase interfacial shear strength between the fibre and matrix resin.

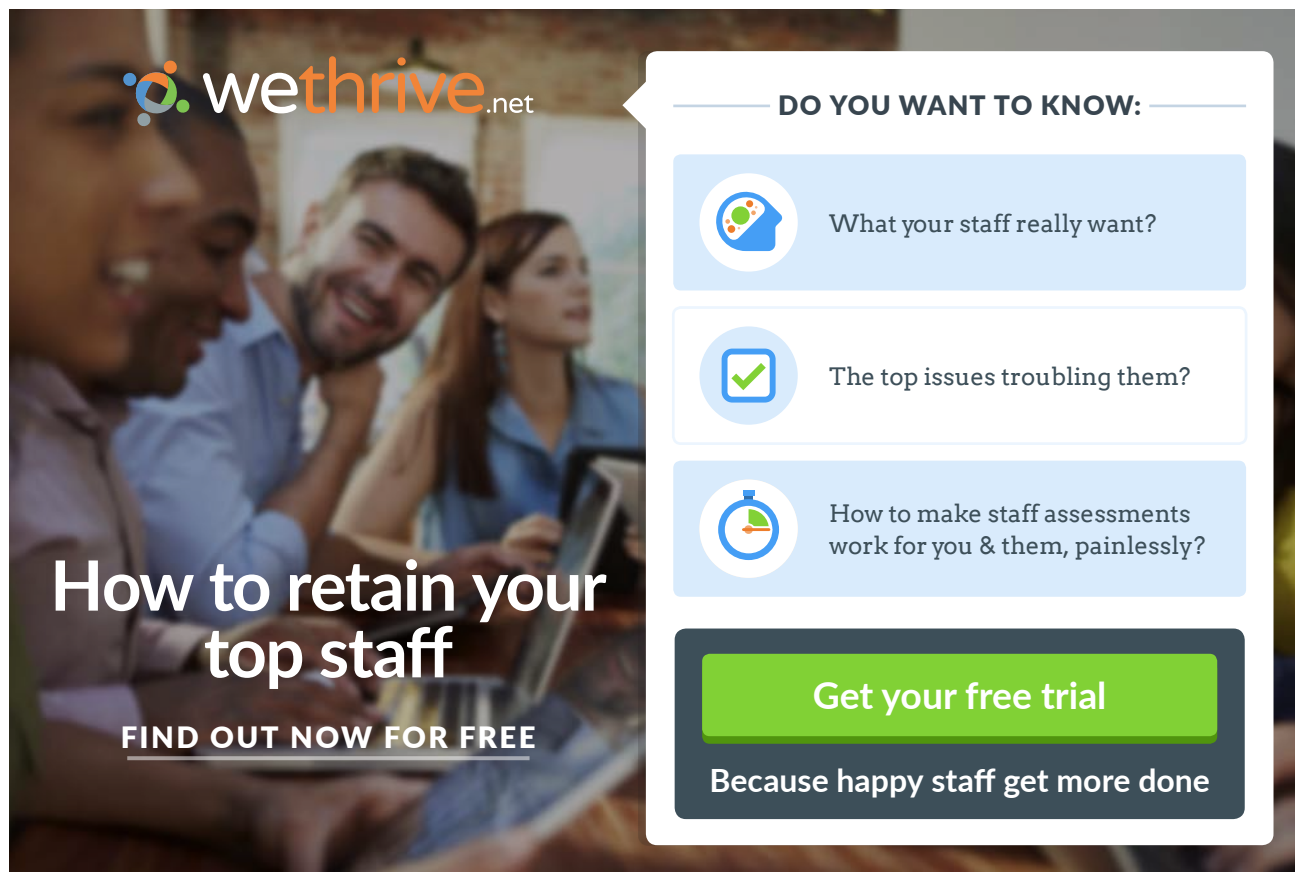
Carbon fibres are mostly used with epoxy matrices, hence the sizing is predominantly epoxy-based and low in molecular weight to encourage fibre pliability and spreadability. However, research is underway to create sizings with chemistries that suit the variety of matrix resins now in demand for end-use applications (McConnell 2009).

Also, composites based on high-temperature resins, such as polyimides, BMIs and PEEK, can suffer from poor oxidative stability with sizings not formulated to match the requirements of matrix resin properties (Akay and Spratt 2008). The functional groups provided by the traditional epoxy-compatible sizings do not chemically react with polyimides and consequently weak interfacial shear strengths result. Furthermore, high temperatures involved in processing temperatures during manufacture and in end-use environments can degrade the epoxy sizing and, as a result, weaken the fiber/matrix interface, producing voids and delaminations (Mason 2004).

Different sizing formulations may be applied to fibres depending on the the type of production method to be employed, for example, infusion or prepregs-autoclave processes,

In the case of chopped versus continuous fibers, sizings will differ to provide different spreadability and good infiltration into the fibre bundles in the case of chopped fibres.

Electropolymerization, as the name suggests, polymerises different species onto the fibre surface. This process could potentially serve the dual role of surface treatment and sizing; or it could be performed on a conventionally surface-treated fibre, directly replacing sizing (Mason 2004).



wethrive.net

How to retain your top staff

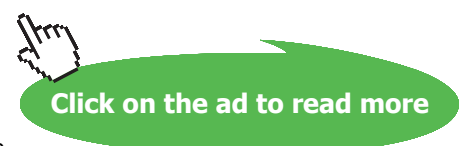
FIND OUT NOW FOR FREE

DO YOU WANT TO KNOW:

- What your staff really want?
- The top issues troubling them?
- How to make staff assessments work for you & them, painlessly?

Get your free trial

Because happy staff get more done



Organometallic coupling agents, based on titanium and zirconium, have been successfully used for most engineering fibres, including polyaramid and UHMWPE fibres, with chemically inert smooth surfaces. Other surface modification techniques suitable for most fibres include **plasma**, an ionized gas, corona discharge ((which is basically an ‘air-plasma’ of excited oxygen and ozone radicals and ions), laser irradiation, and high-energy UV irradiation treatments.

The physical surface treatment techniques of corona and oxygen-plasma pretreatments have also been used with thermoplastic matrices. The surface free energy of the thermoplastic matrix polymer needs to be increased significantly, and the treatments lead to this by generating an increase in the surface concentration of polar groups.

In crystalline thermoplastic-matrix composites, the fibre-matrix interface affects the mechanism of crystallisation generating an “interphase” region where the morphology of crystallinity is different than that exhibited in the bulk of the polymer. The morphology of semicrystalline polymers, such as polypropylene and nylons are affected by the presence of reinforcing fibres, such as carbon, glass, polyaramid and natural fibres: the fibre surface induces additional nucleation sites causing **transcrystallinity**, which grows perpendicularly to the fibre direction until the growing front impinges with spherulites nucleated in the bulk. This generates a band of transcrystalline interphase, see Figures 1.16 and 1.17, which enhances interfacial adhesion.

It should be noted, sometimes, the fibre-sizing surface is referred to as the ‘interface’ while the sizing-matrix region is referred to as the ‘interphase’.

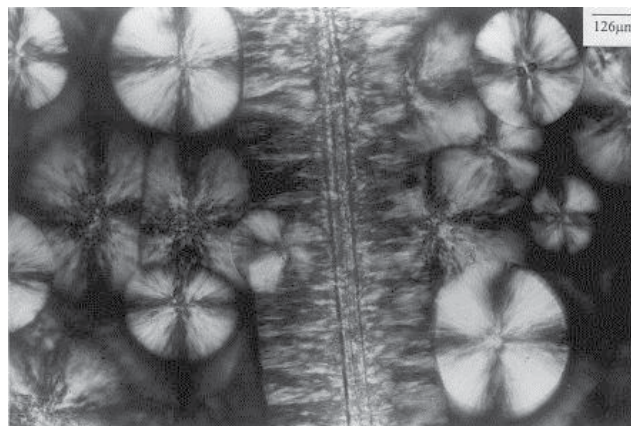


Figure 1.16 Optical micrograph of the transcrystalline layer in dew-retted flax/isotactic polypropylene composite (melting 170°C) (source: Zafeiropoulos et al. 2001)

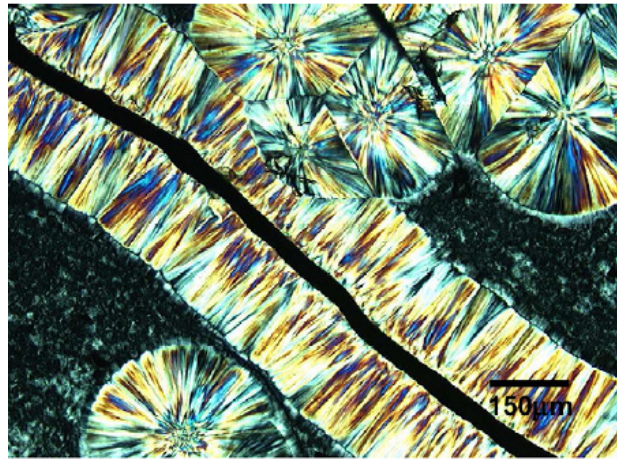


Figure 1.17 Optical micrograph of transcrystalline interphase for polypropylene surrounding the carbon nanotube fibre (isothermally crystallized at 125°C) (source: Zhang et al. 2008)

One other factor to be mentioned is **residual thermal stresses** that can build up at the fibre-matrix interface because of the differential thermal expansion/contraction due to variations in the coefficients of thermal expansion of the component materials, and depending on its magnitude the residual stress can be a source of mechanical weakness at the interface.

1.4.4 Fibre arrangement

In composites, fibres are combined with resin systems in a variety of arrangements to create reinforced engineering materials. With a given resin, the type, amount, diameter, length and orientation of the fibres determine the final properties. The highest strength and modulus values are obtained with unidirectional continuous-fibre composites in the direction of the fibre axis. There is a practical limit of about 70% by volume fibre content that can be added to form a composite, otherwise, there may be too little matrix to support the fibres effectively. In the case of discontinuous-fibre (short fibre) composites, the efficiency of reinforcement suffers because of the reductions in fibre length and alignment. However, discontinuous-fibre composites cost less and offer the mechanical properties required in most ordinary engineering applications.

A structural laminate of composites consists of layers (plies) stacked up in a specific lay-up or ply arrangement, based on the various design criteria imposed on it. A laminate lay-up definition refers to the fibre orientation of successive plies in a laminate with respect to an established reference coordinate system. The fibres in the plies may be continuous or in short length and aligned in one (unidirectional) or more directions. In a unidirectional ply/laminate all the fibres are aligned parallel to each other. Figure 1.18 shows alignment of fibres in different directions in a laminate structure.

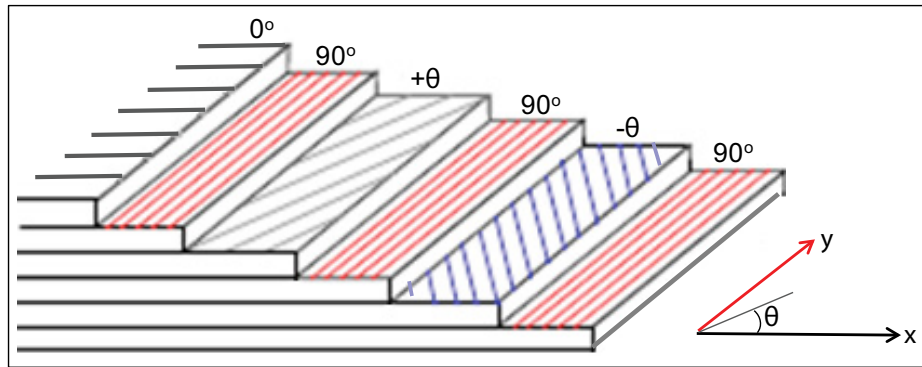


Figure 1.18 An illustration of multi-axial fibre alignment in a laminate

Each **ply (lamina)** is assigned a number representing the direction of the fibre in degrees with respect to the reference axis (x -axis), which is parallel to the long direction of the rectangular panel or structure, where appropriate the sign of the orientation is indicated.

A composite part might require 0° plies to react to the axial (longitudinal) loads, $\theta = \pm 45^\circ$ to react to the shear loads and 90° plies to react to the side (transverse) loads.

Struggling to get interviews?

Professional CV consulting & writing assistance from leading job experts in the UK.

Visit site

 Take a short-cut to your next job!
Improve your interview success rate by 70%.

 **TheCVagency**
Visit theagency.co.uk for more info.



Click on the ad to read more

Laminate lay-ups are expressed by a code that specifies:

- the sequence of plies starting from the tool surface
- the orientation of each ply relative to the reference axis
- number of plies
- the number of successive plies of the same angle by a subscript after the angle
- the sense of the angle plies that are equal in magnitude but opposite in sign by placing positive or negative signs in front of the angles.

A complete set of laminate code is placed within a pair of brackets. If the laminate is symmetric, with an even number of plies, then only the plies on one side of the mid-plane of the laminate are indicated in brackets, followed by the subscript “s” outside the brackets. Symmetric laminates with an odd number of plies are listed with a bar over the centre ply to indicate it being the mid-plane, see Table 1.7. Note that in symmetric lay-ups, the plies become mirror image of one another with respect to the mid-plane/centre-line or the mid-ply. Fabric plies are identified by either placing the ply name or the letter “F” after the ply angle.

Lay-up	code
0°	[0/45/90/90/90/45/0] or [0/45/90/ $\overline{90}$] _s
45°	
90°	
90°	
90°	
45°	
0°	

Table 1.7 Examples of laminate lay-up codes (source: http://nptel.ac.in/courses/Webcourse-contents/IISc-BANG/Composite%20Materials/pdf/Lecture_Notes/LNm2.pdf)

The fibre directions can be arranged to meet specific mechanical properties. The lay-up shown in Figure 1.19 is known as quasi-isotropic, provides isotropic mechanical properties in-plane. Quasi-isotropic properties can also be achieved with 0°, 60° and 120° oriented unidirectional plies.

A quasi-isotropic laminate has either randomly oriented fibre in all directions, or has fibres oriented as described such that equal strength is developed all around the plane of the part.

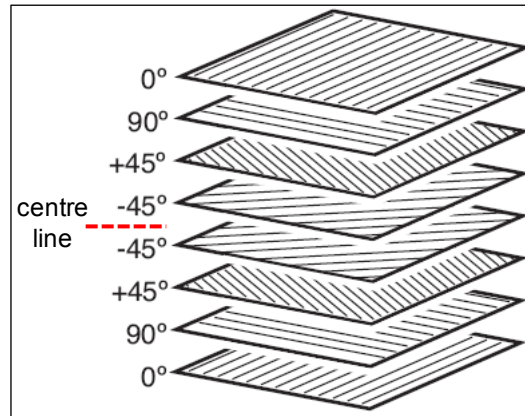


Figure 1.19 Quasi-isotropic orientation of plies

Contribution of ply orientations in Figure 1.19 to laminate performance:

0° plies: give column stability, carry tension and compression.

± 45° plies: give buckling stability and carries shear.

90° plies: carry transverse load, reduce Poisson's effects and helps stability in long and narrow panels.

Reinforcement fibres can be woven into **fabrics**. Fibres running along the length of a roll are referred to as the warp fibres, and those across the width, weft fibres. There are several different fabric styles which are commonly used in the composites industry. Some of these are illustrated in Figure 1.20.

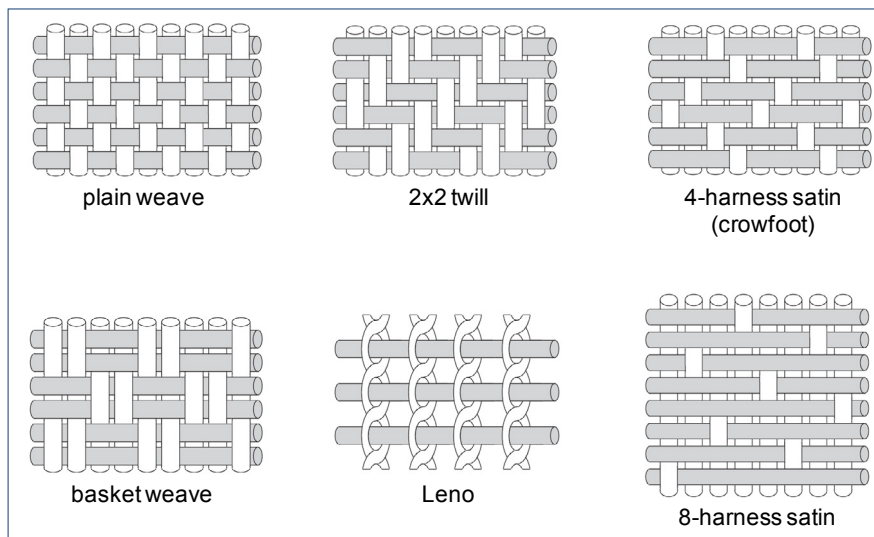


Figure 1.20 An illustration of different fabric patterns (source: JPS Composite Materials)

Different weave patterns exhibit different levels of stability, pliability and, therefore, drapability. In reference to the fabrics included in Figure 1.20, the plain weave is the most stable and the least pliable, whereas the eight-harness satin is the most pliable weave and is used for forming curved surfaces.

The twill weave is more pliable than the plain weave and has better drapability while maintaining more fabric stability than a four or eight harness satin weave. The weave pattern is characterized by a diagonal rib. The fibres pass over and under a number of fibre bundles. A 2×2 twill fabric has warp fibres passing over two fill (weft) yarns and then under two yarns, as in Figure 1.20. Subsequent fibre intercepts are offset by one fibre bundle creating a diagonal, herring bone pattern. The twill is used where tightly woven fabric with high density is required.

The leno weave is used where relatively low numbers of yarns are involved. The leno weave locks the yarns in place by crossing two or more warp threads over each other and interlacing with one or more fill threads.

In woven fabrics there are also different levels of **crimp**, which refers to the amount of bending that is done by thread as it interlaces with the threads that are lying in the opposite direction of the fabric. The level of crimp is expressed in terms of the crimp ratio = (yarn length) / (fabric length). The mechanical properties of fabrics are influenced by the extent of crimping that different weave styles impart, for example:

- plain weave: high crimp, poor mechanical properties
- twill: intermediate properties
- satin: low crimp, good mechanical properties.

The advertisement features a runner in a red top and black leggings on a dirt path at sunrise. The GaiTEYE logo is in the top left. Text on the left reads 'EXPERIENCE THE POWER OF FULL ENGAGEMENT...' followed by 'RUN FASTER. RUN LONGER.. RUN EASIER...'. On the right, technical diagrams of a shoe's sole and foot are shown. A yellow button at the bottom right says 'READ MORE & PRE-ORDER TODAY WWW.GAITEYE.COM' with a hand cursor icon.

Polyester fibre (blue) and Kevlar fibre (straw colour) are used as tracers in GF and CF fabrics to indicate the warp direction. Even with PW fabric, the fibre content may differ in warp and weft directions, and laying up prepreg layers without being aware of warp and weft directions can lead to unsatisfactory outcomes. The variation in the fibre content can occur as a result of the “beating up or battening” process applied to push/consolidate the weft (fill) fibres.

Composites are also produced from thermoplastic fibres as matrix commingled with reinforcement fibres into rovings/tows, which are suitable for filament winding, pultrusion and weaving. These can be combinations of fibres of thermoplastics such as PP, PET or PEEK with GF or CF. Commercial product Twintex® comes as rovings or fabrics made of commingled GF or CF with PP or PET fibres. Figure 1.21 shows a roll of fabric of PP and GF yarns. In the production of composites, the stack of dry fabrics is consolidated into a laminate product by heating above the melting temperature of PP matrix (180°C–230°C) and applying pressure (600 kPa) before cooling under pressure.



Figure 1.21 A roll of PP-GF Twintex fabric

Another example of commingling is PEEK/CF systems, involving separating the respective yarns into open ribbons and then combining them.

Fibres need to be flexible/pliant in order to remain intact under the mechanical stresses and strains imposed during the weaving processes. Flexural flexibility is an inverse function of the fibre diameter as shown below:

Flexibility is defined as inverse of bending stiffness. Consider a fibre as a beam under pure bending and from the engineer’s bending theory,

$$\frac{M}{I} = \frac{E}{R}$$

where, M is the bending moment (or the moment of force), I is the second moment of area, E is the elastic modulus of the material, and R is the radius of curvature that forms when the beam is forced to bend.

It should be noted that as the deflection of the beam increases, the radius of curvature, R , decreases. Therefore, R becomes an indication of stiffness, such that R is directly proportional to stiffness. Accordingly,

Stiffness $\propto EI$, since from the equation of the bending theory $R = EI / M$.

\therefore Flexibility $\propto 1/EI$

where, $I = \pi d^4/64$, and 'd' is the fibre diameter.

Flexibility $\propto 1/Ed^4$

Thus, flexibility of a fibre is inversely proportional to 4th power of the fibre diameter.

Fibres, particularly glass fibres, are also used as **discontinuous-fibre reinforcement** in composites. They are chopped into short lengths varying from 5 to 75 mm and incorporated into composite raw materials in the form of dough moulding compound (DMC) or sheet moulding compound based on various resins but mainly unsaturated polyester. In the SMCs, the fibres are in the form of mats of randomly arranged fibres of 25–75 mm in length. Reinforcement in the form of mats of chopped fibres obviates the weaving process and, therefore, reduces cost but the process is not suitable for controlling fibre alignment to maximise the contribution of the fibres to the properties of the composite. Hand lay-up composite products are usually made from randomly oriented long chopped fibres (chopped-strand mat) and polyester resin.

Short fibres are also incorporated into thermoplastic via the processes of compounding extrusion and/or pultrusion, producing granules/pellets with fibre lengths up to 10 mm long. Products from fibre-containing granules are mainly produced by injection moulding. Base polymers include nylon 6,6, polycarbonate, polyester, polypropylene, polystyrene, PEEK, etc. Reinforcing levels range from 10 to 60 parts by mass. Processing of fibre containing granules, in comparison with the unfilled grades, needs to be controlled to avoid fibre degradation (e.g. lower injection back pressure and screw rotational speeds).

The properties are mainly dictated by fibre content, fibre length and fibre orientation distributions, see Hull (1981 p. 69) and Akay et al. (1995). Fibre orientation in injection moulded fibre reinforced thermoplastics is a function of the melt-flow pattern and also the drag between the flowing melt and the mould surfaces. The resultant fibre orientation is a complex one, however, in a flat plaque moulding there are distinct skin or surface and core layers. The orientation is predominantly longitudinal to the melt-fill direction near the outer/surface layer of the moulding and transverse in the core, see Figure 1.22. The scanning electron microscopy (SEM) micrograph of the specimen taken from the Location (b) indicates the formation of at least three clear layers of fibre orientation. Such anisotropy in fibre orientation results in anisotropic mechanical behaviour of the mouldings. The other physical factor that has a very strong influence on mechanical properties is the fibre content, expressed either in terms of volume, v_f or weight fractions, w_f .

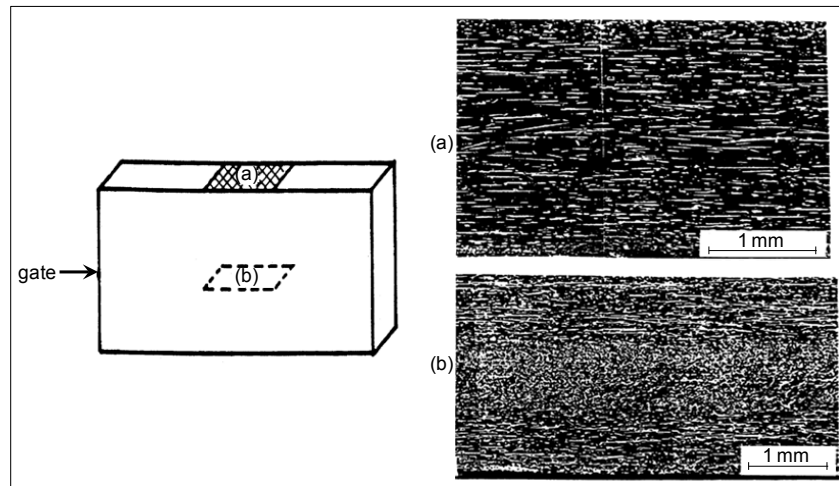


Figure 1.22 SEM micrographs showing tiers of fibre orientation through the thickness of an injection moulded plaque at locations (a) and (b). Material is glass-fibre/polyamide (source: Akay & Barkley 1991)

1.4.5 Fibre and matrix content

One of the methods used to determine the fibre weight percentage in polymer-matrix composites is the resin burn-off method, described in ASTM D2584 – 11: Standard test method for ignition loss of cured reinforced resins. The fibre volume fraction, v_f can be calculated from the fibre weight fraction, w_f :

$$w_f = M_f / M_c \text{ and } v_f = V_f / V_c$$

where, M , V , f and c stand for mass, volume, fibre and composite, respectively.

\therefore the fibre weight fraction, $w_f = \frac{V_f \times \rho_f}{V_c \times \rho_c} = (\text{fibre volume fraction}) \times (\rho_f / \rho_c)$; rearranging gives the equation for the fibre volume fraction, v_f :

$$v_f = w_f \times \left(\frac{\rho_c}{\rho_f} \right)$$

where, ρ is density.

The volume fraction may be expressed in terms of the densities from the rule of mixtures relationship:

$$\rho_c = \rho_f v_f + \rho_m v_m; \text{ assuming zero void content, then}$$

$$\rho_c = \rho_f v_f + \rho_m (1 - v_f); \text{ rearranging gives}$$

$$\rho_c - \rho_m = v_f (\rho_f - \rho_m)$$

$$\therefore v_f = \frac{\rho_c - \rho_m}{\rho_f - \rho_m}$$

The volume fraction may also be expressed in terms of the densities of the component materials and the weight fraction:

The mass (M) of the composite is the sum of the component masses, i. e. $M_c = M_f + M_m$.

In terms of density (ρ) the equation becomes: $\rho_c = \rho_f v_f + \rho_m v_m$

where, m stands for matrix, and $v_f + v_m = 1$ assuming the material is void free.

Expressing in terms of weight fractions, w :

$$v_f = V_f / (V_f + V_m) \text{ or } v_f = (M_f / \rho_f) / (M_f / \rho_f + M_m / \rho_m).$$

$$w_f = M_f / (M_f + M_m) \text{ or } w_f = M_f / M_c \text{ or } M_f = w_f M_c, \text{ and similarly } M_m = w_m M_c.$$

Substituting for M_f and M_m in the above equation for v_f gives

$$v_f = (w_f M_c / \rho_f) / (w_f M_c / \rho_f + w_m M_c / \rho_m) = (w_f / \rho_f) / (w_f / \rho_f + w_m / \rho_m).$$



This e-book
is made with
SetaPDF

SETASIGN

PDF components for PHP developers

www.setasign.com

Substituting for v_f and v_m in $\rho_c = \rho_f v_f + \rho_m v_m$ gives

$$\rho_c = [(w_f/\rho_f) / (w_f/\rho_f + w_m/\rho_m)]\rho_f + [(w_m/\rho_m) / (w_f/\rho_f + w_m/\rho_m)]\rho_m$$

$\therefore \rho_c = (w_f + w_m) / (w_f/\rho_f + w_m/\rho_m)$, since $w_f + w_m = 1$, then

$$\rho_c = 1 / (w_f/\rho_f + w_m/\rho_m). \text{ If } w_f \text{ and } w_m \text{ are in \%}, \text{ then } \rho_c = 100 / (w_f/\rho_f + w_m/\rho_m).$$

Substituting for ρ_c in $v_f = w_f \times (\frac{\rho_c}{\rho_f})$ yields an expression for v_f in terms of w_f , ρ_f and ρ_m :

$$v_f = \frac{w_f/\rho_f}{(w_f/\rho_f + w_m/\rho_m)}$$

Alternatively, by eliminating w_f/ρ and using $w_f + w_m = 1$, the equation becomes

$$v_f = \frac{1}{1 + (\rho_f/\rho_m)[(1/w_f) - 1]}$$

Similarly, v_f can be converted to w_f by the equations:

$$w_f = \frac{v_f \rho_f}{(v_f \rho_f + v_m \rho_m)}$$

$$w_f = \frac{v_f \rho_f}{\rho_m + v_f(\rho_f - \rho_m)}$$

Estimation of cured ply thickness (CPT) from fibre weight in a unit area of prepreg ply, W_f :

$$\text{Fibre density} = \frac{\text{weight of fibres in the prepreg ply}}{\text{volume of fibres in the prepreg ply}} = \frac{\text{weight of fibres in the prepreg ply}}{(\text{prepreg ply area}) \times (\text{CPT}) \times (v_f)}$$

where, v_f is the fibre volume fraction.

$$\therefore \rho_f = \frac{W_f}{(\text{CPT}) \times v_f}; \text{ where, } W_f = \frac{\text{weight of fibres in the prepreg ply}}{\text{prepreg ply area}}$$

Rearranging gives

$$\text{CPT} = \frac{W_f}{\rho_f \times v_f}$$

$$\text{CPT (mm)} = \frac{W_f \text{ (g/m}^2\text{)}}{\rho_f \text{ (g/cm}^3\text{)} \times v_f \times 1000}$$

1.4.6 Void content

The voids in composite materials have been described as arising from two main causes: firstly, incomplete wetting out of the fibres by the resin, which results in entrapment of air and is more likely in systems where the dry fibres are closely spaced and the viscosity of the resin is high; secondly, the presence of volatiles produced during the curing cycle in thermosetting resins and during the melt processing in thermoplastic polymers. The volatiles may be residual solvents, products of chemical reactions or low molecular weight fractions. The void content and distribution depends on fibre volume fraction and distribution, resin properties, and processing conditions such as temperature, pressure and time (Hull 1981, p. 76).

It has been indicated by Stone and Clark (1975) that at low void content (<1.5%), the voids tend to be spherical with diameter 5–20 μm and at higher void contents, the voids are cylindrical and the length can be an order of magnitude greater than the diameter and that the cylindrical voids are generally oriented parallel to the fibres. A wide review on this topic based on many composites by Judd and Wright (1978) has concluded that, regardless of resin, fiber type, or fiber surface treatment, the interlaminar shear strength of a composite decreases by about 7% for each 1% void up to a total void content of about 4%. Other mechanical properties are also affected, although not to the same extent.

Ghiorse (1993) found that in the range zero to 5% void content in carbon fibre epoxy composites, each 1% increase in void decreased the interlaminar shear strength of by 10% and the flexural strength and modulus by 5%.

A simple method of determining **void fraction** is based on density measurements:

$V_{\text{composite}} = (V_{\text{matrix}} + V_{\text{fibre}}) + V_{\text{void}}$; where, V is volume.

By defining $(V_{\text{matrix}} + V_{\text{fibre}})$ as V_{material}

$$\therefore \% \text{ void} = (V_{\text{void}} / V_{\text{composite}}) \times 100 \text{ or } \% \text{ void} = [(V_{\text{composite}} - V_{\text{material}}) / V_{\text{composite}}] \times 100.$$

Expressing in terms of density and mass, $\rho = M / V$, and bearing in mind void content has no mass, gives

$$\% \text{ void} = \{[(M_{\text{composite}} / \rho_{\text{composite}}) - M_{\text{material}} / \rho_{\text{material}}] / (M_{\text{composite}} / \rho_{\text{composite}})\} \times 100$$

$$\% \text{ void} = \{(1/\rho_{\text{composite}} - 1/\rho_{\text{material}}) \rho_{\text{composite}}\} \times 100$$

$$\therefore \% \text{ void} = [1 - (\rho_{\text{composite}} / \rho_{\text{material}})] \times 100 = [(\rho_{\text{material}} - \rho_{\text{composite}}) / \rho_{\text{material}}] \times 100$$

Note that $\rho_{\text{composite}}$ is the experimentally measured density of the sample that includes void, whereas ρ_{material} assumes a completely solid matter. Accordingly, reliable results can only be achieved by accurately measuring $\rho_{\text{composite}}$. For instance, by using very sensitive scales and by weighing the composite sample in air and immersed in liquid, and applying the Archimedes principle

$$\rho_c = \frac{\text{composite weight (in air)}}{\text{composite weight (in air)} - \text{composite weight (in liquid)}} \times \rho_l$$

ρ_l = Liquid density (g/cm³), which becomes one when distilled water is used.

The density of the solid content, i.e. ρ_{material} , may be calculated from the rule of mixtures equation:

$$\rho_{\text{material}} = \rho_f V_f + \rho_m V_m.$$

1.4.7 Core materials

Engineering theory shows that the flexural stiffness of any panel is proportional to the cube of its thickness. The purpose of a core in a composite laminate is therefore to increase the laminate's stiffness by effectively 'thickening' it with a low-density core material. This can provide a dramatic increase in stiffness for very little additional weight.

The advertisement is a dark blue rectangle with a large, stylized lion logo in the background. In the center, the text "YOU THINK. YOU CAN WORK AT RMB" is written in large, white, sans-serif capital letters. In the top right corner, there is a white box containing the Rand Merchant Bank logo (a lion with a key) and the text "RAND MERCHANT BANK" and "A division of FirstRand Bank Limited". Below the logo, it says "Traditional values. Innovative ideas."

Rand Merchant Bank uses good business to create a better world, which is one of the reasons that the country's top talent chooses to work at RMB. For more information visit us at www.rmb.co.za

Thinking that can change your world

Rand Merchant Bank is an Authorised Financial Services Provider



Click on the ad to read more

Figure 1.23 shows a cored laminate under a bending load. Here, the sandwich laminate can be likened to an I-beam, in which the laminate skins act as the I-beam flange, and the core materials act as the beam's shear web. In this mode of loading, it can be seen that the upper skin is put into compression, the lower skin into tension and the core into shear. It therefore follows that one of the most important properties of a core is its shear strength and stiffness.

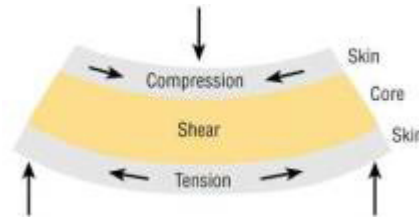


Figure 1.23 Cored laminate under a bending load

In addition, particularly when using lightweight, thin laminate skins, the core must be capable of taking a compressive loading without premature failure. This helps to prevent the thin skins from wrinkling, and failing in a buckling mode.

Stiffness Equations:

The **flexural stiffness** of a flat plate under three-point loading is given by

$$\text{Stiffness (or Rigidity)} = F/\delta = Et^3 (4w/L^3), \text{ in N/mm}$$

where, F is the applied force at midspan, δ is the elastic deflection of the plate at midspan, E is the flexural modulus of the material, t is the plate thickness, w the width, and L is the span.

Therefore, the stiffness of a structure is dependent on the elastic modulus of the material and the geometry of the part, for a plate the thickness being the important parameter.

The stiffness of more complicated structures, such as ribbed plates, corrugations, sandwich beams can be assessed by using **the engineer's bending theory**,

$$\frac{M}{I} = \frac{E}{R}$$

where, M is the bending moment (or the moment of force), I is the second moment of area, E is the elastic modulus of the material, and R is the radius of curvature that forms when the plate is forced to bend, as shown below, Figure 1.24.

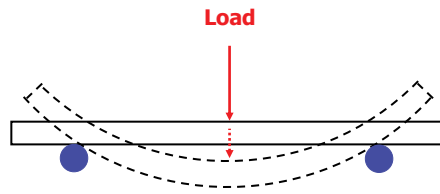


Figure 1.24 Three-point bending of a plate

Note that as the deflection of the plate increases, the radius of curvature, R , decreases. Therefore, R becomes an indication of stiffness, such that R is directly proportional to stiffness. Accordingly,

Stiffness $\propto EI$, since from the equation of the bending theory $R = EI / M$.

Also $I = wt^3/12$, therefore, stiffness $\propto EI$ or Et^3 .

Placing material as far as possible from the neutral axis of bending, which increases t , is generally an effective means of increasing I , and thus, stiffness for a given area of plate cross-section. Separation of plates can be achieved by using honeycomb or foam cores. However, increases in stiffness may also be achieved by the corrugation of a plate or adding ribs to it. The ease with which these structures can be moulded and/or thermoformed in plastics enhances this approach.

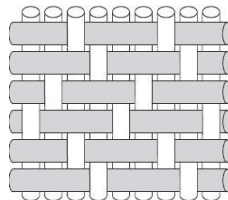
Similarly, the stiffening effect of ribs and corrugations arises from the fact that the geometry results in an increased distance of material from the neutral axis of bending so that the moment of inertia, I , is increased. A stiffening factor may be defined as, $SF = I_{\text{with ribs}} / I_{\text{without ribs}}$.

The value of EI should be kept constant for equal plate deflection or stiffness under a given load.

1.5 Self-assessment questions

1. For a fibre-reinforced composite:
 - a) List the functions of the matrix and fibre phases.
 - b) How does the quality of the fibre-matrix interface influence the strength, stiffness and toughness of the composite?
2. A composite of PMMA and hydroxyapatite contains 36% by weight PMMA. Calculate the volume fractions. Assume specific gravity values of 1.18 for PMMA and 3.16 for HA.
Answer: $v_{\text{HA}} = 0.4$.
3. For a two-component composite with no void content, derive an equation that relates the volume fraction of one of the components to its weight fraction in terms of the densities of the component materials only.
4. Which properties of phenolic resins make them desirable as a matrix for PMCs?
5. What is the purpose of “sizing” in fibre-reinforced composite materials?

6. List the names of the weave patterns for the fabrics used in polymer composites. Compare the properties of these different fabric types with reference to drape and the level of crimp.
7. Show the stack of layup sequence for the code $[\pm 45/\overline{90}]_s$.
8. Show the stack of layup sequence for the code $[0 / \pm 45 / 90]_s$.
9. The Laminate composed of plies of 0° and 90° is called:
 - a) symmetric laminate
 - b) unsymmetric laminate
 - c) cross-ply laminate
 - d) angle ply laminate.
10. The properties of a PMC are determined by:
 - a) the properties of the fibre/resin
 - b) the ratio of fibre to resin in the composite (fibre volume fraction)
 - c) the geometry and orientation of the fibres in the composite
 - d) all of the above.
11. The pre-cursor material used for the manufacturing of carbon fibre is:
 - a) polyamide
 - b) polyacrylonitrile
 - c) graphite
 - d) epoxy resin.
12. Aramid fibre is produced from:
 - a) rayon
 - b) PAN
 - c) PTFE
 - d) polyamide (poly-para phenylene terephthalamide).
13. Which of the following are the properties of Kevlar?
 - a) synthetic organic fibre
 - b) poor compressive strength
 - c) good resistance to impact
 - d) hygroscopic
 - e) all the above.
14. Identify the type of weave pattern shown in the figure below:



- a) 4-harness satin weave
- b) plain weave
- c) 8-harness satin weave
- d) Leno weave.

15. Fibres of different types inserted into weave in a specific pattern is called:
- a) fringer
 - b) tracer
 - c) cursor
 - d) none of the above.
16. The ability of fabric or prepreg to conform to a contoured surface is known as:
- a) symmetry
 - b) smoothness
 - c) balanced
 - d) drape.
17. Hygroscopic refers to:
- a) capable of absorbing water
 - b) capable of repelling water
 - c) capable of absorbing and retaining atmospheric moisture
 - d) change in properties due to moisture absorption and temperature change.

Answer: c



Discover the truth at www.deloitte.ca/careers

Deloitte.

© Deloitte & Touche LLP and affiliated entities.



Click on the ad to read more

18. Which matrix system is suitable for up to 300°C under dry conditions?

- a) epoxy resin
- b) phenolic
- c) polyimide
- d) BMI.

Answer: c

19. The difference between Kevlar and Nomex is that:

- a) Kevlar has meta-oriented aromatic rings, making it about five times stronger than Nomex. Nomex has para-oriented rings with 120° bond angles, which help it not melt at high temperatures.
- b) Kevlar has para-oriented aromatic rings, making it about five times stronger than Nomex. Nomex has meta-oriented rings with 120° bond angles, which help it not melt at high temperatures.
- c) Kevlar has meta-oriented aromatic rings, making it about five times weaker than Nomex. Nomex has para-oriented rings with 120° bond angles, which help it not melt at high temperatures.
- d) Kevlar has para-oriented aromatic rings, making it about five times stronger than Nomex. Nomex has meta-oriented rings with 120° bond angles, which help it melt at high temperatures.

Answer: (b).

20. Nomex is used for:

- a) bullet-proof vests
- b) firefighter uniforms.

21. Kevlar is used for:

- a) bullet-proof vests
- b) firefighter uniforms.

22. When would a satin-weave fabric be used in preference to a plain-weave fabric in composites?

23. Write the chemical formulae of the reagents for the polymerisation of phenolics, and describe the chemical differences between the phenolic resole and novolac resins.

24. Distinguish between interface and interphase between the fibres and thermosetting and thermoplastic matrices.

25. Write the names and the chemical formulae of the reagents for the polymerisation of epoxy resin, and give the chemical equation for the formation of linear epoxy prepolymer.

26. Use suitable equations to show which properties and features affect the stiffness of a composite plate.

27. How can the fibre volume fraction of an autoclave-laminated plate made from CF-epoxy resin prepreg be determined in a non-destructive manner?

Hint: relation of the cured ply thickness to the areal fibre weight in prepreg

28. Define the terms specific elastic modulus and specific tensile strength. Why is expressing properties in this manner important in comparing engineering materials?

2 Processing and forming methods

Fibre composites offer many desirable material properties such as high strength and stiffness for a given mass and allow directional tailoring of properties; but their processing/fabrication can be laborious and pose difficulties. A list of the fabrication techniques is given below:

Fabrication techniques include:

- impregnation of fibres with resin to produce “prepregs”
- laminate formation from prepregs – by hand or tape laying, vacuum bagging and autoclave curing
- contact moulding: spray and hand lamination
- sheet moulding compound (SMC) and dough moulding compound (DMC)
- pultrusion
- filament winding
- fibre placement (ideally 3-D) and resin injection, resin transfer moulding (RTM) or resin infusion
- compression moulding (e.g. DMC and SMC)
- reinforced reaction injection moulding (RRIM) and structural RIM (SRIM)
- glass mat thermoplastics (GMT)
- injection moulding of short/long fibre-reinforced thermoplastics
- shear controlled orientation technology (SCORTEC).

2.1 Open-mould processes (Contact moulding)

2.1.1 Hand lay-up

The process is illustrated in Figure 2.1. Resins are impregnated by hand into fibres by brushes and/or rollers, which also work air bubbles out. Resins (thermoset) need to be low in viscosity to be workable by hand, and fibres, usually glass fibre, can be in the form of chopped strand mat, woven, stitched or bonded fabrics, singly or in combination. The layers are built up until the required part thickness is achieved and, normally, the laminate is left to cure under standard atmospheric conditions.

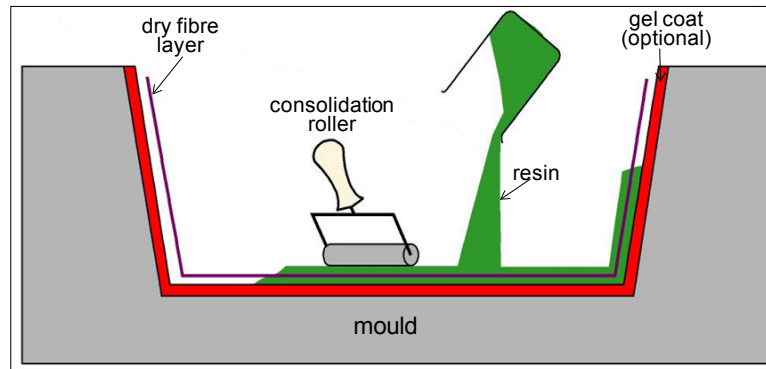


Figure 2.1 Illustration of hand lay-up process (source: SP Systems)

Popularly known as the “Bucket and brush” method, the hand lay-up has been widely used for many years. It is a labour intensive process that uses low cost mould/tooling, particularly if room-temperature cure resins are used. Higher fibre contents and longer fibres can be incorporated in products than those made with spray lay-up. It lends itself to sandwich construction (foam or balsa-wood cores) and inserts can readily be incorporated. As well as being a high labour-intensive process, some of the other disadvantages include volatile organic compound (VOC) emissions, health & safety concerns over the exposure of operators to hazardous chemicals, therefore subject to regulations such as COSHH, and product quality and variability dependent on operator expertise.

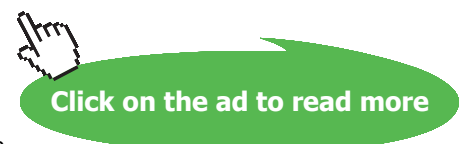
The advertisement features a group of diverse people holding a large green banner with the text: "I WANT TO CHANGE DIRECTION, AND THE WORLD." Below the banner, the website "GOT-THE-ENERGY-TO-LEAD.COM" is displayed. A woman in a business suit is sitting on the ground, holding a briefcase. The RWE logo is in the bottom left corner, with the tagline "The energy to lead".

**I WANT TO CHANGE DIRECTION,
AND THE WORLD.**

GOT-THE-ENERGY-TO-LEAD.COM

We believe that energy suppliers should be renewable, too. We are therefore looking for enthusiastic new colleagues with plenty of ideas who want to join RWE in changing the world. Visit us online to find out what we are offering and how we are working together to ensure the energy of the future.

RWE
The energy to lead



The most common health problem for the workers is the skin condition, dermatitis. Resins, hardeners, catalysts and additives used in lay-up and spray-up are all possible sensitizers. The uncured resin dust from finishing operations can also cause these allergic reactions. Sensitization is an allergic reaction that some workers can develop suddenly after years of handling a material without any reaction. However, once sensitized, contact with even a small amount of the same material can cause a severe outbreak that may spread widely over the body.

2.1.2 Spray lay-up

The process (Figure 2.2) involves the spraying of chopped fibre rovings and catalysed resin mixture into a pre-prepared mould, rolling the deposited layer to remove air and curing the resin (thermoset), normally under standard atmospheric conditions. Spray-up is a faster process and is less labour intensive than hand lay-up, and it also offers potential for automation with robots. Drawbacks include the possibility of more air entrapment, short fibre lengths at a random orientation, difficulty in controlling thickness and resin-to-glass ratios, only one moulded surface, no significant consolidation pressure and generation of waste, especially when overspray is significant.

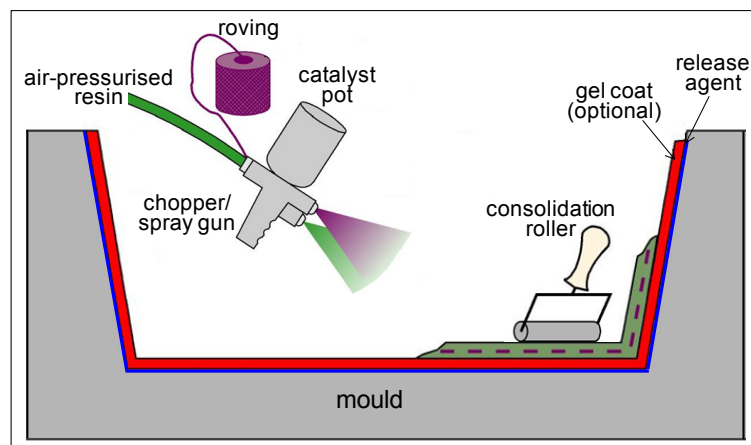


Figure 2.2 Illustration of spray lay-up process

Health & safety concerns exist over the exposure to chemicals and their VOC emissions and noise in spray booths, particularly if the process is not automated. Contact with catalysts used to initiate resin curing can cause eye/skin burns. A serious concern is over the high styrene monomer content used to thin resins such as polyesters and act as the crosslinking agent: styrene and most of the commonly used solvents, such as acetone and methyl ethyl ketone (MEK), can form flammable or explosive vapour concentrations under normal room temperatures and cause breathing difficulties. Protective measures include the use of overspray containment flanges.

Another skin problem, glass itch, is caused by glass fibres rubbing on the skin and irritating it, which can arise during both hand lay-up and spray lay-up processes. Glass fibres can also be so fine as to cause respiratory problems.

Hazardous substances are regulated, and government agencies such as Occupational Safety and Health Administration (OSHA) of USA provides good work practices to follow when working with these substances and sets permissible exposure limits, e.g. 50 parts per million (ppm) for styrene, for employees to be exposed to during an eight-hour work shift. There is as yet no EU harmonisation in this respect, the limit for styrene monomer exposure is set at different levels: ranging from 20 ppm in Germany to 100 ppm in the UK. Companies are expected to establish effective health and safety management systems to control the risk factors and ensure compliance with regulations.

Centrifugal casting is a variant of the lay-up processes, such that chopped strand mat is placed into a hollow, usually cylindrical, mould then the resin is added, the mould is closed, heated and rotated until the resin is cured. Alternatively, continuous roving is chopped and directed onto the inside walls of the rotating mould together with thermosetting resin or thermoplastic powder. The heat is transferred through the walls of the mould to soften and fuse thermoplastics or cure the thermosetting resin (some thermosets are chemically cured without external heat). Centrifugal force of rapid rotation forces the resin to conform to the shape of the mould. The process is similar to the rotational moulding process except here the rotation is usually around a single axis. Centrifugal Casting is used for making cylindrical, hollow shapes such as tanks, pipes and poles.

bookboon.com

Corporate eLibrary

See our Business Solutions for employee learning

[Click here](#)

Management Time Management

Problem solving Self-Confidence Effectiveness

Project Management Goal setting Motivation Coaching

[Click on the ad to read more](#)

69

Download free eBooks at bookboon.com

2.1.3 Prepreg, vacuum bag and autoclave

Preimpregnation of fibres with polymer matrix via one of the methods shown in Figure 2.3 produces prepreg plies, which basically become a raw material for many fabrication processes to produce composite products. The thermosetting resins in prepregs are only partially cured and are in a tacky state to facilitate consolidation in the subsequent processes. The tackiness has a certain tack/shelf life and, therefore, the rolls of prepreg are kept in cold storage prior to production. The prepreg needs to be defrosted prior to usage, usually overnight, and its “out life” indicates the time it can remain usable at workshop temperature.

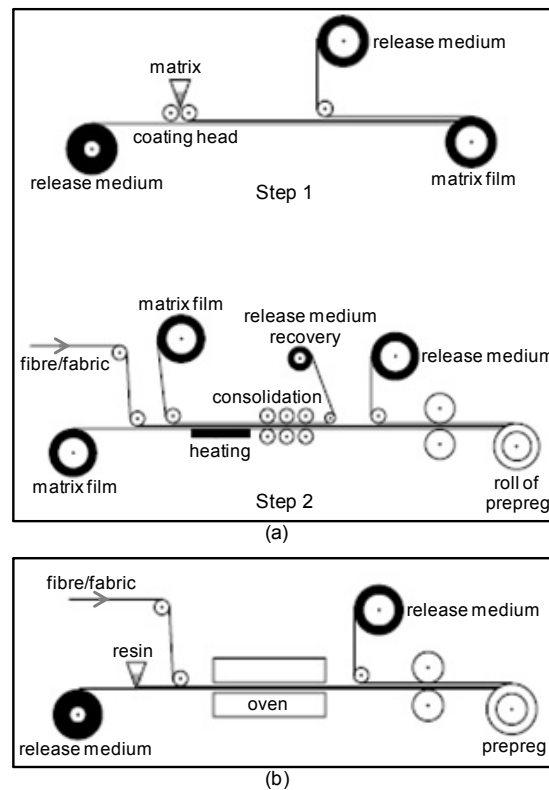


Figure 2.3 Illustration of prepreg processes: (a) film transfer route and (b) solution route (source: Hexcel)

Prepregs are employed in various processes such as vacuum bag processing and autoclave processing. For either one of these processes, the prepreg plies (lay-ups) are stacked on to a tool (mould) surface in a given fibre orientation arrangement, covered with flexible bagging film, see Figure 2.4, and consolidated by applying both heat and pressure in an autoclave or under vacuum (generating a consolidation pressure of 1 atmosphere) in an air circulating oven. **Vacuum bag processing** is suited to components with thin sections and large sandwich structures. High processing pressures under **autoclave processing** allow the moulding of thicker sections and complex shapes.

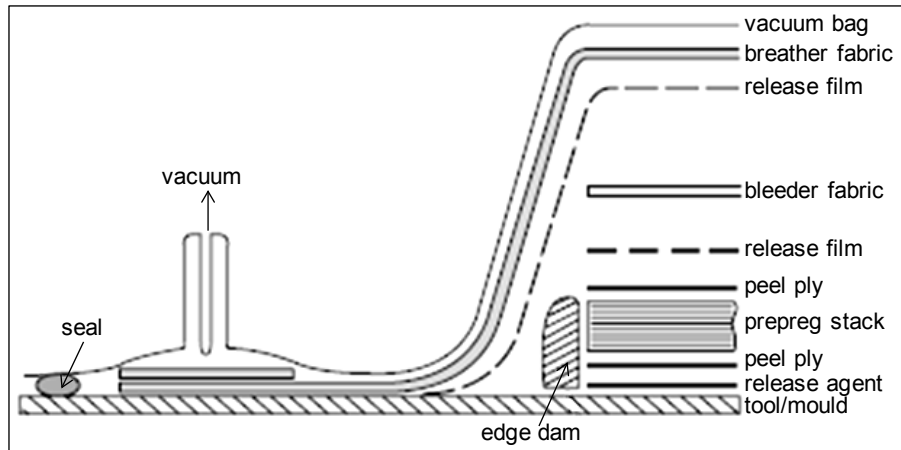


Figure 2.4 Detail of vacuum bag lay-up (source: Hexcel)

The functions of most of the consumable-material layers shown in Figure 2.4 are self explanatory, and briefly: **peel ply** is a perforated layer that allows free passage of volatiles and excess matrix during the cure and provide a clean surface for further lamination, secondary bonding or coating. **Bleeder fabric** usually made of felt of glass fibre and absorbs the excess matrix. The matrix flow can be regulated by the quantity of bleeder to produce composites of known fibre volume content. **Release film** (slightly perforated) prevents adhesion, hinders flow of matrix but allows the passage of air and volatiles into the breather layer above. **Breather fabric** allows gas flow under vacuum and ensures uniform vacuum pressure. Thicker breathers are needed when high autoclave pressures are used. Edge dam restricts resin flow and maintains the component edge shape. Not all the consumable-material layers are always used; some of them are optional, depending on the component made and the quality required.

The lay-up preparation requires **debulking** by applying vacuum suction at specific points in the lay-up sequence to ensure full mechanical consolidation of the prepreg plies. Vacuum is also employed during the curing process to remove air and volatiles and consolidate the lay-up.

A suitable **cure cycle** is applied depending on the type of resin, processing method and the lay-up geometry that is used. In autoclave (effectively a pressurised oven) processing of the composite part, the curing conditions of vacuum, pressure, heat up rate, cure temperature and cool down rate are controlled. The pressure exerted on the lay-up is normally within the range 300–700 kPa (3–7 bar or 44–102 psi). Excessive pressures should be avoided in processing sandwich constructions (consisting of prepreg skins and honeycomb/foam core) in order to avoid movement of the core and telegraphing (where honeycomb cells are visible through the composite skins) – it may be necessary to process in two or three operations/stages.

Two-stage curing is the most commonly used technique for manufacturing sandwich constructions, such as Formula One car chassis: the first facing skin is laid-up on the tool, vacuum bagged and cured. The cured skin is retained on the tool and the subsequent components added, i.e. adhesive layers, core and outer facing skin. The whole assembly is then bagged and cured.

Thermal stresses occur during the cooling of a cured laminate from the processing temperature down to room temperature, also due to any subsequent heating and cooling in usage. If thermal stresses are balanced in a laminate then there should be no distortion. This is achieved by symmetric arrangement of plies. Unsymmetrical laminates suffer distortion upon heating or cooling, because of the variations in the coefficients of thermal expansion parallel (α_{\parallel}) and perpendicular (α_{\perp}) to the fibre direction. Examples of symmetric and non-symmetric angle-ply and cross-ply laminates are shown in Figure 2.5.

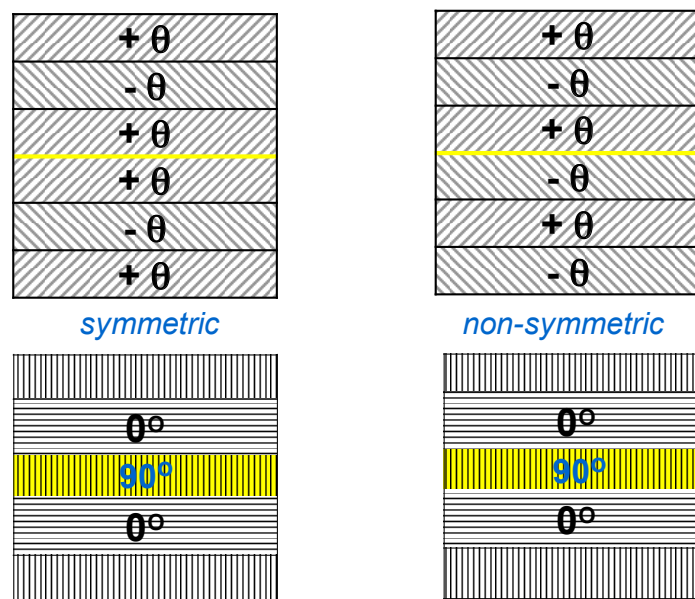


Figure 2.5 Symmetric and non-symmetric angle-ply and cross-ply laminates

Figure 2.6 shows examples of distortions in some non-symmetric angle-ply laminates, and in a well-bonded two-layered cross-ply laminate, which will curl up towards the ply with the lower coefficient of expansion on heating.

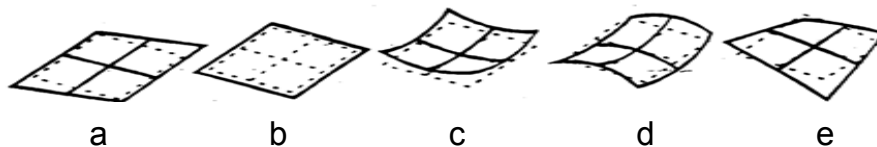


Figure 2.6 Effect of temperature increase on flat plates: (a) off-axis unidirectional ply; (b) symmetric crossply laminate; (c) non-symmetric laminates of isotropic plies; (d) non-symmetric crossply laminate (produces a double curvature distortion); (e) non-symmetric angle-ply laminate (source: Powell 1994)

A wide variety of polymer foam cores with densities from 30 kg/m^3 to 400 kg/m^3 are used in composite sandwich structures, including PET, e.g. Airex; polymethacrylimide (PMI), e.g. Rohacell; PS, and styrene-acrylonitrile copolymer (SAN), e.g. Corecell; PU, e.g. Kapex; and PVC. Rohacell exhibits good strength and stiffness, high dimensional stability and can be used at elevated temperatures. However, high cost limits its use to aerospace components: helicopter rotor blades, ailerons and stringer profiles in pressure bulkheads. PS foam is low cost, its mechanical properties are relatively poor and normally used with epoxy resins because styrene in polyester resin acts as a solvent for PS. It can be easily shaped and is extensively used in surf board manufacture. PVC and PU foams are resistant to styrene and, therefore can be used with polyester resins.

Honeycomb/corrugated cores are made from aluminium, resin-impregnated paper or polymers: made by selectively bonding layers of scored material and then expanding the stack to produce a regular cellular structure. Alternative manufacture includes bonding together corrugated thermoplastic extrudates. It should be remembered that galvanic corrosion may occur if carbon fibres are in contact with aluminium in a moist environment. Nomex (DuPont aramid) is used for aerospace quality honeycombs. It should, however, be noted that aramid is hydrophilic.



Brain power

By 2020, wind could provide one-tenth of our planet's electricity needs. Already today, SKF's innovative know-how is crucial to running a large proportion of the world's wind turbines.

Up to 25 % of the generating costs relate to maintenance. These can be reduced dramatically thanks to our systems for on-line condition monitoring and automatic lubrication. We help make it more economical to create cleaner, cheaper energy out of thin air.

By sharing our experience, expertise, and creativity, industries can boost performance beyond expectations. Therefore we need the best employees who can meet this challenge!

The Power of Knowledge Engineering

Plug into The Power of Knowledge Engineering.
Visit us at www.skf.com/knowledge

SKF

Long cure cycles are required because the large autoclave mass takes a long time to heat up and cool down. Heat up rates (1–3°C/min) need to be selected to ensure even temperature distribution on the tooling and composite components. The cured component cooled to room temperature at 3°C/min. A typical autoclave cure cycle is a two-step process, see Figure 2.7. First, vacuum and pressure are applied while the temperature is ramped up to an intermediate level and held there for a short period of time. Intermediate dwells are often chosen at a temperature where the resin is at the optimum viscosity for removal of air and volatiles from the part. The resin also begins wetting the fibres at this stage. In the second ramp up, the temperature is raised to the final cure temperature and held for a sufficient length of time to complete the cure reaction. The viscosity of the resin should be at a level that permits adequate consolidation and fibre wetting, while avoiding excessive flow and subsequent resin starvation. Similar to temperature, it may also be more suitable to increase the pressure incrementally.

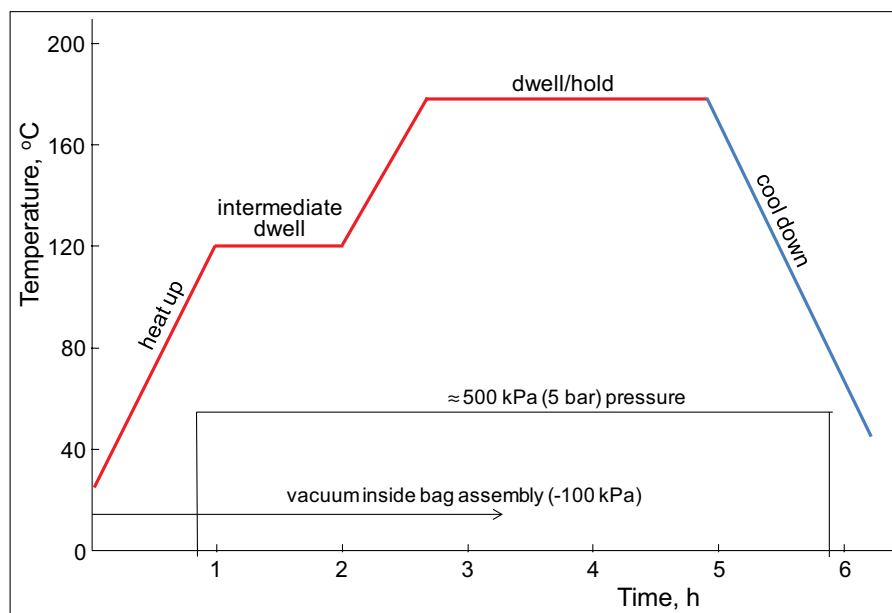


Figure 2.7 A cure cycle in an autoclave for an epoxy resin prepreg lay-up

Tape laying employs a computer-numerically controlled technique for laying prepreg reinforcement tape of various widths, using thermoset or thermoplastic matrix, and applying it on the tool surface by a tape application robot. It is a suitable process for producing high quality aerospace parts with flat or low curvature surfaces.

Production of some complex-shaped components may necessitate the use of **intensifiers** to exert pressure at component locations such as corners that are difficult to pressurise under normal autoclave pressure. Pressure intensifiers are hard rubber pads/profiles incorporated in the bag to ensure that the area concerned receives full pressure to consolidate the laminate. The concept is illustrated subsequently in Figure 2.12 for a matched-tool assembly for the production of a rib-stiffened plate.

An analogous composite material to prepregs is **glass mat thermoplastics (GMTs)**. This semi-finished intermediate product was developed primarily as a substitute for sheet metal in some applications in the automotive industry. GMT is produced in flat sheets/panels, typically 3–4 mm thick, in which long (>12.5–100 mm) or continuous fibres are arranged in random form in a thermoplastic matrix. The fibre content typically ranges 15–40% by weight. Sheets of GMT are produced on an extrusion line consisting of an extruder, double belt press (the double-band press), heating and cooling units and a cutting unit. Thermoplastic melt is extruded between the continuously fed layers of glass-fibre mats forming, therefore, a continuous sheet of glass-mat-reinforced thermoplastic, which is cut into GMT blanks at the end of the processing line following the cooling/solidification of thermoplastic matrix. The specifically dimensioned pre-cut GMT blanks are further processed on a GMT production line into products by a thermoforming, press stamping or moulding operations.

Further details and the diagrams of these processes for GMT production are presented by Schemme (2008). He has also described the so-called Advanced GMT, which combines the advantages of conventional GMT processing of random mats with woven fabrics or unidirectional (UD) fibre layers. The number and position of the fabrics or UD layers can be chosen in any combination that leads to customized solutions for processability, properties and cost-effectiveness. Advanced GMTs were used in 1998 for the production of heavy-duty under-body skid-plates and bumper beams. Since then Advanced GMT has also been employed in the production of spare wheel pans, rear axle supports and rear doors. These parts have the following in common: complex geometry; good crash features due to high energy absorption and ductile fracture behaviour; and high stiffness/weight ratio.

GMTs are viable alternatives to thermosetting prepregs: the process times are shorter; the material costs are lower (particularly with commodity polymers such as polypropylene and polyesters as matrix).

2.1.4 Filament winding

In filament winding continuous fibre strands/tows or ribbons are impregnated with resin and wound onto a rotating mandrel at a numerically controlled pre-programmed pattern to produce a tubular shape, see Figure 2.8. The pressure on the part is normally applied by fibre tension, which affects fibre volume fraction and void content as well as the level of consolidation. Pressure can also be applied if the part is cured in an autoclave after the winding process.

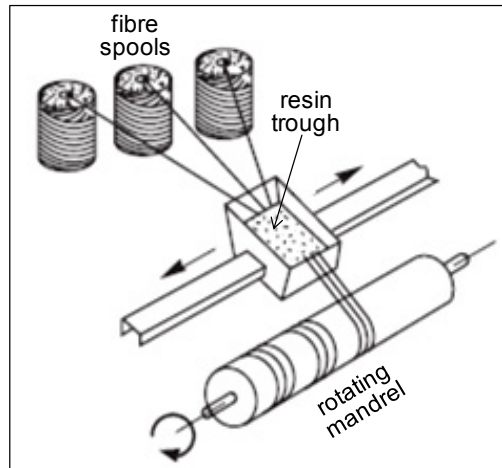


Figure 2.8 Filament winding (source: Molded Fiber Glass Companies 2003)

The matrix used is generally a thermosetting resin, the use of a thermoplastic matrix involves either passing the fibres through a vat of polymer powder where the fine powder adheres to the fibres electrostatically, or by using fibres that are already coated with the molten polymer by an extrusion process. However, the fibre ribbons coated with a thermoplastic need to be heated at the point of contact with the mandrel (e.g. using a heating torch) to sufficiently soften it and then pressure is applied locally with a consolidation roller to achieve bonding.

With us you can
shape the future.
Every single day.

For more information go to:
www.eon-career.com

Your energy shapes the future.

e-on



The mandrels are either removed from the finished products if they are collapsible or soluble, or remain in the product as a liner. Smart mandrels can also be adopted for some complex shapes. These are made from fibre-reinforced shape memory polymer (SMP) hollow tubes. The tube is softened, placed in a split-mould, in the shape of the mandrel, and is pushed against the mould contours with air pressure. After it is cooled, the SMP becomes rigid and maintains the moulded shape. The rigid mandrel is then coated with a mould release and used for the winding of a composite part; with such a mandrel the heat of cure has to be below the glass-transition temperature of the SMP. Following the filament winding process, the mandrel is reheated to above its softening temperature and it resumes its original tube shape and can be extracted from the cured part.

The complexity/capacity of the filament-winding machines are characterised by the degrees of movement freedom that they offer: usually three orthogonal and three rotational axes are possible. For example, in hoop winding the angle is just below 90° , in axial winding 0° (difficult to maintain fibre tension), polar winding, where the threads are run almost horizontally to the axis of the mandrel, for domed ends or spherical components (fibres constrained by bosses on each pole of the component), and helical winding. Some examples of complex winding patterns are shown in Figure 2.9.

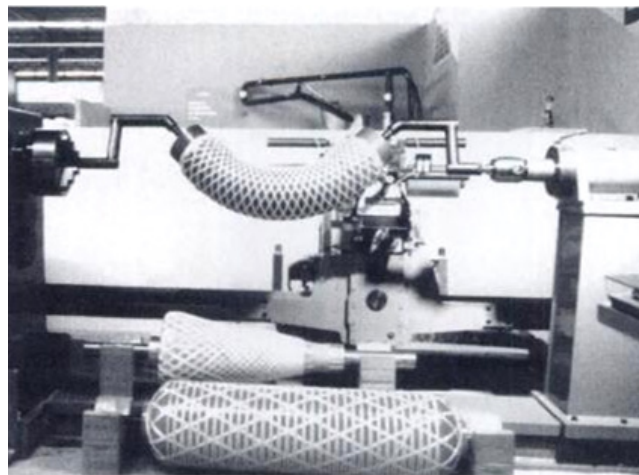


Figure 2.9 Filament winding (source: Bunsell & Renard 2005, p. 159)

2.1.5 Bladder moulding/Pressure-bag moulding

The process, mainly for the production of hollow sections such as tubes, is similar to matched-die compression moulding, except the male half of the mould is a flexible/deformable bladder/bag. The layup, in the form of prepreg or preform, and bladder assembly is placed inside a mould (e.g. a clamshell mould) that defines the outer surface of the part; and as the composite is heated, the bladder is inflated so as to conform the material to the shape of the mould cavity and bring about consolidation, see Figure 2.10. The inflatable bladder is either manufactured from silicone rubber or a shape memory polymer. Unlike a rubber bladder, the SMP bladder is initially rigid and is inflated when it softens under the heat applied for curing. Once the cure cycle is complete, the air pressure is released and as the mould cools down the SMP bladder shrinks to its original hose-like shape and detaches from the cured part and is removed. The curing is either conducted in an oven or by heaters attached to the mould. A pressure regulator may regulate the amount of pressure applied to the material by the flexible bladder as the bladder presses the material against the forming tool.

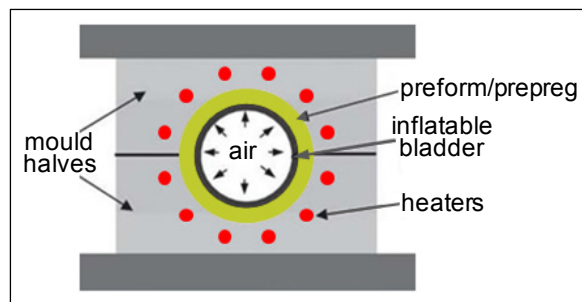


Figure 2.10 Bladder moulding of a tubular shape

The process is suitable for manufacturing with woven or braided preforms from comingled yarns to produce items such as tennis racquets and bicycle frames. The comingled yarns consist of a mixture of reinforcing fibres, e.g. CF or GF, and thermoplastic-matrix fibres such as polypropylene or a polyamide (e.g. nylon 12).

2.2 Closed-mould processes

2.2.1 Compression moulding

This is a common industrial process whereby typically a charge of DMC, SMC or flat sheets of prepregs placed into the lower half of a heated matched mould, the mould halves are then closed and pressed together to conform the material into the final shape and where it is allowed to cure, see Figure 2.11. The charge is usually preheated prior to placement into the mould. Preheated polymer becomes softer resulting in shortening the moulding cycle time. The method is used mostly for moulding thermosetting resin-based materials, but some thermoplastic composite parts may also be produced by compression moulding.

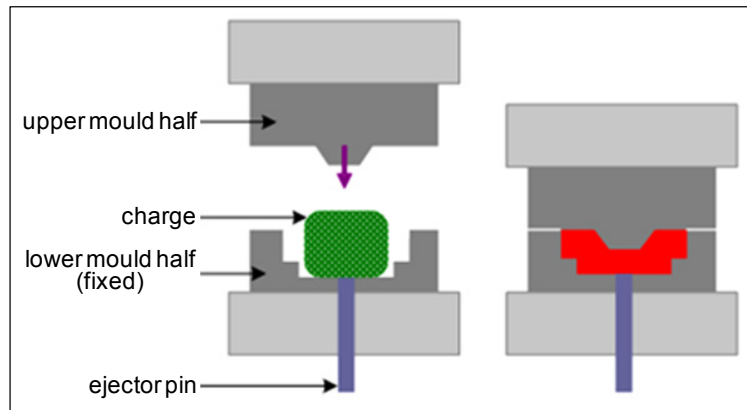


Figure 2.11 Compression moulding (source: Kopeliovich 2012)

The tool, particularly for moulding complex prepreg layups, can also be assembled in such a way that the pressure required is applied in an autoclave, and the tool assembly may incorporate rubber **pressure intensifiers** to provide additional pressure, particularly in locations that require extra pressure for good consolidation, see Figure 2.12.

The advertisement features a background image of a lecture hall with rows of wooden chairs. A large blue arrow points from the word 'be' on the left to 'your degree' on the right. The text 'Be greater than.' is prominently displayed, followed by 'consulting | technology | outsourcing'. The Accenture logo and tagline 'High performance. Delivered.' are in the bottom right. A small copyright notice '© 2013 Accenture. All rights reserved.' is visible on the right side.

be > your degree

Bring your talent and passion to a global organization at the forefront of business, technology and innovation. Discover how great you can be.

Visit accenture.com/bookboon

Be greater than.
consulting | technology | outsourcing

accenture
High performance. Delivered.

© 2013 Accenture. All rights reserved.



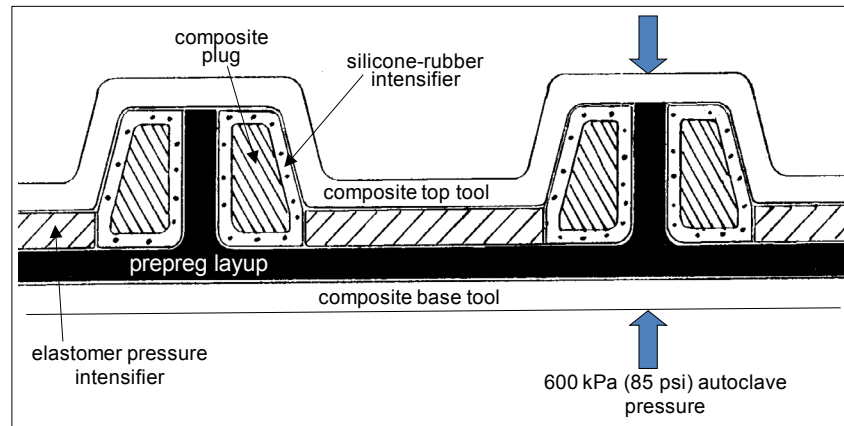


Figure 2.12 An illustration of the use of a pressure intensifier in a matched-tool assembly

A similar concept to that of pressure intensifiers, called **trapped rubber moulding** or **thermal expansion moulding**, also utilises the greater thermal expansion of the rubber medium compared with the rigid tool to generate all the required pressure. Prepeg layers are wrapped over blocks of rubber and the lay-up is then restrained in a composite tool with a low coefficient of thermal expansion and the assembly is then heated in an oven. As the temperature increases, a high differential thermal expansion takes place between the tool and the rubber plug generating high pressures to consolidate the lay-up. An aluminium layer may also be used to provide pressure by means of such differential thermal expansion.

The method enables the production of complex shapes in a single cure cycle, thus reducing the number of joints and parts.

2.2.2 Pultrusion

Pultrusion is a continuous method of manufacturing, see Figure 2.13, whereby fibre rovings/mats of randomly oriented fibres and veils are mechanically gripped and pulled (hence pultrusion) from their spools/bobbins on creels through a resin bath to impregnate/coat the reinforcement with resin, then through a heated die to give the shape of the final cross section of the part and the cured profile is finally pulled to the saw (a flying cut-off saw) for cutting to length. Two distinct pulling systems are used: a caterpillar counter-rotating track or a hand-over-hand hydraulic reciprocating clamp.

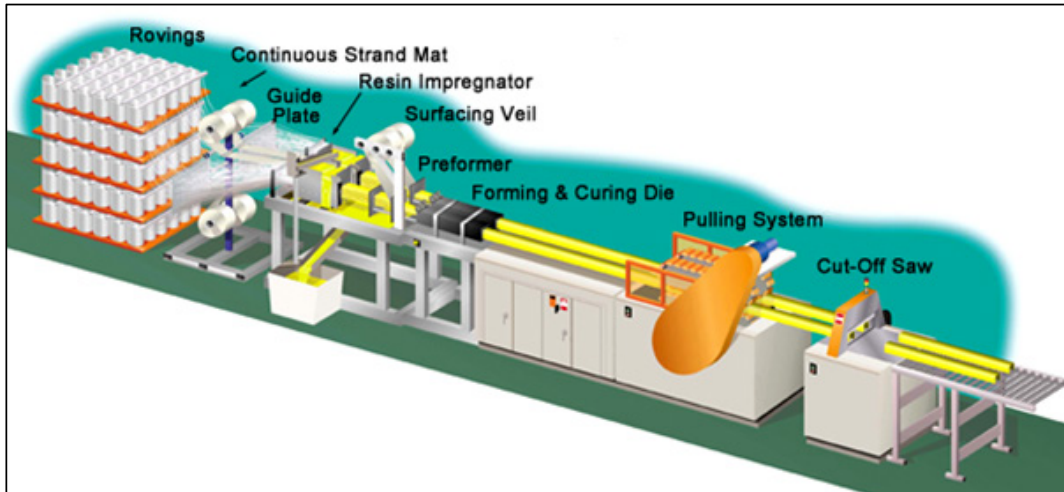


Figure 2.13 Pultrusion line (source: J&J Mechanic)

It is a low-cost, high-volume method to produce continuous lengths of reinforced plastic profiles of uniform cross sections with fibres aligned mainly along the longitudinal axis of the part. Pultrusion is ideally suited for customised shapes; some standard products include rods, bars, angles, tubes/channels, and I-beams. Normally a thermosetting resin such as polyester is used; however, it is also possible to use thermoplastics. The resin impregnation consists of a simple pull through a resin bath, see Figure 2.14, or by employing a pressure/vacuum impregnation device. The tension on the reinforcement material needs to be controlled as in filament winding.



Figure 2.14 Open-bath pultrusion forming (source: Martin Pultrusion)

Figure 2.15 shows the material layup in a channel section: **fibre roving** provides the high longitudinal strength in the product and also the tensile strength needed to pull the other reinforcements through the die; continuous **fibre mat** provides transverse mechanical properties, and the **resin** binds the composite together. Surfacing **veils** are non-woven materials, composed of uniformly distributed glass fibre strands or non-woven fabric of PET fibres that add reinforcement at the surface of a laminate and provide a smooth, resin-rich, durable surface. The veil surfaces improve the external appearance of the composite by blocking the fibre glass reinforcements close to the surface from striking through and affecting the surface appearance. The veil surfaces improve the external appearance of the composite by blocking the fibre glass reinforcements close to the surface from striking through and affecting the surface appearance. The use of veils may also improve weatherability and degradation resistance and increase die life.

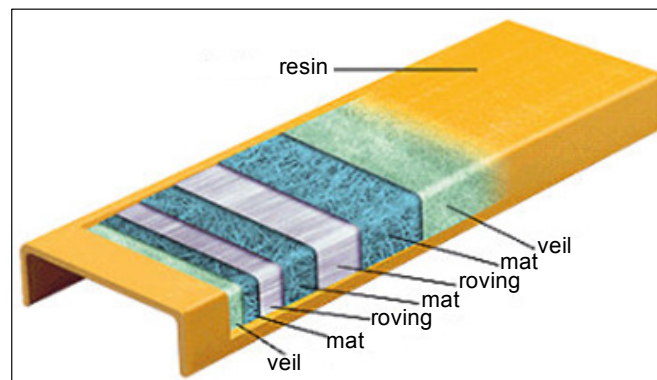


Figure 2.15 Layers across a pultruded profile (source: Iten Industries)

“I studied English for 16 years but...
...I finally learned to speak it in just six lessons”
Jane, Chinese architect

ENGLISH OUT THERE

Click to hear me talking before and after my unique course download

2.2.3 Liquid composites moulding

Processes that cut out the intermediate operation of prepreg manufacturing and bring together the matrix and fibre ingredients of a composite directly in the mould for producing the final shape of a part are known as liquid composites moulding (LCM). LCM processes include resin transfer moulding (RTM) or resin infusion such as liquid resin infusion (LRI), resin film infusion (RFI), Seeman Composites Resin Infusion Molding Process (SCRIMP), patented by TPI Technology, Inc.), resin infusion under flexible tooling (RIFT), vacuum-assisted resin injection system (VARI), used in the production of Lotus cars, vacuum-assisted resin transfer moulding (VARTM), etc. These processes, where liquid resin progresses through dry fibrous preforms, are developed as an alternative processing route to prepreg-based manufacturing.

2.2.3.1 Resin transfer moulding

In the resin transfer moulding process, the dry fibre preform is laid into the lower half of a matched mould. The mould is then closed and clamped, and resin is injected into the cavity. Catalyzed, low-viscosity resin is pumped in under pressure, displacing the air and forcing it out through the vent holes at the mould edges, until the mould is filled. In vacuum-assisted resin injection (VARI), vacuum is applied to the vent ports to assist in drawing the resin into the fibre preform and removing any trapped air, see Figure 2.16.

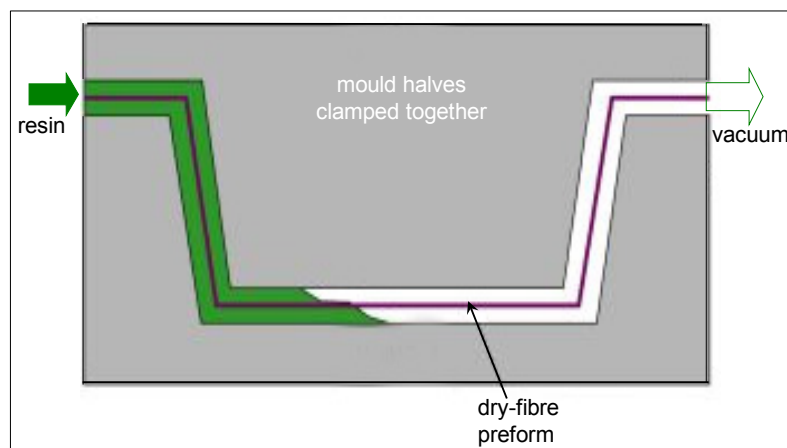


Figure 2.16 An illustration of RTM (source: SP Systems)

Thermosetting resins such as epoxy, polyester, vinylester and phenolics are generally used, although high temperature resins such as bismaleimides are also used, requiring higher process temperatures.

Moulds for this low-pressure production method are usually made from a fibre-reinforced plastic composite or a composite mould with a nickel-shell mould face. RTM parts, like compression moulded parts, have two finished surfaces, gel coats may be applied to the mould surface prior to moulding to provide a high-quality surface finish. Finished products by this method include automotive body parts, aircraft parts, bathtubs, and containers.

2.2.3.2 Liquid resin infusion moulding

Liquid resin infusion is a similar process to RTM, except only one side of the component has a moulded finish. Briefly, the process involves the placement of all the dry fibrous preforms together with cores (honeycomb cores to be avoided) or inserts in the mould, which are then vacuum bagged. The resin is drawn in by vacuum and gravity from its container into/over the distributor fabric/mesh placed over the top of the reinforcement lay-up/preform, which provides enhanced resin flow over the lay-up. This high permeability distributor fabric allows resin to seep into the lay-up by through-thickness flow, achieving full wet-out of the reinforcement (hence, using this method, the liquid has only to diffuse through the preform/lay-up thickness, not across the part width as in RTM), see Figures 2.17. Typical resins used are polyester, vinyl ester, and epoxy with many being UV cure initiated.

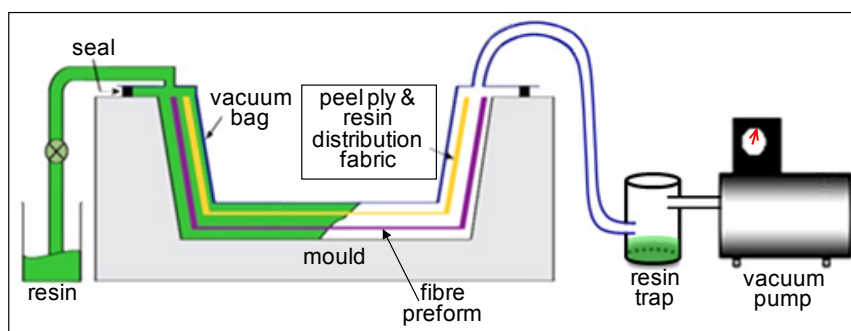


Figure 2.17 An illustration of RIFT process (source: Gurit Product Catalogue 2014, p. 75)

The resin infusion process only requires low resin pressure and the tooling is less expensive (only one side of the component has a moulded finish) than RTM rigid moulds, particularly as mouldings increase in size, tools become larger and mould clamping forces become excessive.

Many composite fabricators have recognised the advantages of the process and it is now successfully employed in a broad range of industries, including the marine, wind energy, automotive and aerospace sectors. However, the process produces only one moulded surface, large parts take a relatively long time to fill (Figure 2.18 shows an example of filling a plaque by the infusion process) and low resin viscosity means lower thermal and mechanical properties. On the other hand, compared with hand lay-up, the resin infusion process results in very low void content and excellent mechanical properties due to the relatively high fibre content, and this process is also more desirable environmentally and health and safety wise since there is no resin exposure.

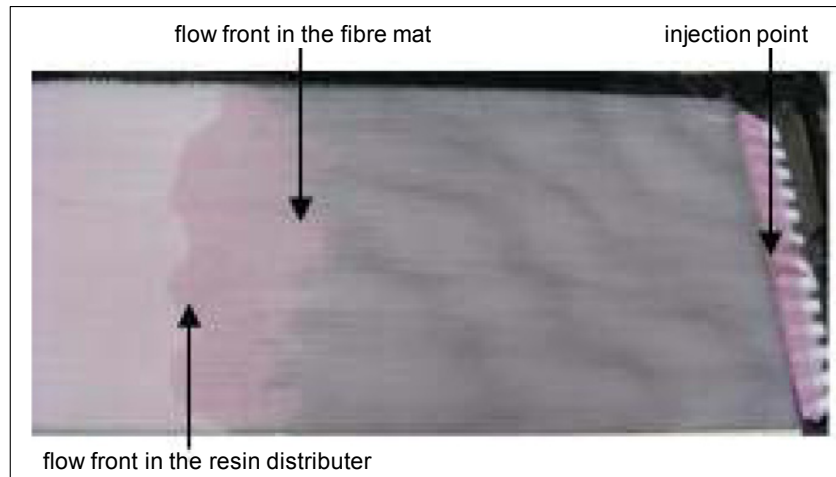


Figure 2.18 Resin infusion process (source: Visconti et al. 2006, p. 226)

Variations of RIFT technique include the Resin Infusion between Double Flexible Tooling (RIDFT), which is described by Thagard et al. (2004). In the RIDFT concept, the forming of the entire tooling and wetted reinforcements occurs together into the final part shape where it is then cured and removed as a finished part. The resin infusion and fibre wetting takes place within a double flexible vacuum bag that is initially a flat shape and then the entire wetted reinforcement and flexible tooling is shaped into a specified part by vacuum forming.

An advertisement for Duke University's Fuqua School of Business Global MBA program. The background is a grey world map. In the top left corner is the Duke University logo: "DUKE THE FUQUA SCHOOL OF BUSINESS". In the center, the text "BUSINESS HAPPENS" is written in large, black, sans-serif capital letters. Below this, the website "www.fuqua.duke.edu/globalmba" is displayed, with "globalmba" in blue. At the bottom left is an orange button with the text "Learn More >". On the right side, there is a circular collage of six diverse people's faces. In the center of this collage, the word "HERE." is written in large, bold, black, sans-serif capital letters.

In the RIFT process, instead of liquid resin, partially cured resin (B-stage) in film form can also be used as matrix. Sheets of resin film are interleaved with the dry fibre layers into a stack to be processed, see Figure 2.19.

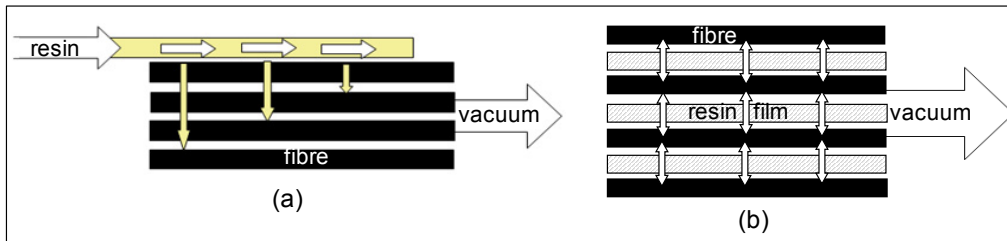


Figure 2.19 Schematic representation of (a) the liquid resin infusion along the distributor medium and down the fibrous preform, (b) the resin film infusion process [note that the bagging film (above) and mould tool (below) are omitted for clarity] (source: Summerscales et al. 2005)

2.2.4 Reinforced reaction injection moulding

Reinforced reaction injection moulding (RRIM) is a variant of reaction injection moulding (RIM). A dispensing machine is employed for the process where the components (parts) of a rapid curing resin system are combined and mixed together, then injected into a mould cavity. The resin rapidly reacts and cures to form a solid polymer. Mixing of the component materials involves either mechanical mixing or high-speed impingement immediately before dispensing the mixture. The mixing head needs to be flushed with a suitable solvent to avoid clogging. Figures 2.20 and 2.21 show aspects of a resin dispensing system employed in RIM processes.

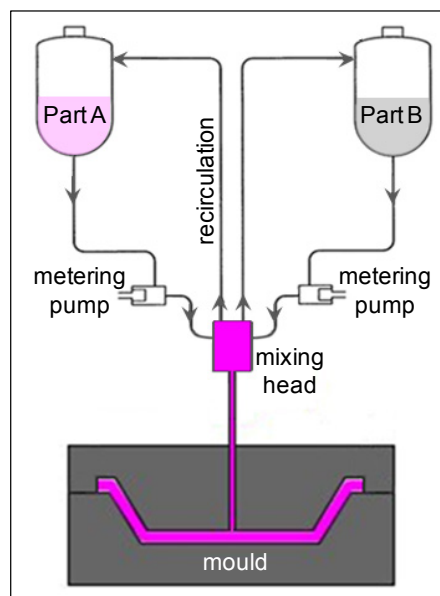


Figure 2.20 An illustration of the principles of RIM process

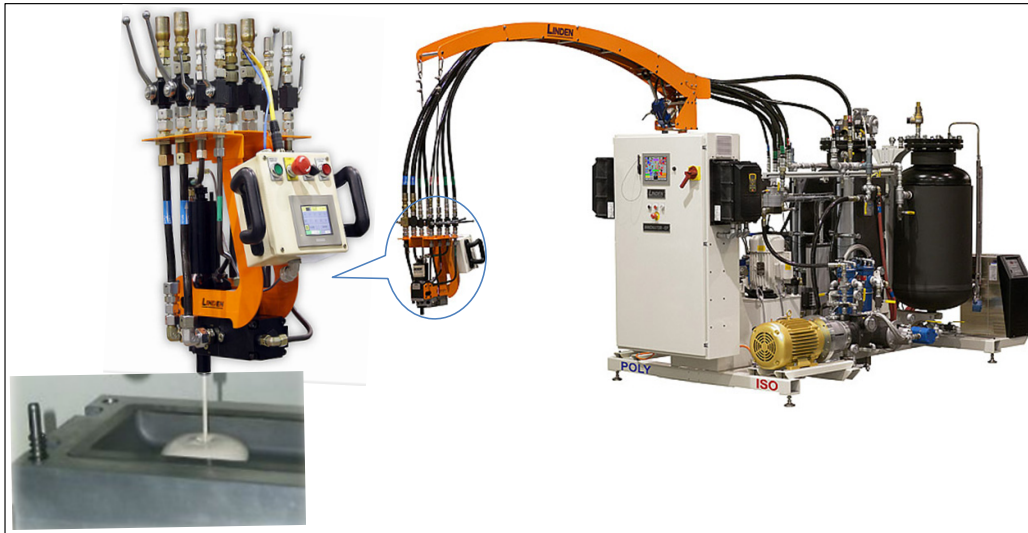


Figure 2.21 A dispensing unit with its magnified mixing head for polyurethane RIMs (source: Linden Industries)

Polyurethanes (produced by combining polyols and isocyanates) and nylon 6 (by monomer casting and anionic polymerisation at relatively low temperatures, about 100°C, provide fast moulding cycles well suited for automotive and furniture applications). Common RIM parts include automotive bumpers, fender and panel components, appliance housings, and furniture items.

Join American online LIGS University!

Interactive Online programs
BBA, MBA, MSc, DBA and PhD

Special Christmas offer:

- ▶ enroll **by December 18th, 2014**
- ▶ **start studying and paying only in 2015**
- ▶ **save up to \$ 1,200** on the tuition!
- ▶ Interactive Online education
- ▶ visit ligsuniversity.com to find out more!

Note: LIGS University is not accredited by any nationally recognized accrediting agency listed by the US Secretary of Education. More info [here](#).



In RRIM, the fibres are either placed within a closed mould as preform prior to resin injection or added as chopped short fibres to resin to form slurry before injection. When short fibres or flakes are mixed with resin prior to injection to produce a relatively uniform/isotropic product, the process is called RRIM, however, where a preform or reinforcing mat is placed into the mould and then resin injected, the process is called structural reaction injection moulding (SRIM or SRRIM).

2.2.5 Injection moulding

A normal injection moulding machine, described elsewhere (Akay 2012, p. 60), is used for moulding fibre reinforced thermoplastic granules/pellets. These feed stocks are identified as short-fibre reinforced thermoplastics (SFT) and long-fibre reinforced thermoplastics (LFT), see Figure 2.22. The fibre lengths, in granules/pellets, are normally less than 1 mm for SFTs, and typically 10 mm long for LFTs such as “Verton”. Reinforcing levels range from 10 to 70% by weight. Production of “Verton” is by a pultrusion process (by passing continuous fibres through a die where impregnation with molten polymer occurs and the cooled/solidified pultruded rod is cut into pellets at the end of the pultrusion line), rather than extrusion compounding. Polymers used include nylon 6,6, polycarbonate, polyester, polypropylene, polystyrene, PEEK, etc. LFTs have become well established over the recent years as engineering materials for structural applications, particularly in the automotive industry, offering weight reduction (therefore fuel economy), high volume of productivity, damping ability (attenuates noise and vibrations/shocks), parts reduction/consolidation and economic benefits. Furthermore, in view of the end-of-life vehicle (ELV) EU directive, the ease of recycling of LFT (compared with fibre reinforced thermoset matrices) is also becoming an increasingly important factor.



Figure 2.22 Granules/pellets of SFT and LFT

Processing of fibre containing granules, in comparison with the unfilled grades, needs to be controlled to avoid fibre degradation (e.g. lower injection back pressure, typically 25–50 psi (0.17–0.34 MPa), and screw rotational speeds, 30–70 rpm should be used). Feed throat from hopper to machine must have sufficient opening to prevent bridging of long pellets, or the hopper should be fitted with a vibrator. Normally, reinforced materials require higher mould temperatures than non-reinforced materials. This helps achieve a smoother, more blemish free surface by providing a resin rich skin on the moulded part. Tooling considerations include adopting short sprues, round runners with no sharp corners and minimum gate thickness of 2 mm.

The properties are mainly dictated by fibre content, fibre length (fibre degradation during processing can result in sharply reduced mechanical properties) and fibre orientation distributions. Fibre orientation in injection moulded fibre reinforced thermoplastics is a function of the melt flow pattern and also the drag between the flowing melt and the mould surfaces (e.g. shearing flow between the faster moving core region and nearly solidified skin). The resultant fibre orientation is a complex one, however, in a flat plaque moulding there are distinct skin/surface and core layers, see Figure 2.23. The orientation is predominantly longitudinal to the melt-fill direction in the surface and transverse in the core. Such anisotropy in fibre orientation results in anisotropic mechanical behaviour of the mouldings.

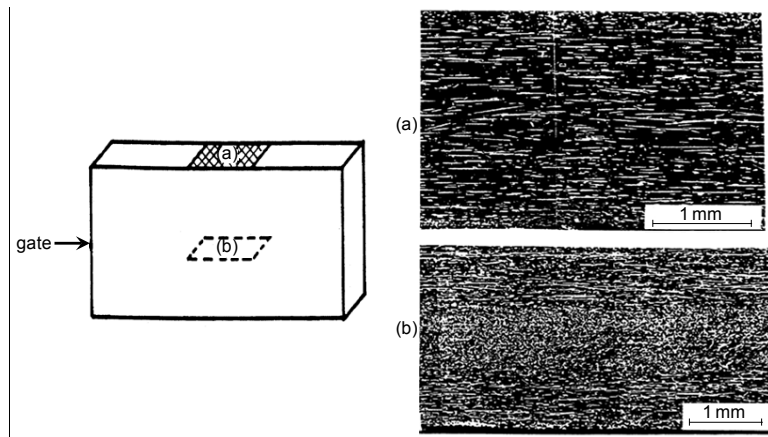


Figure 2.23 SEM micrographs showing tiers of fibre orientation through the thickness of an injection moulded plaque at locations (a) and (b). Material is glass-fibre/polyamide (source: Akay & Barkley 1991)







#gobeyond

MASTER IN MANAGEMENT

Because achieving your dreams is your greatest challenge. IE Business School's Master in Management taught in English, Spanish or bilingually, trains young high performance professionals at the beginning of their career through an innovative and stimulating program that will help them reach their full potential.

- Choose your area of specialization.
- Customize your master through the different options offered.
- Global Immersion Weeks in locations such as Rio de Janeiro, Shanghai or San Francisco.

Because you change, we change with you.

www.ie.edu/master-management

mim.admissions@ie.edu





Shear Controlled Orientation Technology (SCORTEC) developed at Brunel University to control orientation in injection moulded and extruded short fibre composites: shear-controlled orientation in injection moulding (SCORIM), which is also referred to as multi-live feed injection moulding or push-pull injection moulding, and shear-controlled orientation in extrusion (SCOREX). These are melt oscillation techniques that create uniform alignment of fibres in the direction of melt fill. Other improvements are claimed to be minimisation of weld-line effects, sink marks and voids, and greater dimensional stability. For further information on the subject refer to Avery (1998, p. 138).

Injection moulding of thermosetting plastics, sometimes known as direct screw transfer, is very similar to the injection moulding of thermoplastics except that the plasticisation is achieved at low temperature (60–95°C) and the curing occurs in the mould, which is at a temperature that produces rapid cross-linking (150–200°C). The material remains in the mould until it is cured sufficiently to be stable in shape (i.e. has green strength), when it can be demoulded although still hot.

The main difference between the moulding machines for thermoplastics (TPs) and the thermosetting plastics (TSs) is the design of the screw: in injection of TPs, the screw exerts significant compression on the melt along the barrel, whereas for TSs the screw has a compression ratio of nearly one (the ratio of the feed zone channel depth to the meter zone channel depth, with a value of about 3 for general purpose screws to process TPs) in order to avoid shear heating of the resin, causing premature curing in the barrel. Similarly, any other components/features, such as the check rings, that can restrict resin flow and cause resin stagnation should be avoided with TSs.

The resin incorporated with filler (e.g. glass fibre, wood flour cotton flock, talc, etc.) and additives (e.g. curing agents, inhibitors, stabilisers, colourants, etc.) is partially polymerised and formed into granules for moulding purposes. The resin would have long shelf life if stored under appropriate conditions. The most commonly used resins are phenolics, and others that are employed to various extents include melamines, polyesters, silicones and epoxies. Some of these resins are specifically formulated/developed for injection moulding. For injection moulding, the fibre reinforced thermosets should flow easily at the barrel temperature without curing and/or separating into resin, fibre and filler components, and should cure rapidly at the mould temperature. Refer to Chanda & Roy (2007, p. 2–21) for further information on this subject.

To select the best composite fabrication process (Miracle & Donaldson 2001, p. 11), the designer generally chooses the process that will provide an acceptable-quality component for the lowest cost. In evaluating cost and quality, however, tooling cost, production rate, materials cost, desired part finish, and many other factors (e.g. safety, health and environment) must be considered. Only after considering all the pertinent factors that the fabrication method (or the material) should be selected.

2.3 Wood-plastic composites

WRAP (Waste and Resources Action Programme) (U.K.) had developed a number of targets for plastic and wood recycling to be achieved in 2004. One such target was to identify at least one new technology to produce a composite product using recycled polymer resins with wood. To meet this objective and to assist the wood programme target of identifying new end markets, WRAP commissioned Optimat Ltd in partnership with MERL to conduct a study (WRAP 2003) of wood plastic composites (WPCs).

Wood-plastic composite refers to any material that contains wood and thermosetting or thermoplastic polymers. Thermosets include resins such as epoxies and phenolics. Thermoplastics include polymers such as polyethylenes, polypropylene and polyvinyl chloride. WPCs extend the concept of “wood composites” beyond the traditional compressed materials such as particleboard and medium density fibre board, and lend themselves to be processed with the familiar, mass production, polymer processing equipment of extrusion and injection moulding.

The main constituents of WPC are wood flour, thermoplastics, all PE grades, PP and PVC, and various additives such as lubricants/processing aids, antioxidants, UV absorbers, coupling agents/compatibilisers and impact modifiers. WPCs typically contain 30% to 60% wood filler (mainly in the form of approximately 40 mesh (i.e. 40 openings per inch) wood floor) (reported by Forest Products Laboratory). Most WPCs are made with polyethylenes (approximately 80%), mainly high-density polyethylene (HDPE), both virgin and recycled, for use in exterior building components, however, some WPCs are also made from polypropylene and polyvinyl chloride (approximately 10% each). Because of the limited thermal stability of wood only the thermoplastics with melting points not greater than 200°C are normally used in WPCs.

Coupling agents are especially valuable in polyolefin WPCs because they overcome the incompatibility between the polar wood chemistry and nonpolar resin matrix. These include chemically modified (usually maleated) polyolefins made by grafting maleic anhydride onto the polymer backbone through reactive extrusion. Newer developments include chemically modified polyolefins, such as maleated HDPE, long-chain chlorinated paraffin, or treatment of the wood fibres with a sizing stabilizer to act as a compatibiliser before compounding.

Lubricants increase throughput and improve WPC surface appearance. WPCs can use standard lubricants for polyolefins and PVC, such as ethylene bis-stearamide (EBS), zinc stearate, paraffin waxes, and oxidized PE. EBS with zinc stearate is widely used in wood-HDPE. However, there are new alternatives because metal stearates are known (Sherman 2004) to decouple the maleic anhydride of maleated coupling agents, cancelling the effectiveness of both lubricant and coupling agent. Alternative lubricants have been developed that contain no metallic stearates.

Adding wood fibres to commodity plastics such as polyethylenes and polypropylene increases their density. The density of the wood cell wall is about 1.44–1.50 g/cm³, the porous anatomy of solid wood results in overall densities of about 0.32–0.72 g/cm³ when dry. Wood flour is compressible and as filler the degree of collapsing or filling will depend on variables such as particle size, processing method and melt/additive viscosity. In composites wood densities approaching the wood-cell wall density can be found, particularly, in high-pressure processes such as injection moulding.

Industrial applications of lignocellulosic filled thermoplastics go back to the late 1960s, and in the 1990s the industrial production of wood filled thermoplastic polymers became more wide spread (Gardner & Murdock). WPCs lend themselves to be manufactured using conventional polymer processing techniques such as extrusion and injection moulding. One of the largest segments (80%) of the wood filled thermoplastic industry concentrates on the production of wood plastic composite decking and railings as a replacement for preservative treated wood and the more expensive durable wood species such as redwood and teak. Other common applications include exterior building and construction panels/claddings and outdoor furniture items. Some of the positive attributes of wood filled plastic composite lumber compared with wood is its durability, low maintenance, no painting, insect and decay resistance, and it will not warp, splinter or crack, is denser and thus holds screws better, and can be manufactured to be resistant to ultraviolet light.

SMS from your computer
...Sync'd with your Android phone & number

FREE
30 days trial!

Go to
BrowserTexting.com

and start texting from
your computer!

BrowserTexting

The advertisement features a laptop on the left displaying a web interface with a list of contacts and a text message conversation. A blue double-headed arrow connects the laptop to an HTC smartphone on the right, which also displays a text message conversation. The background is a light blue gradient with a dark blue diagonal banner in the top right corner.

Recent market trends as well as technology trends are covered by Gardner et al. (2008): highlighting the advantages of WPC technology as being weight reduction of the products and enhancement of mechanical properties for structural uses (e.g. by using engineering plastics such as PET, Nylon 66 and ABS). Several strategies have been described to overcome the thermal degradation risk of the wood when being processed at high processing temperatures with high melting point/plasticising temperature (230–270°C) engineering plastics.

2.3.1 Extrusion of WPC boards

The processes that can be used in the manufacture of WPC products are compounding, extrusion, injection moulding and pultrusion. Compounding produces wood composite pellets for processors who do not want to blend their own material and just use a single screw extruder for production rather than invest in a compounding extruder. However for significant volumes of production it may be more economic to compound in-house.

Compounding involves melting the plastic and blending in the wood. In a properly compounded WPC, the individual wood particles are thoroughly mixed throughout a continuous plastic matrix. Each individual wood particle should be completely encapsulated by plastic with no fibre-to-fibre contact. On a compounding extrusion line, the molten wood-plastic mixture is then converted into products such as decking boards.

The process of **twin screw extrusion** will be expanded upon here. The process is normally used to both compound and manufacture WPC products. The machines can be co-rotating or counter-rotating twin-screw extruders. The counter rotating system is more commonly used for producing wood composite profiles. Rauwendaal (1981) concluded that the co-rotating extruder appears to be best suited for melt blending operations, while the counter-rotating extruder seems to be preferred in operations where solid fillers are dispersed in a polymer matrix. WRAP Report (2003) compares different extrusion systems, including conical and parallel twin screw designs.

The Weber website lists the advantages of counter-rotating twin screw extruders, which includes:

- low shear rates and comparably moderate melt temperatures
- high torque
- degassing option (a requirement in WPC)
- self-cleaning and therefore narrow range of dwell time distribution
- high pressure build up capacity with low increase in temperature (important in WPC, high temperatures degrade wood flour)
- many different types of materials can be processed (dry blend, compounds, pellets etc.)
- high output consistency throughout the whole speed range due to system force feed.

Elements of a typical twin screw compounding and profiling extrusion line is shown in Figure 2.24.

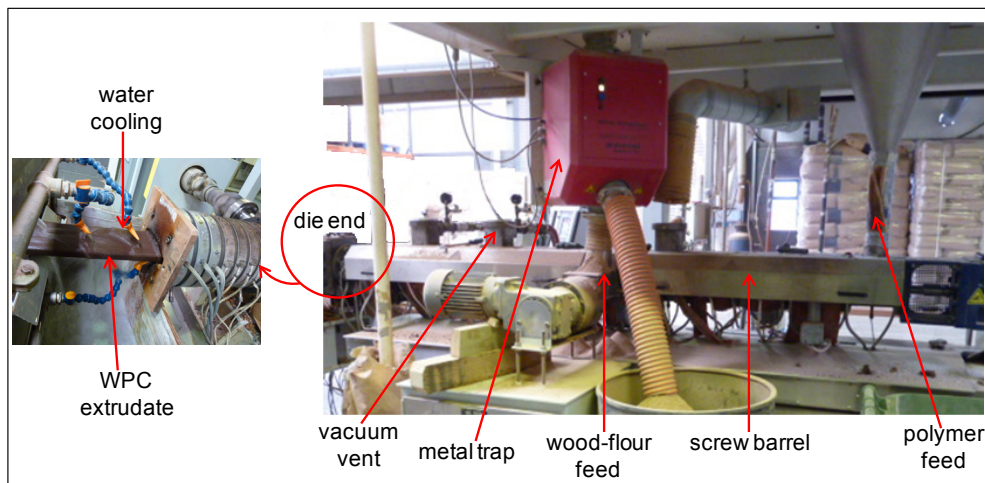


Figure 2.24 Features of a WPC extruder

It is important that the water content of the wood flour stock used in production is controlled: if it is too high then the fibres are attracted to each other rather than the polymer and resist dispersion, the moisture in the wood flour also reacts with the coupling agent and reduces the amount available to bond fibres to the polymer. Normally maleic anhydride coupling agent reacts with the hydroxyl polar groups in wood and forms strong covalent ester bonds. The wood flour needs to be dried before processing in order to achieve good bonding between wood and polymer. The levels of drying recommended include weight % moisture contents of less than 0.5% (Sherman 2004), less than 1% (Gardner and Murdock) and around 2% moisture content or less by Chelsea Center for Recycling and Economic Development (2000) to facilitate adequate mixing with the polymer. The drying of the wood flour is potentially the most dangerous part of the WPC processing.

It is also vital that the plastic used is clean and free of any non-plastic contaminant. This excludes a number of waste streams such as post-consumer waste and waste plastic from end-of-life vehicles, which can contain various types of plastics and be contaminated with metal clips, nails, etc. Some composites, however, can accommodate a small amount of waste paper. The amount of paper must be very consistent and should be within the limits of 5%–8% (Chelsea Center for Recycling and Economic Development (2000)). The main polymer used in the manufacture of WPC boards is recycled LDPE and HDPE. Presence of any higher melting point polymer regrinds in the feed stock, if unplasticised during processing and not filtered by the screen pack/breaker plate, would remain as inclusion in the product, see Figure 2.25.

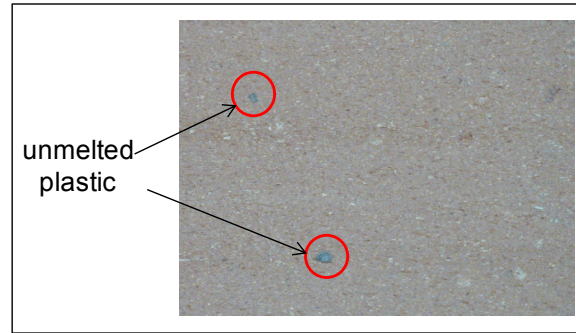


Figure 2.25 Unmelted regrind plastic in extrudate

The extruder screws are modular, allowing different elements/segments and screw geometries to be assembled to accomplish the required mixing for a given production. Screw elements that are used in twin-screw extruders include several types of conveying, kneading and mixing elements. Conveying elements with low pitch length (restrictive elements) are used at the end of the melting zone to work the material, generating higher shear heat to enhance melting. These elements (Figures 2.26) often supplied as individual pieces provide flexibility in configuring a screw. Kneading blocks perform both distributive and dispersive mixing depending on the number of elements in a block of a given length and the widths of the individual elements (disks): higher numbers increase distributive mixing and so do the narrow disks but the wider disks provide better dispersive mixing. These topics are covered in greater detail by Giles et al. (2005) and Chung (2000).

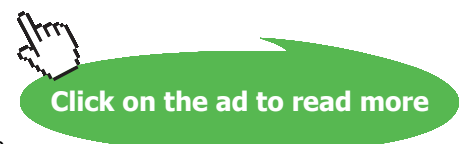
The Wake

the only emission we want to leave behind

Low-speed Engines Medium-speed Engines Turbochargers Propellers Propulsion Packages PrimeServ

The design of eco-friendly marine power and propulsion solutions is crucial for MAN Diesel & Turbo. Power competencies are offered with the world's largest engine programme – having outputs spanning from 450 to 87,220 kW per engine. Get up front!
Find out more at www.mandieselturbo.com

Engineering the Future – since 1758.
MAN Diesel & Turbo



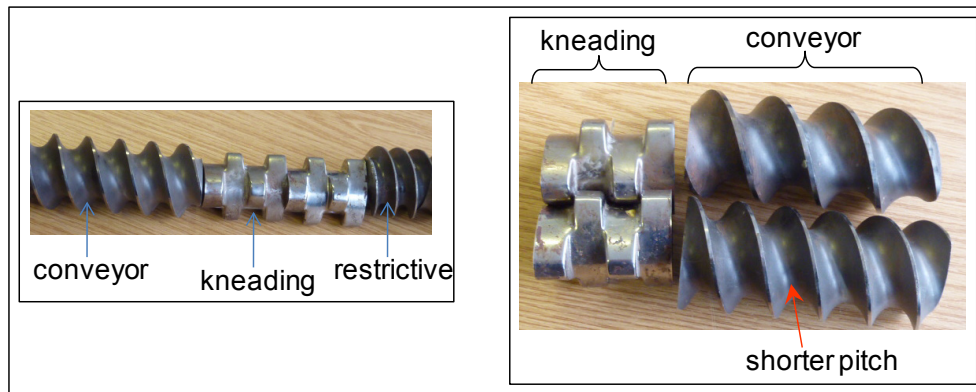


Figure 2.26 Examples of different screw elements

Mixing elements contain cut-outs and are designed to convey material forward in the barrel, while dividing and recombining the melt stream to provide mainly distributive mixing. They can suffer excessive wear, see Figure 2.27, and with some material mixes, e.g. wood flour and a polymer, this may happen in a short period of time and therefore needs to be regularly monitored to ensure proper mixing.



Figure 2.27 Photographs of a new and a worn-out mixing element

Poorly distributed wood fibres, called “wood spots” (Hanawalt 2012) are a common quality problem when the wood contains excessive fines or when the extruder is too worn to achieve good mixing. Figure 2.28 shows a clear example of agglomerated wood flour as a result of poor mixing.



Figure 2.28 Photograph of wood flour scooped out of a “wood spot”

The raw material is loaded to an extruder by gravimetric feeders and twin-screw side feeders. In some compounding extruders, the plastic and wood are fed simultaneously into the extruder. In others, the wood is fed downstream after the plastic has been melted as shown in Figure 2.24.

Since wood flour or fibre is a low bulk density material, an extra feeder is used to force it into the extruder. These feeders are known as a “crammer” or “side-stuffer”.

In either case, after the plastic has been melted (by heating the extruder barrel and by heat generated through the screw action) and the wood thoroughly mixed-in, moisture removal can take place. Moisture removal is accomplished through the use of atmospheric and vacuum vents. Water vapour and any other gaseous matter are sucked out by a vacuum pump. The vacuum-vent opening houses a vertical auger, a short screw, to force the wood flour that goes up to the vent back into the barrel to minimise its loss. After mixing and moisture removal, the compound can be pumped through a strand die for pelletizing or can be extruded through a profile die directly into products, as demonstrated here. In counter-rotating extrusion additional discharge equipment (e.g. melt pump) is required to pump the material through the die.

The extrudate produced is water cooled and cut to length and processed further as required. Figure 2.29 shows the extrusion of board, e.g. for decking, and its on-line cutting, sanding and moulding/profiling. The surface roughening and profiling helps prevent slip and improve grip in applications such as decking. Moulding also serves a decorative purpose. Figure 2.30 shows the rotary profile cutter employed.

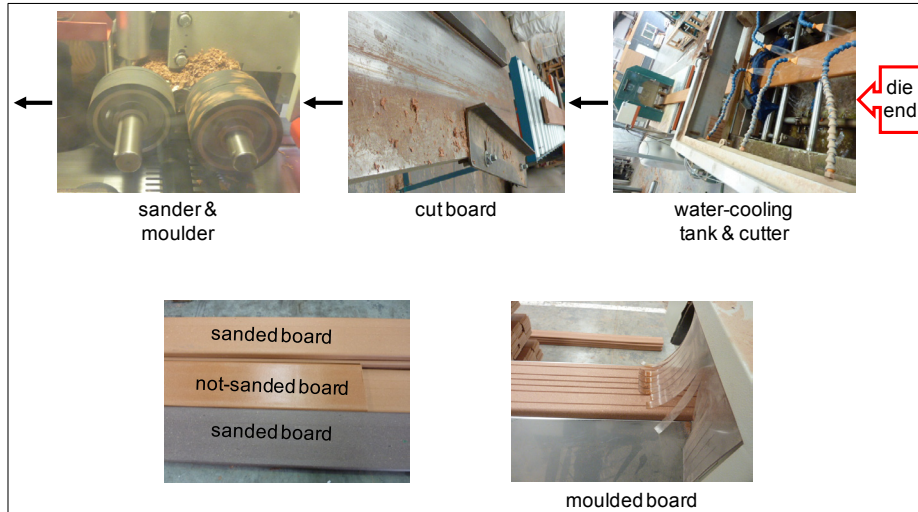


Figure 2.29 Post-extrusion cooling, cutting, sanding and moulding operations

TURN TO THE EXPERTS FOR **SUBSCRIBE** CONSULTANCY

Subscribe is one of the leading companies in Europe when it comes to innovation and business development within subscription businesses.

We innovate new subscription business models or improve existing ones. We do business reviews of existing subscription businesses and we develop acquisition and retention strategies.

Learn more at [linkedin.com/company/subscribe](https://www.linkedin.com/company/subscribe) or contact Managing Director Morten Suhr Hansen at mha@subscribe.dk

SUBSCRIBE - to the future



Figure 2.30 The rotary profile/moulding cutter

WPC production generates significant scrap, which can be regranulated and added to the feedstock as regrind. A typical granulator is shown in Figure 2.31. A granulator has a rotary knife that cuts the solid waste into sufficiently small pieces so the granules will pass through holes in a screen and exit the machine. Most regrind is granulated so that it passes through an approximately 10 mm screen. Screen sizes range from 6 to 14 mm: smaller screens slow down the throughput of the granulator, and therefore affect the cost.



Figure 2.31 Photographs of a WPC granulator

2.4 Other processing considerations

2.4.1 Machining of composites

The following properties/factors should be taken into account when machining composites:

- material heterogeneity in composition and anisotropy in structure, similar to wood
- low heat dissipation
- low coefficient of thermal expansion: hot tool expands more rapidly than the work-piece
- fibre-composite materials wear out cutting tools more rapidly than traditional engineering materials. The tools need to be tipped with hard wearing abrasive substances as in diamond-tipped tools/bits
- tool durability and initial cost: high speed steel, carbide, boron nitride or polycrystalline diamond
- more expensive cutting tools may be cost-effective when costs are calculated over tool-life time, and produce better surface finish.

Composites machining is dusty, messy and hard on tools. Glass fibre is more abrasive than carbon, which causes tools to wear faster, and carbon fibre is more brittle than glass fibre and generates a finer dust that can pose larger cleaning issues. Machinery needs to be cleaned of the cutting debris regularly in order to avoid damage to the equipment: items such as filters on the electronics cabinets need to be changed frequently.

For reasons of health and safety, it is also essential to minimise dust and decomposition products that arise from machining by extraction at source, or entrapment in a stream of gas or water. In most operations the dust is released in a finite area and can be collected by a vacuum system. However the operator must always wear recommended personal protective equipment such as a dust mask, gloves (cut edges can be very sharp) and ear plugs during the machining operations of composite materials.

A suitable coolant will be used for high-heat cutting operations to reduce the chance of degrading the resin in the part, which also keeps cutting tool edge temperatures under control and prevents the removal of diamond or carbide coating from the tool's substrate.

There are various ways of machining composites either manually or on computer numerical control (CNC) machine tools. Milling machines, saws (e.g. using diamond-tipped rotary wheels, see Figure 2.32) or diamond impregnated stainless steel wire), drills and lathes are some of the most common machines that use mechanical shear as the primary method of material removal. Other methods include water-jet cutting and laser cutting. Some of these techniques are detailed in the text book by Strong (2008 p. 367):

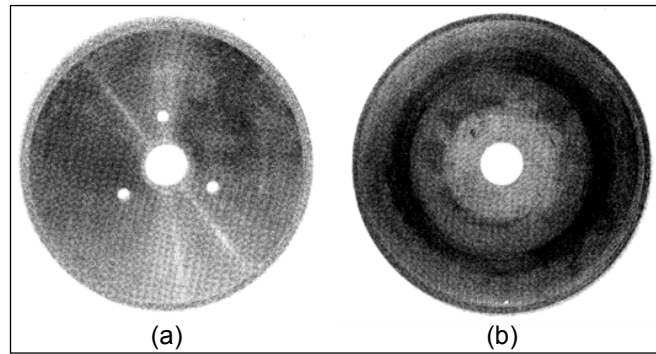


Figure 2.32 Diamond-tipped rotary wheels: (a) fresh tip, (b) worn tip

In **laser cutting** the beam is focused onto the workpiece and melts/burns the material away. There is no cutting force; therefore it is suitable for cutting fragile pieces. Collimation of the beam enables holes to be drilled that are too small to be drilled mechanically, e.g. in the manufacture of printed circuit boards. The thermal effects can be problematic: in some cases, for instance, it is difficult to remove the burnt material, which may remain in the cut, dissipate the incoming light energy and block further cutting. Cutting speeds depend on workpiece thickness, type of material, and the power of the laser. Typical values are 0.5 to 3 m/min. Carbon fibre composites are difficult to machine with lasers because of their thermal conductivity, aramid composites are easily machined with lasers and glass fibre composites yield an intermediate outcome.

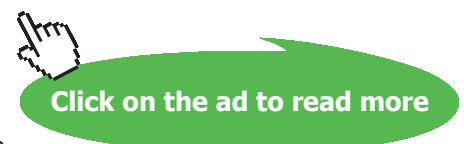
wethrive.net

How to retain your top staff
FIND OUT NOW FOR FREE

DO YOU WANT TO KNOW:

- What your staff really want?
- The top issues troubling them?
- How to make staff assessments work for you & them, painlessly?

Get your free trial
Because happy staff get more done



In **diamond wire cutting**, the diamond-impregnated wire moves to and fro (a sawing action) over the surface to be cut. It is a relatively slow process, but the temperature rise at the cut is only a few degrees. The kerf (material lost in making the cut) is typically 10% greater than the diameter of the wire.

Water-jet cutting: a high pressure water jet either by itself or mixed with an abrasive grit, e.g. garnet, is used as the source of energy (hydromechanical) for machining. The method is suitable for materials ranging from soft rubber to tool steel. Water, pressurised to about 300 MPa using a water pump, is mixed with grit and passes through a nozzle of tungsten carbide (approximately 0.8 mm diameter) at a flow speed of 850 m/s. In order to avoid delamination in cutting composite laminates, a hole is mechanically drilled at a corner of the work-piece and the water jet is applied starting from the drilled hole and then moved to the desired area.

Waterjet cutting produces less cutting force than most of the mechanical methods, can dwell in one spot for some time without widening the cut width and generally requires only clamping to support the part. The cut is approximately $0.5\text{--}2.5 \pm 0.4$ mm wide and tapered. The cutting speed is controlled by back pressure sensed from the resistance to the water jet and depends on the thickness of the work-piece and the type of material being cut, typically ranging from 1.5 m/min for 25 mm to 18 m/min for 3 mm thick parts for composite laminates. The quality of the cut depends on the hardness and strength of the fibres, for example, the cut is much rougher with boron fibres than with softer aramid fibres. With some demanding jobs such as thick steel, the jet will operate as a hammer drill until the water jet is through the material and then moves on.

When abrasives such as garnet are entrained in the water stream, the jet becomes powerful enough to cut through 4" (≈ 100 mm) thick carbon-fibre/epoxy or magnesium boron carbide without creating heat-affected zones. The thickness of the work-piece depends on the softness or hardness of the material being cut as well as the finish desired. Soft materials are cut with water only, while hard materials require a stream of water mixed with fine grains of abrasive garnet.

Some applications in waterjet cutting are involved with hollow structures. The hollow space tends to disperse the jet and not produce desirable results. The cutting stream does not remain cohesive after cutting through the upper layer, causing a poor edge quality on the next layer(s).

Water absorption by the part may be an issue, especially for materials with weak fibre-matrix interfaces and for composites with aramid fibres, more so under high waterjet pressures. The waterjet cutting process is quite noisy and requires ear protection, and the water requires good filtration to minimise jet wear.

Waterjet cutting has been compared with other techniques, for example, Sloan (2010) has compared it with rotary tool cutting, Shanmugam et al. (2002) have compared it with laser cutting as well as comparing plain waterjet cutting with abrasive waterjet cutting.

The abrasive waterjet doesn't create damaging heat in the cutting process unlike lasers. The abrasive waterjet outperforms routers when finishing carbon or graphite fibre epoxy structures: the abrasive waterjet's light and compact cutting head fits in spaces inaccessible to the router, waterjets will not cause cracking, fraying or delamination. Additionally, waterjets do not require an operator to focus on feed rates.

2.4.2 Joining of composites

Parts are assembled together by joining to produce a larger size, a complex geometry or a hybrid structure with different materials. Composites may be joined by mechanical means, i.e. bolting and riveting, chemically, i.e. by adhesive bonding, or by one of many welding techniques.

2.4.2.1 Mechanical joining

The common mechanical-joint designs are shown in Figure 2.33. The straight lap joint is the simplest but it is non-symmetric and therefore the joint is always subject to shear forces when mechanically loaded. The other designs produce joints that are less prone to shear, but require the use of more material.

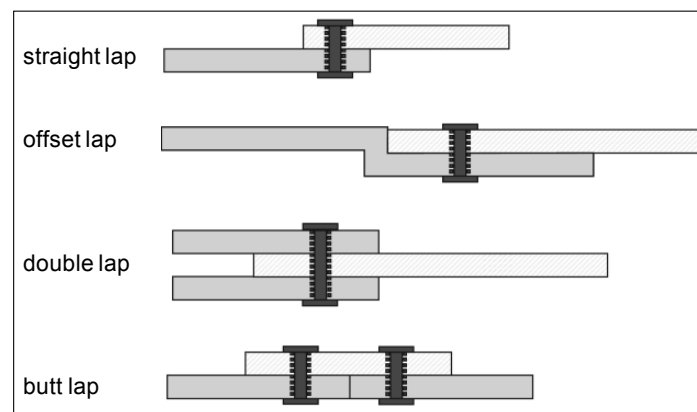


Figure 2.33 Mechanical joint designs (source: Strong (2008, p. 360))

Other factors to consider besides the type of joint include the lay-up of the composite laminate, fastening composites to other materials, size and geometry of the joint and the level of tightening of the joint. Drilling damages composites. Special drill bits designed for composites should be used to minimize heating of the matrix and fraying of the fibres. A modified high-speed steel drill bit used in machining Kevlar is shown in Figure 2.34. It provides three sharp contact points and the specimens were drilled at 2400 rev/min on a backing of 25 Shore D rubber to avoid fraying at the cut edges (Akay& Mun 1995). Using woven fabrics as the innermost and outermost plies also reduces drilling damage.

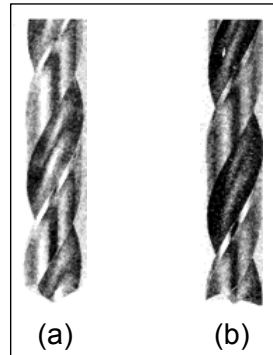


Figure 2.34 Drill bits: (a) standard, (b) modified

The type of material used in the joint is important, particularly in joining carbon fibre composites. Carbon fibre is electrically conductive and forms galvanic cells with metals, leading to galvanic corrosion with certain metals such as aluminium (C and Al are at opposite ends of the electrochemical series), much less of a concern with titanium and nickel. This can be prevented by inserting a thin glass-fibre composite layer in the joint to separate the carbon-fibre composite and metal parts.

Typical failure modes at a mechanical joint include: pin bearing, shear-out, cleavage, tension or a combination of these, and direct failure of substrate or fastener material. The level of tightening (torque) applies compressive stress in the unreinforced direction of the laminate and can cause surface crushing of the materials joined together and/or change the nature of stresses generated on the joint. However, in properly tightened fasteners premature failure due to localised composite delamination or fibre disintegration into fibrils ('brooming') is avoided and the bearing strength of composites significantly increases, see Figure 2.35. Quasi-isotropic layups provide the highest pin-bearing strength.

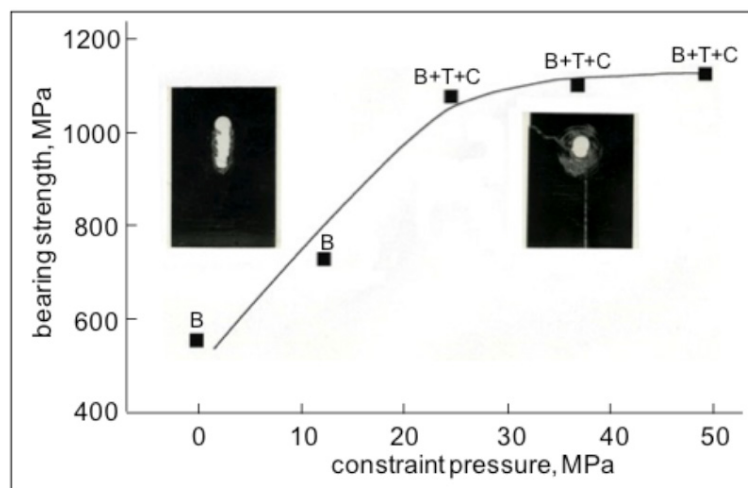
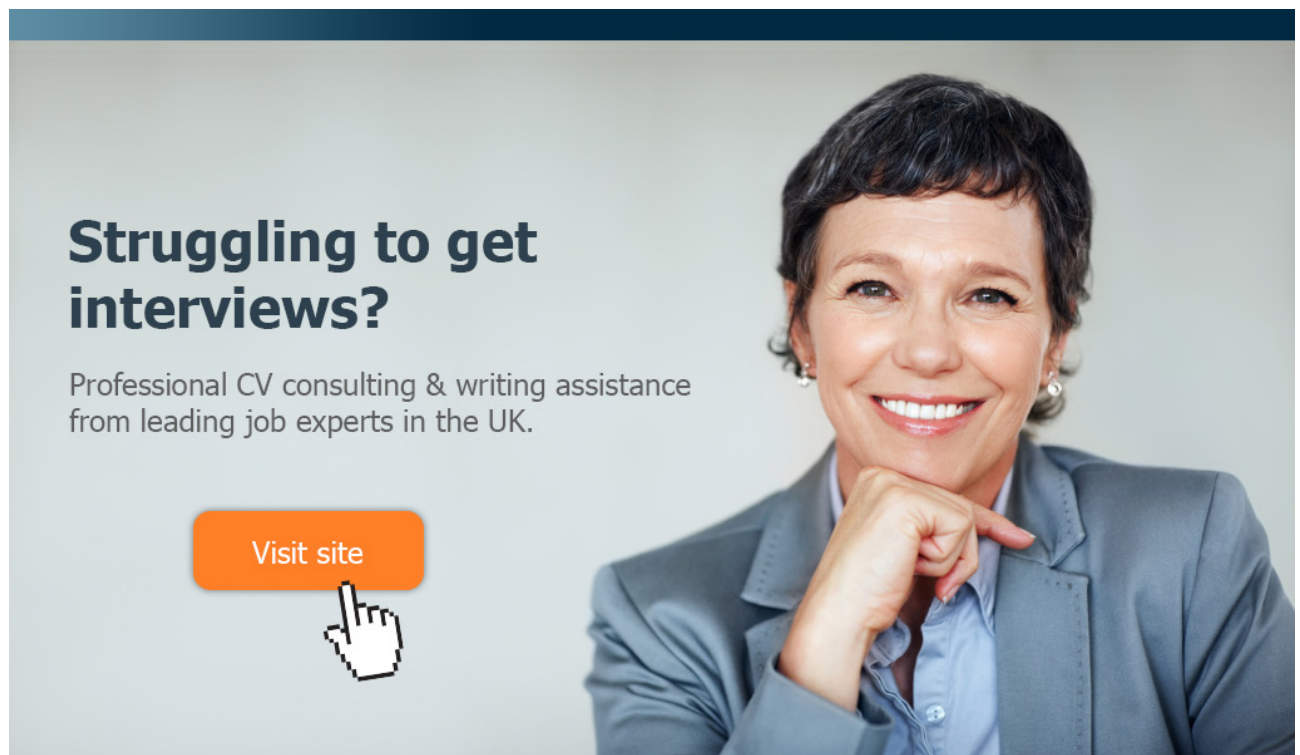


Figure 2.35 Bearing strength vs. constraint pressure for a CF/epoxy resin composite system with associated failure modes indicated as B – bearing, T- tension and C – cleavage (source: Akay 1992)

The size and geometry of the joint also dictates the mechanical behaviour of the joint: the ratio of edge distance to fastener diameter (e/d) should be at least 3:1 (e = the distance from the centre of the hole to the edge or the end of the part; d = fastener or pin-hole diameter), the ratio of fastener width to the hole diameter (w/d) should be at least 4:1 and a distance of 3 to 4 diameter should be placed in between adjacent fasteners for composites of various lay-up configurations.

2.4.2.2 Adhesive bonding

The concept of marrying metal and composite materials to create aerospace components dates from the early 1950s. The metal bonding process, in which metal parts are adhesively integrated with prepreg and/or honeycomb core and cured, is still used to make a wide variety of aerospace structural parts such as flaps, spoilers, rotor blades, interior bulkheads and even entire wings. The process offers advantages, such as good impact resistance and repairability, as well as good strength-to-weight ratio, despite their higher weights compared with composites-only structures. Adhesive bonding often enables designers to eliminate mechanical fasteners, which means a smoother part surface and better aerodynamic performance (Black 2003).



Struggling to get interviews?

Professional CV consulting & writing assistance from leading job experts in the UK.

Visit site

 Take a short-cut to your next job!
Improve your interview success rate by 70%.

 **TheCVagency**
Visit theagency.co.uk for more info.

The common types of adhesively-bonded joints are shown in Figure 2.36. The type of joint should be selected carefully to achieve maximum performance under a given mode of loading. Figures 2.37 and 2.38 delineate which joint-designs are good and which ones to avoid: the ideal performance is achievable under compressive loading, acceptable performance in shear, but tensile loading should be avoided, particularly in peel and cleavage modes. A straight-butt joint under tension is not stable because, as shown in the diagram, a slightly off-centre force will cause a crack to propagate through the joint. A similar problem can occur with a corner joint, if an indirect force is applied, it can result in the introduction of a cleavage force into the joint.

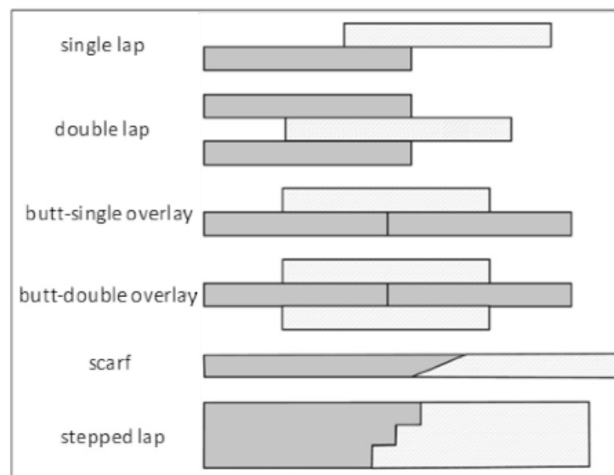


Figure 2.36 Adhesively-bonded joints (source: Strong 2008 p. 364)

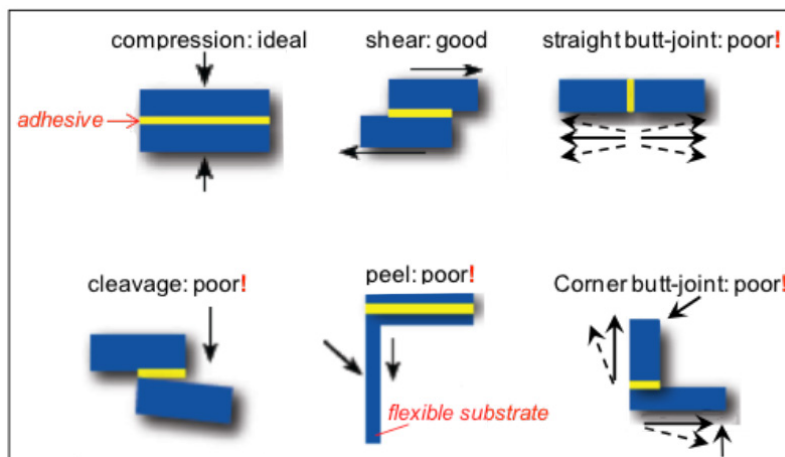


Figure 2.37 Rating of bonded-joint designs (source: Permabond)

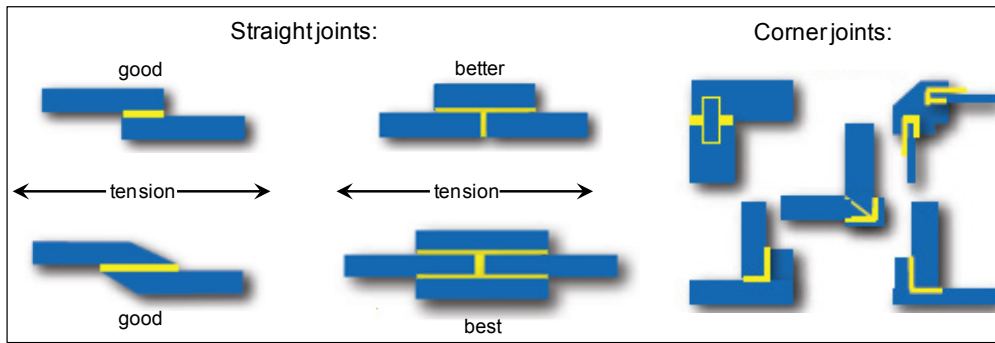


Figure 2.38 Suggested improvements for poor joints (source: Permabond)

Adhesives undergo a chemical reaction, e.g. polymerisation/crosslinking, or physical change (melting/solidification) during the bonding process. Structural adhesives are mainly thermosetting systems such as epoxy resins, modified acrylics, phenolics, polyurethanes, cyanoacrylates, silicones, etc.

However, even with advanced adhesive formulations, it remains critical to prepare surfaces: for composites this normally includes a degrease-abrade-degrease-dry sequence to remove any grease/oil and/or particle residues left on the surfaces so that the adhesive will bond properly. Shot-blasting to abrade surface is inappropriate with composites, it tends to remove too much substrate. Plastic bead blasting (or similar blast media) permits greater control of material removal. The metallic parts to be joined to a composite part may be chemically etched, for example, with chromic acid anodizing solution, which deposits a thin, protective oxide coating on the metal in preparation for adhesive bonding. They are then primed with an adhesive epoxy primer (i.e. a paint-like epoxy material) ready to be cured with the composite layup.

Achieving good metal-to-composite bonds is difficult. Because metals usually have a higher coefficient of thermal expansion than composites, especially carbon and aramid composites, the bonds can break if the structure is subject to large temperature swings. That is often why co-cured metal-to-composite bonds fail even before the part is put into service. Also, aluminum oxidizes rapidly, making it difficult to achieve a good bond to this metal. For these reasons, mechanical fasteners are often specified when joining composites to metals.

Whenever possible, multiple composite parts should be joined together during cure. This process is called “co-curing” and results in the strongest composite-to-composite bond. It also has the advantage of reducing part count and minimizing related machining operations.

2.4.2.3 Welding

Thermoplastic composites, such as PEEK-CF (APC2) laminates, are typically joined by welding using one of the following methods:

- mechanical: vibration, rotational/spin, friction stir, ultrasonic, orbital
- electromagnetic: infrared, microwave, laser beam, dielectric/high frequency, induction and resistance
- externally heated: hot plate, hot bar, impulse, hot gas, extrusion.

In resistance welding an electrically resistive implant is placed at the joint (it can be metal wire or mesh or carbon fibre and it stays in the joint) and as the current passes through, it heats up and provides the necessary heat for bonding.

In induction welding a coil is used to generate high frequency alternating magnetic field that induces eddy currents and hence heat in the joint material for welding (a conducting implant would be needed in the joint in non carbon-fibre composites). Refer to TWI Report (2011) and Lizotte & Cramer (2008) for further information on induction and resistance welding.

gaiTeye
Challenge the way we run

**EXPERIENCE THE POWER OF
FULL ENGAGEMENT...**

.....

**RUN FASTER.
RUN LONGER..
RUN EASIER...**

**READ MORE & PRE-ORDER TODAY
WWW.GAITEYE.COM**

Hybrid joints such as mixed-adhesive, bolted-bonded, and riveted-bonded joints are also used in order to benefit from the advantages of different techniques. Adhesive joints with functionally graded materials are also used to achieve a true uniform stress distribution along the joint overlap.

Fractures/cracks in low melting point thermoplastic products can be welded/repared using a hand-held hot-air gun welder. Hot air hand welding uses a spool of thermoplastic strand to perform the weld. It is a manual process and therefore the quality of the weld depends on the dexterity of the operator. The hot air (or inert gas) is required to simultaneously transmit heat into the product and the welding strand/rod to allow the fusion to take place.

2.4.3 Repair

Composite laminates are used in a wide range of applications some of which are for important structural components, and when damaged they need to be repaired to assure safety and performance and for cost effectiveness. Damage to composite components is not always visible to the naked eye and the extent of damage is best determined for structural components by suitable non destructive test (NDT) methods.

Repair techniques are heavily dependent on details of the structure and, therefore, selected based on a specific case. However, there are basic fundamental steps of composite repair listed below that apply in general (Netcomposites, <http://www.netcomposites.com/guide/repair/65>):

- assess damage (extent and degree)
- remove damaged material
- treat contaminated material
- prepare repair area
- conduct/complete repair
- inspect repair for quality assurance (e.g. for delaminations, inclusions, proper cure)
- restore surface finish.

Repairs for composite laminates include uniform lap, stepped lap, tapered-sanded (scarf) and step-sanded, see Figures 2.39, 2.40 and 2.41. For consolidation of the repair plies, vacuum-bagging (provides consolidation pressure of 1 atmosphere) is used for advanced composite repairs. The assembly is placed inside an air oven for curing or over a heater mat for in field conditions. Autoclave processing is used for the repair of high quality structural components, where the processing conditions of vacuum, pressure, heat up rate and cure temperature are controlled. Testing, often using non-destructive test methods, is required to ensure long-term success of the repair.

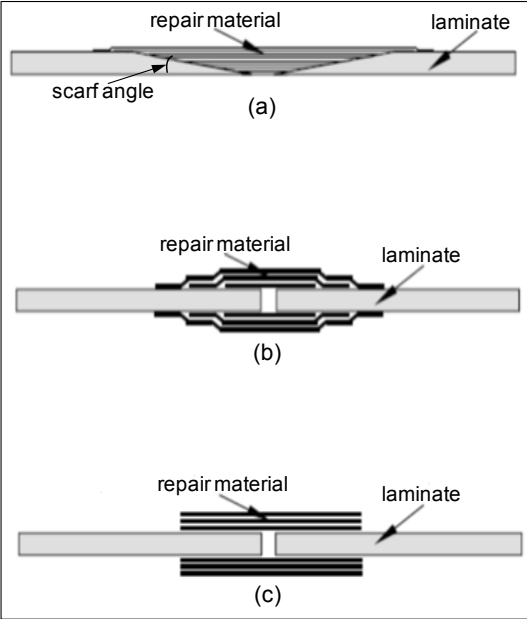


Figure 2.39 Illustration of some of the repair methods: (a) scarf (b) stepped lap (c) uniform lap (source: Ahn & Springer 2000)

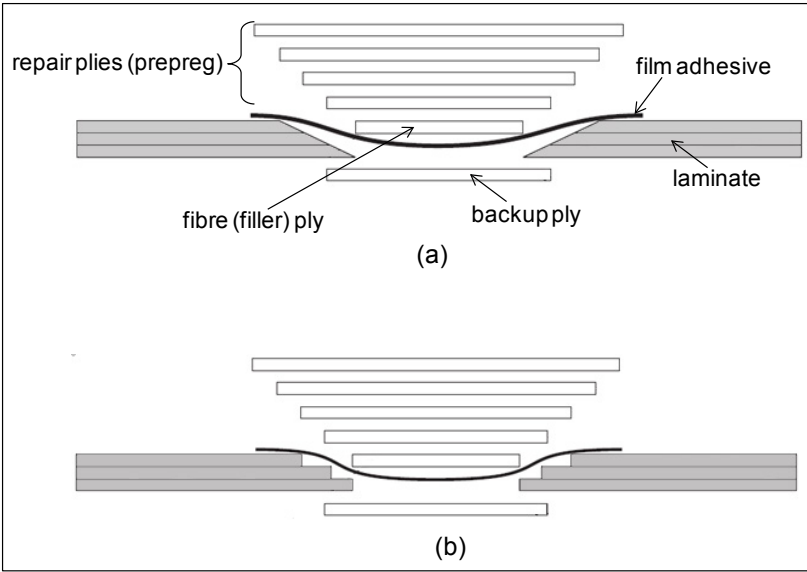


Figure 2.40 Elements of sanded-repair methods: (a) scarf (b) step (source: Hexcel 1999)

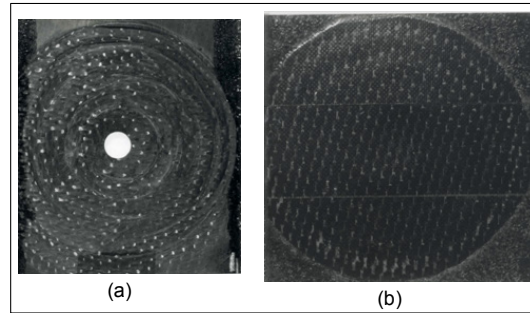
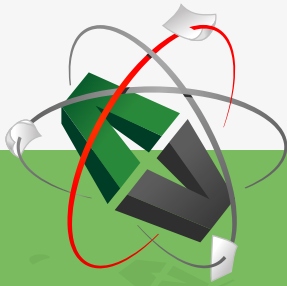


Figure 2.41 Damaged CF-epoxy laminate: (a) step-sanded and (b) repaired areas

In comparison scarfing is normally easier to produce. Stepping leaves abrupt edges and butt joints in each repaired ply. Stepping is also hard to do without cutting through and damaging the underlying plies. Repairing can be done using prepreg as repairing material or with wet lay-up of the repair material.

Work reported by Ahn & Springer (2000) includes evaluation of composite repairs in relation to types of repair, geometric factors, cure cycle, specimen moisture content and test temperatures. They have shown that the failure loads were higher with the prepreg repair (scarf and stepped lap) than with the wet lay-up repair for specimens dried and tested at approximately 20°C. However, the failure loads were lower in the prepreg repair than with wet lay-up repair when the specimens were moisturized and tested at approximately 80°C.

This e-book
is made with
SetaPDF



SETASIGN

PDF components for PHP developers

www.setasign.com



The effects of the following geometric factors on the failure load were evaluated:

- for the scarf repair: the scarf angle and the number of external plies
- for the lap repair: the shape of the repair plies (stepped or uniform), the length of the repair plies (lap length), and the number of repair plies per side.

Internal damage, caused by low velocity/energy impact, is common in composites. Repair of such barely-visible damage is important: to detect and repair so that failures do not progress to catastrophic failure. Damage, when detected, is usually repaired in the field by hand, however, **self-repairing polymer composites** ensure the repair of undetected damage. Repair chemicals are released from within the composite itself. The hollow fibres or nano tubes are embedded in the matrix, and the chemicals they carry are released wherever and whenever cracking or other matrix damage occurs. The repair chemical flows into the crack, and crack faces are rebounded as illustrated in Figures 2.42. For further information and actual experimental examples refer to Dry (2005 and 2008).

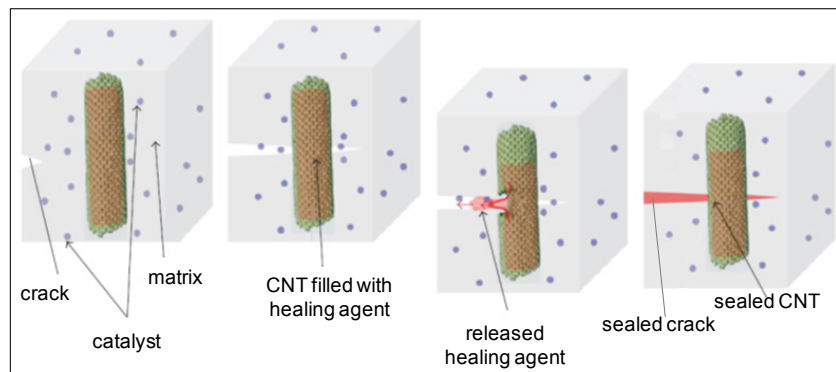


Figure 2.42 Concept of the self-healing process using carbon nanotubes (CNT) (source: Lanzara et al. 2009)

2.5 Self-assessment questions

1. Briefly describe pultrusion, filament winding and prepreg production processes, indicating the advantages and the disadvantages of each.
2. What is the role of each layer in vacuum bag assembly?
3. What are the main autoclave and vacuum bag/oven processing parameters?
4. What are the advantages and disadvantages when autoclaves are used for curing?
5. Describe the mechanism by which rubber pressure intensifying occurs in tooling during composites manufacturing, and indicate what the main advantage of employing rubber pressure intensifiers is.
6. Draw a diagram for a two-step autoclave cure cycle for an aerospace grade epoxy resin prepreg lay-up, indicating all the processing parameters with their typical values and briefly describing the purpose of curing in two stages.
7. Describe a prepreg sandwich construction.

8. Briefly describe the fabrication and uses of structural composite sandwich panels.
9. Distinguish between the composite production methods of Resin Transfer Moulding (RTM) and hand lay-up.
10. Describe the resin infusion process, and indicate why it may be preferred compared with other similar processes.
11. Name three cutting processes and indicate their advantages and disadvantages in cutting composite parts.
12. Indicate two advantages and disadvantages of adhesive bonding versus mechanical joining of composites.
13. Give examples of symmetric and non-symmetric arrangements of unidirectional continuous fibre containing polymer plies in the production of flat laminates. Why is the symmetry in the stacking of the plies important?
14. 'The conditions under which short-fibre reinforced thermoplastics are processed by injection moulding have significant effects on the mechanical properties of the component made.' Briefly discuss this statement.
15. Describe, by sketching appropriate graphs/diagrams, the significance of the critical fibre length in short fibre reinforced composites. What precautions can be taken during injection moulding of a PMC to minimise the mechanical degradation of the fibres?



The advertisement features a dark blue background with a large, stylized white graphic of a lion's head. In the center, the text "YOU THINK. YOU CAN WORK AT RMB" is written in large, white, sans-serif capital letters. In the top right corner, there is a white rectangular box containing the Rand Merchant Bank logo (a lion with a key) and the text "RAND MERCHANT BANK", "A division of FirstRand Bank Limited", and "Traditional values. Innovative ideas."

Rand Merchant Bank uses good business to create a better world, which is one of the reasons that the country's top talent chooses to work at RMB. For more information visit us at www.rmb.co.za

Thinking that can change your world

Rand Merchant Bank is an Authorised Financial Services Provider



Click on the ad to read more

3 Estimation of mechanical properties

3.1 Continuous fibre composites

Fibre composites are anisotropic in their mechanical behaviour, e.g. variation in Young's modulus (E) occurs depending on the direction of applied load with respect to the fibre alignment. The extreme scenario is illustrated in Figure 3.1 for a unidirectional fibre (f) reinforced matrix (m).

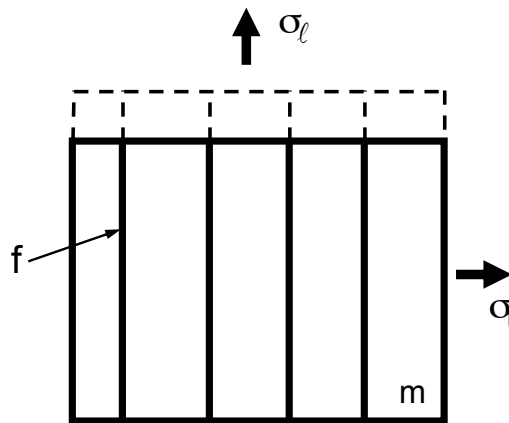


Figure 3.1 Longitudinal and transverse loading of a UD composite

Two alternatives are considered: the applied stress (σ) is longitudinal (L) or transverse (T) to the fibre direction.

(a) $\sigma //$ fibres:

Assume uniform strain (i.e. isostrain).

Then, the stress carried by the composite is estimated by a **law (rule) of mixtures equation**.

$\sigma_c = \sigma_f v_f + \sigma_m (1 - v_f)$; where, v_f is the fibre volume fraction.

or in terms of E : $\sigma_c = E_f \epsilon_f v_f + E_m \epsilon_m (1 - v_f)$

since $\epsilon_c = \epsilon_m = \epsilon_f$ i.e. the isostrain condition

$$\therefore E_{c,L} = \frac{\sigma_c}{\epsilon_{c,L}} = E_f v_f + E_m (1 - v_f)$$

b) $\sigma \perp$ fibres:

Assume uniform stress.

The net strain in the composite is, therefore, the sum of the contributions from the matrix and the fibre. Accordingly, the strain experienced in the composite is estimated by the law of mixtures relationship.

$$\text{i.e., } \varepsilon_c = \varepsilon_f v_f + \varepsilon_m (1-v_f)$$

since, $\sigma_c = \sigma_f = \sigma_m$, i.e. the isostress condition

$$\therefore E_{c,T} = 1 / \left(\frac{v_f}{E_f} + \frac{(1-v_f)}{E_m} \right)$$

$$\text{or } \frac{1}{E_{c,T}} = \frac{v_f}{E_f} + \frac{(1-v_f)}{E_m} \text{ (an inverse rule of mixtures relationship).}$$

The inverse rule of mixtures relationship (Reuss Model) obtained under transverse loading is a poor approximate for $E_{c,T}$, since the strain and stress distribution in the matrix is not uniform (Hull 1981, p. 86) and DoITPoMS (2004–2014)) and it is demonstrated that a better estimate is the semi-empirical Halpin-Tsai expression:

$$E_{c,T} = \frac{E_m(1 + \xi\eta v_f)}{(1 - \eta v_f)}$$

where, $\eta = \frac{(E_f/E_m) - 1}{(E_f/E_m) + \xi}$, and ξ depends on the shape and aspect ratios of the fibres, fibre packing geometry (hexagonal or square) and regularity, and loading conditions.

A graphical representation of these two extreme anisotropy in moduli, and other intermediate levels of anisotropy, achievable by fibre arrangement are shown in Figure 3.2.

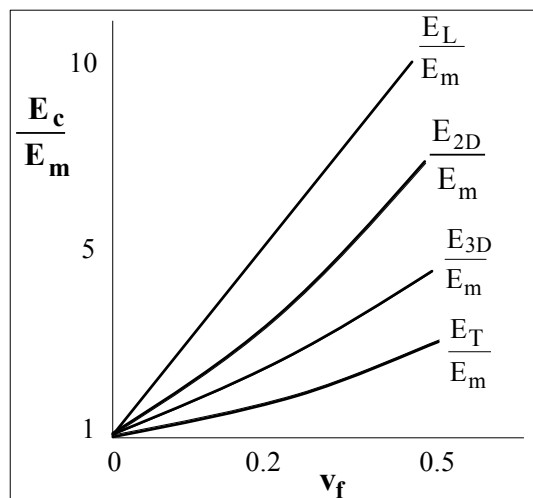


Figure 3.2 Elastic moduli vs. fibre volume fraction for various fibre arrangements for a composite with $E_f/E_m = 25$.

The graph compares the longitudinal (E_L) and transverse (E_T) elastic moduli of unidirectionally-oriented fibre composites with the elastic moduli where the same amount of fibres are arranged orthogonally in plane (E_{2D}) and in bulk (E_{3D}) as illustrated in Figure 3.3. Although the modulus E_{2D} is high compared with that of E_T , it is lower than E_L of a uniaxially oriented composite. Thus, in order to achieve isotropy in modulus in a plane, the maximum possible modulus, E_L , is sacrificed.

Fibres may be oriented in 3-D to give truly isotropic composites, although this is generally difficult to achieve in fabrication. In the case of 3-D composites, there is an even greater sacrifice in the maximum achievable modulus, E_T .

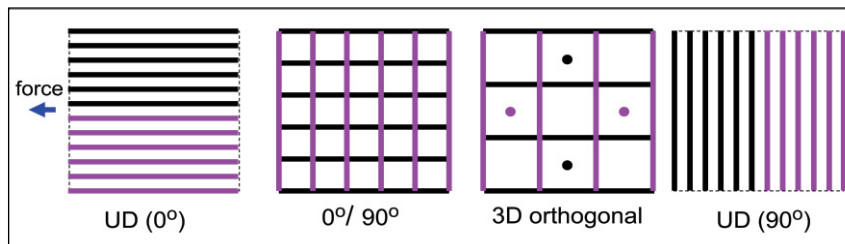


Figure 3.3 Arrangement of the same number of fibre strands in different alignments to the direction of applied force



Discover the truth at www.deloitte.ca/careers

Deloitte.

© Deloitte & Touche LLP and affiliated entities.



Click on the ad to read more

Control of properties in any direction in a plane is possible through careful lamination (i.e. controlled lay-up of individual plies). Typical laminate may contain layers (plies) which alternate by 90° (cross-ply) or by 60° (quasi-isotropic). With quasi-isotropic laminates the properties are nearly the same in all directions in the plane.

Anisotropy is also strongly exhibited in material strength as shown in Figure 3.4 for the ultimate tensile strength (UTS).

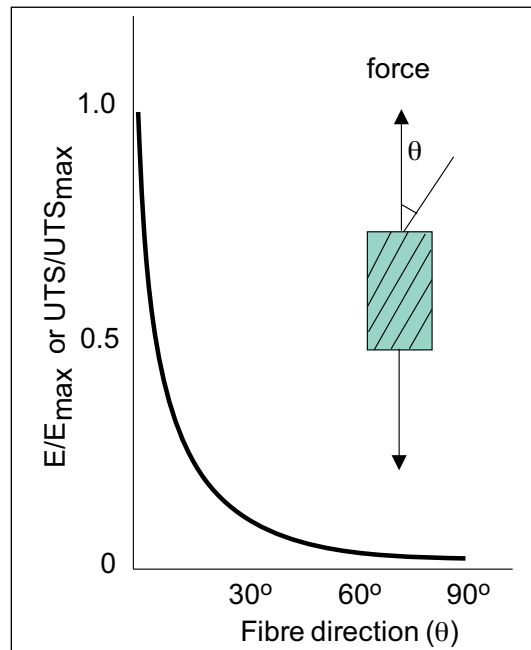


Figure 3.4 Mechanical properties vs. fibre orientation

The reinforcement for polymer/fibre composites within a single ply can take the form of unidirectional (UD) fibres, woven rovings or chopped strands. Briefly these compare as follows:

Maximum strength and stiffness can only be achieved with UD fibres (in the fibre direction). Planar isotropy (at the expense of strength and stiffness) is offered with woven roving and chopped fibres. Although complete planar isotropy can exist in a ply of chopped fibres, woven roving is weaker and less stiff at ± 45° to fibres. Woven rovings also suffer from the fibre bending (crimping) at the cross-over points. Lower stresses are supported along the chopped fibres compared with continuous UD and woven fibres. The extent of fibre volume incorporation into a fibre/resin composite is highest for UD fibres and lowest for chopped fibres. Continuous fibres are more expensive. Manufacturing is easier (better drape and fibre placement) with woven and chopped fibre mats.

The rule-of-mixtures relationship for a composite incorporating two or more fibres within a single matrix may be expressed as:

$$E_c = \eta_{IA} \eta_{oA} v_A E_A + \eta_{IB} \eta_{oB} v_B E_B + v_m E_m$$

where, subscript A and B represent fibre types, v volume fraction, and η_l and η_o are length correction and orientation efficiency factors, respectively.

Laminate theory is the main mathematical tool for determining the property relationship between plies and laminate: with this approach, the elastic properties of laminates can be calculated from the properties and orientation of individual plies. The details of the laminate theory can be found in many textbooks, including Hull (1981 p. 101).

Longitudinal tensile strength of UD composites, $\sigma_{c,L}^*$, depends on the strain (ϵ) at failure values of the fibre and the matrix. For $\epsilon_f^* > \epsilon_m^*$, see Figure 3.5, depending on the fibre volume content (v_f), two failure processes are envisaged as illustrated in Figure 3.6: at low fibre content $\leq v_f'$, when the matrix fractures and all the loads are transferred to the fibres, the low numbers of fibres cannot support this load and break, thus the strength of the composite is estimated by

$$\sigma_{c,L}^* = v_f \sigma_f + (1 - v_f) \sigma_m^*$$

I WANT TO CHANGE DIRECTION,
AND THE WORLD.

GOT-THE-ENERGY-TO-LEAD.COM

We believe that energy suppliers should be renewable, too. We are therefore looking for enthusiastic new colleagues with plenty of ideas who want to join RWE in changing the world. Visit us online to find out what we are offering and how we are working together to ensure the energy of the future.

RWE
The energy to lead



Click on the ad to read more

When $v_f > v_f'$, the matrix takes only a small proportion of the load since $E_f > E_m$ so that when the matrix fractures the transfer of additional load to the fibres is insufficient to cause the fibres to fracture as well and, provided it is still possible to continue to transfer the load to the fibres, the load on the composite laminate can be increased until the tensile strength of the fibres is reached. Therefore,

$$\sigma_{c,L}^* = v_f \sigma_f^*$$

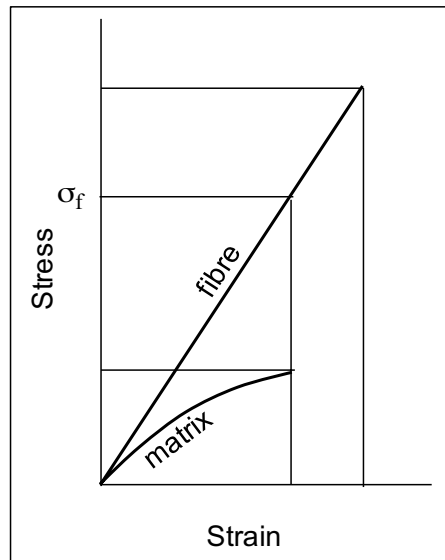


Figure 3.5 Stress vs. strain curves for fibre and matrix (source: Hull 1981, p. 128)

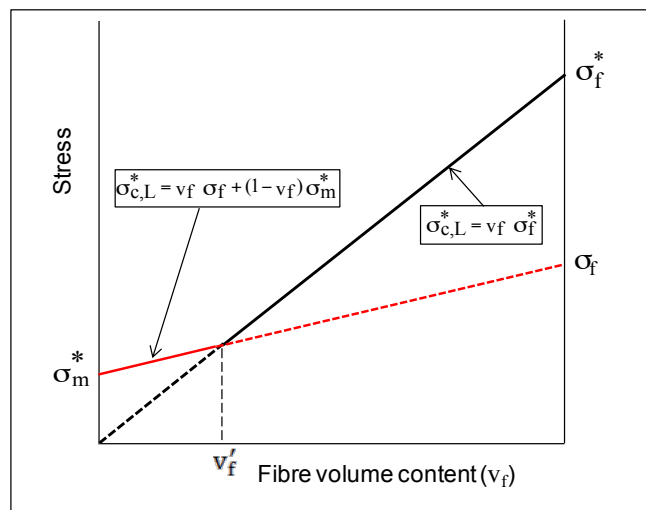


Figure 3.6 Variation of fracture strength of UD laminae with v_f for $\epsilon_f^* > \epsilon_m^*$ (source: Hull 1981, p. 128)

By considering the above two equations for $\sigma_{c,L}^*$ as simultaneous equations, the cross-over point, v_f' , where the change in failure mechanism occurs can be determined to be:

$$v_f' = \sigma_m^* / (\sigma_f^* - \sigma_f + \sigma_m^*)$$

For $\epsilon_m^* > \epsilon_f^*$, see Figure 3.7, also depending on the fibre volume content (v_f), two failure processes are envisaged as illustrated in Figure 3.8: at low fibre content $\leq v_f'$, when the fibre fracture occurs the extra load on the matrix is not sufficient to fracture the matrix. However the presence of the broken/ineffectual fibres in the matrix tantamount to a reduction in matrix content by the amount of failed fibre content and, in turn, a progressive reduction in the load carrying capacity of the matrix, σ_m^* , with increasing fibre content, thus the strength of the composite is estimated by

$$\sigma_{c,L}^* = (1 - v_f) \sigma_m^*$$

When $v_f > v_f'$, the load transferred to the matrix when fibres fracture is too high to be supported by the matrix and it also fractures when the fibres fracture, and so

$$\sigma_{c,L}^* = v_f \sigma_f^* + (1 - v_f) \sigma_m^*$$

By considering the above two equations for $\sigma_{c,L}^*$ as simultaneous equations, the cross-over point, v_f' , where the change in failure mechanism occurs for $\epsilon_m^* > \epsilon_f^*$ case can also be determined:

$$v_f' = (\sigma_m^* - \sigma_m) / (\sigma_f^* + \sigma_m^* - \sigma_m)$$

bookboon.com

Corporate eLibrary

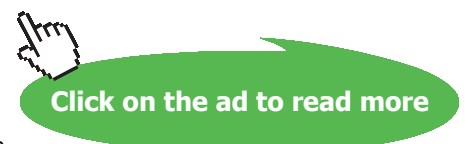
See our Business Solutions for employee learning

[Click here](#)

Management Time Management

Problem solving Self-Confidence Effectiveness

Project Management Goal setting Motivation Coaching



Substituting values for carbon fibre and epoxy resin, it can be shown for both cases that v_f' is very small compared with $v_f = 0.4-0.7$ for most industrial laminates, indicating that the matrix contribution to the longitudinal tensile strength of PMCs is small and can be neglected.

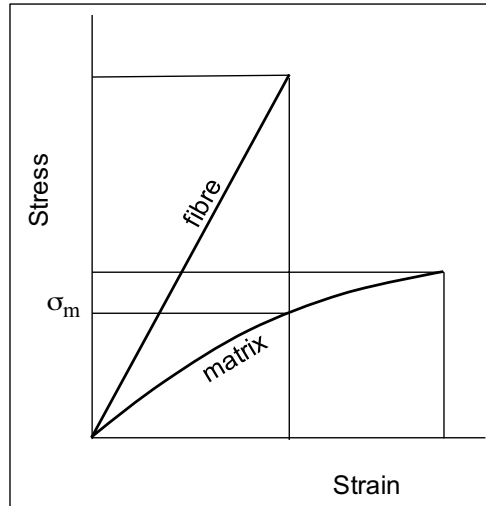


Figure 3.7 Stress vs. strain curves for fibre and matrix (source: Hull 1981, p. 130)

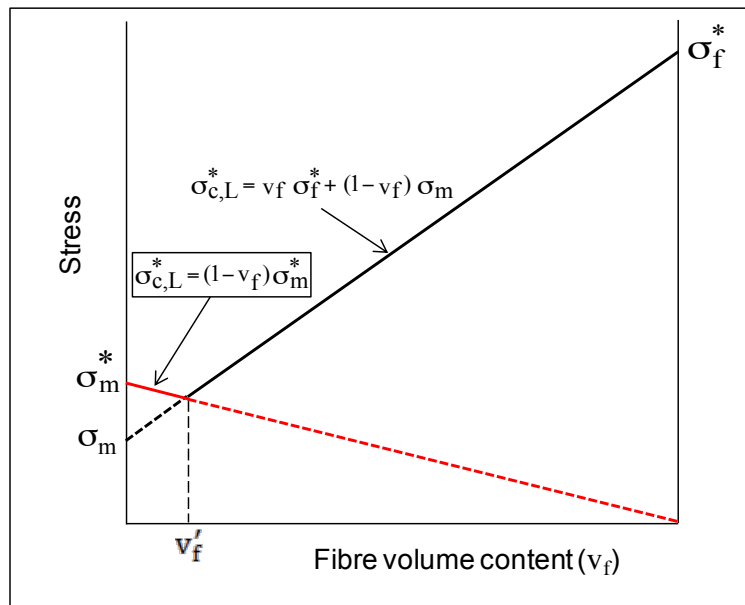


Figure 3.8 Variation of fracture strength of UD laminae with v_f for $\epsilon_m^* > \epsilon_f^*$ (source: Hull 1981, p. 130)

Inaccuracies exist in estimations for longitudinal strength, including the reality that the fibre strength is not constant along its length for a given type of fibre; instead there is a range of strengths, described by Weibull statistics, due to varying flaw sizes along each fibre. Weibull distribution function (see Hull 1981, p. 132) describes scatter that exists in experimentally measured strength values for brittle materials.

3.2 Short (discontinuous) fibre composites

In short-fibre reinforced composites, see Figure 3.9, at the ends of fibres the load is transferred back to the matrix and hence the composite will deform to a greater extent than a similar volume fraction continuous fibre composite. Therefore, the simple rule of mixtures equation is modified such that this lowering of material stiffness (elastic modulus) is accounted for:

$$E_{c,L} = KE_f v_f + (1-v_f) E_m$$

where, K is the fibre efficiency parameter which depends on v_f and the E_f/E_m ratio.

$K < 1$; usually $K = 0.1 - 0.6$.

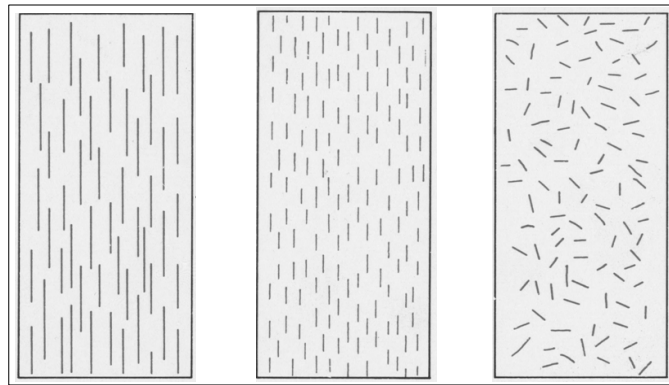


Figure 3.9 Sketch of various discontinuous fibre arrangements (source: Callister 2007, p. 587)

3.2.1 Transfer of stress from matrix to fibres and the concept of critical fibre length, ℓ_c

When a composite is under a tensile load, the difference in the elastic moduli of the matrix (E_m) and the fibre (E_f) (where $E_f > E_m$) results in a differential movement (deformation) at the fibre surface (i.e. fibre/matrix interface). This differential response at the interface generates shear (friction) stresses at the fibre surface which in turn is transferred to the fibres as tensile stresses; hence, the fibres bear the major part of the applied load and act as reinforcement. The human body is a good example of stress transfer between the parts of a composite body, where external loads experienced by the body are transferred to the bones via flesh/muscle. Figure 3.10 also illustrates the concept of load transfer.



Figure 3.10 An illustration of load transfer (source: Google image)

The maximum load bearing capacity of a material is dictated by its strength, therefore, a minimum fibre length, known as **the critical fibre length** (l_c), is required for the build up of tensile stress to reach the level of its tensile strength as demonstrated in Figure 3.11. It can be seen that as the specimen is extended the load is transferred to the fibre from both ends and the resultant stress (σ) builds up along the fibre reaching an apex value (tensile strength, σ_F^*) in the middle of the fibre.

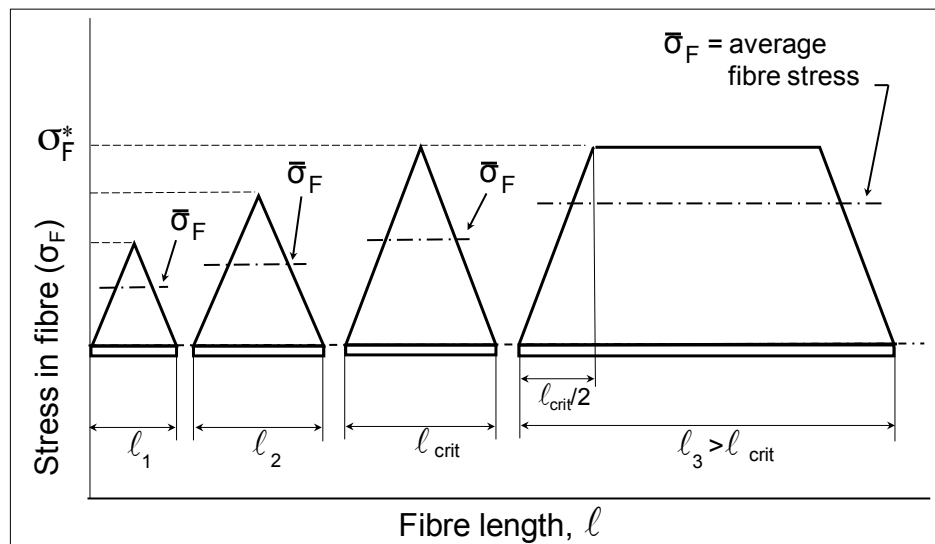


Figure 3.11 Development of stress along a fibre vs. fibre length

It can be appreciated from Figure 3.11 that in short fibre reinforced composites, a minimum fibre length, l_c , is required in order to achieve the reinforcing potential of the fibres, i.e. to enable them to support stresses up to their tensile strength level. The critical fibre length can be estimated for a composite system from the properties of the fibre and matrix components as shown in the following derivation.

For a composite (e.g. a fibre embedded in matrix) under stress,

$$\text{shear force at fibre-matrix interface} = \tau (2\pi r \delta x)$$

where, τ is the interface shear strength, r fibre radius and δx is an increment of fibre length.

Tensile force generated in the fibre = $\delta\sigma(\pi r^2)$

where, $\delta\sigma$ is the tensile stress generated in δx length of the fibre.

Balancing the forces:

$$\int_0^{\sigma_f^*} \pi r^2 \delta\sigma = \int_0^{\ell_c/2} \tau 2\pi r \delta x$$

$$\therefore \pi r^2 \sigma_f^* = \tau 2\pi r \frac{\ell_c}{2}$$

$$\therefore \ell_c = \frac{\sigma_f^* r}{\tau}$$

where, σ_f^* is the fibre tensile strength, and ℓ_c is the critical fibre length.

Longitudinal tensile strength, $\sigma_{c,L}^*$, of UD short-fibre composites:

The longitudinal composite strength can be estimated by the rule of mixtures equation;

$$\sigma_{c,L}^* = \bar{\sigma}_f V_f + \sigma_m V_m \quad (1)$$

where, $\bar{\sigma}_f$ is the average stress in the fibre at composite failure, σ_m is the matrix stress at composite failure.

Brain power

By 2020, wind could provide one-tenth of our planet's electricity needs. Already today, SKF's innovative know-how is crucial to running a large proportion of the world's wind turbines.

Up to 25 % of the generating costs relate to maintenance. These can be reduced dramatically thanks to our systems for on-line condition monitoring and automatic lubrication. We help make it more economical to create cleaner, cheaper energy out of thin air.

By sharing our experience, expertise, and creativity, industries can boost performance beyond expectations. Therefore we need the best employees who can meet this challenge!

The Power of Knowledge Engineering

Plug into The Power of Knowledge Engineering.
Visit us at www.skf.com/knowledge

SKF

The average, $\bar{\sigma}_f$, can be expressed in terms of fibre properties using the stress vs. fibre length graph (Figure 3.12) for a fibre length $\ell > \ell_c$.

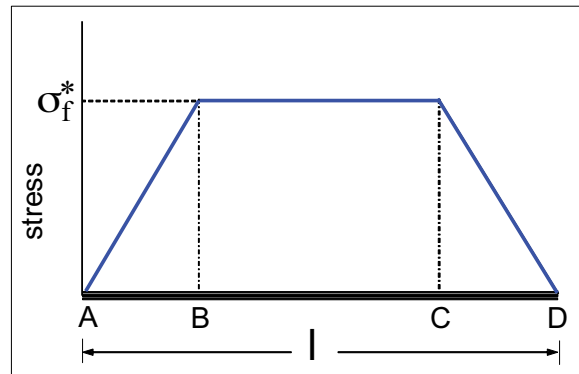
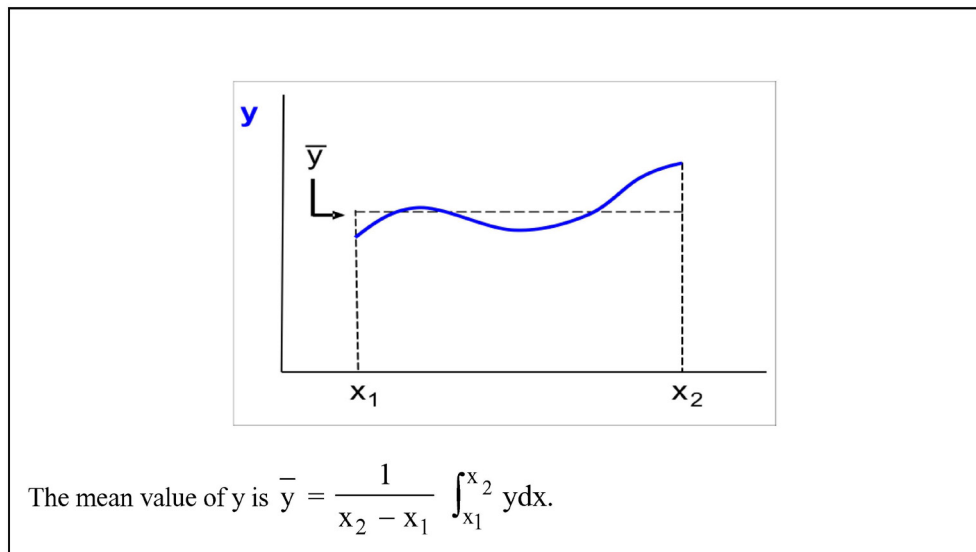


Figure 3.12 Stress (σ_f) vs. fibre length (ℓ)

Note that the mean value of a function $y = f(x)$ can be determined from its integral (i.e. the area under the curve) as shown in the text-box below.



Consider $y = \sigma_f$ and $x = \ell$; therefore from Figure 3.12, determine the area under the stress (σ_f) vs. fibre length (ℓ) graph, and divide it by the length, ℓ , in order to estimate $\bar{\sigma}_f$:

Note that the portions of the length ℓ , $\overline{AB} = \overline{CD} = \ell_c / 2$.

$$\text{Accordingly, } \bar{\sigma}_f = \left[\frac{1}{2} \left(\sigma_f^* \frac{\ell_c}{2} \right) + \sigma_f^* (\ell - \ell_c) + \frac{1}{2} \left(\sigma_f^* \frac{\ell_c}{2} \right) \right] / \ell$$

$$\text{i.e., } \bar{\sigma}_f = \left(\frac{\ell - \ell_c}{\ell} + \frac{\ell_c}{2\ell} \right) \sigma_f^* \text{ or } \bar{\sigma}_f = \left(1 - \frac{\ell_c}{2\ell} \right) \sigma_f^*$$

substituting in Equation (1) gives:

$$\sigma_{c,L}^* = \left[\left(1 - \frac{\ell_c}{2\ell}\right) \sigma_f^* \right] v_f + (1 - v_f) \sigma_m$$

where, σ_f^* is the tensile strength of the fibre and σ_m is the stress in the matrix at composite failure.

$$\text{For } \ell = \ell_c; \quad \sigma_{c,L}^* = \frac{\sigma_f^* v_f}{2} + \sigma_m (1 - v_f)$$

$$\text{For } \ell > \ell_c \text{ (i.e., fibres fracture first): } \sigma_{c,L}^* = \left(1 - \frac{\ell_c}{2\ell}\right) \sigma_f^* v_f + (1 - v_f) \sigma_m$$

For $\ell \gg \ell_c$ (at least 10 times), then the composite can be treated as a continuous fibre composite and, thus, the simple law of mixtures can be used to determine the strength (since in the above equation $(\ell/2\ell)$ becomes negligibly small for large values of ℓ).

$$\sigma_{c,L}^* = \sigma_f^* v_f + \sigma_m (1 - v_f).$$

When the build-up of stress in the fibre is insufficient to cause fibre fracture, i.e. when $\ell < \ell_c$ matrix fails first:

$$\bar{\sigma}_f = \frac{\left[\frac{1}{2} \left(\frac{\ell}{2}\sigma_f\right) + \frac{1}{2} \left(\frac{\ell}{2}\sigma_f\right) \right]}{\ell} = \frac{1}{2} \sigma_f = \frac{\ell\tau}{2r}, \quad \text{since } \ell \text{ (fibre length to transfer stress, } \sigma_f) = \frac{\sigma_f r}{\tau}$$

$$\therefore \sigma_{c,L}^* = \frac{\ell\tau}{2r} v_f + \sigma_m (1 - v_f)$$

where, τ is the interface shear strength and σ_m^* is the matrix tensile strength.

Therefore, three different equations (as derived above) can be used to estimate the strength of a short fibre reinforced composite, depending on the average fibre length of the composite with respect to the critical fibre length.

3.3 Failure mechanisms that result in composite toughness

Toughness in composites is not so obviously predictable from its component materials, since fibres and rigid thermosetting polymers often used as matrices are not by themselves materials that exhibit toughness. However, composites besides introducing excellent strength and stiffness-to-weight ratios and good corrosion resistance, do also introduce good toughness.

The toughness in composites does not arise from the inherent characteristics of the component materials but rather from the failure mechanisms that operate during the material fracture process.

There are various mechanisms through which fibres render the composite tougher. Fibres form a barrier to a propagating crack, stopping it from running straight through the material. Fibres either stop the crack or cause it to deflect, thus, expending the energy of the crack and rendering it harmless.

The deflection of the cracks can occur in different forms including debonding of the fibre-matrix interface. Debonding can, in some circumstances, lead to a large-scale deviation of the crack tip and force it to run parallel with the fibres rather than across the fibres, resulting in an effective blunting of the crack. Cracking may then proceed on some other plane, remote from the original crack plane, with a resultant increase in the complexity of the fracture face and increase in composite toughness. Debonding (usually) leads to fibre pull out which requires high energy and, thus, makes a major contribution to the toughness. The toughening mechanisms of debonding and fibre pull-out are illustrated in Figure 3.13.

With us you can
shape the future.
Every single day.

For more information go to:
www.eon-career.com

Your energy shapes the future.

e.on



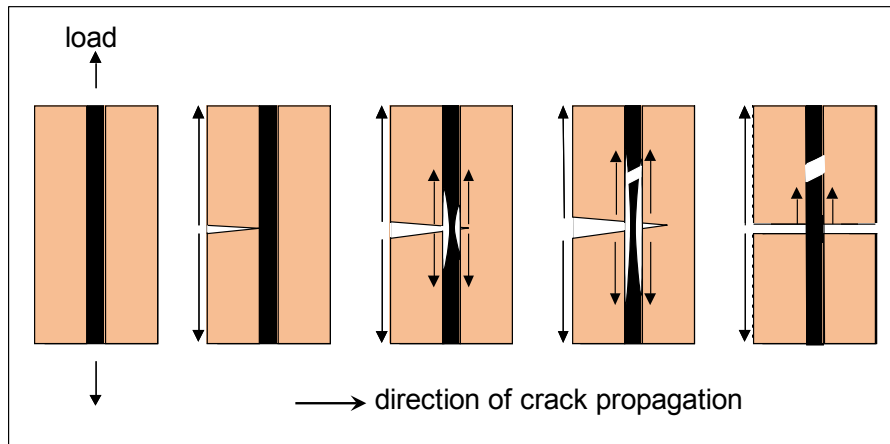


Figure 3.13 Illustration of fibre debonding and fibre pullout processes

3.3.1 Debonding

The process of debonding creates new surfaces in the composite and therefore requires energy, which is estimated as follows:

The Poisson's contraction effect, as a result of tensile loading of the fibres, causes the separation of the fibres from the matrix. Thus, the energy of debonding per fibre, W_D , can be calculated by equating it to the strain energy released in the fibre as the stress relaxes with debonding.

$$W_D = (\sigma_D^2 / 2E_f) \cdot (\text{volume of fibre debonded})$$

where, σ_D is the stress to cause debonding and $(\sigma_D^2 / 2E_f)$ is the strain energy (i.e. elastic energy per unit volume of the fibre, see text-box below) that was released at debonding.

The strain energy is defined as below:

$$\text{Strain energy} = \frac{\text{energy absorbed by the material under elastic deformation}}{\text{volume of the material}}, \text{ J/m}^3$$

$$\text{Strain energy} = \frac{\text{stress} \times \text{strain}}{2}; \left(\frac{\text{N}}{\text{m}^2} \right) \left(\frac{\text{m}}{\text{m}} \right) = \frac{\text{J}}{\text{m}^3}$$

Strain = stress / E

$$\therefore \text{strain energy} = (\text{stress})^2 / 2E.$$

The strain energy released in the fibre and expended for **debonding** can be calculated in terms of the fibre and matrix properties as follows:

The strain energy is only partially released upon debonding, as shown in the force displacement curve in Figure 3.14, since some of the energy remains in the debonded fibre when it is re-gripped by the matrix upon its expansion to regain its original diameter. (Note that, the process of debonding involves overcoming of both chemical and physical bonds between the fibre and the matrix: accordingly, the strain energy is only partially released upon debonding, since the physical bonding is re-established upon the instant return of the fibre to its original diameter when it is re-gripped by the surrounding matrix.)

Further work is required to overcome the physical interfacial squeeze for the onset of the pull out process of the debonded fibres and for the subsequent continuation of the frictional sliding of the fibres.

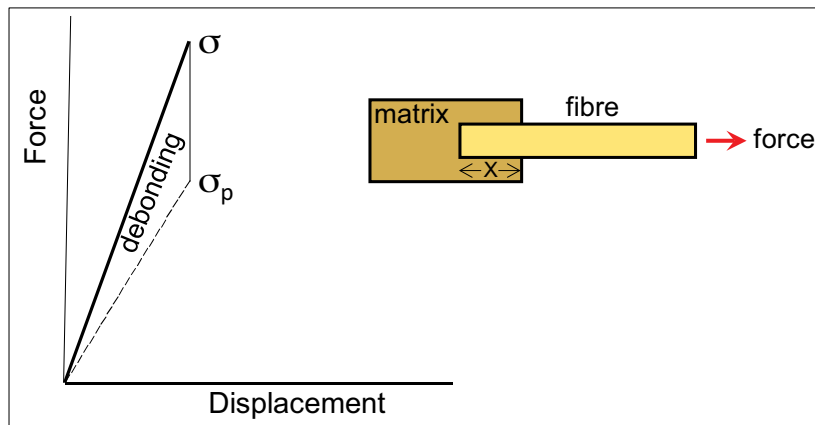


Figure 3.14 Schematic force vs. displacement relationship at debonding of fibre-matrix interface

By reference to Figure 3.14, σ_D can be calculated:

$$\sigma \text{ (tensile stress in the fibre)} = \sigma_D + \sigma_p$$

$$\therefore \sigma_D \text{ (stress to cause debonding)} = \sigma - \sigma_p$$

σ_p , **pull-out stress**, can be determined from balancing forces on the fibre following debonding and immediately before the onset of pull-out from its socket in the matrix.

Tensile force generated in the fibre = interfacial shear force between the fibre and the matrix.

i.e., $\sigma_p (\pi d^2/4) = \tau [(\pi d) x]$, where x is the pull-out length, d is the fibre diameter and τ is the interfacial shear stress.

$$\text{Rearranging gives } \sigma_p = (4 \tau x) / d$$

$$\therefore \sigma_D = \sigma - \sigma_p = \sigma - (4 \tau x) / d.$$

Substituting for the volume of the debonded section of the fibre and for the portion of the stress in the fibre that causes debonding in the equation $W_D = (\sigma_D^2 / 2E_f) \cdot (\text{volume of fibre debonded})$

gives W_D :

$$W_D = \frac{\pi d^2}{8E_f} \int_0^x \left(\sigma - \frac{4\tau x}{d}\right)^2 dx$$

Integrating gives
$$W_D = \frac{\pi d^2}{8E_f} \left[\frac{1}{3} \left(\sigma - \frac{4\tau x}{d}\right)^3 \left(\frac{-d}{4\tau}\right) \right]_0^x$$

$$\therefore W_D = \frac{\pi d^2}{3(8)E_f} \left[-\frac{d}{4\tau} \left(\sigma - \frac{4\tau x}{d}\right)^3 + \frac{d\sigma^3}{4\tau} \right]$$

This has a maximum value when $x = \frac{\ell_c}{2} = \frac{(\sigma_f)d}{4\tau}$ and $\sigma = \sigma_f$ (i.e. stress in the fibres reach the fibre tensile strength value, σ_p at $x = \ell_c/2$). Note that the first term in brackets becomes zero when $\frac{\ell_c}{2} = \frac{(\sigma_f)d}{4\tau}$ and $\sigma = \sigma_f$ is substituted.

(Note that E_f and σ_f are the elastic modulus and the tensile strength of the fibre).

$$\therefore W_{D(\max)} = \frac{\pi d^2}{24E_f} \frac{d\sigma_f^3}{4\tau} = \frac{\pi d^3 \sigma_f^3}{96E_f \tau}$$

Note that the critical fibre length, $\ell_c = \sigma_f d / 2\tau$, $\therefore d = 2\tau \ell_c / \sigma_f$

Rearranging and substituting gives

$$W_{D(\max)} = \frac{\pi d^2 \sigma_f^3}{96E_f \tau} \left(\frac{2\tau \ell_c}{\sigma_f} \right)$$

$$\therefore W_{D(\max)} = \frac{\pi d^2 \sigma_f^2 \ell_c}{48E_f} \text{ per fibre,}$$

For aligned fibres, the equation can be modified to include the volume fraction of fibres, v_f (see the text-box below), and express the maximum debonding energy per unit-cross-sectional area of composite as:

$$W_{D(\max)} = \frac{\sigma_f^2 \ell_c v_f}{12E_f} \text{ per unit area,}$$

Note that the number of fibres per unit area of a UD composite, $n = v_f / (\pi d^2/4)$ as described below:

The area of the fibres in a cross-section A of the composite = $A v_f$.

\therefore the number of the fibres in $A = A v_f / a_f$, where a_f is the cross-sectional area of a fibre,

\therefore the number of fibres per unit area of the composite, $n = (A v_f / a_f) / A = v_f / a_f$.

The unit of n is, for example, 100 fibre/m², etc.

3.3.2 Fibre pullout

Fibre pullout occurs following debonding (see Figure 3.15) in short fibre reinforced composites and in the case of continuous fibre composites after debonding and fibre fracture. After debonding a continuous fibre is loaded to failure over a 'gauge length' equal to the debonded length and it may break at any point within this region. The broken ends will retract and in the process of regaining their original diameter, the fibres will be re-gripped (or squeezed) by the resin. In order to permit further opening of the crack and, ultimately, to separate the two parts of the sample, these broken ends must be pulled out of the matrix.

© 2013 Accenture. All rights reserved.

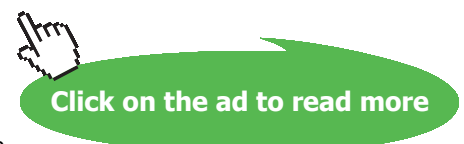
be > your degree

Bring your talent and passion to a global organization at the forefront of business, technology and innovation. Discover how great you can be.

Visit accenture.com/bookboon

Be greater than.
consulting | technology | outsourcing

accenture
High performance. Delivered.



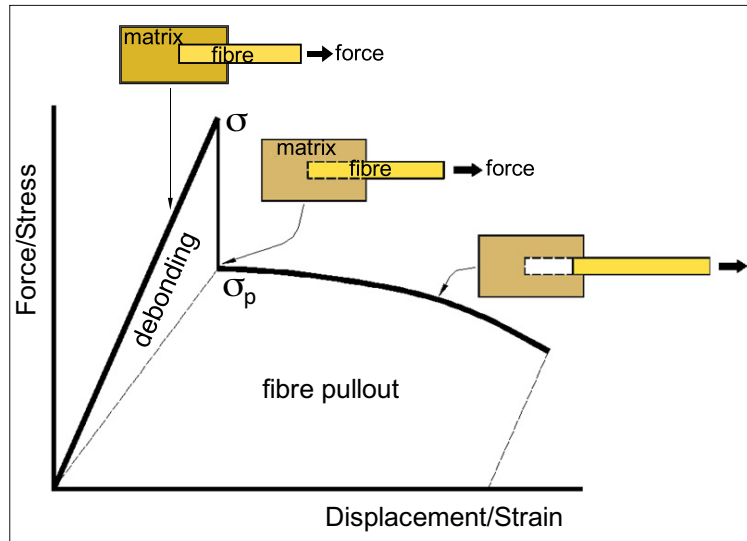


Figure 3.15 Schematic stress vs. strain relationship for fibre debonding and fibre pullout

Consider a UD-aligned short fibre composite material containing a volume fraction v_f of fibres of length ℓ as in Figure 3.16.

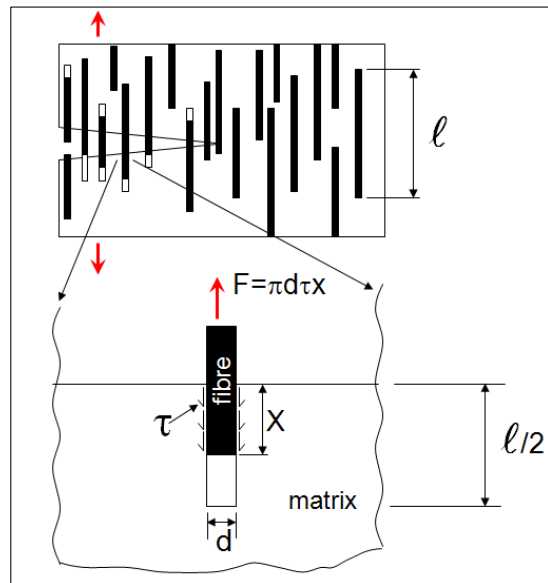


Figure 3.16 Fibre pullout during crack propagation

The work done (W_p) in pulling out a single fibre of embedded length x can be determined:

Pullout force, $F = (\sigma_p) (\text{area})$, i.e., $F = (4\tau x/d) (\pi d^2/4)$

$\therefore F = \pi d \tau x$.

Toughness of the composite improves by fibres pulling out of the fracture surface, therefore absorbing energy, as the crack opens.

$$W_p = \int_0^x F \delta x = \int_0^x \pi d \tau x \delta x = \left[\pi d \tau \frac{x^2}{2} \right]_0^x$$

where δx is an increment of pull-out length.

$$\therefore W_p = \pi d \tau \frac{x^2}{2}$$

The maximum length of fibre that can be pulled out is $\ell_c/2$. Substituting $x = \ell_c/2$ gives the maximum work to pull out a fibre to be

$$W_{p(\max)} = \pi d \tau \frac{\ell_c^2}{8},$$

$$\text{substituting } \ell_c = \frac{\sigma_f d}{2\tau} \text{ gives, } W_{p(\max)} = \frac{\pi d^2 \sigma_f \ell_c}{16} \text{ per fibre.}$$

A comparison of the energies required for debonding and pull-out, i.e., $W_{p(\max)} / W_{D(\max)} = 3E_f / \sigma_p$ shows that the energy associated with pull-out is much greater than the energy of debonding, since $E_f \gg \sigma_p$.

The maximum pull-out energy per unit-cross-sectional area of the composite can be expressed as:

$$W_{p(\max)} = n \frac{\pi d^2 \sigma_f \ell_c}{16}, \text{ where } n = 4v_f / \pi d^2$$

$$W_{p(\max)} = \frac{\sigma_f v_f \ell_c}{4} \text{ per unit area}$$

$$\text{or substituting for } \ell_c = \sigma_f d / (2\tau), W_{p(\max)} = \frac{v_f d \sigma_f^2}{8\tau} \text{ per unit area.}$$

When the units are in SI, the result is Nm/m^2 .

$$W_{p(\max)} = \text{energy/area,}$$

$$\therefore \text{energy in a given cross-sectional area of the composite} = W_{p(\max)} \cdot (\text{x-area}).$$

Note that the composite toughness ought to increase by raising the fibre volume content, increasing the fibre diameter, or using stronger fibres. However, improving the fibre/matrix bond or using a matrix with high yield strength will usually reduce the toughness because it inhibits debonding and therefore reduces the occurrence of pull-outs and it also offers a greater resistance to the process of pull-out.

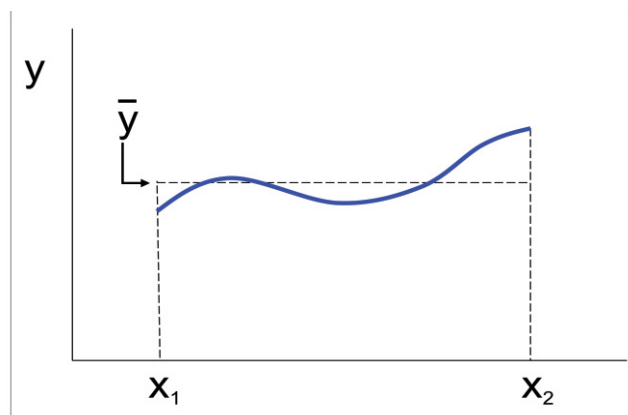
The mean value of pull-out work done per fibre for a population of fibres with embedded lengths zero to x is:

$$\bar{W}_p = \frac{1}{x} \int_0^x W_p \delta x = \frac{1}{x} \int_0^x \pi d \tau \frac{x^2}{2} \delta x$$

$$\bar{W}_p = \frac{1}{x} \pi d \tau \frac{x^3}{2(3)} = \frac{\pi d \tau x^2}{6}$$

From the following plot of 'y' against 'x', note that the mean value of y is

$$\bar{y} = \frac{1}{x_2 - x_1} \int_{x_1}^{x_2} y \delta x, \text{ where } y \equiv W_p \text{ and } (x_2 - x_1) \equiv x.$$



x will vary between 0 and $\ell/2$, therefore the average pull-out work done per fibre becomes:

$$\bar{W}_p = \frac{\pi d \tau \ell^2}{24} \text{ for } \ell \leq \ell_c.$$

For $\ell > \ell_c$, the effective fibre length for pull-out is ℓ_c , therefore $\bar{W}_p = \pi d \tau \ell_c^2 / 24$.

However, when $\ell > \ell_c$, not all the fibres contribute to the pull-out. The number of fibres contributing would depend on the magnitude of ℓ and ℓ_c . The condition for pull-out is that the embedded fibre length $\leq \ell_c / 2$. See Figure 3.17 for the definition of embedded fibre length.

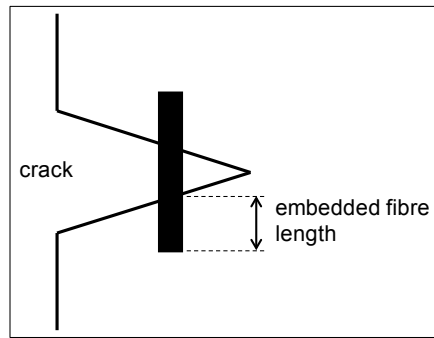


Figure 3.17 Illustration of an embedded fibre length at the opening of a propagating crack

The probability of pull-out, therefore, increases as ℓ_c increases. But, for a given ℓ_c , the probability decreases as ℓ increases. The numbers of fibres contributing to pull-out, hence, are directly proportional to the value of ℓ_c but are inversely proportional to the value of ℓ .

$$\therefore \bar{W}_p = \left(\frac{\ell_c}{\ell}\right) \frac{\pi d \tau \ell_c^2}{24} \text{ for } \ell > \ell_c$$

A schematic representation of the variation of the work of pull-out or crack propagation (i.e. toughness) with the fibre length, ℓ , is shown below (Figure 3.18). For small ℓ , the work of pull-out increases with fibre length because the pull-out length is increasing. It reaches a maximum value at ℓ_c and then drops because fibre fracture occurs for $\ell > \ell_c$ and the amount of pull-out decreases.

“I studied English for 16 years but...
...I finally learned to speak it in just six lessons”
Jane, Chinese architect

ENGLISH OUT THERE

Click to hear me talking before and after my unique course download



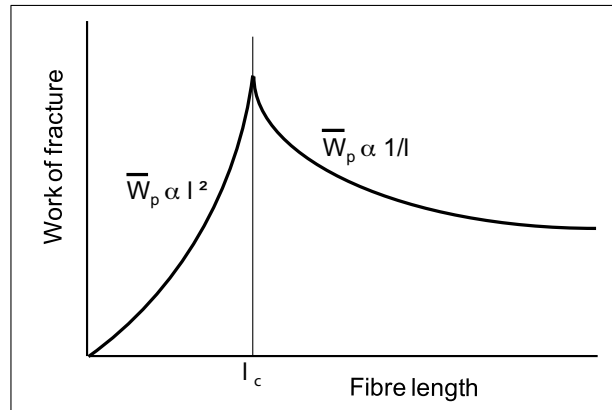


Figure 3.18 Variation of work of fracture per fibre with fibre length

Toughness alongside the primary objectives of stiffness and strength offered by fibre reinforced composites is most desirable in high-performance engineering applications such as the body work for Formula-1 racing cars. However, where toughness is a primary consideration for plastics, then, there are more efficient ways of achieving this both cost wise and productivity by, for instance, incorporating fine rubber crumbs into a polymer as in HIPS. In rubber filled plastics, a crack intersects and stretches rubber particles as illustrated in Figure 3.19: the particles act as little springs, clamping the crack shut, and therefore increasing the load required for the crack propagation.

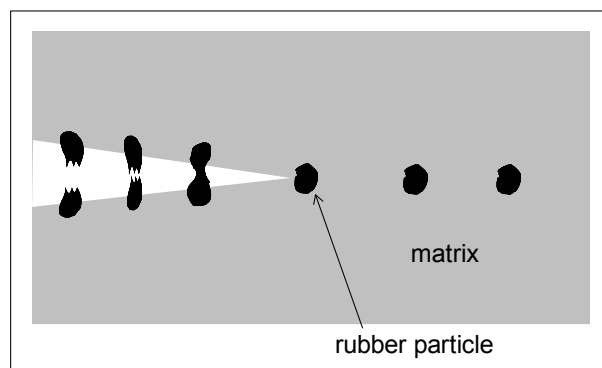


Figure 3.19 Mechanism of plastic toughening with rubber particles

Other failure mechanisms, such as dewetting or crazing are also experienced in particulate filled plastics depending on the elastic moduli of the component materials as illustrated in Figure 3.20. In dewetting, cavitation occurs at the poles of the particles, and in crazing, microcracks form around fillers. These failure mechanisms affect mechanical properties, e.g. crazing is complementary to impact strength.

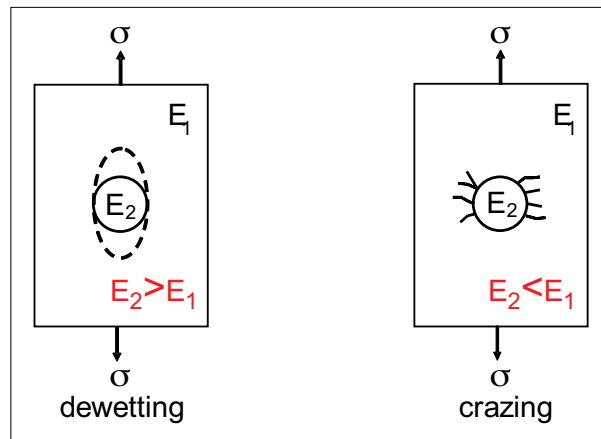


Figure 3.20 Types of failure around particles in a polymer matrix

3.4 Self-assessment questions

1. A polyester (PE) matrix composite contains discontinuous glass fibres (GF) of $5\ \mu\text{m}$ radius and $500\ \mu\text{m}$ average fibre length. If the shear strength of PE is $25\ \text{MPa}$ and the fracture strength of the GF is $2\ \text{GPa}$, comment on the efficiency of fibre reinforcement.

Answer: $\ell (=500\ \mu\text{m}) > \ell_c (=400\ \mu\text{m})$, \therefore the reinforcement is efficient.

2. How can 2-D and 3-D isotropy in the mechanical properties of continuous fibre reinforced composites be achieved? Explain briefly if the achievement of the isotropic behaviour compromises any of the attractive properties of such composites.
3. Demonstrate the anisotropy in the mechanical properties of continuous unidirectional fibre reinforced composites on a plot of Young's modulus vs. fibre volume fraction. Describe how the extent of anisotropy may be reduced and on the same graph also demonstrate the consequences of change in the magnitude of anisotropy.
4. Derive an expression for the Young's Modulus of a unidirectional continuous fibre reinforced polymer-matrix composite in terms of its component moduli when a tensile load is applied parallel to the fibres. Would this expression also be appropriate for predicting the elastic modulus of a short-fibre reinforced composite? Give a brief explanation.
5. A polymer resin of $3.4\ \text{GPa}$ elastic modulus is reinforced with 40% by volume glass fibres of $69\ \text{GPa}$ modulus. The resulting composite is placed under load such that the applied stress in the matrix is $5.7\ \text{MPa}$ and on the fibres $116.4\ \text{MPa}$, calculate the corresponding strains in the matrix and the fibres. Comment on this result.
6. For a UD continuous fibre reinforced composite, show on a graph how the longitudinal tensile strength varies with fibre content. Assume the strain to failure value of the matrix is greater than that of the fibre. Give the relevant equations and define all the terms used in your answer.

7. For a UD continuous fibre reinforced composite, where the strain to failure value of the matrix is greater than that of the fibre, calculate what should be the minimum fibre content above which the tensile strength of the composite increases in linear proportion with fibre content. In your answer, consider as negligible the stress carried by the matrix if the matrix also fails at the time when the fibres break. Take the values for the tensile strength of the matrix and the fibre to be 70 MPa and 2 GPa, respectively.

Answer: $v_f' = 3.4\%$

8. Calculate the axial failure stress for a composite composed of 30% borosilicate glass matrix and 70% Kevlar fibre, assuming that if one of the components fails the entire applied load is transferred to the other component. The tensile strength and the elastic modulus values are 3 GPa and 130 GPa for Kevlar fibre, and 0.1 GPa and 64 GPa for the matrix, respectively.

Answer: $\sigma_{c,L}^ = 2100 \text{ MPa}$*

9. The ratio of the length to the diameter of a fibre is called:
- the aspect ratio
 - the critical ratio
 - the elastic ratio.

DUKE
THE FUQUA
SCHOOL
OF BUSINESS

BUSINESS HAPPENS
HERE.

www.fuqua.duke.edu/globalmba

Learn More >



10. Tensile tests were conducted on a series of short glass-fibre reinforced polyamides with various fibre volume fractions. A plot of elastic moduli values against the fibre volume fractions produces a straight line with a slope of 16 GPa. Determine the fibre reinforcing efficiency, given that the elastic moduli of the matrix and the fibre are 3 GPa and 80 GPa.

Answer: $K = 0.24$

11. Briefly explain the origins of thermal stresses in fibre-resin composites and the effects of the stresses on the product.
12. Explain the concept of 'critical fibre length', ℓ_c , in relation to short-fibre reinforced injection mouldings. Derive an equation for ℓ_c and clarify the factors that dictate the load-transfer between the matrix and the fibres.
13. Calculate the ratio of the average fibre length to the critical fibre length required to ensure that the average tensile stress generated along the fibres was 75% that of the tensile strength of the fibre.

Answer: $\ell / \ell_c = 2$.

14. For a continuous fibre reinforced polymer, use a diagram to explain how the Young's modulus of the composite varies with fibre orientation and fibre content.
15. In terms of the fibre failure stress derive an equation for the average tensile stress that develops along a short fibre, which is longer than the critical fibre length, embedded in a polymer matrix that is subjected to a tensile force along the fibre axis. Determine what the ratio of the average fibre length to the critical fibre length should be in a discontinuous fibre reinforced composite to ensure that its strength in tension was 95% that of the strength exhibited if the fibres in the composite were continuous.

Answer: $\ell / \ell_c = 10$.

16. Short carbon fibres of 10 mm diameter, 230 GPa elastic modulus and 2.9 GPa tensile strength are to be used to reinforce nylon 6,6 of 2.8 GPa elastic modulus at 30% by volume fibre content. If the design stress for the composite is 300 MPa, calculate the load transfer length for the fibres, and indicate if this length is longer than or shorter than the critical fibre length, state your reason. Take the interfacial shear strength between the components of the composite to be 4 MPa. Indicate any assumptions made in your calculation.

Answer: Assume iso-strain and that the maximum stress is transferred to the fibre under the composite design stress. $E_c = 71$ GPa and $(\sigma_f)_{\max} = 972$ MPa.

$\ell_t = [(\sigma_f)_{\max} \times d] / 2\tau$, substituting values gives $\ell_t = 1.2$ mm, which is less than ℓ_c since the fibre tensile strength > 972 MPa.

17. For a fibre, partially embedded in matrix, with the aid of a graph illustrate the stress vs. strain relationship for fibre debonding and fibre pullout processes. Clearly define all the symbols used in your answer.
18. Define the elastic strain energy for a material, and for a specimen under tensile load derive an equation for the strain energy in terms of an important mechanical property of the material. Clearly define all the symbols/terms used in your answer.

19. How would you determine the total energy absorbed during the fracture of a composite from its stress strain curve?
- The gradient of the linear region of the curve
 - The area under the plot times the mass of the composite
 - The area under the plot times the volume of the composite
 - The area under the plot.

Answer: (c)

20. Illustrate the failure processes of fibre debonding and fibre pull-out for a fibre reinforced composite material.

21. What is the most significant energy absorbing mechanism during composite failure?

- Matrix deformation
- Fibre Fracture
- Fibre Pull-out
- Crack deflection and interfacial debonding.

Answer: (c)

22. Illustrate the failure process of dewetting and crazing in a particulate-filled polymer composite.

23. Explain, using a sketch, the mechanism of failure by crazing in a particulate-filled polymer under a tensile load. Briefly describe how the crazing influences the mechanical behaviour of a plastic material.

Join American online LIGS University!

Interactive Online programs
BBA, MBA, MSc, DBA and PhD

Special Christmas offer:

- ▶ enroll **by December 18th, 2014**
- ▶ **start studying and paying only in 2015**
- ▶ **save up to \$ 1,200** on the tuition!
- ▶ Interactive Online education
- ▶ visit ligsuniversity.com to find out more!

Note: LIGS University is not accredited by any nationally recognized accrediting agency listed by the US Secretary of Education. More info [here](#).



24. Explain, using a sketch, the mechanism by which well-bonded rubber particles toughen a polymer.
25. A uni-directionally aligned continuous fibre reinforced resin system is to be prepared. The fibre-to-matrix ratio of elastic moduli is 26. Calculate the required fibre volume content so that the resultant composite has a Young's modulus 11 times that of the resin.

$$\text{Answer: } v_f = 0.4$$

26. Show if it is possible to achieve a unidirectional continuous fibre-reinforced polyester of minimum 1.45 GPa tensile strength and 1.8 maximum specific gravity. The tensile strength and specific gravity of the glass fibre and the polyester resin are, respectively, 3.5 GPa; 2.5 and 50 MPa; 1.35.

Answer: not possible, since, at least, $v_f = 0.41$ is required to achieve the tensile strength, which renders the specific gravity greater than specified.

27. Is it possible to produce a uni-directional continuous aramid-fibre/epoxy-resin composite having longitudinal and transverse moduli of elasticity (E) of 35 GPa and 5.2 GPa, respectively? State reasons. Assume E of the epoxy is 3.4 GPa and that of aramid fibre 124 GPa.

$$\text{Answer: } v_f = 0.26 \text{ for } E_{c,\ell}, \text{ but } v_f = 0.35 \text{ for } E_{c,t}.$$

28. Compute the longitudinal strength of an aligned carbon-fibre/epoxy-matrix composite of $v_f = 0.2$, average fibre diameter of 12 μm , average fibre length of 8 mm, fibre fracture strength of 5 GPa, interface strength of 60 MPa, matrix stress at composite failure of 6 MPa and matrix tensile strength of 60 MPa.

$$\text{Answer: } \ell_c = 0.5 \text{ mm}, \therefore \sigma_{c,\ell}^* = 1048 \text{ MPa}.$$

29. Compute the longitudinal tensile strength of an aligned glass-fibre/epoxy-matrix composite of $v_f = 0.25$, average fibre diameter of 15 μm , average fibre length of 0.5 mm, fibre fracture strength of 3.5 GPa, interface strength of 100 MPa, matrix stress at composite failure of 5.5 MPa and matrix tensile strength of 60 MPa.

$$\text{Answer: } \sigma_{c,\ell}^* = 652 \text{ MPa}$$

30. For a single fibre embedded in a polymer matrix, the maximum work or energy required for debonding, $W_{D(\text{max})}$, and for fibre pull out, $W_{P(\text{max})}$, are given as:

$$W_P(\text{max}) = \pi d \tau \frac{\ell_c^2}{8}; \quad W_D(\text{max}) = \frac{\pi d^2 \sigma_f^2 \ell_c}{48 E_f}$$

- Express the maximum work required to pull out fibres from a unit area of the composite in terms of its fibre volume content and the fibre tensile strength.
 - Show that the energy associated with the fibre pull-out, $W_{P(\text{max})}$, is much greater than the energy of the fibre-matrix debonding, $W_{D(\text{max})}$.
31. Calculate the critical length of the fibres in mm and hence tensile strength of the composite in MPa for a polymer-matrix composite containing aligned short fibres at 40% volume content. The fibres have an average diameter of 20 μm and length of 5 mm. The fibre has a tensile strength of 3 GPa, and the matrix has a yield strength of 100 MPa and a tensile strength of 120 MPa.

$$\text{Answer: } \ell_c = 300 \mu\text{m}; \sigma_{c,\ell}^* = 1272 \text{ MPa}.$$

4 Mechanical and thermal properties

4.1 Introduction

The addition of high strength fibres to a polymer matrix can greatly improve mechanical properties such as ultimate tensile strength, flexural modulus, and temperature resistance. Examples are illustrated in the Table 4.1 for various injection moulded polymers with and without glass fibre reinforcement. The level of improvement becomes much more pronounced with continuous fibre reinforcement, particularly with fibres such as carbon fibre.

Polymer type	Ultimate tensile strength (MPa)		Flexural modulus (GPa)		HDT at 1.8 MPa load (°C)	
	Unfilled	With 30% GF	Unfilled	With 30% GF	Unfilled	With 30% GF
Polyetheretherketone	90	150	4	10	160	285
Polyphenylene sulfide	70	140	5	11	120	260
Epoxy	70	150	2.5	25	175	200
Phenolic	60	90	3	20	180	250
Thermoset polyester	60	140	3	8	130	220
ABS	40	90	2.5	7	90	110

Table 4.1 Typical property values for filled and unfilled polymers (source: MatWeb)

It is important that a full description of a composite material is given when documenting its properties, including fibre content and arrangement, void content, and the level of cure for thermosetting polymers. Sims (1999, p. 407) has covered the particular requirements of composites in determining their mechanical properties, and has also presented (Sims, 2007) lists of ISO and EN standard test methods for various constituent fibres, compound specifications, laminate test methods and thermal analysis test methods for polymer-matrix composites, and also some product specific test methods. Similarly a list of standards, which includes ISO as well as ASTM and BS method, is presented by Hexcel-Qualification Laboratory (2011). A basic description of some of the test methods for characterisation of PMCs is given here.

The **fibre content** of a composite can be obtained by a burn off test according to EN ISO 1172 (1998): the composite specimen is calcinated at about 650°C for approximately one hour to burn off polymer/resin and leave behind the non-combustible fibre. The standard also describes a methodology for determination of the content of any soluble filler present. ISO 14127 (2008), *Method A* specifies three different resin removal procedures for the determination of the mass of fibre in the composite (viz. a combustion procedure, a procedure by digestion in nitric acid and a procedure by digestion in a mixture of sulfuric acid and hydrogen peroxide).

The **void content** can be determined by experimentally measuring the densities of the matrix, the fibre and the composite, and comparing the measured and calculated densities for the composite in accordance with EN ISO 7822 (1999).

The **degree of resin cure** in thermosetting PMCs can be assessed using the Barcol hardness test, ASTM D2583 (2007), which is a simple non-destructive test used as a convenient quality check on the cure of laminates such as chopped-strand mat composites. More sophisticated and rigorous techniques involve the employment of dynamic mechanical analysis (DMA) or DMTA, dielectric thermal analysis (DETA) or dielectric analysis (DEA) and differential scanning caloriometry (DSC) to determine the glass-transition temperature of the material that reflects the degree of curing of the resin. See Table 4.2 for the relevant test methods.

ie business school

#1 EUROPEAN BUSINESS SCHOOL
FINANCIAL TIMES 2013

#gobeyond

MASTER IN MANAGEMENT

Because achieving your dreams is your greatest challenge. IE Business School's Master in Management taught in English, Spanish or bilingually, trains young high performance professionals at the beginning of their career through an innovative and stimulating program that will help them reach their full potential.

- Choose your area of specialization.
- Customize your master through the different options offered.
- Global Immersion Weeks in locations such as Rio de Janeiro, Shanghai or San Francisco.

Because you change, we change with you.

www.ie.edu/master-management | mim.admissions@ie.edu | f t in YouTube U

Property	Test method		
	ASTM	ISO	CRAG
Resin/fibre/void content	C613-1997(2008), D 3171-2011, D2584-2011	1172, 14127: 2008	1000
Void/volatiles content	D3530-1997(2008), D2734-2009	7822	1001
State of cure (by Barcol hardness)	D2583-2007		
Resin gel time	D3532-2012		
Fabric areal weight	D3776-2009		
Density	D792-2000, D1505-2010	1183-1:2012	800
DMA/DMTA properties	D4065, D4473, D4440, D5279	6721:2012 (twelve parts)	
DEA/DETA properties	E2038, E2039		
DSC properties	D3418-2008, E1356-2008	11357:2011 (seven parts)	
DTUL (deflection temperature under load)/HDT (heat deflection temperature)	D648	75-3	
Vicat softening temperature	D1525		306
CTE (linear), out-of-plane	E831		
CTE (linear), in-plane	D696, E228		801
Thermal conductivity	C177	8302	
Thermal diffusivity	E1461		
Specific heat	E1269, C351		
Moisture content	D4019-1988		
Moisture conditioning	D5229-2012		902
Moisture diffusivity	D5229		

Table 4.2 Test methods for structural, thermal and moisture properties

4.2 Tensile properties

Tensile tests are conducted, most popularly, to determine material strength and stiffness (Young's modulus), which are generally determined in two perpendicular directions to accommodate anisotropy that usually exists in the composite laminates. The test methods (see Table 4.3) include ISO 527-5 (2009) (also Parts 1 and 4) and ASTM D3039 (2008). The tensile properties of the composites, as covered in the previous chapter, are highly dependent on fibre content and fibre orientation, but the types of fibre also have a strong bearing on properties. Figure 4.1 shows a basic comparison of the main fibre types in terms of the tensile stress-strain behaviour along the fibre axis for UD fibre reinforced epoxy laminates. The fibre contents by volume are approximately 60% for CF composites and 50% for GF and Aramid composites. The tests are conducted in the fibre direction.

Property	Test method		
	ASTM	ISO	CRAG
Tensile (longitudinal)	D3039, D7205, D3916	527-Parts 1, 4 & 5, 11566	300
Tensile (transverse)	D3039, D5450		301
Tensile (multidirectional)			302,303
Compression	D3410, D695, D6641	14126	400-402
In-plane shear	D3518, D5448, D3846	14129	101
In-plane shear modulus by plate twist		15310	
Short beam interlaminar shear	D2344	14130	100
Double-notch shear	D5379 (Iosipescu)		
V-notched rail shear	D7078, D4255		
Flexure	D7264, D790, D6272, D6415, D4476	14125	200
Open-hole compression	D6484	12817	
Open-hole tensile	D5766		
Bearing	D5961	12815	700
Double-shear bearing	draft		
Charpy impact	D6110	179	
Izod impact	D256, D4812	180	
Falling-weight impact	D3763, D7136	6603	
Compression after impact (CAI)	D7137	18352	403
Mode I fracture toughness	D5528	15024	
Mode II fracture toughness	draft	15114	600
Mixed Mode I-Mode II fracture toughness	D6671		
Tension-tension fatigue	D3479	13003	500
Tension-compression fatigue			500
Bearing fatigue	D6873		
Fatigue crack propagation	E647		

Table 4.3 Test methods for mechanical properties

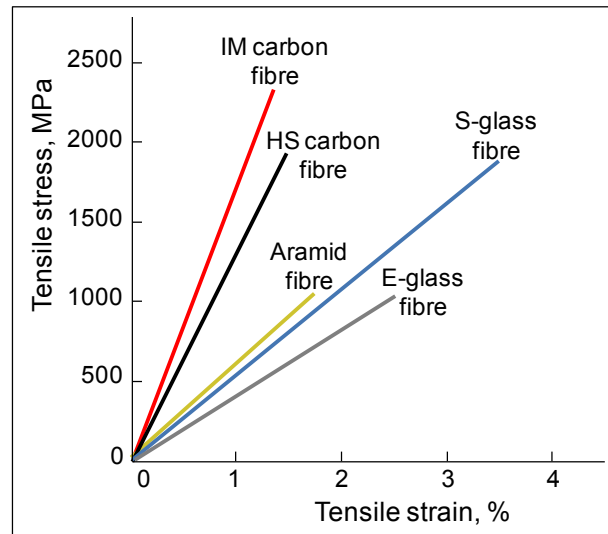


Figure 4.1 Tensile stress-strain plots for various UD composites with different types of fibres (IM – intermediate modulus, HS – high strength) (source: Netcomposites)

4.3 Compressive properties

Compression testing is particularly difficult for PMCs due to the occurrence of macro- and micro-buckling. Most composites are available as relatively thin sheets of laminates (2–4 mm thick) and specimens taken from these sheets would not be suitable for compression tests as they fail by Euler column buckling. Three approaches (Sims, 1999, p. 414) have been used to avoid specimen buckling:

- increased specimen thickness, limited by machine capacity
- short test piece/specimen height (i.e. short gauge length) – most popular approach
- support jig on faces of specimen, for example as used in ASTM D695; however the level of support and load carried by the jig is unknown.

In practice, a short gauge length of 10 mm for a 2 mm thick specimen of unidirectionally reinforced composite or 25 mm for a 4 mm thick fabric or mat reinforced specimen is most frequently used. Standard tests methods for compression testing are given in Table 4.3.

Figure 4.2 shows the compressive stress-strain behaviour along the fibre axis for the same composite systems tested for tensile properties.

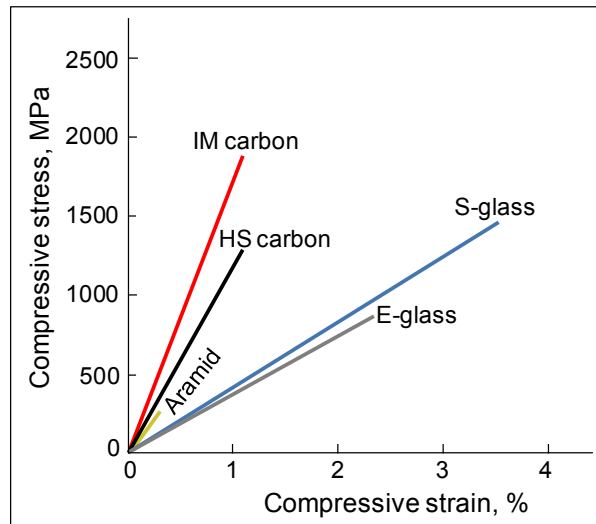


Figure 4.2 Compressive stress-strain plots for various UD composites with different types of fibres (source: Netcomposites)

The graphs in Figures 4.1 and 4.2 show the strengths and maximum strains of the different composites at failure. The gradient of each graph also indicates the stiffness (elastic modulus) of the composite: the steeper the gradient, the higher the stiffness. The graphs also show how some fibres, such as aramid, display very different properties when loaded in compression, compared with loading in tension.

SMS from your computer

...Sync'd with your Android phone & number

FREE
30 days trial!

Go to

BrowserTexting.com

and start texting from your computer!

BrowserTexting



4.4 Flexural properties

Flexural testing, see Figure 4.3, is a convenient method of obtaining equivalent data to that obtained under tension. Sims (1999, p. 416) has indicated the difficulties in drawing parallels between these modes of testing: under flexure a proportion of the measured deflection occurs in shear rather than in flexure, resulting in a modulus 1% lower than that achieved by tensile test. This variation is even greater with composites: about 10% with flexure data obtained at a span length of $16 \times$ specimen thickness. Therefore, in order to obtain a comparable value the span/thickness ratio of 40 is recommended for composites reinforced with UD fibres.

It is also a difficulty that different failure modes are experienced with different types of composites: those with mat reinforcement fail in tension, while specimens of composites with UD fibres often fail on the compression face by micro-buckling assisted by the local compression and shear loads at the mid-loading roller of three-point flexure fixture. Figure 4.4 shows different types of failure modes under flexural loading. A four-point flexure (Figure 4.5) loading delays the initiation of compressive failure by reducing the load on the central loading rollers, and also does not generate shear forces in the mid-span area.

The test standards include ISO 14125 (1998) and ASTM D7264 (2007) that specify for both 3-point and 4-point loading modes.

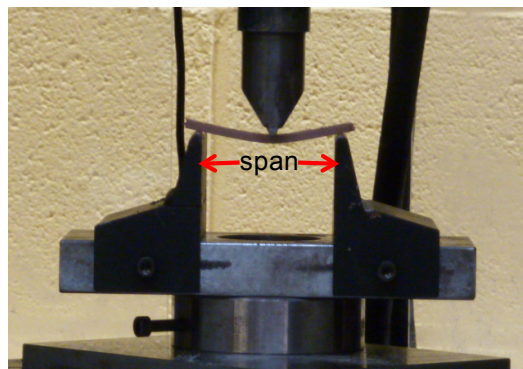


Figure 4.3 A test under 3-point loading arrangement

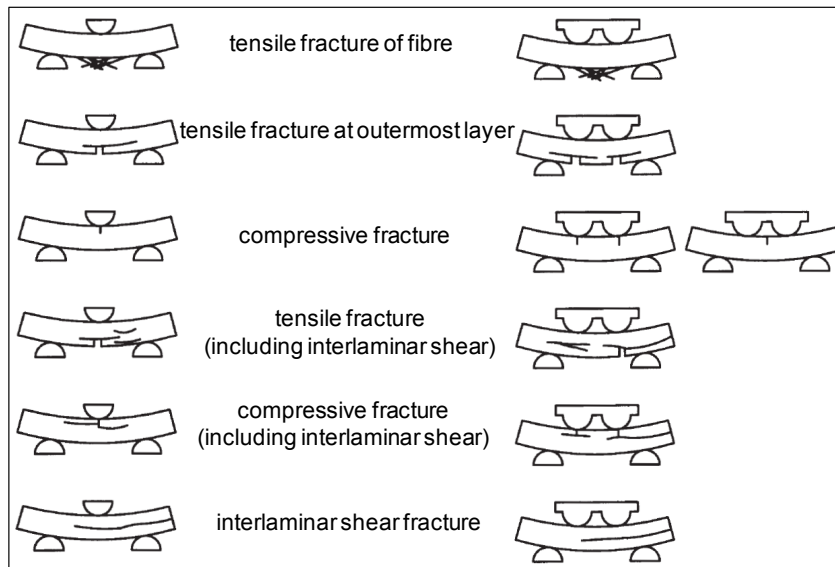


Figure 4.4 Failure modes (tensile-initiated and compression-initiated, remote from the loading points, are acceptable failure modes. Failures initiated by interlaminar shear are not acceptable) (source: DIN EN ISO 14125 (1998))



Figure 4.5 Three and four-point flexure test fixtures (note that with this setup the upper adapter is connected to 4-point loading head) (source: Wyoming Test Fixtures)

Three-point flexural moduli (E) and strength (σ) values for various UD and plain-weave fabric prepreg-laminate composites (epoxy matrix) are given in Table 4.4.

Property	E-glass laminate (50% by vol. fibre)		Aramid laminate (50% by vol. fibre)		HS-CF laminate (60% by vol. fibre)		IM-CF laminate (60% by vol. fibre)	
	UD	fabric	UD	fabric	UD	fabric	UD	fabric
σ_L , MPa	1200	700	550	400	1800	1000	1400	1200
E_L , GPa	42	20	40	25	120	65	140	75

Table 4.4 Flexural properties of various composite laminates under 3-point bending (source: Hexcel, 2013)

4.5 Shear properties

There are various test methods to enable characterisation of in-plane and through-thickness interlaminar shear properties:

- 1) Inter-laminar shear strength (ILSS) is measured by 3-point bending of a short beam in accordance with, for example, ASTM D2344M -00(2006). Figures 4.6 and 4.7 show a test fixture and the modes of failure, and Figure 4.8 shows typical load-displacement graphs for a glass-fibre reinforced polyester system. Specimens should undergo an interlaminar shear failure for a valid test by the standard, as other failure modes frequently occur, such as tension for mat reinforced materials or compression for fabric reinforced materials.

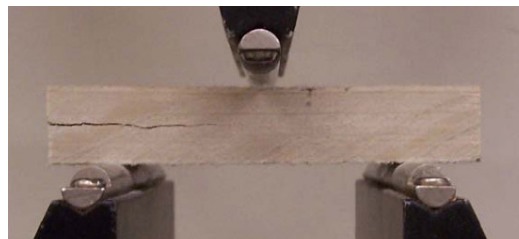


Figure 4.6 Short-beam flexure test set up: showing shear failure of a FRP specimen (source: D'Alessandro 2010)

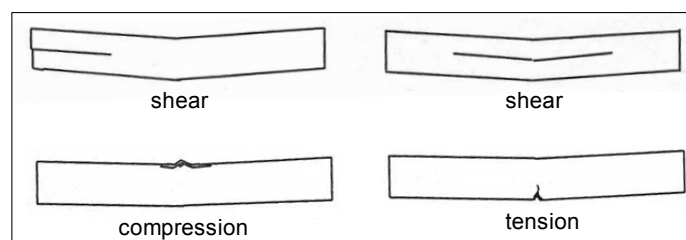


Figure 4.7 Failure modes in the short-beam test

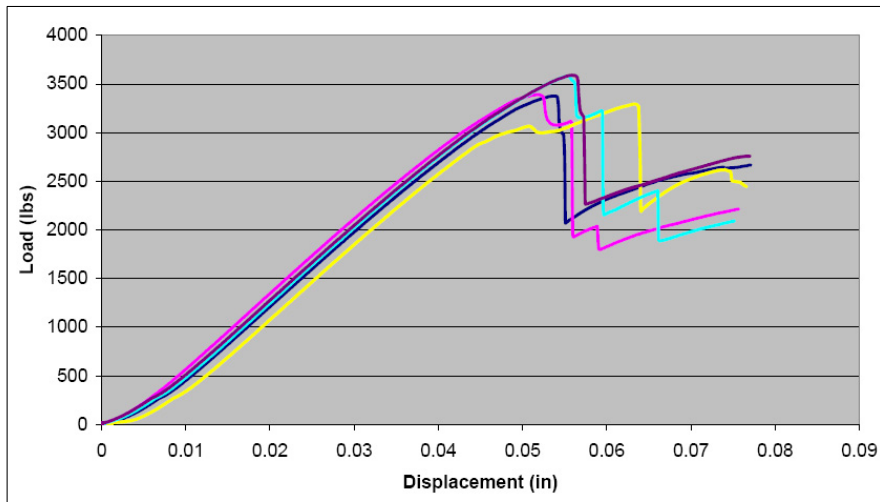


Figure 4.8 Interlaminar shear load-displacement graphs for FRP specimens (source: D'Alessandro 2010)

- 2) Modulus and strength data can be obtained in-plane shear testing in accordance with, for example, ASTM D3518M – 94(2007).
- 3) Modulus and strength data can also be obtained by a double-notch shear test conducted in accordance with, for example, ASTM D5379M – 2007. Figure 4.9 shows the Iosipescu fixture that is used in conducting this test.

The Wake

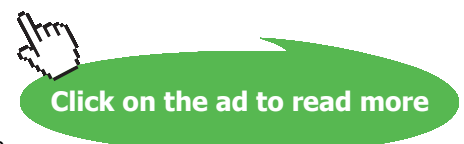
the only emission we want to leave behind

Low-speed Engines Medium-speed Engines Turbochargers Propellers Propulsion Packages PrimeServ

The design of eco-friendly marine power and propulsion solutions is crucial for MAN Diesel & Turbo. Power competencies are offered with the world's largest engine programme – having outputs spanning from 450 to 87,220 kW per engine. Get up front! Find out more at www.mandieselturbo.com

Engineering the Future – since 1758.

MAN Diesel & Turbo



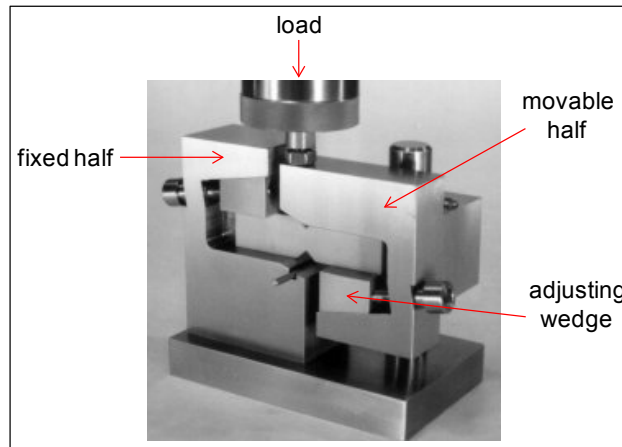


Figure 4.9 Iosipescu shear test set up (source: Wyoming Test Fixtures 2000)

- 4) In-plane shear modulus can be determined by the plate twist method in accordance with BS EN ISO 15310:2005.

Values of ILSS (σ_L) for UD (0°) and in-plane shear modulus (G_{LT}) and strength (σ_{LT}) for various UD ($0^\circ/90^\circ$) and plain-weave fabric prepreg-laminate composites (epoxy matrix) are given in Table 4.5. The fibre contents in the laminates are as indicated in Table 4.4.

Property		E-glass laminate		Aramid laminate		HS-CF laminate		IM-CF laminate	
		UD	fabric	UD	fabric	UD	fabric	UD	fabric
Interlaminar shear	σ_L , GPa	75	50	60	50	80	70	80	70
	σ_{LT} , MPa	60	55	45	40	95	80	95	80
In-plane shear	G_{LT} , GPa	4	4.2	2.1	4	4.4	5.5	4.4	5

Table 4.5 Shear properties of various composite laminates (source: Hexcel, 2013)

4.6 Impact and fracture toughness properties

A background perspective on impact testing of composites is summarised by Adams (2012): “The impact response of composite materials was of only minor interest prior to the introduction of carbon fibre in the mid-1960s. Before that time, the composites in use were primarily reinforced with glass fibres, which performed well under impact loads. This soon proved not to be true for carbon fibres, which are relatively brittle. But since their static strength and stiffness properties were very attractive, development of carbon fibre reinforcements for structural applications continued. However, by the early 1970s the need to characterize the impact response of carbon fibre composites was evident.”

The notched Charpy (ISO 179-1:2010 and ISO 179-2:1997 or ASTM D6110 – 10) and Izod (ISO 180 or ASTM D256 – 10) tests are, in general, not meaningful for composites, and ISO 179 recommends that only unnotched specimens should be tested. The main concern is the inconsistent modes of failure: e.g. in composite specimens tested by Charpy tests, all three basic failure modes (i.e. tension, compression and shear) are exhibited in the same specimen.

Alternatively, tests are conducted on flat plaques or disks using falling-weight (also known as drop weight or falling dart) impact testers with hemispherical impactors. The tests can be conducted in accordance with ISO 6603-1:2000 (not instrumented, e.g. “staircase method”) or ISO 6603-2:2000 and ASTM D3763 – 06 (instrumented). Instrumentation, although expensive, allows more information to be obtained from an impact test, and is now relatively well developed, generally accepted and widely used. All of the impact process can be documented in terms of force and displacement, which then enables the computation of various force, deflection and energy data at different points throughout the test, e.g. at the peak, at a particular event, and at complete specimen fracture.

4.6.1 Instrumented impact tests

Instrumented impact can be performed either on a falling-weight tester, see Figure 4.10, or on a pendulum-type instrument. Most instrumented drop-weight testers allow users to also perform the Izod and Charpy tests by changing the impact striker and specimen support fixture on the instrument.

With instrumented impact, the tip of the falling dart or the pendulum’s hammer is fitted with a load cell. The force-time data during the actual impact event are stored by a high-speed data-acquisition system. These data can be used to generate curves showing force, energy, velocity, and deformation versus time. By analyzing these curves, one can determine the force, energy, and deformation necessary to initiate a crack and to cause total failure; the rate sensitivity of a material to impact loading, and the temperature of a material’s transition from ductile to brittle failure mode.

Variable parameters on a typical drop tower impact system include the mass and height of the impactor, impact velocity and impact energy. Manufacturers, e.g. Instron, produce drop-weight machines with capacities range from 0.7 J up to approximately 28 kJ for testing a wide variety of plastic, metal, and composite materials.

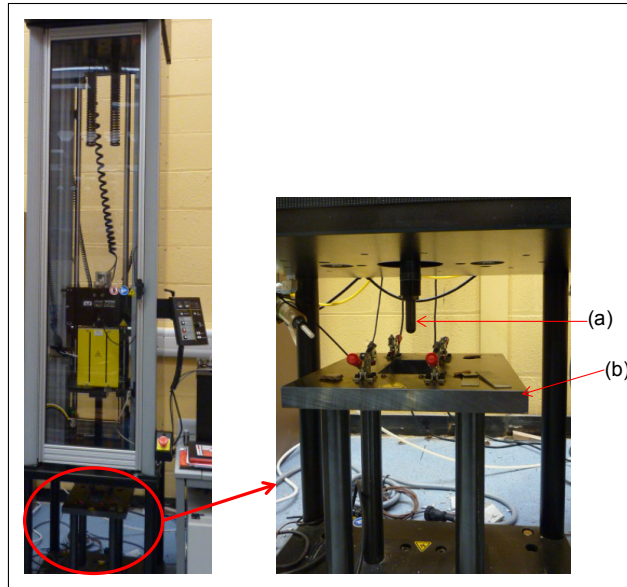


Figure 4.10 Instrumented drop-weight tower: (a) hemispherical-tipped plunger, (b) support platform for flat specimens

Figure 4.11 shows Charpy impact force-deflection traces with associated tested specimens for UD epoxy-CF composites (63 wt% fibre content), where fibres are aligned normal to the line of impact. The complex/rough fracture path includes an axial split failure, along the fibre direction, at the tip of the notch as indicated by the arrow in Figure 4.11 (a).

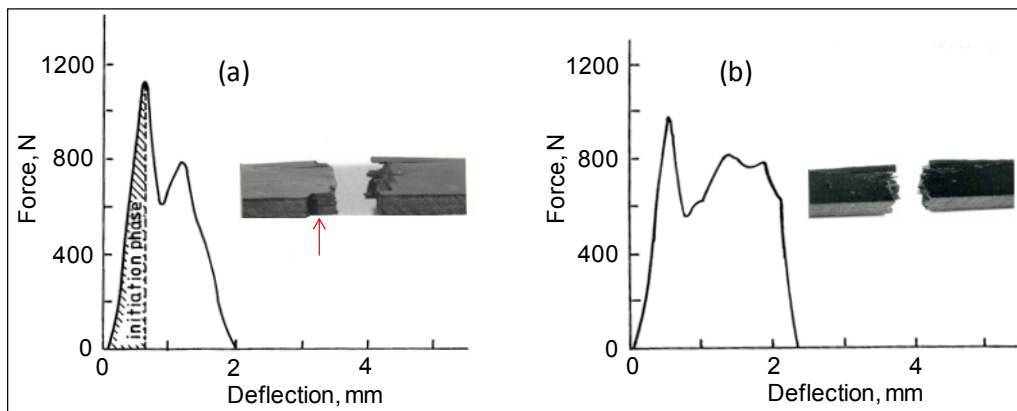


Figure 4.11 Force-deflection traces and fractured test pieces for edge-on impacted longitudinal (a) notched and (b) un-notched specimens (source: Akay 1990)

Figure 4.12 shows the failure processes involved in impact testing of a cellular core composite sandwich panel. The panel is 12.5 mm thick, consisting of approximately 2 mm thick face-skin and 0.6 mm thick back-skin epoxy-CF composite laminates, and closed-cell Rohacell foam (based on polymethacrylimide) core. The face skin consists of a five-ply laminate ($45^\circ/90^\circ/90^\circ/90^\circ/45^\circ$) of 8-HS fabric prepreg with 63 wt% CF content, and the back skin consists of a three-ply laminate ($/90^\circ/45^\circ/90^\circ$) of PW fabric prepreg plies of 60 wt% CF content. The figure clearly shows two main peaks associated with the failures of the composite-laminate skins: as expected the impact energy (as indicated by the area under the force-deflection peak) associated with the failure of the face skin is much greater than that of much thinner back skin.

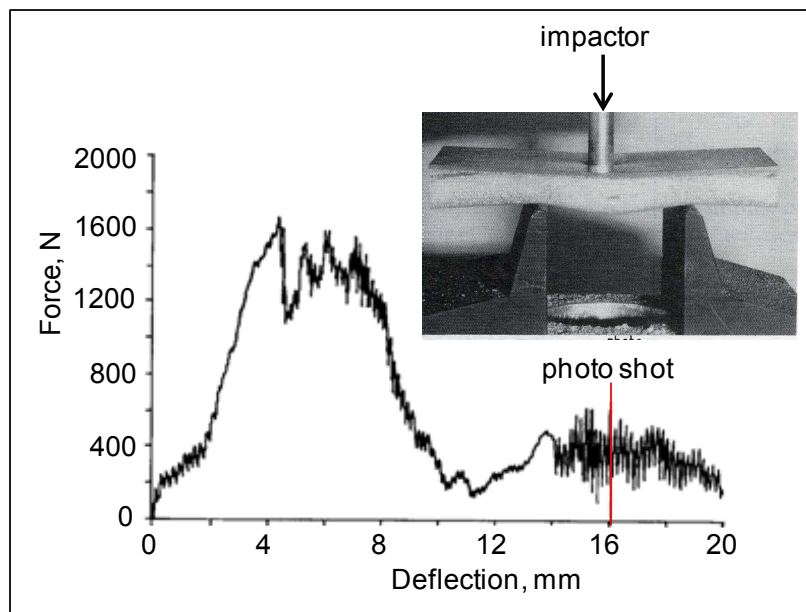


Figure 4.12 Force-deflection trace for a foam-core composite panel impacted with a hemispherical plunger (approximately 13 mm diameter) (the red marker indicates the instant when the flash photography was triggered) (source: Barkley & Akay 1992)

4.6.2 Fracture toughness

Susceptibility to interlaminar failure is a major weakness of advanced laminated composites. Laminated composite materials have their primary failure path between the plies: in Mode I, the crack is propagated along the interlayer/interply plane under tension following the procedures outlined in ISO 15024 (2001) and ASTM D5528-01 (2007) standards. A thin film (e.g. PTFE) is laminated into the composite in the midplane to act as a starter notch in a double cantilever beam (DCB) specimen.

As well as in tensile deformation (Mode I), deformation can occur by in-plane shearing (i.e. sliding) (Mode II), and by out-of-plane shearing (i.e. tearing) (Mode III). These different loading modes are illustrated in Figure 4.13. Shear modes considered are end-notched flexure (ENF), involves three-point bending of a specimen which contains a starter delamination at one end; stabilized ENF, a four-point versions of ENF; and end-loaded split (ELS), where shear stresses are generated by bending down a DCB specimen (i.e. loaded as a cantilever) in a specialised fixture as specified in the Draft International Standard ISO/DIS 15114 (2011).

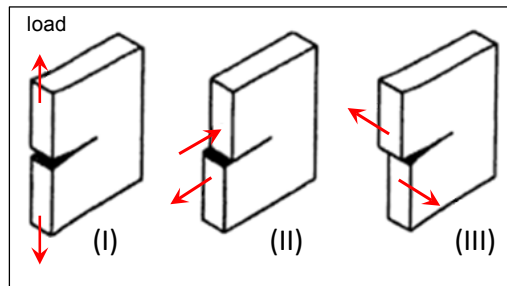


Figure 4.13 An illustration of the loading modes I, II and III

During the DCB test, the onset of delamination movement from the precrack and subsequently at various delamination length increments as specified in the standard methods are marked on the load-displacement trace, see Figure 4.14.

TURN TO THE EXPERTS FOR **SUBSCRIPTION** CONSULTANCY

Subscribe is one of the leading companies in Europe when it comes to innovation and business development within subscription businesses.

We innovate new subscription business models or improve existing ones. We do business reviews of existing subscription businesses and we develop acquisition and retention strategies.

Learn more at [linkedin.com/company/subscribe](https://www.linkedin.com/company/subscribe) or contact
Managing Director Morten Suhr Hansen at mha@subscribe.dk

SUBSCR✓**BE** - to the future

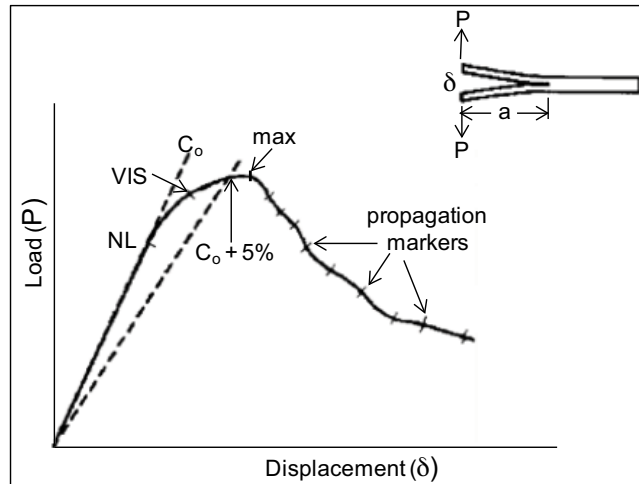


Figure 4.14 Load-displacement trace from DCB test

The initial delamination length, a_0 , subsequent delamination lengths during the crack propagation, a ($a = a_0 +$ the measured delamination length increments) and the corresponding load, P , and displacement, δ , values are recorded. These data, together with the width of DCB specimen, B , allow the calculation of the Mode I critical strain energy release rate (Mode I interlaminar fracture toughness), G_{Ic} , from the simple beam theory expression for the strain energy release rate, G_I , of a perfectly built-in (i.e. clamped at the delamination front) DCB:

$$G_I = \frac{3P\delta}{2Ba}$$

By inserting in the equation for G_I the values for load, displacement associated with growth at a particular crack length, a , the fracture toughness, G_{Ic} , at that crack length can be determined. In this test method, a resistance curve (R curve) showing G_{Ic} as a function of delamination length can be generated to characterise the initiation and propagation of a delamination in a unidirectional specimen.

There are different ways of determining the initiation value of G_{Ic} from the load-displacement data as shown on Figure 4.14: these include G_{Ic} calculated using the load and displacement values at the point of deviation from linearity on the load-displacement curve, i.e. the point of non-linearity (NL); or at a visually (e.g. determined by a microscope) observed initiation on the edge of the specimen (VIS), or at the point on the load-displacement curve where the initial compliance C_0 has increased by 5%, however, the data associated with the maximum-load value should be used if the 5% offset compliance line intersects the curve beyond the maximum point (i.e. 5% or max). Note that compliance $C = \delta / P$.

The main reason for the observed resistance to delamination is the development of fibre bridging, see Figure 4.15, which results from growing the delamination between two 0° unidirectional plies (not an occurrence between plies of dissimilar orientation). Hence in 0° UD laminates G_{Ic} propagation values calculated beyond the end of the implanted insert are questionable, and an initiation value of G_{Ic} measured immediately ahead of the implanted crack starter is preferred by ASTM. Alternative views promote testing from a precrack generated ahead of an insert (which may introduce fibre bridging to the specimen prior to the measurements).

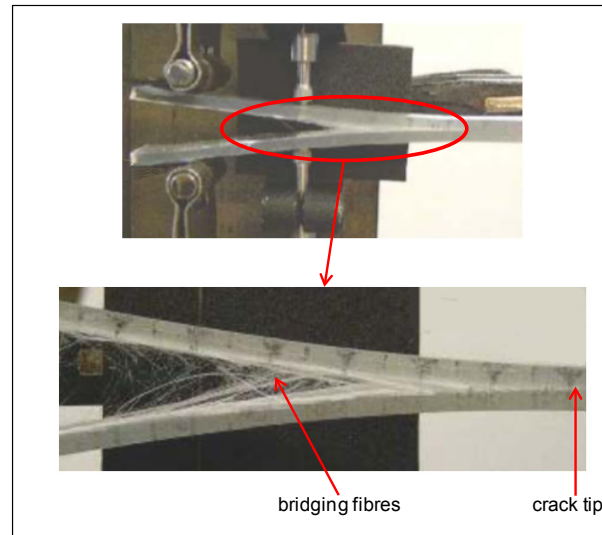


Figure 4.15 Fibre bridging in glass fibre/polyester ($v_f = 43\%$) DCB specimen (source: Szekrenyes 2005)

The ENF and stabilized ENF (SENF) tests enable the determination of the critical strain energy release rate (Mode II interlaminar fracture toughness) for the initiation of a delamination under Mode II loading. The ELS test enables both initiation and propagation values of G_{Ic} to be determined.

Some interlaminar fracture toughness values for unidirectional CF/epoxy resin, CF/polyether sulphone and CF/polyether ether ketone composite systems are presented in Table 4.6.

Composite fibre/matrix	Fracture toughness (G_{Ic}), J/m ²		
	fracture mode	initiation	propagation
T300/6376	Mode I	270	270
	Mode II (ELS)	600	–
	Mode II (ENF)	650	–
XAS/913	Mode I	280	280
	Mode II (ENF)	660	–
T300/914	Mode I	140	140
	Mode II (ENF)	720	–
T800/924	Mode I	220	250
	Mode II (ELS)	440	600
AS4/PES	Mode I	800	2020
	Mode II (ELS)	1230	1840
	Mode II (ENF)	1290	–
AS4/PEEK	Mode I	1680	2420
	Mode II (ELS)	1740	3160
	Mode II (ENF)	1820	–

Table 4.6 Typical values of interlaminar fracture toughness for various composites (source: Robinson & Hodgkinson 2000 p. 172)

An evaluation of the fracture-mechanics test methods for sandwich composite panels has been presented by Adams et al.

wethrive.net

How to retain your top staff
FIND OUT NOW FOR FREE

DO YOU WANT TO KNOW:

- What your staff really want?
- The top issues troubling them?
- How to make staff assessments work for you & them, painlessly?

Get your free trial
Because happy staff get more done



4.6.3 Compression after impact

In a full penetration drop-weight impact test, the results of interest are the maximum force and the energy absorbed to maximum force, and/or the total energy absorbed during the full penetration process. Alternatively, the test panel may be subjected to a prescribed level of impact energy, selected to induce local damage without puncture. The induced surface damage may be barely visible and is referred to as barely-visible impact damage (BVID). Non-destructive testing techniques, such as ultrasonic C-scan, are used to quantify the extent of internal damage. The impact causes delamination between the ply layers, plus some associated fibre and matrix damage without necessarily showing any blemish on the impacted surface. The impact energy applied is considered to be equivalent to a tool dropped by a maintenance engineer or debris thrown up from a runway during take-off or landing.

BVID can cause a reduction in mechanical properties: compressive strength is particularly susceptible to such localised material degradation. To gauge this, a compression after impact (CAI) test can be conducted in accordance with a recognised standard test method, e.g. ASTM D7137 (2012) or ISO 18352 (2009). The test assesses the damage tolerance of a panel (e.g. an aircraft wing skin). Testing involves inducing impact damage on 100 mm by 150 mm panels on an instrumented drop-weight impact tester using the ISO 6603-2 (2000) method. The damaged panels are then subjected to a uniform in-plane compressive force along its 100 mm long edges. The specimen is simply supported along all four edges to inhibit buckling as shown in Figure 4.16.

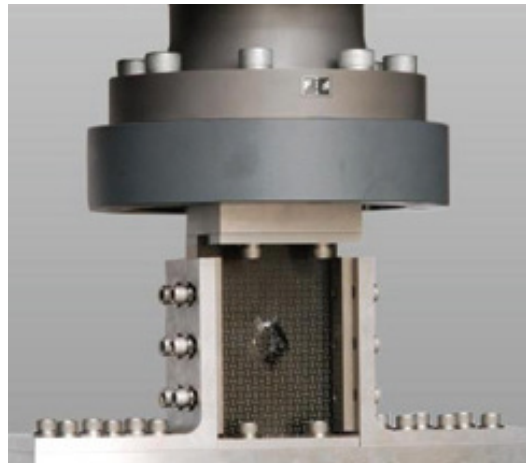


Figure 4.16 Compressive residual strength support fixture with specimen in place

A schematic plot of compressive strength after impact against impact energy is presented in Figure 4.17.

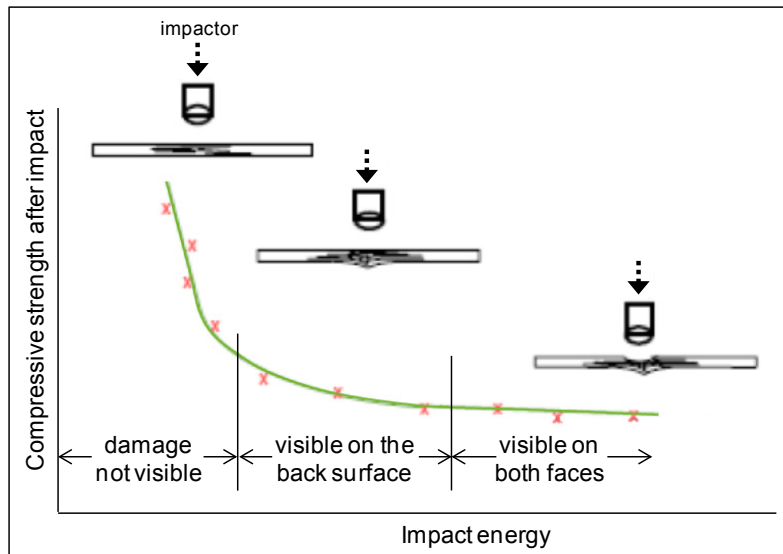


Figure 4.17 Effects of impact on composite laminates (source: Roach & Duvall)

Experimental data is given in Figure 4.18 for PW carbon fibre/epoxy resin composite panels (10-ply laminates of 2.2 mm thickness). The associated ultrasonic C-scans for these specimens showing the level of impact damage prior to compression testing is shown in Figure 4.19. Note that for the same impact energy level, as would be expected the damaged area is smaller for the toughened epoxy system.

Struggling to get interviews?

Professional CV consulting & writing assistance from leading job experts in the UK.

[Visit site](#)

Take a short-cut to your next job!
Improve your interview success rate by 70%.

 **TheCVagency**
Visit theagency.co.uk for more info.

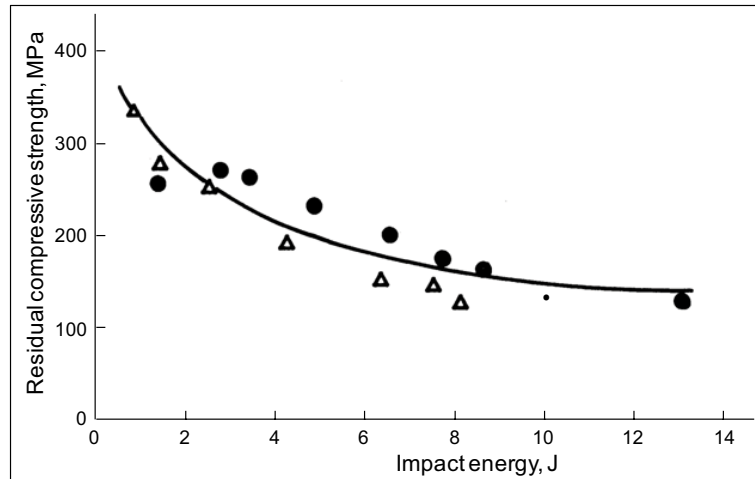


Figure 4.18 Residual compressive strength vs. incident impact energy for: (Δ) PW CF/epoxy, (●) PW CF/toughened epoxy (source: Akay 1988)

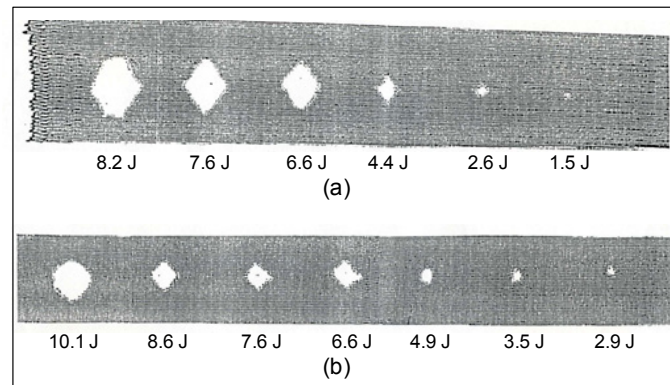


Figure 4.19 C-scans of impact-damaged test pieces: (a) PW CF/epoxy, (b) PW CF/toughened epoxy (source: Akay 1988)

An account of post-impact residual compressive strength of composite sandwich panels is given here by summarising a study (Akay & Hanna 1990) conducted on panels containing Rohacell (polymethacrylimide foam) and Nomex honeycomb cores. The results for three different panels are presented here. The face skins for the panels consisted of approximately 2 mm thick 8-harness (8H) satin weave fabric CF/epoxy laminate, and the back skins of approximately 0.6 mm thick PW fabric CF/epoxy laminate. The cores were approximately 12.5 mm thick and consisted of 51 kg/m³ density Rohacell foam for Panel A, 48 kg/m³ density and 3.1 mm cell opening Nomex honeycomb for Panel B, and 71 kg/m³ density Rohacell foam for Panel C. The panel specimens of 76 mm by 127 mm were impacted on their face skins at various energy levels up to 10 J. The extent of damage, confined to the face skin and the core, was measured by ultrasonic scanning, see Figure 4.20 for the C-scans.

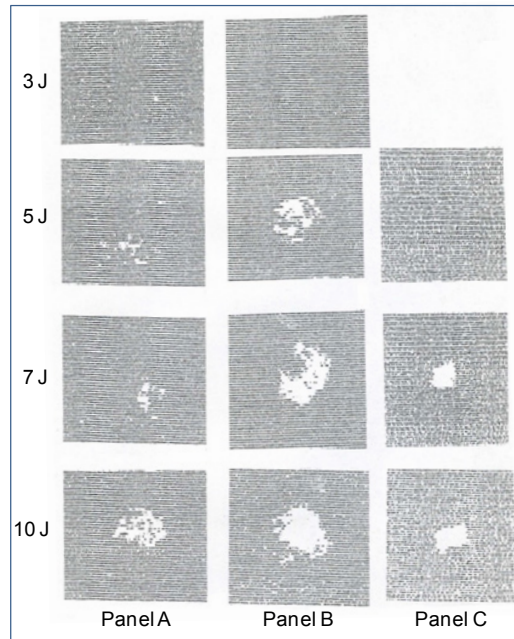


Figure 4.20 C-scans of impact-damaged composite sandwich panel pieces
(source: Akay & Hanna 1990)

Damage was detected by C-scan at a 3 J incident impact level but was only visible beyond 5 J.

gaiTEYE
Challenge the way we run

**EXPERIENCE THE POWER OF
FULL ENGAGEMENT...**

.....

**RUN FASTER.
RUN LONGER..
RUN EASIER...**

**READ MORE & PRE-ORDER TODAY
WWW.GAITEYE.COM**

Figure 4.21 shows that, as would be expected, compressive load to failure for undamaged Rohacell panels increases with foam density. With impact damaged specimens, the load to failure reduces asymptotically as the incident impact energy level increases. It is also clear that Rohacell 51 panels had limited residual capacity. Rohacell 71 and Nomex honeycomb panels exhibited identical capacity.

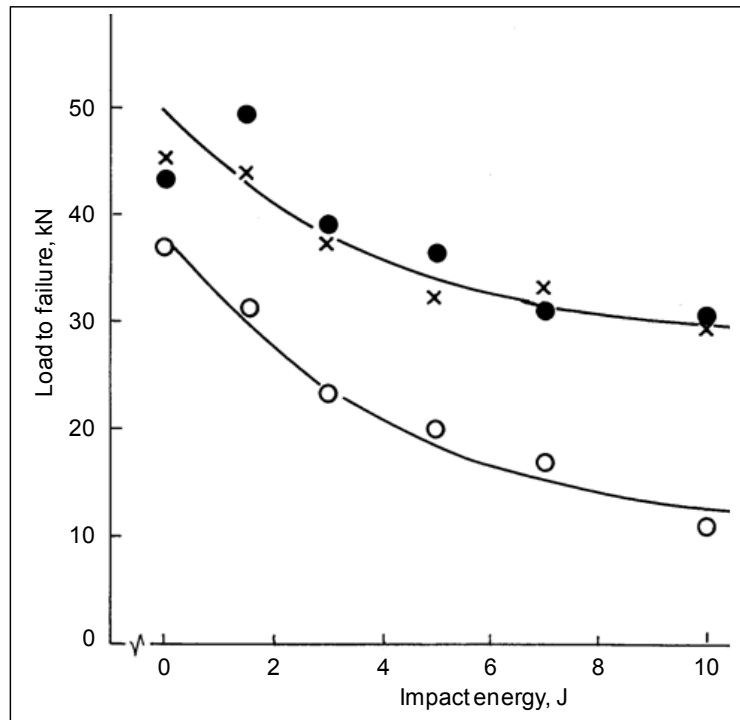


Figure 4.21 Compressive load to failure vs. incident impact energy for: (o) Panel A, (x) Panel B, and (•) Panel C CF/toughened epoxy (source: Akay & Hanna 1990)

4.7 Bearing strength

Mechanical fastening is usually the only feasible means of joining highly loaded composite (thick) components. In mechanical fastening, the bolt bears down on the faces of holes passing through the joint members; the resulting bearing failure causes elongation of the hole, allowing bending and subsequent fatigue of the bolt or substructure.

Bearing strength of the composites is, therefore, particularly relevant in bolted joints. Successful adoption of bolted joints depends on a clear understanding of pin bearing strength, which is of critical importance since such joints are employed in critical engineering applications such as aerospace structures. The serious accident that an Airbus 300 jet aircraft suffered in 2001 during its flight from New York to Santo Domingo, Dominican Republic, caused the death of 260 people on board and five people on the ground. The accident was attributed to the tail of the plane breaking off from the fuselage under the force of swirling wakes generated by another jetliner flying at a path, approximately 1.2 km away. The tail assembly of the aircraft was constructed from carbon-fibre/ polymer composite and bolted on to the fuselage and the failure had occurred in the vicinity of the bolted joints as shown in Figure 4.22. The figure shows that the tail assembly has snapped off at the bolted joints, however without closer inspection, it is difficult to conclude whether the failure is caused by an inherent weakness in the composite material or by an actual aspect of the joint.

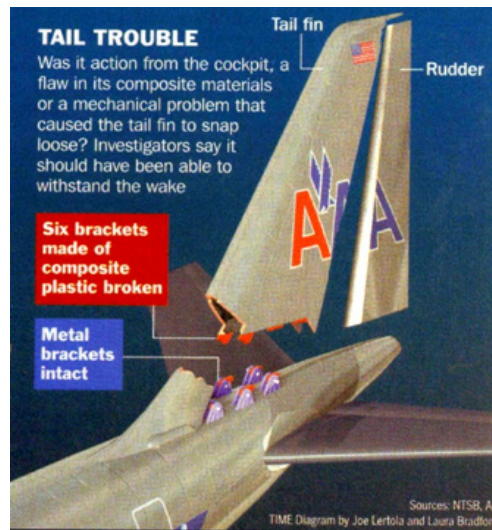


Figure 4.22 Illustration of the aircraft tail section failure at the November 2001 crash (source: TIME, November 26, 2001)

The bolted joints are vulnerable to bearing failures, where the mode of failure is complex and depends on factors such as the structure and properties of the materials joined together, the size and the geometry of the joint, e.g. the pin-hole diameter, thickness and width of the lug, the distance between the centre of the hole and the free end (edge) of the fastener lug, and the level of clamping force applied to the joint (see Akay 1992 and Akay & Mun 1995, Baker et al. (2004, p. 289)). Various failure modes are possible: the main modes are end-section bearing (i.e. crushing failure ahead of the bolt), net-section tension (tensile failure across the reduced section), edge-section shear (double shear out parallel to the direction of load) and end-section cleavage (tear out or split forward of the bolt), see Figure 4.23. In addition, any mixture of these failure modes may also be experienced, such as bearing-tension-cleavage combination or tension-shear, etc. Furthermore, bolt-head pulling through the laminate (a problem particularly with deeply countersunk holes) and bolt failure due to bearing failure can also occur.

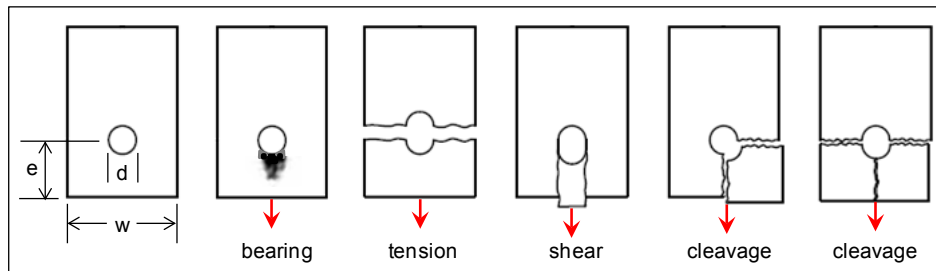


Figure 4.23 Failure modes

A standard test method for bearing strength of polymer-matrix composites is given in ASTM D5961 (2010), ISO 12815:2013 and for polymer-matrix composites in CRAG test method 700 (Curtis 1988). The tests are normally conducted in tensile mode, employing a test fixture shown in Figure 4.24. The test produces a load-displacement graph (see Figures 4.25 and 4.26), from which the bearing strength properties expressed in terms of the maximum stress sustained by the specimen, the stress at initial failure and the stress at which the bearing hole is deformed by 4% of its diameter may be determined.

This e-book
is made with
SetaPDF



SETASIGN

PDF components for PHP developers

www.setasign.com



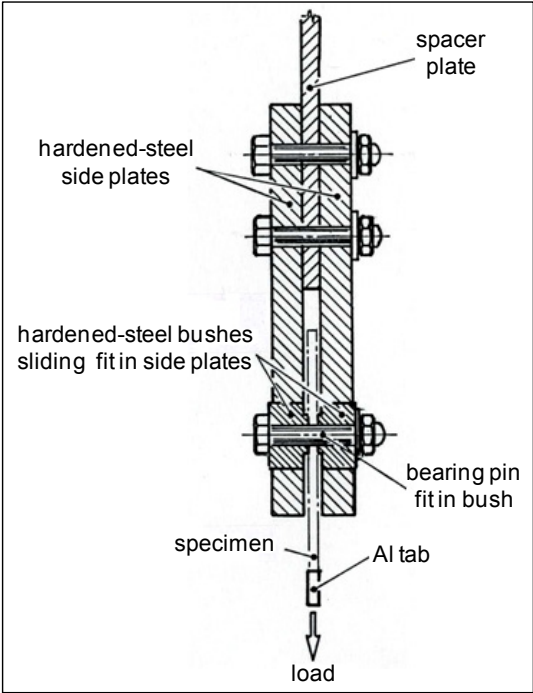


Figure 4.24 An illustration of specimen test fixture for bearing strength

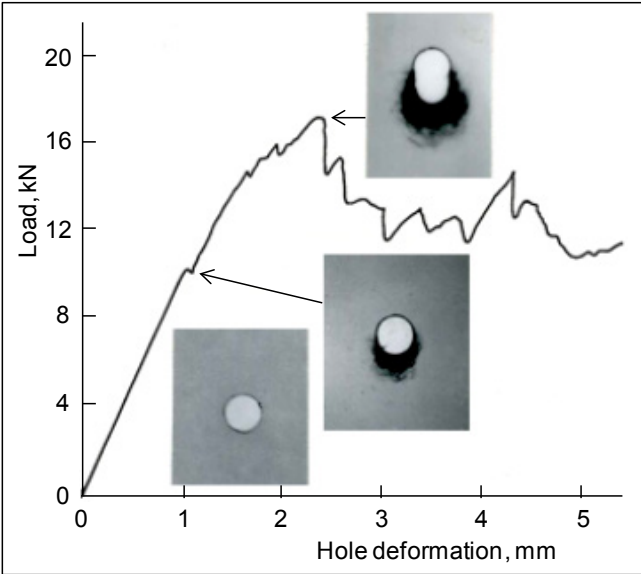


Figure 4.25 Typical load-displacement curve with X-ray micrographs of specimens at various levels of load for CF/epoxy composite (loading at 1 mm/min via 4.8 mm diameter pin) (source: Akay 1992)

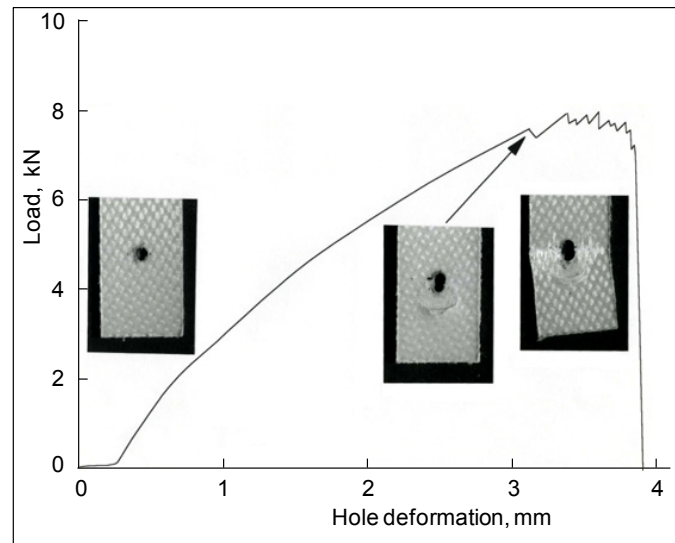


Figure 4.26 Typical load-displacement curve with photographs of specimens at various levels of load for Kevlar/epoxy composite (source: Akay & Mun 1995)

The bearing strength and the type of failure that occurs depends on the ratio of the specimen width to the diameter of the pin-hole (w/d), the ratio of the edge distance to the diameter of the hole (e/d), and also the clamping force (or constraint pressure) applied to the bolted assembly as shown in Figure 4.27.

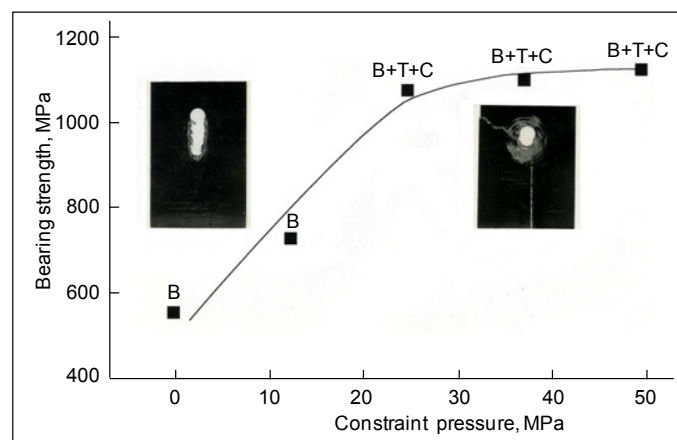


Figure 4.27 Bearing strength vs. constraint pressure for a CF/epoxy resin composite system with associated failure modes indicated as B – bearing, T- tension and C – cleavage (source: Akay 1992)

4.8 Fatigue and wear

Wear is a material surface damage caused by cyclic straining of one or both of the components that are in contact. The standard test methods (see Akay (2012, p. 204) and Franek et al. (2009) can be employed in wear testing of PMCs, while accounting for the anisotropic nature of the material arising from fibre orientation and fibre ends.

A definition of **fatigue** has been given as the ultimate failure of a material or a component by the application of a varying load whose maximum amplitude, if continuously applied, is insufficient to cause failure (Hull, 1981, p. 221). The test entails cyclic loading of a specimen/component, usually under constant amplitude and frequency, to either failure or for a given number of cycles (fatigue life). Note that for CFRP materials used in aerospace applications, 10^6 cycles is typically identified as the material's design fatigue life.

One of the common ways of representing fatigue is by constructing an S-N curve, where N is the number of cycles to failure at the stress (or strain) level (S) required to fail the sample. The actual shape of the S-N curve varies from one material to another. It should be noted that for many applications variable amplitude and frequency loading is more representative of service conditions, but such a variable pattern of loading is more complicated and requires software packages such as Instron Wavemaker to enable the input of variable waveforms (spectral loading).

Various shapes of waveform can be used for testing; these include triangular, square, trapezoid, saw-tooth as well as sinusoidal form, which is normally considered.

**YOU THINK.
YOU CAN WORK
AT RMB**

 **RAND
MERCHANT
BANK**
A division of FirstRand Bank Limited
Traditional values. Innovative ideas.

Rand Merchant Bank uses good business to create a better world, which is one of the reasons that the country's top talent chooses to work at RMB. For more information visit us at www.rmb.co.za

Thinking that can change your world

Rand Merchant Bank is an Authorised Financial Services Provider



Click on the ad to read more

Fatigue of metals has been studied for over a century and despite significant advances it remains a major cause of catastrophic failure of structures. Composites, on the other hand, have high potential for fatigue resistance. However, this should not lead to complacency in evaluation of fatigue in composites: Harris (1999, p. 130) states, “It is not uncommon for users of composite materials, even in the aerospace industry, to express the belief that composite materials – specifically, carbon-fibre-reinforced plastics – do not suffer from fatigue. This is an astonishing assertion, given that from the earliest days of the development of composites, their fatigue behaviour has been a subject of serious study, and what is usually implied is that, because most CFRP are extremely stiff in the fibre direction, the working strains in practical components at conventional design stress levels are usually far too low to initiate any of the local damage mechanisms that might otherwise have led to deterioration under cyclic loads.

The idea of using composites, especially CFRP, only at very low working strains raises two important issues. The first is the obvious one that by using expensive, high-performance materials at small fractions of their real strength, we are over-designing or, in more cost-conscious terms, we are using them uneconomically. The second is that since anisotropy is a characteristic that we accept and even design for in composites, a stress system that develops only a small working strain in the main fibre direction may easily cause strains normal to the fibres or at the fibre/resin interface that may be high enough to cause the kind of deterioration that we call fatigue damage. In designing with composites, therefore, we cannot ignore fatigue. And it follows directly that, in addition to needing to understand the mechanisms by which fatigue damage occurs in composites, we need access to procedures by which the development and accumulation of this damage, and therefore the likely life of the material (or component) in question, can be reliably predicted.”

A similar reminder is given by Kelly (1989, p. 77), “The fatigue properties of composites are anisotropic, i.e., directionally dependent, and can be dangerously low in some directions. This warrants careful use of composites based on proper understanding of the mechanisms that govern the fatigue behaviour.”

Fatigue testing can be conducted on specimens or on actual parts. The subject is covered here only with respect to test coupons: these include undamaged as well as pre-conditioned/damaged specimens, e.g. those with machined holes and notches, where the response of materials and components to the presence of stress raisers such as holes and notches is tested. Tests are also conducted on notched specimens applying fracture mechanics to measure the rate of growth of cracks as a function of the stress intensity factor under cyclic loading. For crack propagation, da/dN data, the number of cycles required to extend a crack of length, a , by a length da is monitored with increasing stress.

4.8.1 Fatigue of undamaged coupons

The details of the fatigue testing for PMC samples are described in ASTM D 3479:2012 and ISO 13003:2003 standard methods: a continuously alternating mechanical load or displacement is applied at a constant amplitude and frequency to the specimen under test until the specimen either fails or reaches a certain number of fatigue cycles. By testing specimens at each of several percentage levels of the ultimate stress or strain a plot of the stress or the strain versus number of fatigue cycles can be constructed. This plot provides information as to the fatigue life of the material or how many fatigue cycles the material can sustain at a certain stress/strain level before failure will occur.

The standards mentioned above make recommendations for tests under tensile mode of loading; the ISO standard also includes the flexural loading mode. In general, a fatigue test can be performed under load or under displacement (or strain) control. Tensile tests normally use load control, whereas the flexural loading is conducted under displacement/deflection control.

Under tensile loading mode, different fatigue regimes such as tension-tension, compression-compression, etc. may be adopted (see Figure 4.28).

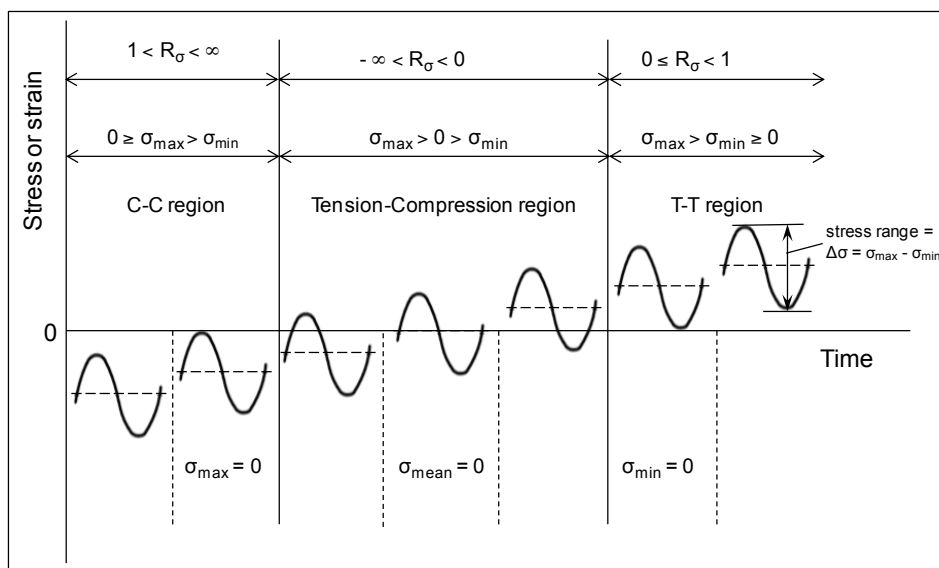


Figure 4.28 Examples of fatigue regimes: C – compression, T – tension (source: ISO 13003)

The sign and the value of the parameter R indicates the regime of loading used. R is the ratio of the minimum stress, strain or displacement to the maximum stress, strain or displacement within a fatigue cycle. Accordingly,

$$\text{stress ratio, } R_{\sigma} = \sigma_{\min} / \sigma_{\max}$$

$$\text{strain ratio, } R_{\epsilon} = \epsilon_{\min} / \epsilon_{\max}$$

displacement ratio, $R_d = d_{\min} / d_{\max}$,

load ratio, $R_F = F_{\min} / F_{\max}$,

Therefore, for instance, $R = -1$ is fully reversed tension-compression of equal magnitude, $R = 0.1$ is tension-tension cycling where the maximum value is ten times the minimum value, and similarly $R = 10$ is compression-compression where the maximum value is ten times the minimum value, etc.

By testing specimens at various % levels of the ultimate stress or strain, an S-N curve can be plotted. This plot provides information as to the fatigue life of the material or how many fatigue cycles the material can sustain at a certain stress level before failure will occur. ISO recommended fatigue stress levels for a tensile-test procedure, suitable for glass-fibre-reinforced plastics, are typically 80, 55, 40 and 25% of the UTS (with higher values for flexural tests or for CFRP).

In an S-N curve, stress can be replaced with load, stiffness, moment, torque, strain, deflection, or crack propagation. Alternatively, it can be expressed as normalised values with respect to the values of the relevant properties obtained under static conditions.



Discover the truth at www.deloitte.ca/careers

Deloitte.

© Deloitte & Touche LLP and affiliated entities.



Click on the ad to read more

Temperature of the specimen should be monitored during the test: autogenous (self generated) heating is limited, according to the standards, to a 10°C temperature rise. The test frequency is set at 2–5 Hz for glass-fibre-reinforced plastics in order to limit the autogenous heating. Higher frequencies can be employed for carbon-fibre-reinforced plastics because of the lower strains applied and the better heat dissipation due to the higher thermal conductivity of the material.

The fatigue failure mechanisms for unidirectional composites loaded in the fibre direction is described in various references such as Kelly (1989, p. 77) and Gamstedt & Andersen (2001, p. 20) using a fatigue-life diagram (see Figure 4.29). The strain rather than stress is used on the illustration since strain is roughly the same in fibres and the matrix while stress differs in the two phases depending on the volume fraction of fibres and the elastic moduli of the two phases. The axial strain level in a longitudinal composite is globally the same for the fibres and the matrix. The strain description also offers an advantage for multidirectional laminates, since all plies are globally subjected to the same strain for in-plane loading, i.e. no significant bending. The static strain to failure is in practice controlled by the strain to failure of the fibres.

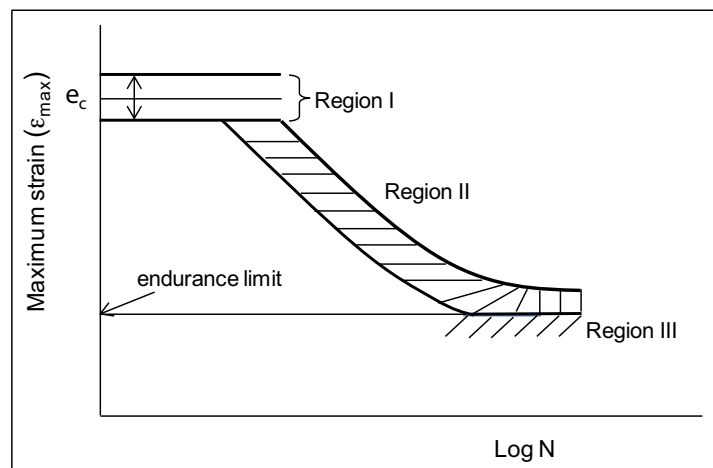


Figure 4.29 Fatigue-life diagram for UD composites loaded in fibre direction

The diagram is divided into three regions: in Region I, the strain level generally coincides with the scatter band of the static strain to failure of the composite (ϵ_c), since virtually all the load is carried by the fibres in conventional polymer-matrix composite materials. From a design point of view, the fatigue behaviour in Region I is not of central interest, since the lifetimes are short (damage growth is cycle independent) and strain levels can be analysed in terms of static strains to failure.

Region II is also called the progressive region. Damage mechanisms responsible for the downward slope of this region are progressive matrix cracking, matrix shear yielding and fibre-matrix debonding/successive fibre breakage (see Figure 4.30), and these govern fatigue life. The slope of the S-N curve is a measure of the resistance/sensitivity of the material to fatigue.

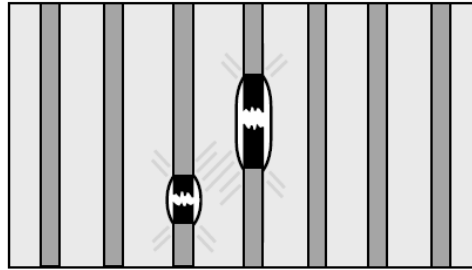


Figure 4.30 Fibre breakage by debonding and yielding
(source: Gamstedt & Andersen 2001 p. 22)

The objective is to design against the fatigue limit, i.e. structure dimensions are chosen so that strains or stresses above the fatigue limit are not allowed in the composite. Below the fatigue limit (endurance limit), no failure is expected within an indefinitely long time or a certain chosen high number of cycles, say 10^8 cycles. Labelled as Region III, the strain levels here are so small that damage does not develop at all, and the material behaves perfectly elastically in cyclic loading, or any progression of damage becomes constrained and arrested by the inherent heterogeneous microstructure of the composite (i.e. the matrix cracks remain arrested by the fibres). However, cracking in this region can allow environmental ingress and lead to degradation in systems with environmentally sensitive fibres, such as glass fibres.

Composites tend to stabilize early under fatigue loading through the following mechanisms, each of which absorbs energy or redirects the energy to other parts of the structure:

- matrix micro-cracking
- debonding: blunting of cracks at the fibre surface which reduces further crack growth and transfers the load to the fibre
- delaminations between layers which may relieve internal cure stresses
- energy dissipation resulting through matrix viscoelastic damping.

Examples of S-N curves are shown in Figures 4.31–4.37. Figure 4.31 shows typical fatigue-life curves for unidirectional composite laminates of glass-fibre/epoxy, carbon-fibre/epoxy and Kevlar/epoxy that were tested under cyclic tension-tension loading. In the figure, the maximum applied cyclic tensile strain (ϵ_f) is expressed in the normalized fatigue strain (ϵ_f / ϵ_o) form, where it is divided by the static tensile failure strain of the composite (ϵ_o). Of the three materials, the glass-fibre/epoxy is the most sensitive to cyclic loading and suffers the worst level of fatigue deterioration at a given number of cycles. High susceptibility of glass-fibre/epoxy to fatigue-induced failure under tension-tension loading is due to the low stiffness of the glass fibre reinforcement, resulting in damaging levels of strains in the matrix.

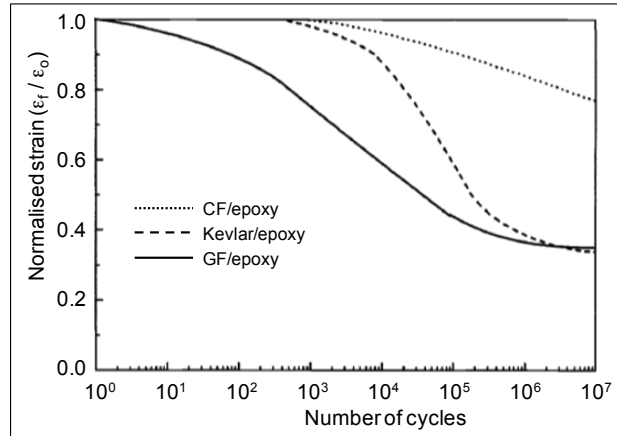


Figure 4.31 Fatigue-life curves for unidirectional composites subject to tension-tension loading (source: Baker et al. 2004 p. 244)

Figure 4.32 shows that the static tensile modulus and strength of $[0/90]_s$ glass-fibre/epoxy composites decrease rapidly with increasing numbers of load cycles before reaching a constant level.

**I WANT TO CHANGE DIRECTION,
AND THE WORLD.**

GOT-THE-ENERGY-TO-LEAD.COM

We believe that energy suppliers should be renewable, too. We are therefore looking for enthusiastic new colleagues with plenty of ideas who want to join RWE in changing the world. Visit us online to find out what we are offering and how we are working together to ensure the energy of the future.

RWE
The energy to lead



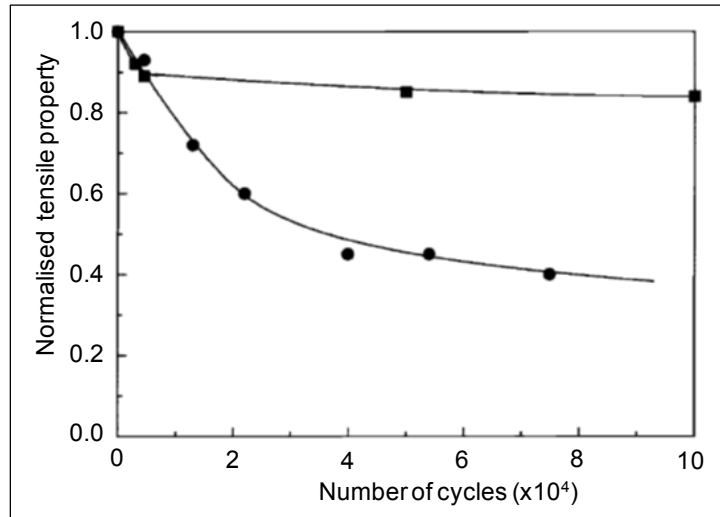


Figure 4.32 Effect of number of tensile load cycles on the (■) Young's modulus and (•) tensile strength of a $[0/90]_s$ glass/epoxy composite (source: Baker et al. 2004 p245)

A comparison of the fatigue responses of composites containing continuous and well-aligned discontinuous fibres (chopped fibres 3 mm long) is shown in Figure 4.33. The results are for unidirectional composites of the same carbon/epoxy system, XAS/914, with 35 % fibre volume content.

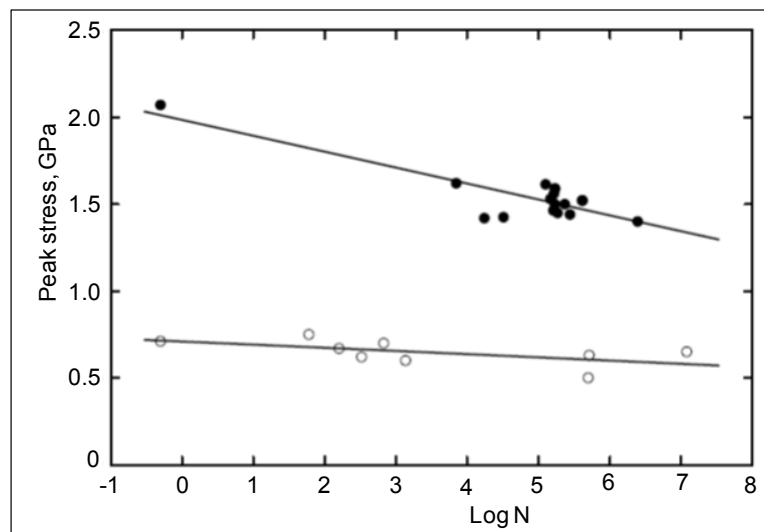


Figure 4.33 Stress/logN-life data for unidirectional composites of XAS/914 carbon/epoxy laminates reinforced with (•) continuous and (o) discontinuous fibres ($R = 0.1$) (source: Harris et al. 1990)

Figure 4.34 shows the influence of frequency on the fatigue behaviour for a graphite-fibre reinforced PEEK composite.

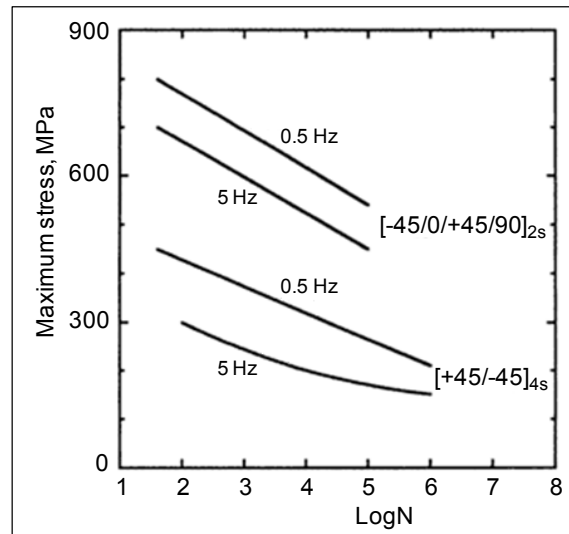


Figure 4.34 Frequency effect on fatigue life of graphite/PEEK (source: Carlile et al. 1989 p199)

In a study (Akay & Aslan 1995), where PEEK containing 30% by weight carbon fibre was evaluated as hip implant, the S-N fatigue data, see Figure 4.35, were obtained by testing injection moulded bar specimens in four-point bending in the saline solution at 37°C. Specimens were conditioned in the saline solution for six months prior to testing. The support span to specimen depth ratio was 12 to 1 and the load span was half of the support span. The frequency of the sinusoidal loading was 1 Hz. The test was conducted in load control mode with a stress ratio (R_o) of 0.1. Tests were continued until the specimens failed or up to 10^6 cycles.

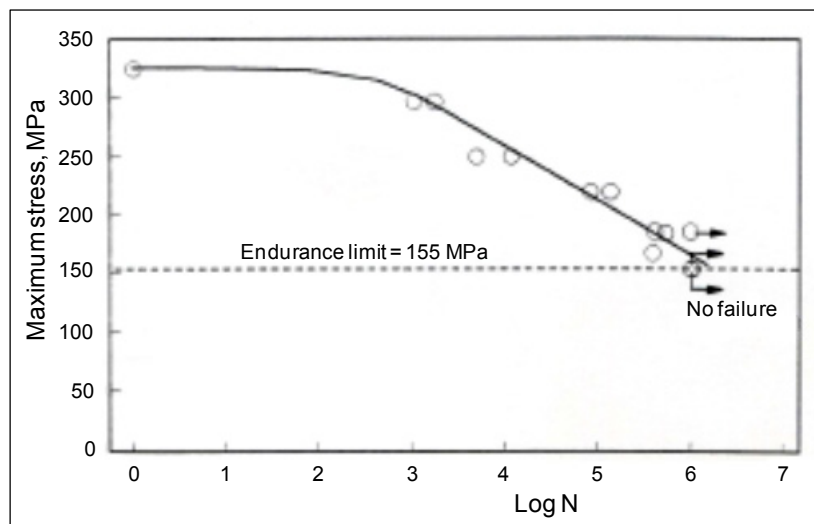


Figure 4.35 S-N fatigue curve for CF/PEEK composite tested in saline solution at 37°C (source: Akay & Aslan 1995)

Figure 4.36 shows the influence of fibre direction with respect to the applied load (off-axis angle, θ). The high level of anisotropy is clearly illustrated: the fatigue limit strain falls sharply with increasing off-axis angle to 0.1% for glass-fibre/epoxy composites.

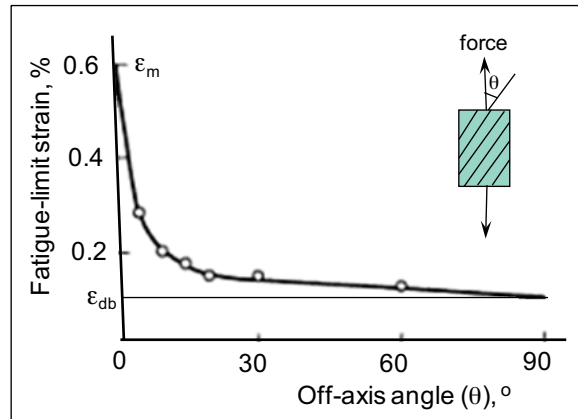


Figure 4.36 Variation of the fatigue limit with the off-axis angle. ϵ_m is the fatigue limit of the matrix and ϵ_{db} is the strain to debonding of fibres from matrix (source: Kelly 1989 p. 79)

In Figure 4.37 a comparison of the fatigue performance under tension-tension and flexural loading regimes is made for a unidirectional graphite-fibre/epoxy system.

bookboon.com

Corporate eLibrary

See our Business Solutions for employee learning

[Click here](#)

- Management
- Time Management
- Problem solving
- Self-Confidence
- Effectiveness
- Project Management
- Goal setting
- Motivation
- Coaching



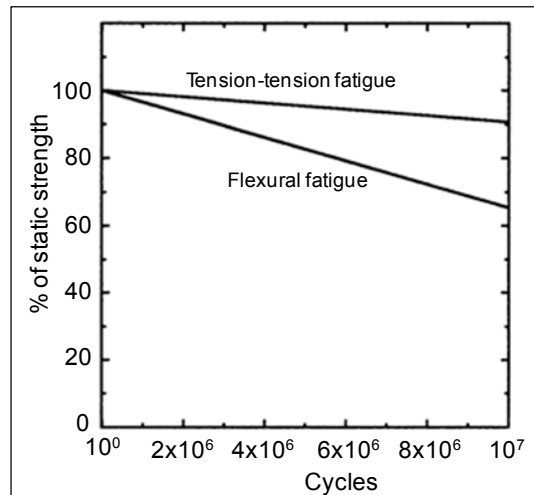


Figure 4.37 Comparison of tension-tension and flexural fatigue lives of a unidirectional graphite/epoxy (source: Mallick 1997 p. 844)

4.8.2 Fatigue of damage-containing coupons

Constant amplitude fatigue testing on undamaged coupons under axial load usually exhibit very flat S-N curves, indicating an insensitivity of life to cyclic loading. Fatigue performance is, however, influenced by out-of-plane loading and in the presence of damage. The fatigue performance of some defined-damage containing specimens will be covered below.

4.8.2.1 Fatigue evaluation of open-hole coupons

The open-hole-tension (OHT) test is a well-established static method for determining the effect of a hole on the tensile strength of thermoset and thermoplastic fibre-reinforced plastic composites. The test specimens, consisting of a strip of rectangular cross-section with a centrally located circular hole, are also tested under fatigue loading. The specimen geometry and dimensions and test methods are described in the standard test methods such as ISO 13003:2003 and ASTM D 5766 –11, ASTM D 3479:2012 and ASTM D7615 –11.

The test is detailed in the National Physical Laboratory Measurement Good Practice Guide No.101 (Gower et al. 2007 p. 24) for laminates of a unidirectional (UD) carbon fibre-reinforced epoxy pre-preg of approximately 57% fibre volume content. The lay-up used was quasi-isotropic $(+45^{\circ}/0^{\circ}/-45^{\circ}/90^{\circ})_{2s}$, and the coupons are tested under tension-tension fatigue regime with $R=0.1$. For the OHT fatigue tests, stress levels of 55, 70 and 80% of the static OHT ultimate tensile strength were used and tests were run to 10^4 , 10^5 , 5×10^5 , 10^6 and 10^7 cycles. No failure occurred even after 10^7 cycles.

The residual OHT strength shows an initial increase with increasing fatigue cycles, then returns to approximately the static UTS value. This is explained (Gower et al. 2007 p. 28) in terms of the stress/strain concentration around the hole: the presence of a hole lowers the tensile strength of the material. At stress levels lower than the static OHT strength, the action of fatigue causes gradual damage growth in the form of matrix micro-cracking, ply splitting and delamination (the stress/strain levels are not high enough to cause fibre fracture), which in turn relieves the stress concentration around the hole. As the tensile strength of the material is dominated by the 0° plies which may contain matrix cracking but no fibre fracture, the residual tensile strength is higher than the static OHT strength measured for un-fatigued specimens.

The trend for residual modulus values is that a decrease with increasing fatigue cycles is seen; the decrease being larger at the higher stress levels.

The open-hole-compression (OHC) fatigue test is described in the standard test methods such as ASTM D7615 –11. Unlike the OHT specimens, shorter open-hole-compression (OHC) specimen design is used for compression fatigue tests to avoid the specimen buckling. The above identified CFRP was OHC fatigue tested under both compression-compression ($R = 10$) and tension-compression ($R = -1$) regimes as described in the National Physical Laboratory Measurement Good Practice Guide No.101. The test frequency for these and OHT tests was 5 Hz.

A comparison of the static OHC compressive strength (ultimate compressive strength, UCS) was made with the residual OHC strength values: specimens were subjected to compression-compression fatigue at 55 and 70% of the mean static OHC compressive strength for 10^4 , 10^5 , 5×10^5 and 10^6 cycles, and then tested for residual static OHC strength. The residual strength values achieved were generally within the scatter of the UCS values; however at the 70% stress level the residual OHC strength values at around 10^6 cycles were slightly higher than the maximum ultimate strength recorded. This indicates that as in the OHT tests, the stress/strain concentration factor due to the hole is relieved due to damage initiation and propagation around the hole after fatigue loading. Damage induced due to fatigue loading is clearly visible in the X-ray image shown in Figure 4.38. As in the OHT fatigue specimens, the damage has propagated longitudinally along the lines tangent to the edge of the hole. With further fatigue cycles, this damage would grow further resulting in detachment of the centre section and reduction in residual strength to below the static ultimate OHC strength.

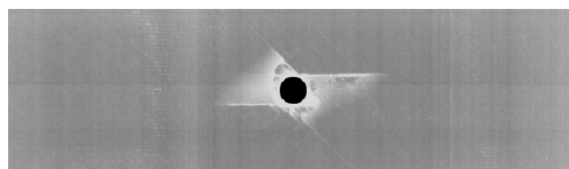


Figure 4.38 X-radiography image of OHC fatigue specimen (at 70% of static UCS after 10^6 cycles)
(source: Gower et al. 2007 p. 33)

From the data presented in the NPL Guide, it has also been shown that the fully reversed fatigue regime is much harsher than compression-compression as the fatigue life at corresponding stress levels is significantly reduced.

4.8.2.2 Fatigue evaluation of filled-hole coupons

The material is usually evaluated for the effect of a rivet or a bolt shaft in testing filled-hole coupons. The test, e.g. ASTM D6873 – 08, involves inserting a metallic pin into the drilled hole and subjecting the test coupon to cyclic bearing forces in tension, compression or reversed tension and compression modes to full failure of the specimens, to a pin displacement (e.g. a hole elongation of 40%) or to a maximum cycle count of, say, one million.

Work is presented on bearing fatigue properties for various CF/epoxy laminates (Akay 1992) and Kevlar/epoxy laminates (Akay & Mun 1995). Figure 4.39 shows an S-N curve for a Kevlar/epoxy laminate: sinusoidal load-amplitude tests were conducted at 1 Hz in positive-positive mode using a base load of 0.4 kN and a range of preset maximum loads. The tests were continued to full failure of the specimens or to a maximum cycle count of one million. Failure modes in the figure are designated as B (bearing), T (tension), C (cleavage), Br (remote bearing at the washer end) and Br(T) (tensile failure that coincides with the remote bearing rather than across the reduced section).



Brain power

By 2020, wind could provide one-tenth of our planet's electricity needs. Already today, SKF's innovative know-how is crucial to running a large proportion of the world's wind turbines.

Up to 25 % of the generating costs relate to maintenance. These can be reduced dramatically thanks to our systems for on-line condition monitoring and automatic lubrication. We help make it more economical to create cleaner, cheaper energy out of thin air.

By sharing our experience, expertise, and creativity, industries can boost performance beyond expectations. Therefore we need the best employees who can meet this challenge!

The Power of Knowledge Engineering

Plug into The Power of Knowledge Engineering.
Visit us at www.skf.com/knowledge

SKF

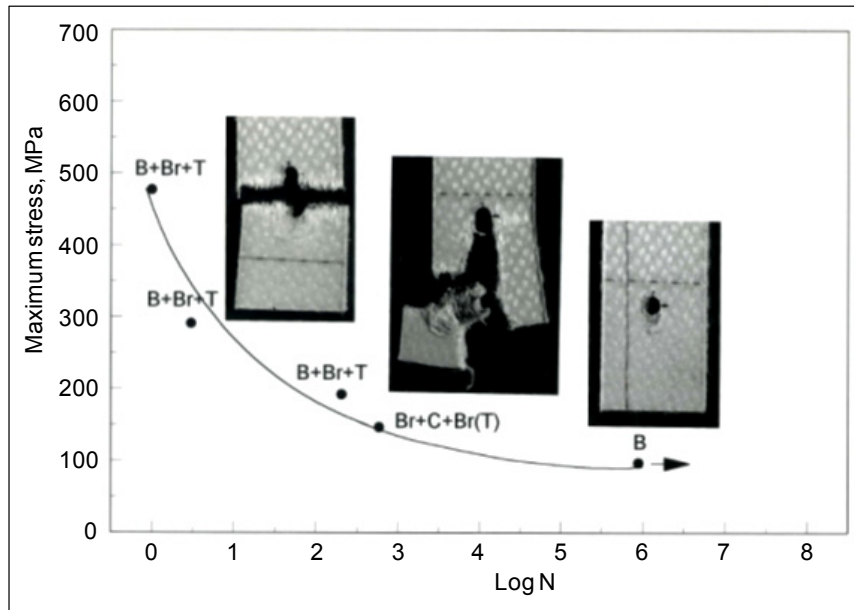


Figure 4.39 S-N curve for Kevlar/epoxy laminates (source: Akay & Mun 1995)

Figure 4.39 represents the tests conducted on oven cured laminates of Kevlar 49-285 fibre/Brochier 1454 epoxy resin; the work (Akay & Mun 1995) also included testing of autoclaved laminates as well as tests conducted on Kevlar 49-285 fibre/Fiberite MXM 7714 epoxy resin laminates.

The specimen which did not fracture up to $N = 10^6$ suffered limited hole deformation by bearing (see Figure 4.39). At higher stress levels, the fatigue failure was accompanied by initial pronounced remote bearing (Br) at the washer edge and a final failure by net tension, particularly at (fatigue stress amplitude) / (static strength) ratios $> 50\%$, and by a cleavage-tension combination at (fatigue stress amplitude) / (static strength) ratios in the range 25% to 50%.

4.8.2.3 Fatigue evaluation of laminate plates with impact damage

The compression-after-impact (CAI) testing for laminated fibre-reinforced plastic materials, where the critical loading mode (compression) is directly linked to the predominant and critical damage type (i.e. delamination), is common within the aerospace industry. CAI may be conducted under static and/or fatigue loading. In both cases the first thing is to induce barely visible impact damage (BVID) on the specimen. BVID is defined as a 0.3 mm deep dent caused by the impact event. The next phase is the assessment/measurement of the level of impact damage by non-destructive inspection, and then conducting compression tests to determine the residual compression properties. The relevant standard test methods include ASTM D7137 – 12, BS ISO 13003:2003 and BS EN ISO 14126: 1999.

Selection of the most appropriate fatigue regime should be made after considering the dominant defect type present in the material. For CAI specimens this is delamination, and the critical loading mode is compression. Therefore it is most appropriate for CAI tests to be carried out under compression-compression fatigue loading ($R = \sigma_{\min} / \sigma_{\max} = 10$). The values of σ_{\min} (equivalent to maximum compressive stress) are calculated as various percentages of the measured mean static CAI strength. The maximum, mean and amplitude stress values (see Figure 4.40) for definitions) could then be calculated using $R = 10$.

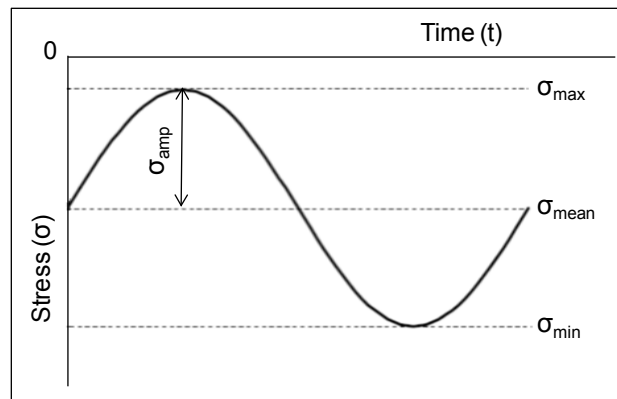


Figure 4.40 Nomenclature for compression-compression fatigue cycle

With us you can
shape the future.
Every single day.

For more information go to:
www.eon-career.com

Your energy shapes the future.

e.on



In the National Physical Laboratory Measurement Good Practice Guide No.10, the results of the tests conducted on autoclave cured UD and quasi-isotropic lay-up (+45°/0°/-45°/90°)_{2s} carbon fibre-reinforced epoxy laminates of approximately 57% fibre volume content are presented: a test frequency of 5 Hz was used after checks were made using a surface mounted thermocouple as to the extent of autogenous heating during loading. It was found that there was little or no rise in the temperature of specimens at this fatigue rate. Specimens were tested until failure occurred or the fatigue life was reached, in this case 2×10^6 cycles. Specimens that reach the fatigue life without failure are identified as ‘run-outs’. In order to compare the fatigue performance of CAI specimens to the undamaged fatigue performance, a number of fatigue tests were also undertaken on plain compression specimens, see Figure 4.41.

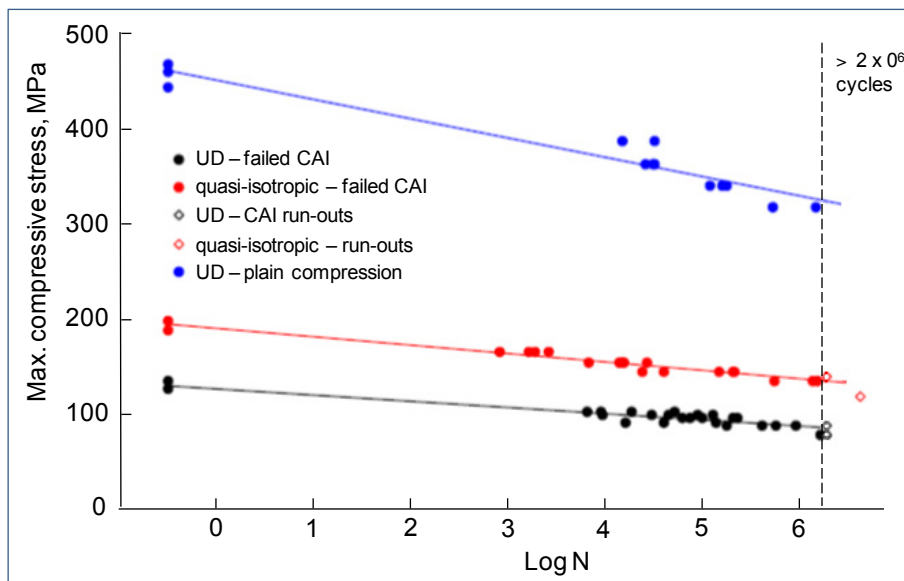


Figure 4.41 Fatigue test results for CAI and plain compression specimens (source: (Gower et al. 2007 p. 21)

4.8.2.4 Fracture mechanics approach to fatigue testing

Materials contain defects/cracks of some form and magnitude, and cracks that do not propagate under a static load may grow under a cyclic load of the same magnitude. When the crack length (a) reaches a critical value after a number of cycles (N) of loading and the stress intensity factor $K = K_c$, then fatigue fracture occurs.

The fatigue life depends on the crack propagation rate. ASTM E647 – 13e1 test method covers the determination of fatigue crack growth rates from near-threshold value of K to K_{max} . Figure 4.42 shows an experimental set up for three-point loading of a single-edge notched bending (SENB) specimen. The lower rollers of the test fixture are held against the stops with rubber bands. A crack opening displacement (COD) clip gauge, employed to measure the crack opening displacement, is placed on the knife edges that are attached to the specimen.

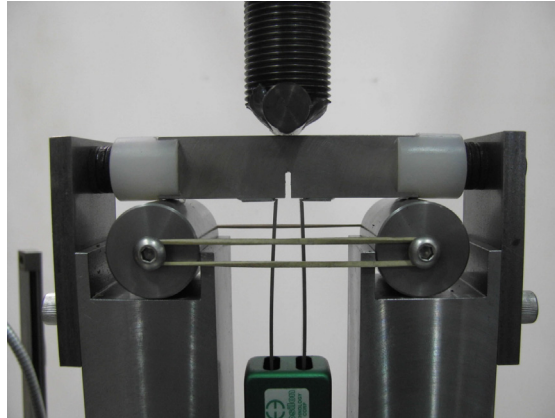


Figure 4.42 Experimental set up for a fatigue crack growth test (source: Google image)

A material's resistance to stable crack extension under cyclic loading is characterised by expressing fatigue crack growth rate, da / dN , as a function of crack-tip stress-intensity factor range, $\Delta K = K_{\max} - K_{\min}$, as shown in Figure 4.43.

An advertisement for Accenture featuring a background image of a lecture hall with rows of wooden chairs. A large blue arrow points from the word 'be' to the phrase 'your degree'. The text 'Be greater than.' is prominently displayed, followed by 'consulting | technology | outsourcing'. The Accenture logo and tagline 'High performance. Delivered.' are also present. A small copyright notice '© 2013 Accenture. All rights reserved.' is visible in the top right corner.

be > your degree

Bring your talent and passion to a global organization at the forefront of business, technology and innovation. Discover how great you can be.

Visit accenture.com/bookboon

Be greater than.
consulting | technology | outsourcing

accenture
High performance. Delivered.

© 2013 Accenture. All rights reserved.

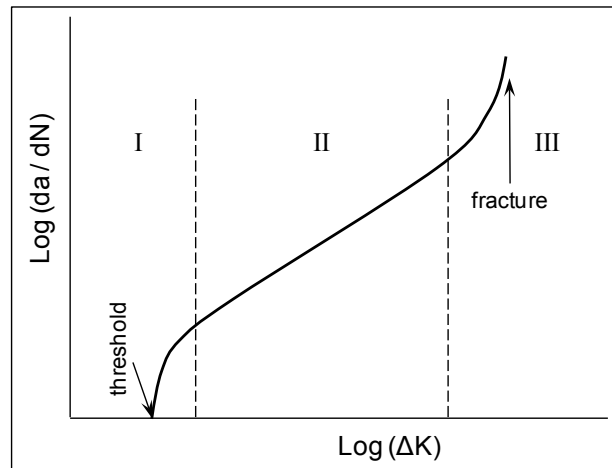


Figure 4.43 Fatigue crack growth rate as a function of stress-intensity factor range

There are three distinct regions to the crack growth rate curve: Region I represents the initial stages of crack growth in the specimen, where a threshold value of ΔK is identified below which cracks will not propagate (analogous to the endurance limit defined in $S-N$ data). In Region II, a linear relationship exists between the crack growth rate and the stress-intensity factor range; and in Region III, the crack growth accelerates as the ΔK reaches ΔK_c , and the material fractures. Region II enables an estimation of the crack-growth rate to be made over the major part of the fatigue life for a given crack length using a power-law relationship (also known as the Paris-Erdogan equation), which relates the sub-critical crack growth under a fatigue stress regime, $\frac{da}{dN}$, to the stress intensity factor range, ΔK , as in equation below.

$$\frac{da}{dN} = C\Delta K^m$$

where a is the crack length, N is the number of load cycles, and C and m are empirical material constants that depend on material properties, test frequency, applied mean load, etc. $\Delta K = K_{max} - K_{min}$, where K_{max} and K_{min} are the maximum and the minimum stress-intensity factors.

Paris-Erdogan equation can be used to quantify the residual fatigue life (in terms of load cycles) of a specimen for a particular crack size. Defining the crack intensity factor as

$$K = Y\sigma\sqrt{\pi a},$$

where σ is a uniform tensile stress perpendicular to the crack plane and Y is a dimensionless parameter that depends on the specimen geometry, similarly the range of the stress intensity factor is

$$\Delta K = Y\Delta\sigma\sqrt{\pi a},$$

where $\Delta\sigma$ is the range of cyclic stress amplitude. Y takes the value 1 for a centre crack in an infinite sheet.

Substituting for ΔK in the Paris equation gives

$$\frac{da}{dN} = C (Y\Delta\sigma\sqrt{\pi a})^m.$$

For relatively short cracks, Y can be assumed as independent of a and the differential equation can be solved via separation of variables.

$$\int_0^{N_f} dN = \int_{a_0}^{a_c} \frac{da}{C (Y\Delta\sigma\sqrt{\pi a})^m} = \frac{1}{C (Y\Delta\sigma\sqrt{\pi})^m} \int_{a_0}^{a_c} a^{(-\frac{m}{2})} da.$$

Integration yields the number of cycles to failure (the fatigue lifetime) N_f to be

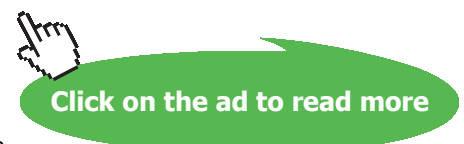
$$N_f = \frac{2 (a_c^{\frac{(2-m)}{2}} - a_0^{\frac{(2-m)}{2}})}{(2-m)C (Y\Delta\sigma\sqrt{\pi})^m},$$

where a_c is the critical crack length at which instantaneous fracture will occur, and a_0 is the initial crack length at which fatigue crack growth starts for the given stress range $\Delta\sigma$.

"I studied English for 16 years but...
...I finally learned to speak it in just six lessons"
Jane, Chinese architect

ENGLISH OUT THERE

Click to hear me talking before and after my unique course download



An example log-log plot of da/dN against ΔK is shown in Figure 4.44 for 30% by weight short carbon fibre containing PEEK injection moulded bars. The detail of this work is presented elsewhere (Akay & Aslan 1995) and, basically, entails testing of SENB specimens in three-point bending. The tests were performed on an Instron servo-hydraulic machine at a frequency of 1 Hz. The K-increasing method was used for the crack-growth rate and the K-decreasing method for the threshold stress intensity factor range (ΔK_{th}) determinations in accordance with ASTM E647. Figure 4.44 includes data representing three different specimens, and the variations in the slopes produced by the data in Region II are due to the fibre orientations encountered at the tip of the propagating cracks. ΔK_{th} was determined to be approximately $3.8 \text{ MPa m}^{1/2}$.

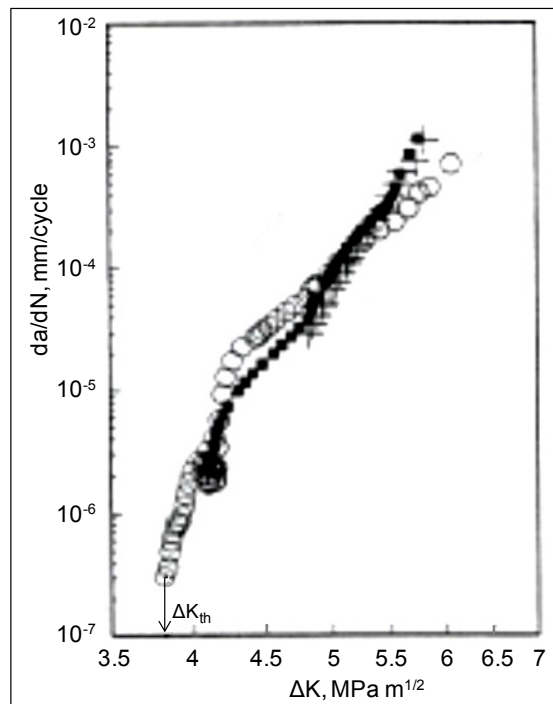


Figure 4.44 Fatigue crack growth rate curve for 30% by weight short CF reinforced PEEK
(source: Akay & Aslan 1995)

4.9 Differential scanning calorimetry

Materials are increasingly required in situations that challenge the thresholds of their thermal capabilities. It is therefore important to understand material behaviour at different temperatures. Thermal analysis techniques such as differential scanning calorimetry (DSC) and its variants; dynamic mechanical analysis (DMA) or dynamic mechanical thermal analysis (DMTA), and measurement of heat distortion (deflection) temperature (HDT)/deflection temperature under load (DTUL) are tools that provide a variety of important information.

DSC measures the temperatures and heat flow associated with transitions in materials as a function of time and temperature, enabling measurement of relaxation temperatures, micro-structural composition (e.g. crystallinity, degree of cure (degree of crosslinking)), thermal stability, etc. There are several standard methods for conducting DSC measurements: ISO 11357-1:2009 (seven parts), ASTM D3418 –12e1 and ASTM E1356 – 08, for the thermal analysis of polymers, polymer blends, and polymer matrix composites. The standards describe methods for measuring properties, such as

- physical transitions (glass transition (T_g), phase transitions such as melting (T_m) and crystallization (T_c), polymorphic transitions, etc.), and the amount of energy (joules/gram) which a sample absorbs/releases while undergoing transition (ΔH_m and ΔH_c)
- chemical reactions (polymerization, crosslinking and curing of elastomers and thermosets, etc.)
- stability to oxidation
- heat capacity.

The properties which are popularly measured using DSC are indicated on Figure 4.45. The increase in heat flow at T_g is caused by the polymer having a higher heat capacity above the T_g than below it. Heat capacity is the amount of heat necessary to generate a specific temperature increase in a material. Therefore, the sudden upward slope at the T_g indicates that the equipment was required to supply more heat to the sample head to maintain a constant heating rate.

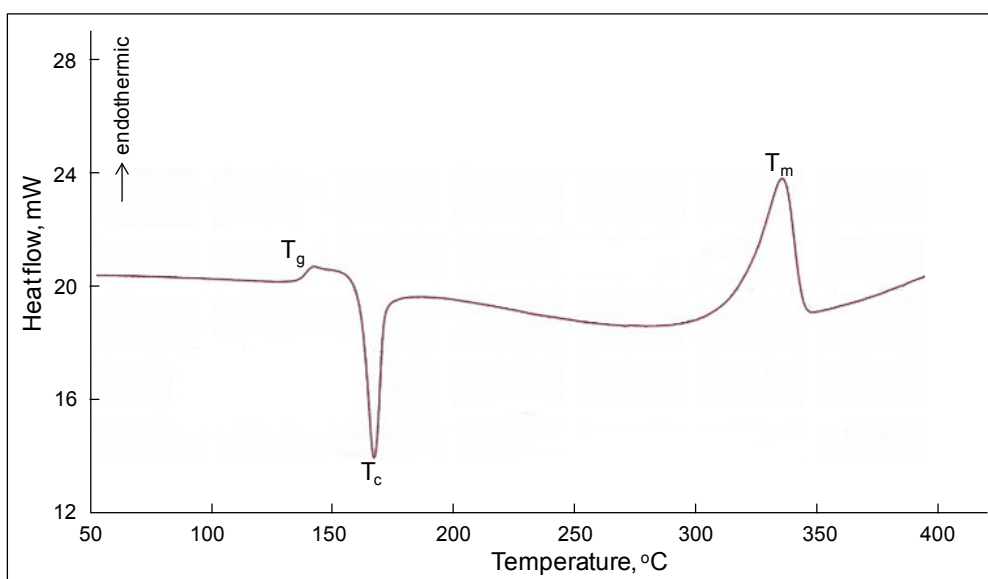


Figure 4.45 DSC scan of PEEK (source: Intertek Plastics Technology Laboratories)

Figure 4.46 shows DSC traces for an Araldite epoxy adhesive (bisphenol A and epichlorhydrin based). The green curve represents the first heating of the material, when an exothermic curing (crosslinking) occurs at 129°C, releasing a heat of reaction of 344 J/g. The cured resin is subjected to a second DSC run (the red trace), indicating a glass transition at 100°C and an associated change in the specific heat capacity by the value $\Delta C_p = 0.35 \text{ J/(gK)}$. The DSC runs are conducted at 5 K/min heating and 40 K/min cooling rates.

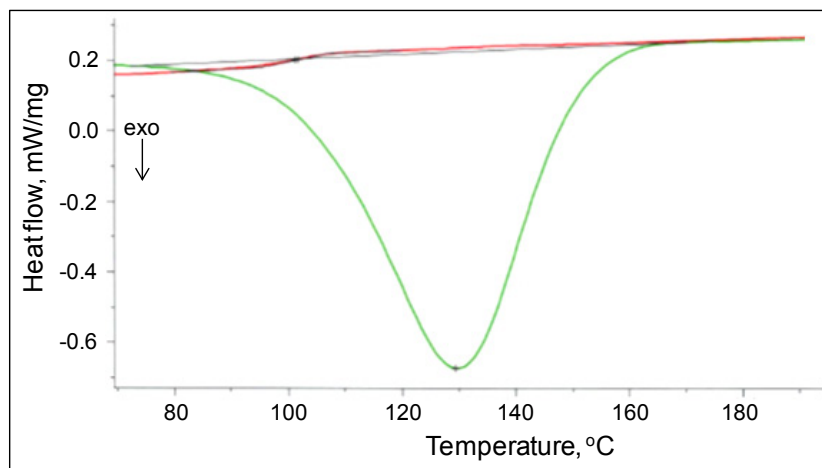


Figure 4.46 DSC traces for an Araldite epoxy adhesive (source: Netzsch GmbH)

The advertisement features the Duke University logo (DUKE THE FUQUA SCHOOL OF BUSINESS) in the top left. The central text reads "BUSINESS HAPPENS" in large black letters, with "HERE." in bold black letters inside a circular collage of diverse people's faces. Below this is the website "www.fuqua.duke.edu/globalmba" and an orange button with the text "Learn More >".



4.10 Dynamic mechanical thermal analysis

Dynamic mechanical thermal analysis (DMTA) is a technique that measures the modulus (stiffness) and damping (energy dissipation) of materials as they are subjected to cyclic load and deformation. Polymeric materials are viscoelastic in nature, and therefore, their mechanical properties are time, frequency and temperature dependent. DMTA is an excellent technique for characterising the viscoelastic nature of polymers in terms of storage (elastic) modulus, loss modulus and a damping term (loss tangent). Cure behaviour of thermosetting resins can also be determined by DMA.

DMTA/DMA is a versatile technique that can be used in many deformation modes (e.g. tension, compression, torsion) and specimen formats (e.g. coupons, fibres). It is an extremely sensitive technique that enables the identification of weak material relaxation transitions not recognisable/distinguishable by other techniques. There are several standard methods for conducting DMA measurements: ISO 6721:2012 (consists of 12 parts, covering various modes of loading and vibration), ASTM D4065 – 12, ASTM D4473 – 08, ASTM D4440 – 08 and ASTM D5279 – 08.

These methods enable various important properties to be determined, e.g. in ASTM D4065, the significance and uses of the method are indicated as follows:

- determination of elastic and loss moduli and mechanical damping as a function of temperature, frequency or time, or both
- determination of relaxation-transition temperatures of plastics, that is, changes in the molecular motions of a polymer: at transition elastic modulus decreases rapidly with increasing temperature (at constant or near constant frequency) or increases with increasing frequency (at constant temperature). A maximum is observed for the loss modulus as well as for the $\tan \delta$ curve in the transition region.
- evaluation of degree of phase separation in multi-component systems
- characterisation of fillers in filled polymers
- study of effects of certain processing treatments
- determination of stiffness of polymer composites, especially as a function of temperature
- determination of degree of polymer crystallinity compared to a reference/control material
- quality control, specification acceptance, and research work.

Most of these properties obtainable with DMTA for polymers are covered elsewhere (Akay 2012 p. 225). Here, properties associated with polymer-matrix composites and with polymers that are commonly used as matrices in composites are recounted.

Figure 4.47 shows typical DMTA traces for an epoxy resin/CF fabric laminate of $(0^\circ/45^\circ/-45^\circ/90^\circ)_s$ prepreg layup arrangement. A sample of $2\text{ mm} \times 10\text{ mm} \times 40\text{ mm}$ is loaded in 3-point bending at 1 Hz, $\pm 30\text{ }\mu\text{m}$ deformation amplitude. The storage modulus (E') begins to decrease sharply at an extrapolated onset point of 186°C , loss modulus (E'') peaks at 197°C and $\tan \delta$ at 201°C . The composite begins to degrade (perhaps by delamination) at 250°C (indicated by a decrease in E'), which also causes an irregular increase in $\tan \delta$ curve.

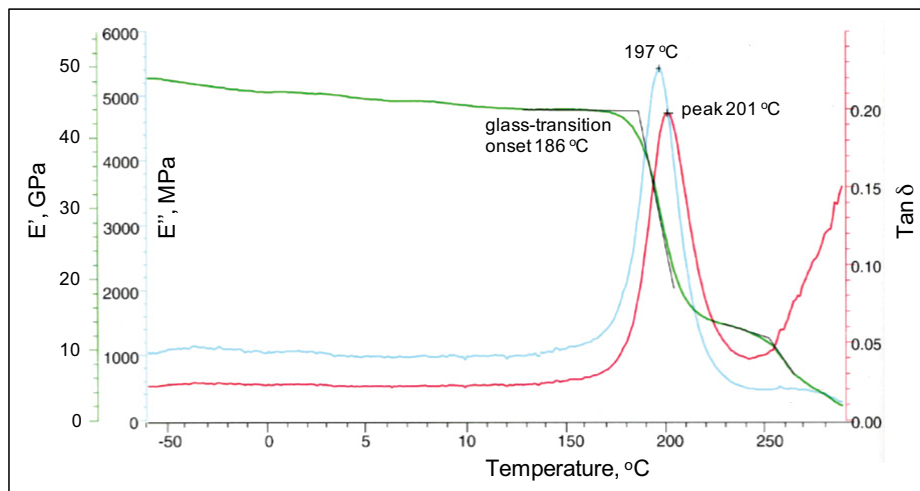


Figure 4.47 DMTA traces for a high performance epoxy resin/CF composite (source: Netzsch GmbH)

Join American online LIGS University!

Interactive Online programs
BBA, MBA, MSc, DBA and PhD

Special Christmas offer:

- ▶ enroll **by December 18th, 2014**
- ▶ **start studying and paying only in 2015**
- ▶ **save up to \$ 1,200** on the tuition!
- ▶ Interactive Online education
- ▶ visit ligsuniversity.com to find out more!

Note: LIGS University is not accredited by any nationally recognized accrediting agency listed by the US Secretary of Education. More info [here](#).



The properties of unidirectional fibre reinforced composites are strongly dependent on the fibre direction, this is also reflected on the dynamic mechanical properties as illustrated in Figures 4.48 and 4.49 for PEEK/continuous AS4 carbon fibre composite of approximately 55% fibre volume content. Samples of approximately 2 mm × 10 mm × 16 mm are DMTA tested in single cantilever bending at 1 Hz, ± 30 μm deformation amplitude.

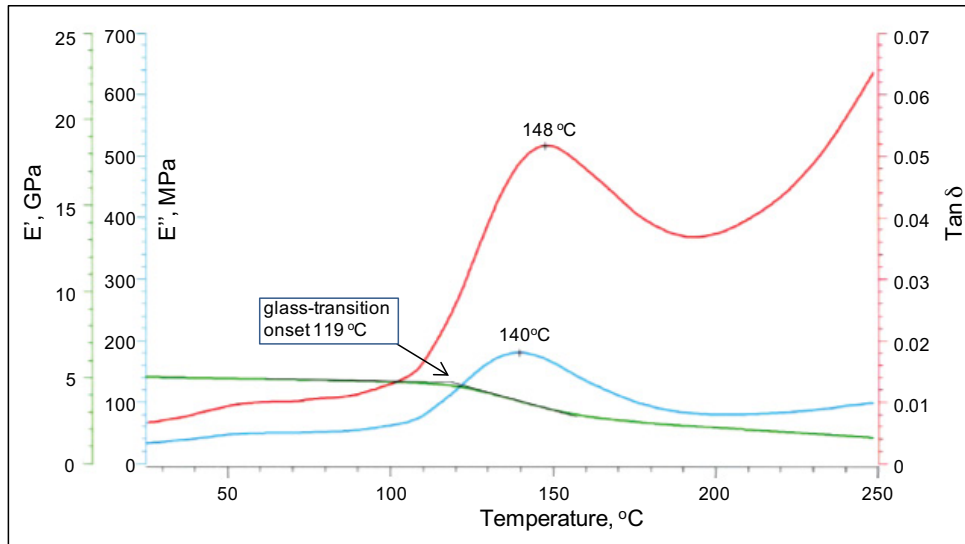


Figure 4.48 DMTA traces for PEEK/CF composite. The fibres are parallel to the specimen width (source: Netzsch GmbH)

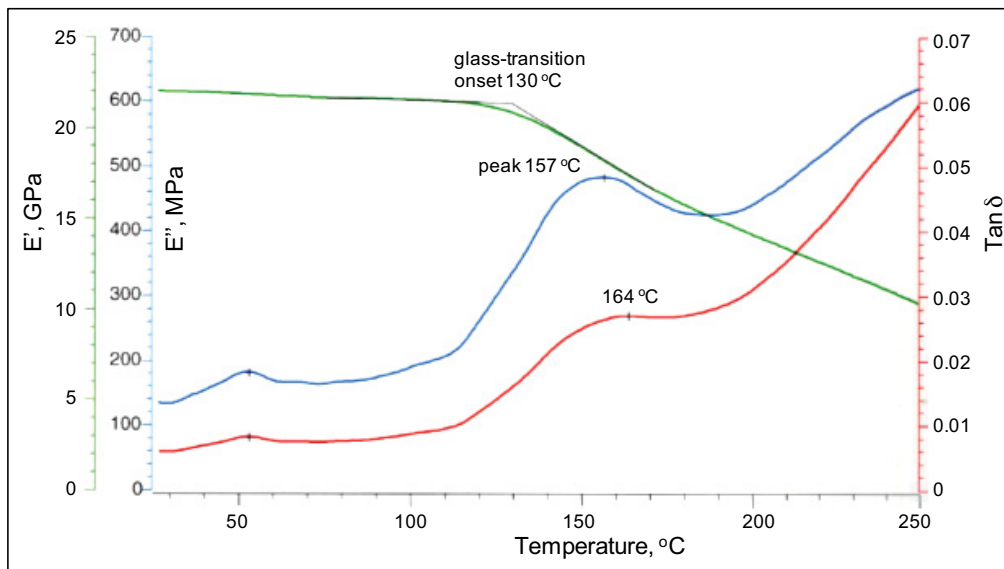


Figure 4.49 DMTA traces for PEEK/CF composite. The fibres are parallel to the specimen length (source: Netzsch GmbH)

A comparison of the figures show that in the case of fibres aligned with the specimen width, the elastic modulus is matrix dominated (Figure 4.48) and is much lower than the one shown in Figure 4.49, where fibres are parallel to the specimen length (i.e. a configuration where the applied load/stress is supported by the fibres) and, therefore, the mechanical properties become dominated by the fibres. The reinforcement of the matrix by the fibres is also reflected in an increase at glass-transition temperature and a decrease in the intensity of the mechanical-damping term $\tan\delta$.

A similar study (Akay 1993) was conducted for autoclave cured (180°C, 600 kPa) unidirectional laminates of CF reinforced epoxy resin (Fibredux 924 epoxy resin and T800 carbon fibre) prepreg of 55% by volume fibre content. Dynamic mechanical properties were determined using a DuPont 983 DMA at 1 Hz, temperature scan rate of 4°C/min and 0.2 mm sinusoidal oscillation amplitude. Test bars of 2 mm × 10 mm cross-sectional area were clamped across a 30 mm clamp separation and forced into flexural deformation. The specimens with fibre alignments along specimen length (i.e. longitudinal fibre alignment) and across specimen length (transverse fibre alignment) were tested in order to study the influence of fibre orientation on properties: in longitudinal fibre arrangement fibres carry the applied load, and therefore as would be expected result in much higher storage modulus values, and also as in PEEK composites show an increase at glass-transition temperature (as indicated by E'' peak) and a decrease in the intensity of the mechanical-damping term $\tan\delta$, see Figure 4.50. However the temperature of $\tan\delta$ maximum, contrary to expectation, shows a large decrease in the longitudinal fibre alignment.

ie business school

#1 EUROPEAN BUSINESS SCHOOL
FINANCIAL TIMES 2013

#gobeyond

MASTER IN MANAGEMENT

Because achieving your dreams is your greatest challenge. IE Business School's Master in Management taught in English, Spanish or bilingually, trains young high performance professionals at the beginning of their career through an innovative and stimulating program that will help them reach their full potential.

- Choose your area of specialization.
- Customize your master through the different options offered.
- Global Immersion Weeks in locations such as Rio de Janeiro, Shanghai or San Francisco.

Because you change, we change with you.

www.ie.edu/master-management | mim.admissions@ie.edu | f t in YouTube

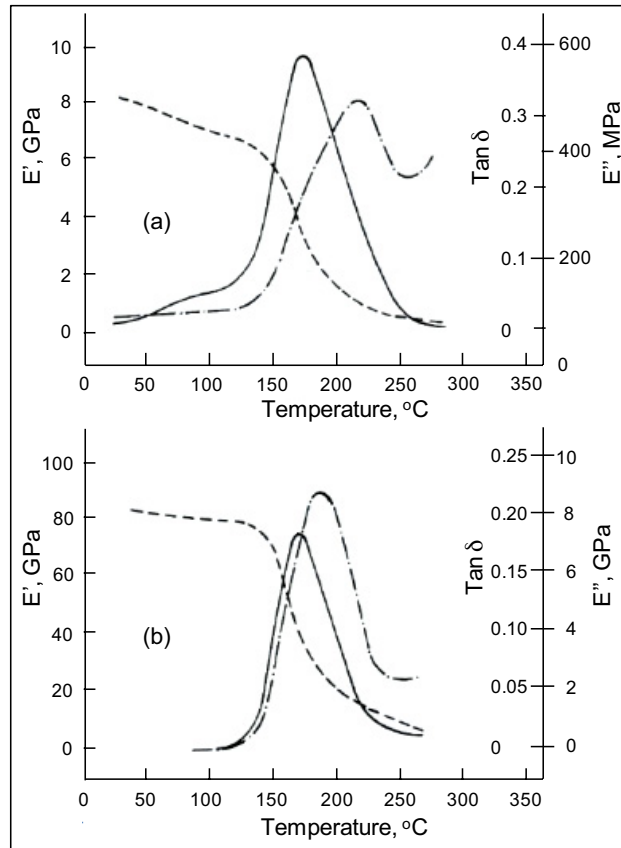


Figure 4.50 Dynamic mechanical properties for CF/epoxy resin at (a) transverse, (b) longitudinal modes of testing (source: Akay 1993)

The anomaly observed with the temperatures where the maxima occurs in $\tan\delta$ peaks is explained in terms of widening of the glass transition region when the specimens are tested in the transverse mode (broader E'' and $\tan\delta$ peaks are obtained as can be seen in Figure 4.50-a). This could be explained in terms of non-uniform compliance in the matrix due to various fibre-resin interactions. Assuming that the fibre-resin interface remains intact then under a given load the matrix at the fibre surface deforms less than the bulk matrix because of the constraint due to the fibre. Furthermore, the matrix around the fibre, the interphase, undergoes chemical modification (e.g. variations in the resin-to-curing-agent ratio) and becomes stiffer than the bulk matrix. These gradients in the elastic modulus of the matrix can yield a broader glass transition than the one due to a single elastic modulus.

One of the advantages of DMTA when studying relaxation transitions in polymers is that the measured values exhibit distinct features such as $\tan \delta$ and E'' peaks. However, it is clear from the figures shown that depending on its definition, different T_g values can be obtained and this can be misleading. Figures 4.50 shows that T_g , expressed as the temperature of $\tan \delta$ maximum, produced higher values in the transverse mode compared with the longitudinal mode by as much as 25°C without any fundamental reason other than the broadening of the transition region. Alternatively, T_g based on the position of E'' maximum reveal an increase in the longitudinal mode compared with the transverse mode (see Figures 4.48 and 4.9): this is more realistic since in the longitudinal mode most of the load is carried by the fibres and thus the matrix experiences a delayed transition. The definition of T_g by E'' peak also coincides more closely with the point of inflection in the E' -curve, where the rate of decrease in stiffness (as indicated by E'') is the highest. Therefore for advanced composites, particularly in thermosets reinforced with unidirectional fibres, T_g by E'' peak becomes a more consistent and appropriate index than the one based on $\tan \delta$ peak.

$\tan \delta$ is not a direct measurement, it is a calculated term ($\tan \delta = E'' / E'$), and therefore, when the transition region broadens, the differences in the rates of decrease in E' and E'' values result in a $\tan \delta$ -peak temperature that is higher than expected for the specimens that produce broader glass-transition regions. Furthermore, for polymeric materials, the glass-transition temperatures taken as the temperature of the maximum $\tan \delta$ indicate higher values than those obtained from DSC measurements. Notwithstanding, all these different means of identifying relaxation-transition temperatures, such as T_g , are widely used, particularly for comparison.

SMS from your computer

...Sync'd with your Android phone & number

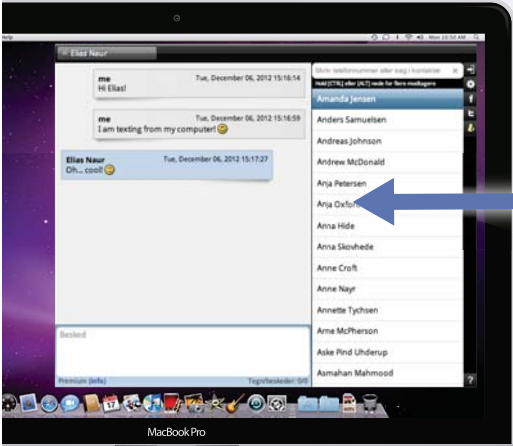
FREE
30 days trial!

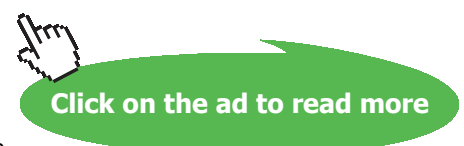
Go to

BrowserTexting.com

and start texting from
your computer!





DMTA is a powerful technique and offers many significant uses, for example, the sensitivity of this technique to variations in cure temperature of thermosetting resins is demonstrated in Figure 4.51. The laminates used in this study (Akay et al. 1994) consisted of 8-HS satin fabric CF/epoxy resin prepreg of 63% by weight fibre content. Eight-ply stacks of prepregs were cured at the recommended autoclave settings of 177°C, 600 kPa for 2 hours. Alternative temperature settings of 130°C, 140°C, 150°C and 160°C were also employed in order to induce different extents of resin curing.

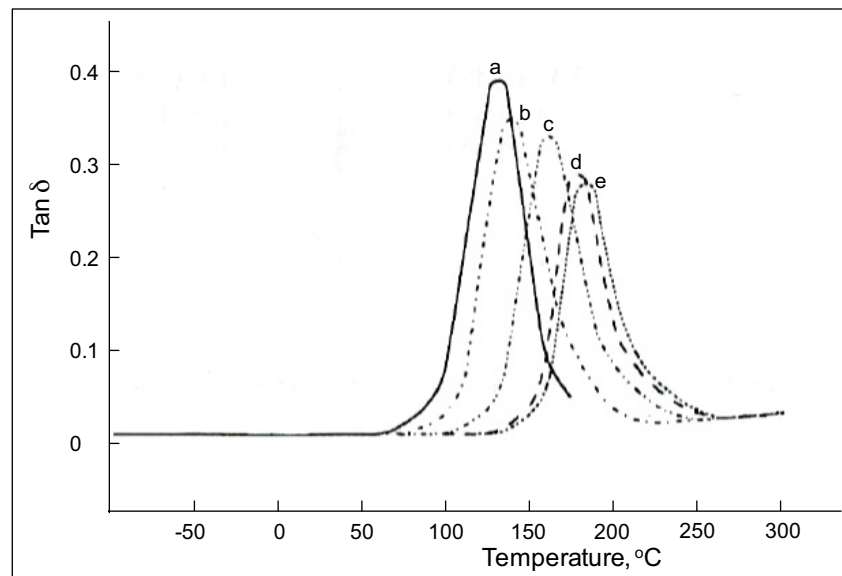


Figure 4.51 Plots of $\tan \delta$ vs. temperature for laminates cured at: (a) 130°C, (b) 140°C, (c) 150°C, (d) 160°C and (e) 177°C (source: Akay et al. 1994)

There is a clear sensitivity between the dynamic mechanical thermal properties (i.e. E' , E'' and $\tan \delta$) and the cure temperature, demonstrated here for $\tan \delta$. Therefore, DMTA becomes an effective technique in raw material “receipt” tests and also as a diagnostic test of any ensuing problems in the performance of the finished components. In this study, it has been shown that static mechanical tests such as compression and ILSS conducted at room temperature are not sufficiently sensitive to distinguish between CF/epoxy resin laminates cured at different autoclave temperatures over a range 130°C to 177°C.

DMTA has also been used in studying thermal ageing of CF/bismaleimide composites (Akay & Spratt 2008). Figure 4.52 shows the DMTA traces for cured laminates of Cycom 5250-4 bismaleimide reinforced with T300 plain-weave carbon fibre fabric at fibre volume fraction of 0.58. DMTA were conducted at 1 Hz, temperature scan rate of 4°C/min and 0.2 mm sinusoidal oscillation amplitude. The processing of the cured laminates consisted of autoclaving at 177°C, 600 kPa (85 psi) for 6 h, followed by a free standing post-curing in an air-circulating oven at 227°C for a further 6 h. Some of the as-cured specimens were further conditioned in air-circulating ovens set at 210°C, 230°C, 250°C for various periods of time up to 2000 h in order to evaluate the effects of thermal ageing: the data extracted from DMTA traces are presented in Figures 4.53 and 4.54.

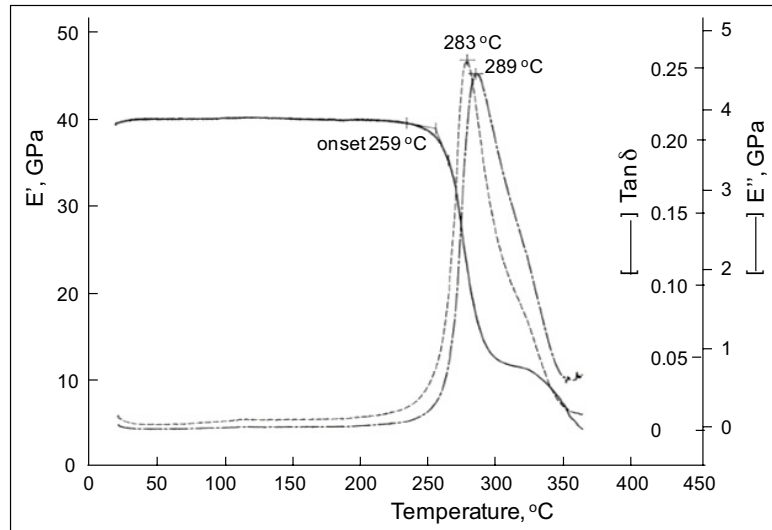


Figure 4.52 DMTA traces for CF/bismaleimide as-cured (unaged) laminate specimens

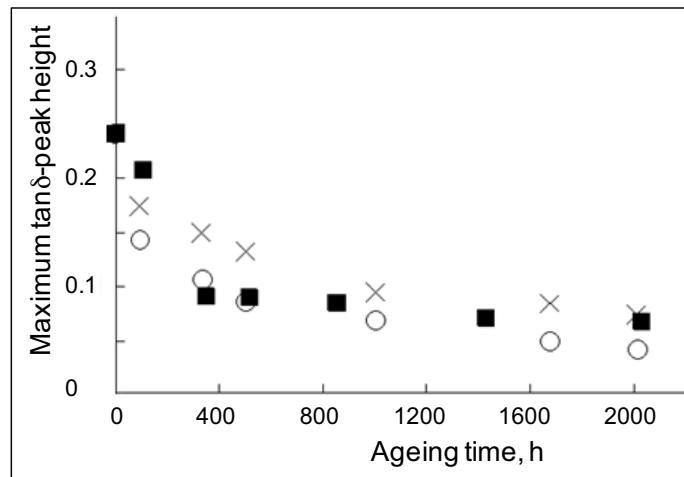


Figure 4.53 Maximum tan δ -peak height vs. ageing time for CF/bismaleimide laminates aged at (■) 210°C, (x) 230°C and (o) 250°C (source: Akay & Spratt 2008)

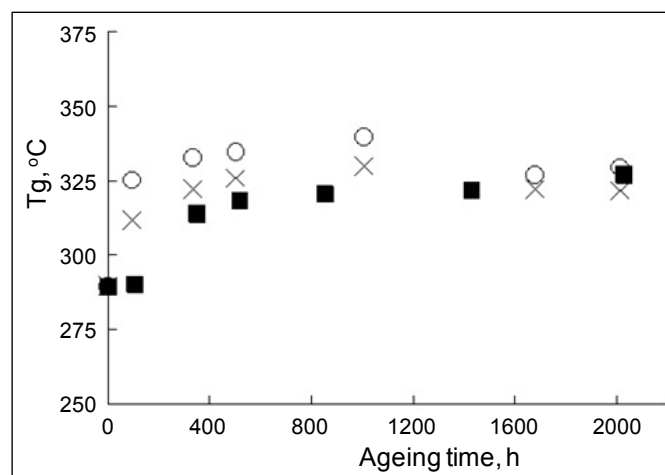


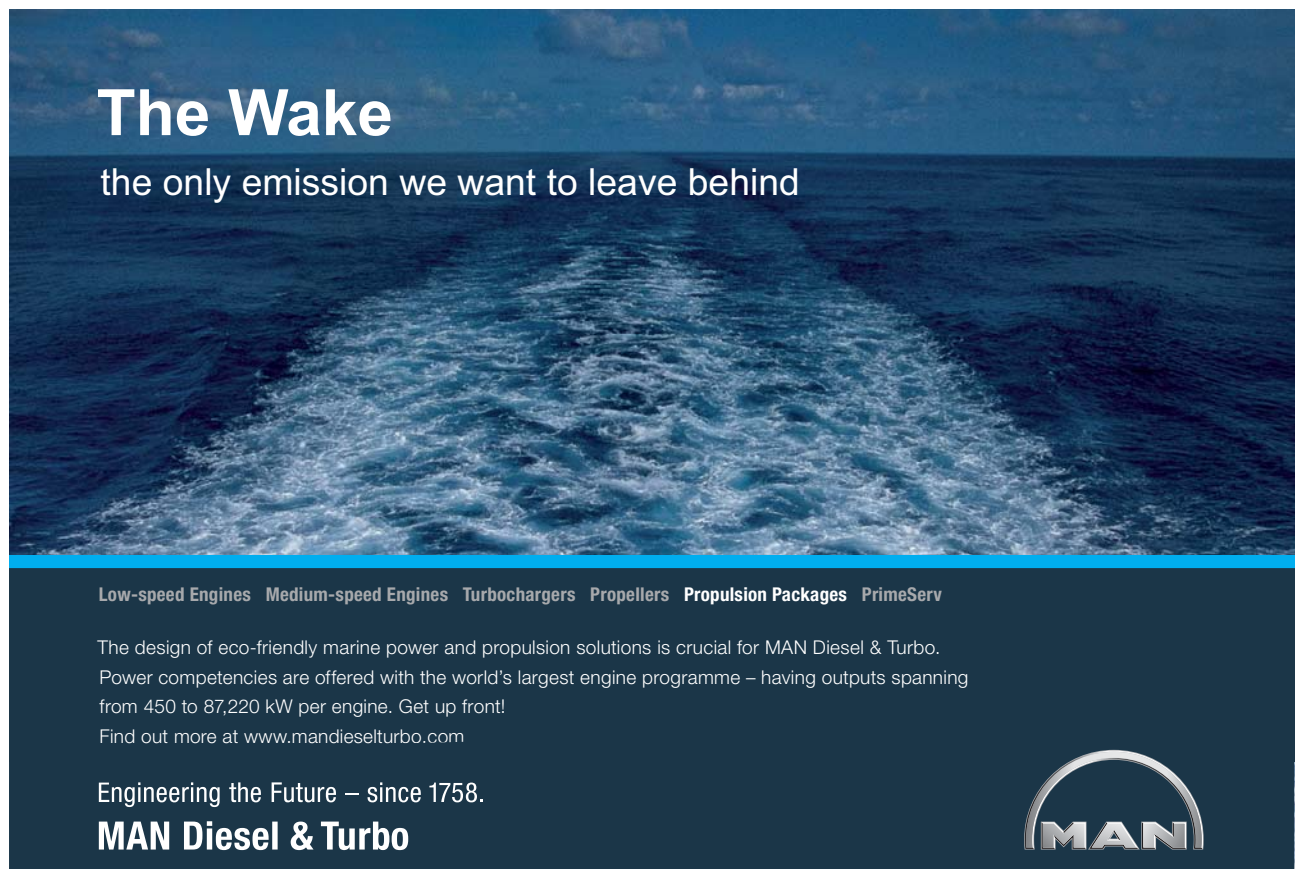
Figure 4.54 Effect of ageing time on T_g for CF/bismaleimide laminates aged at (■) 210°C, (x) 230°C and (o) 250°C (source: Akay & Spratt 2008)

The figures show that T_g (defined as the temperature of the maximum in $\tan \delta$ peak) increases significantly, due to postcuring with increasing ageing temperature and time, reaching a plateau value beyond 1000 h ageing. Postcuring of matrix also decreases damping ability of the material as indicated by the significant drop in the maximum $\tan \delta$ values. These are typical patterns of behaviour in resins as curing/cross linking increases, whereby T_g shifts to a higher temperature and the damping peak becomes squat.

4.11 Environmental effects on properties

Applications of composite materials expose them to a variety of environments that may adversely affect their properties. It is therefore important to understand both the material and the operating environment. The environment must be understood before the suitability of a composite material for a particular application is assessed. These include humidity/moisture, temperature, any radiation and a wide range of chemicals, including fuel, fuel additives, hydraulic fluids, de-icing fluids, paint and paint strippers, dye penetrants, and detergents/cleaning systems.

These chemicals and environmental factors can significantly change the mechanical properties of a composite material. It is important to note that the matrix, fibre, and fibre/matrix interface will be affected differently by the operating environment. It is also important to consider that exposure to these elements in combination, e.g. the combination of humidity and temperature known as hot/wet condition often results in an antagonistic (more damaging) effect in materials.



The Wake
the only emission we want to leave behind

Low-speed Engines Medium-speed Engines Turbochargers Propellers Propulsion Packages PrimeServ

The design of eco-friendly marine power and propulsion solutions is crucial for MAN Diesel & Turbo. Power competencies are offered with the world's largest engine programme – having outputs spanning from 450 to 87,220 kW per engine. Get up front!
Find out more at www.mandieselturbo.com

Engineering the Future – since 1758.
MAN Diesel & Turbo



Immediately after manufacture, the matrix material in a composite material will begin to absorb moisture from humid air, even in an air-conditioned environment. The effect of this absorbed moisture on mechanical performance is critical and needs to be evaluated for specific composite systems.

Moisture diffusion characteristics are described in the literature as Fickian or non-Fickian. The diffusion behaviour of most thermosetting polymers suitable for aerospace applications is Fickian, which is characterized experimentally by an uptake of moisture that reaches an asymptotic/constant value after a period of time. If the weight gain of a sample exposed to constant humidity and temperature is plotted against the square root of time, there will be an initial linear region up to about 60% of the maximum moisture uptake followed by a gradual approach toward a saturation value (equilibrium concentration). A procedure for the determination of moisture absorption or desorption properties in the through-the-thickness direction for laminated polymer matrix composite materials is described in ASTM D5229 / D5229M – 12 .

The level and extent of moisture diffusion are highly dependent on the type of matrix material. Usually fibres do not absorb moisture and therefore are not affected by hygrothermal changes. This is true for carbon, boron, and glass but not for aramid and other polymeric fibres.

In composites containing fibres that are not affected by hygrothermal changes, residual stresses can develop as a result of mismatch of hygrothermal expansions and contractions between the fibres and the matrix: the movement in the matrix is resisted by the fibres.

The moisture plasticises the matrix, significantly lowering T_g and reducing stiffness and strength at elevated temperatures as shown in Figures 4.55–4.65. The effect of the matrix softening on the composite is a reduction in matrix dominated properties, such as shear or compressive strength.

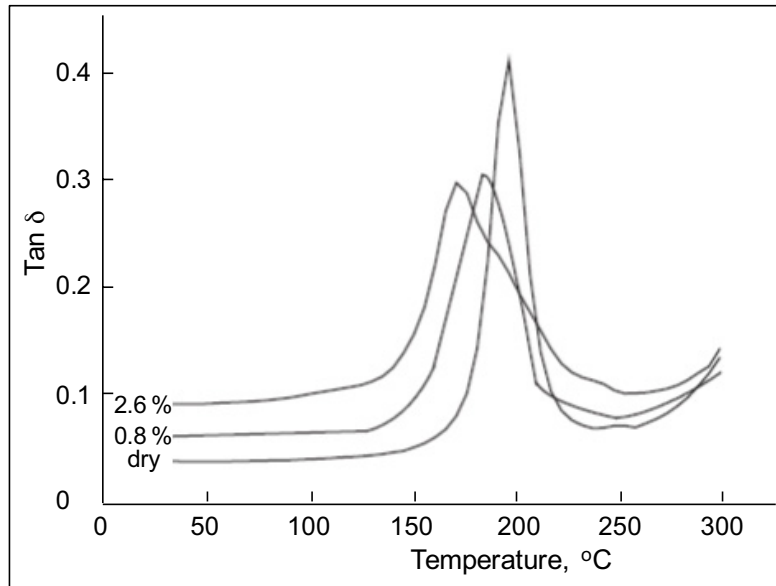


Figure 4.55 Plots of $\tan \delta$ vs. temperature for dry and wet carbon/epoxy laminates (source: Costaa et al. 2005)

Figure 4.55 shows the effect of moisture (0.8% and 2.6% by weight moisture content) on loss tangent for 8-H satin fabric carbon fibre reinforced epoxy (T300/F584) laminates cured in an autoclave at 180°C with pressure of 0.71 MPa. The dynamic mechanical analysis were conducted using TA Instrument's DMA-983 in the three-point bending horizontal measuring mode at settings of 1 Hz frequency, oscillation displacement 0.2 mm and heating rate of 3.0°C/min (Costaa et al. 2005). As can be seen moisture produces a broader and lower $\tan \delta$ -peak (possibly due to inhomogeneous plasticisation of the matrix), similar to the effect of a poor solvent as described in the text book by Nielsen (1974 p. 189).

A study (Akay et al. 1997) on Kevlar fibre/epoxy resin composites also shows the broadening and lowering of $\tan \delta$ -peak with moisture absorption, see Figure 4.56, as well as the generation of two distinct $\tan \delta$ -peaks due to inhomogeneous moisture ingress into the resin, resulting in regions of composite with hardly any moisture absorption. The composite consisted of four-harness (or crowfoot) satin fabric of Kevlar 49-285 fibre and Fiberite MXM 7714 epoxy resin with 48% by volume fibre content. The laminates were oven cured at 127°C for 2h, and a vacuum of 760 mm Hg (≈ 100 kPa) was applied to the debulked stack of plies throughout the oven cure cycle. Specimens were hygrothermally conditioned in an environmental chamber at approximately 70°C and 95% relative humidity to absorb various levels of moisture. DMA-983 was used at 1 Hz frequency, sinusoidal oscillation amplitude of 0.3 mm and a heating rate of 3.0°C/min.

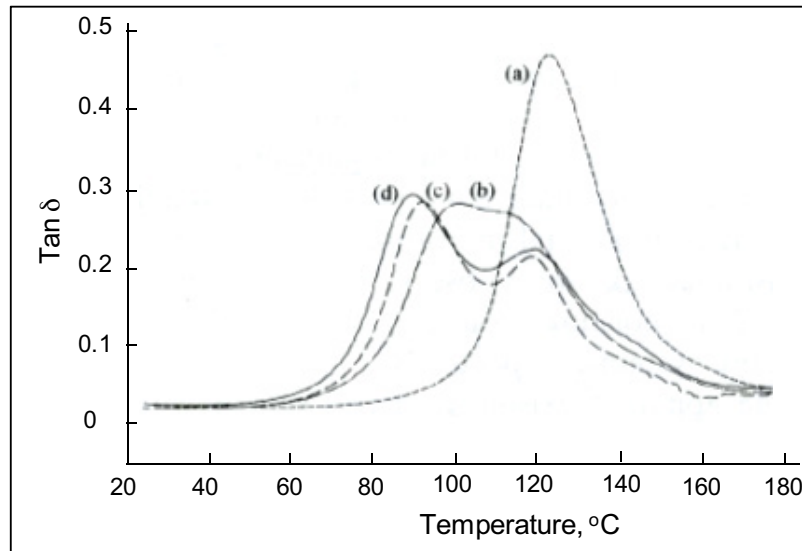


Figure 4.56 Plots of $\tan \delta$ vs. temperature for specimens containing various moisture contents: (a) 0%, (b) 2%, (c) 3% and (d) 3.8% (obtained at 70°C/100% RH) (source: Akay et al. 1997)

Figure 4.57 shows the influence of heat on the transverse (90° direction) tensile stress-strain behaviour of dry and wet composite specimens. The composite was a unidirectional graphite fibre reinforced epoxy resin (AS/3501-5) with 63% by volume fibre content. The wet specimens were conditioned in humidity chambers set at 75% and 95% relative humidities and 70°C, resulting in moisture gains by weight of 1% and 1.6%, respectively. There is a clear deterioration in mechanical performance (reductions in stiffness and strength) in this mode of testing where the matrix sensitivity to hot/wet treatment is exposed. The corresponding stress-strain curves for the composite under longitudinal (0° direction) loading show no significant variation. However, it has also been reported that fibre-dominated properties are adversely affected by embrittlement arising from exposure to very low temperatures. A typical tensile strength reduction for a carbon-fibre-reinforced plastic material exposed to temperatures existing at very high altitude is indicated to be 20–25% (Baker et al. 2004, p. 461).

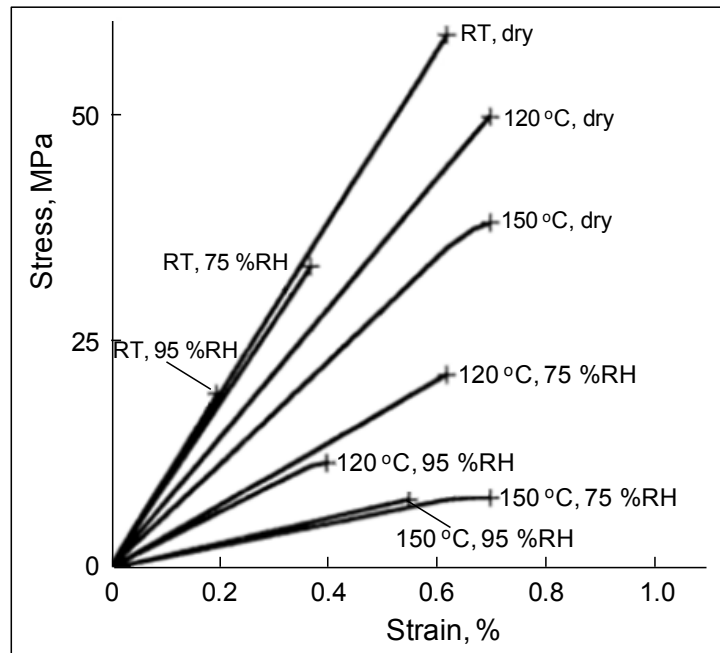


Figure 4.57 Transverse stress-strain curves obtained at different test temperatures for specimens with 1% (75%RH) and 1.6% (95%RH) by weight moisture contents (source: Mallick 1997, p. 869)

TURN TO THE EXPERTS FOR **SUBSCRIPTION** CONSULTANCY

Subscribe is one of the leading companies in Europe when it comes to innovation and business development within subscription businesses.

We innovate new subscription business models or improve existing ones. We do business reviews of existing subscription businesses and we develop acquisition and retention strategies.

Learn more at [linkedin.com/company/subscribe](https://www.linkedin.com/company/subscribe) or contact Managing Director Morten Suhr Hansen at mha@subscribe.dk

SUBSCR✓**BE** - to the future

Figure 4.58 shows the general trends in the variation of tensile and compressive strength with temperature and/or moisture. In “wet” specimens, the composite is fully saturated with moisture. The strength values are expressed as a percentage of the corresponding values at room temperature. Again, it can clearly be seen that the matrix-dominated property, i.e. the compressive strength, is affected by a hot/wet environment. The moisture plasticises the matrix-reducing its strength at elevated temperatures.

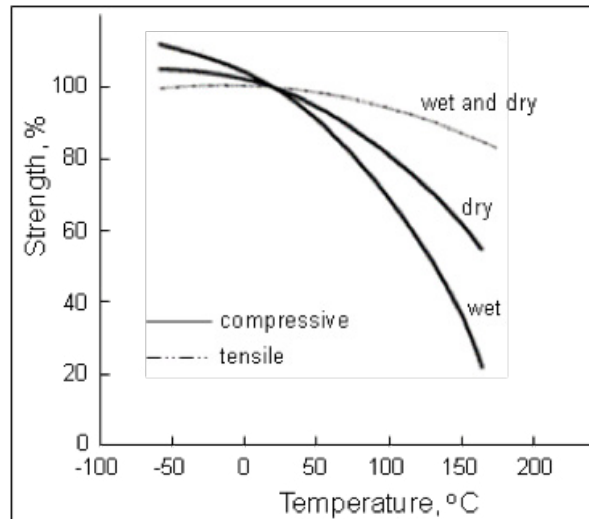


Figure 4.58 Normalised strength vs. temperature for dry or wet graphite/epoxy composite (source: Mallick 1997, p. 870)

Similarly, Figures 4.59–4.61 show the sensitivity of the mechanical properties to the moisture absorption in some Kevlar fibre reinforced epoxy resins. These composites consisted of four-harness (or crowfoot) satin fabric of Kevlar 49–285 fibre reinforced Fiberite and Brochier epoxy resins with 48% by volume fibre content. The laminates were either autoclave or oven cured (details in Akay et al. 1997). Specimens were hygrothermally conditioned in an environmental chamber at approximately 70°C and 95% relative humidity to absorb various levels of moisture. The compressive strength (conducted in accordance with ASTM D695) decreased at a rate of approximately 5% per 1% moisture gain up to approximately 2.5% moisture content (see Figure 4.59). No clear change was experienced in the compressive modulus. The flexural strength (conducted in accordance with ASTM D790) showed a linear decrease with moisture content at a rate of approximately 2% per 1% absorbed moisture (Figures 4.60). No clear changes were indicated in the flexural modulus as can be seen in Figure 4.61.

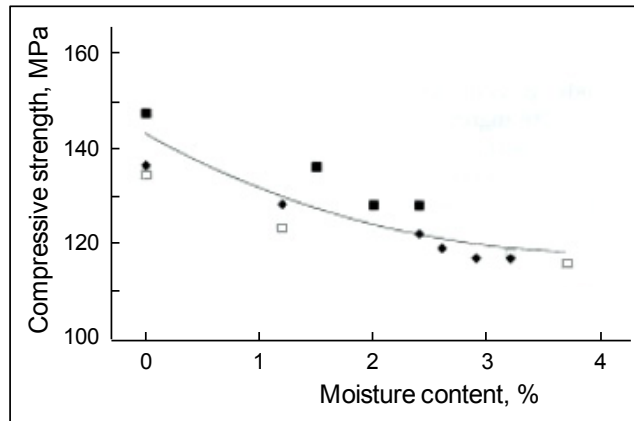


Figure 4.59 Compressive strength vs. moisture content (weight %) for (■) Kevlar/Fiberite (autoclaved), (□) Kevlar/Fiberite (oven cured) and (◆) Kevlar/Brochier (autoclaved) (source: Akay et al. 1997)

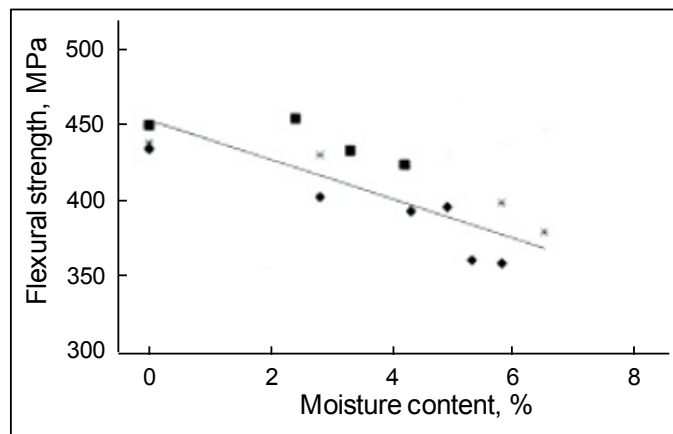


Figure 4.60 Flexural strength vs. moisture content (weight %) for (■) Kevlar/Fiberite (autoclaved), (◆) Kevlar/Brochier (autoclaved) and (*) Kevlar/Brochier (oven cured) (source: Akay et al. 1997)

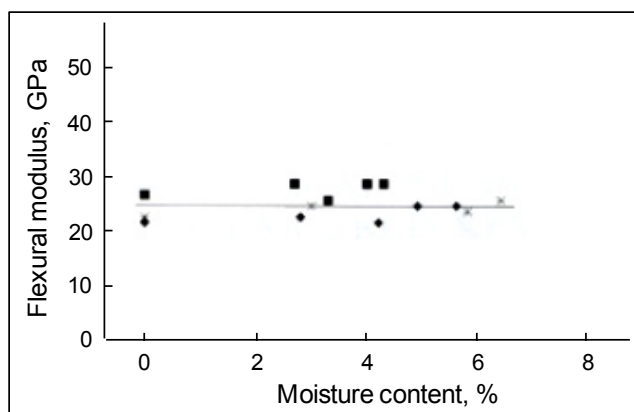


Figure 4.61 Flexural modulus vs. moisture content (weight %) for (■) Kevlar/Fiberite (autoclaved), (◆) Kevlar/Brochier (autoclaved) and (*) Kevlar/Brochier (oven cured) (source: Akay et al. 1997)

The effect of moisture content on T_g of various epoxy resins is presented in Figure 4.62. Properties suffer dramatic reductions above T_g , accordingly, the certification authorities (e.g. JAA, the Joint Aviation Authorities) specify a separation (maximum operating limit safety factor) of 25°C between T_g and a maximum operating temperature (Baker et al., 2004, p. 460).

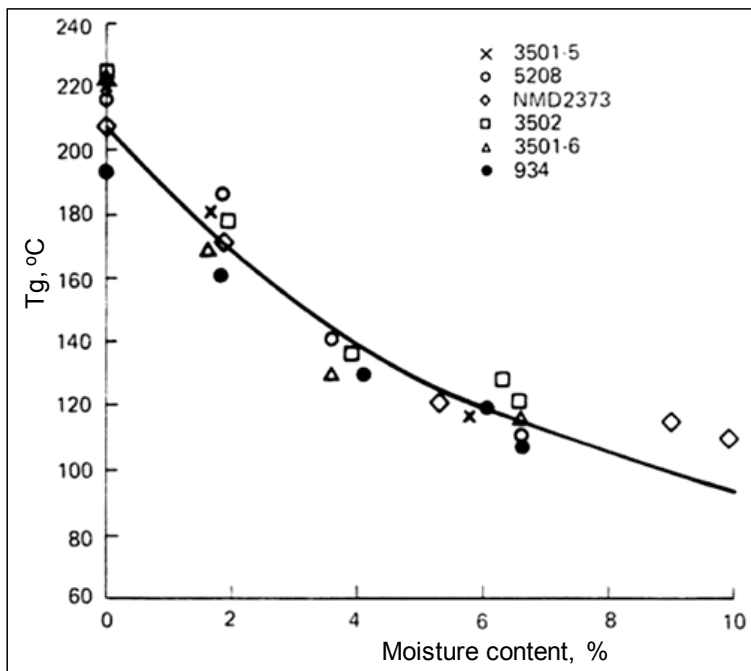


Figure 4.62 Relationship between equilibrium moisture concentration and glass-transition temperature of epoxy resins. T_g measurements were made with a thermomechanical analyser (source: Vinson 1978, p. 14)

Combined temperature/humidity cycling is another consideration and its effects are illustrated in Figure 4.63 for cross-plyed epoxy-based composites reinforced with glass, aramid, and carbon fibres.

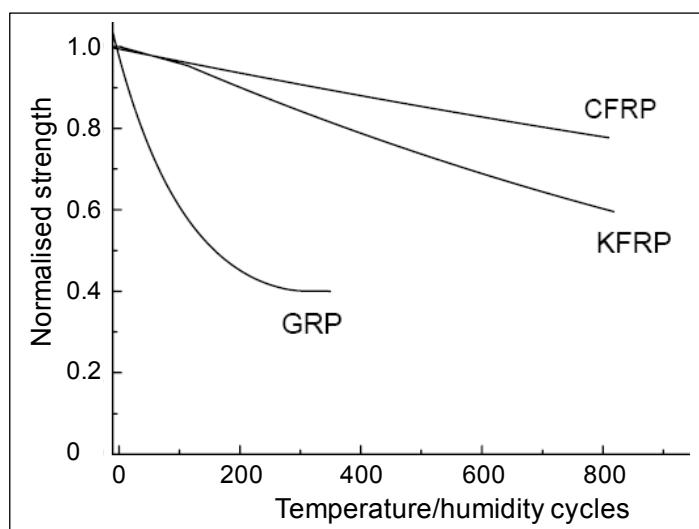
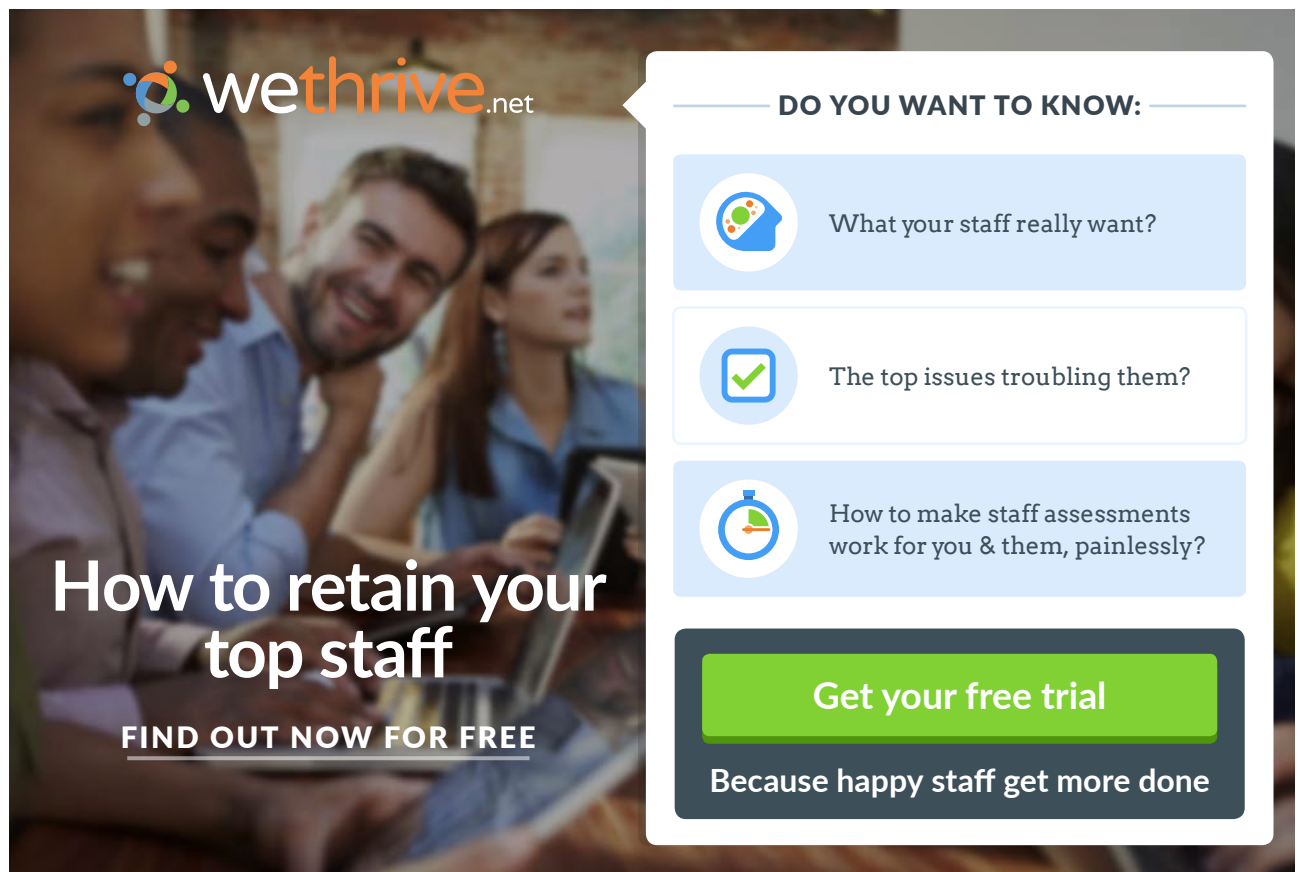


Figure 4.63 Reductions in the strengths of 0°/90° laminates of CFRP, GRP and KFRP as a consequence of temperature/humidity cycling. The cycle consisted of 12 hours at 2°C and 0 %RH, followed by 12 hours at 85°C and 100 %RH (source: Harris 1999, p. 163)

Figure 4.64 shows the general level of sensitivity of various polymer matrices to moisture, where semi-crystalline thermoplastics are indicated as being least prone to moisture. However, some semi-crystalline polymers such as polyamides are hydrophilic and moisture absorption significantly influences their properties. Figure 4.65 shows the influence of moisture on the elastic modulus of injection moulded polyamide 66 and short glass-fibre reinforced polyamide 66 (SGFPA) of 50% by weight fibre content. The study (Akay 1994) has also shown that both unfilled and glass-fibre filled polyamide specimens suffered a deterioration of 35% in UTS, but elongation to failure increased considerably for unfilled PA at equilibrium moisture uptake because of the moisture-induced plasticisation of the polymer. The equilibrium moisture contents were approximately 4.5% and 2.2% respectively for PA and SGFPA specimens conditioned at approximately 60°C and 90 % relative humidity.



wethrive.net

How to retain your top staff

FIND OUT NOW FOR FREE

DO YOU WANT TO KNOW:

- What your staff really want?
- The top issues troubling them?
- How to make staff assessments work for you & them, painlessly?

Get your free trial

Because happy staff get more done

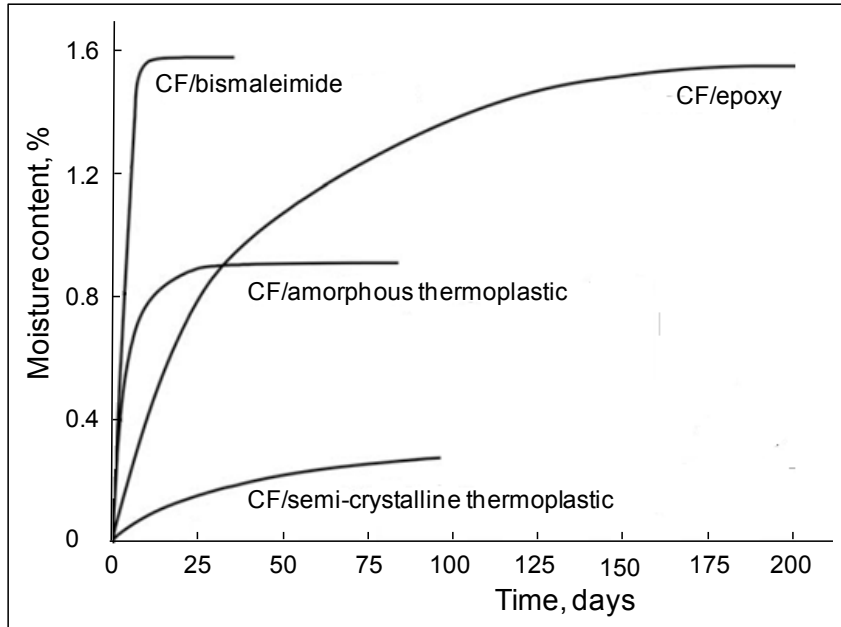


Figure 4.64 Levels of moisture absorption by various PMCs: laminates of 4.3 mm thickness are conditioned at 71°C and 95% RH (source: Campbell 2010)

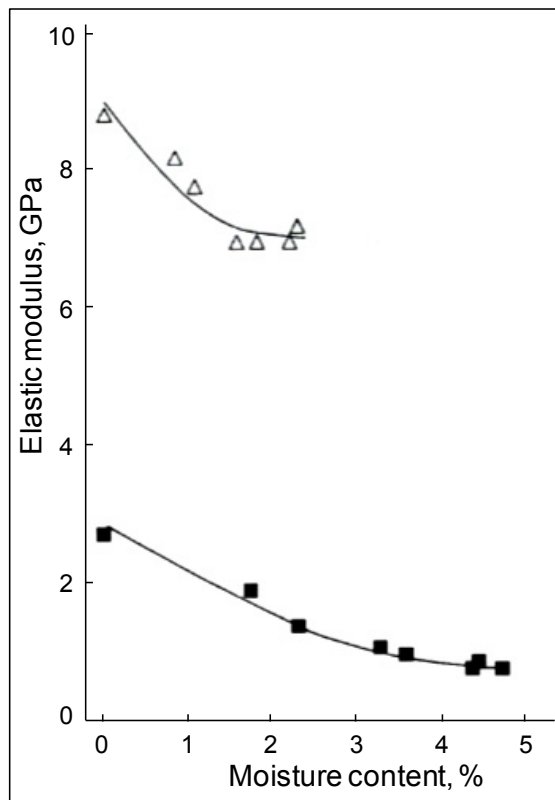


Figure 4.65 Elastic modulus vs. moisture content (weight %) for (■) PA and (Δ) SGFPA specimens (source: Akay 1994)

4.12 Non destructive evaluation

Defects can present a visual blemish but more critically cause a reduction in properties of engineering materials such as composites. It, therefore, becomes important to detect defects in composite structures after manufacture and in service. For example, the strict quality assurance policy of the aviation industry enforces components to be inspected for defects using non-destructive techniques. These can be used either for detecting the presence of damage/defects or for measuring the effects of damage growth via changes in mechanical properties.

ASTM E2533 – 09 standard provides guidelines/information to help engineers select appropriate non-destructive testing (NDT) methods to characterize aerospace polymer matrix composites. Detailed accounts of non-destructive testing/inspection can be found in Vaara & Leinonen (2012), Gower et al. (2007, p. 36), Baker et al. (2004, p. 414), ENG 4793 Module, Strong (2008, p. 298), Kapadia (2007) and NetComposites.

Tables 4.7 and 4.8 list typical manufacturing defects and typical defects that can develop in service, respectively.

Defect	Description
Delaminations	An area of separation between fabric layers in the laminate structure.
Unbond	An area in which two adherends or pre-preg layers failed to bond together.
Disbond	An area in which two adherends have separated at the bondline.
Porosity	The entrapment of pockets of air or gas (es) within a solid material.
Crack	A fracture of material in the laminate that typically extends through the thickness.
Core crush	Damage of the honeycomb core due to impact or excessive pressure during cure.
Foreign object	An inclusion of a foreign substance, such as peel ply, during the manufacturing process.

Tables 4.7 Common defects found in fabricated advanced composite structures (source: Baker, et al. 2004, p. 415)

Defect	Description
Impact damage	Internal damage of composite caused by collision with an external body during flight or docking, typically marked by delaminations, fibre breaking and matrix cracking.
Delaminations	Separation within the composite has occurred generally due to unexpected out-of-plane stresses.
Lightning burns	An area of the composite that has been subjected to high temperatures, causing decomposition and degradation in properties of the matrix.
Disbonding	Interfacial separation in composite/composite or composite/ metal bonded joints due to out-of-plane stresses or, in the case of metallic joints, to environmental degradation.
Core degradation	Areas in honeycomb sandwich panels with cores where water has penetrated leading, in the case of metallic cores, to disbonding and corrosion.

Tables 4.8 Common In-service defects found in advanced composite aircraft structures (source: Baker, et al. 2004, p. 415)

Tables 4.9 and 4.10 list the application of some of the current NDT methods during the life cycle of polymeric matrix composites. It can be seen that no single NDT technique provides all the information necessary to detect all types of defects/concerns. Often it is the geometry of the structure that limits the type of inspection technique that can be used.

NDT technique	Product and process design and optimization	On-line process control	After manufacture inspection	In-service inspection	Health monitoring
Acoustic emission	X	X	X	X	X
Computed tomography			X		
Leak Testing	X	X		X ^A	
Radiography/radioscopy	X	X	X	X	
Shearography	X	X	X	X	
Strain measurement			X		X
Thermography			X	X	
Ultrasound/ultrasonics	X	X	X	X	X
Visual	X	X	X	X	X

Tables 4.9 Application of established NDT methods during the life cycle of PMCs (source: ASTM E2533 – 09)

^A Applicable to composites used in storage and distribution of fluids and gases, for example, filament-wound pressure vessels.

Struggling to get interviews?

Professional CV consulting & writing assistance from leading job experts in the UK.

Visit site

 Take a short-cut to your next job!
Improve your interview success rate by 70%.

 **TheCVagency**
Visit theagency.co.uk for more info.

  Click on the ad to read more

	Acoustic Emission (AE)	Acoustic Impact (AI)	Laser Shearography (LS)	Mechanical Impedance (MI)	Membrane Resonance (MR)	Transient Thermography (TT)	Ultrasonic Amplitude C-Scan (UC)	Ultrasonic Thickness A-Scan (UA)	Ultrasonic Linear B-Scan (UB)	Ultrasonic Depth Scan (UD)	X-Radiography (XR)
Delamination (<10 mm)	7	2	9	4	4	8	9	5	8	9	7
Delamination (>10 mm)	7	5	10	6	6	10	10	8	10	10	7
Crack	7	0	9	0	0	4	0	0	0	0	8
Disbond	2	5	10	6	6	10	10	8	10	10	7
Void	0	1	5	1	1	5	10	6	6	6	10
Impact (BVI)	7	5	10	6	6	8	10	10	10	10	4
Porosity	0	0	8	0	0	6	9	5	6	4	10
Inclusion	0	3	7	4	4	7	9	7	7	6	6
Erosion	0	0	5	0	0	7	7	9	10	10	4
Core splice	0	5	8	5	5	4	6	1	2	0	8
Core disbond	1	10	10	10	10	10	10	8	9	8	5
Core crushing	5	10	5	10	10	5	8	5	5	0	5
Matrix Cracking	10	0	0	0	0	0	0	0	0	0	6
Fibre breakage	10	4	6	4	4	0	0	0	0	0	5
Kissing Bond	0	1	5	1	1	2	1	0	0	0	0
Environment ingress	0	0	4	0	0	10	8	4	5	0	5
Fibre Wrinkling/Waviness	0	0	4	0	0	2	9	1	8	0	2
Fibre and ply misalignment	0	0	2	0	0	2	9	0	1	0	5
Incorrect cure	0	0	0	0	0	0	2	0	5	5	0
Excess resin	0	0	5	0	0	6	5	0	5	8	2
Excess fibre	0	0	5	0	0	6	5	0	5	8	2

Tables 4.10 Applicability of NDT methods to different kinds of defects in composites. Numbers indicate: 10 – high; 7 to 9 – good; 4 to 6 – some; 1 to 3 – limited, and 0 – no applicability (source: Vaara 2012, p. 8)

Acoustic emission (AE) detects sounds emitted by an object (sample or a product) in-service as it is subjected to mechanical/thermal stress. Employment of a single sensor detects the occurrence of the emission, and the location of the emission's source can be found by using several sensors.

Acoustic impact (AI) method uses an acoustic wave to resonate a specimen/structure in its natural frequencies and record the changes in the natural frequency response due to any sub-surface defects. The test is performed by tapping the specimen with an instrumented hammer and detecting the resulting vibrations by an accelerometer or a microphone. AI is mainly used to detect delaminations and disbonds.

Ultrasonics scans the material with ultrasonic energy while monitoring the reflected energy for attenuation (reduction) of the signal. The scanning method most often employed is called C-scan, commonly implemented with separate transducer and receiver that are being moved along matching paths in opposing sides of the sample using water as a coupling agent between the transducer, sample and receiver. A-Scan works on the same principle as C-Scan except that a sound transmitter is placed in direct contact with the part surface via a coupling fluid. The equipment measures the amount of sound reflected back through the part and compares it to a standard.

A slightly modified method called L-scan can detect stiffness of the sample using the wave speed, but requires that the sample density be known.

X-radiography (XR) is the most commonly used radiographic NDT method. X-rays are attenuated when they interact with energy states of electrons in the atoms in the beam's path. The denser the material is and the more material there is the more the x-rays will be attenuated while travelling through the sample. Therefore, any variation in the shade/intensity in the x-ray image/trace means that there is either a difference in the material density/material thickness. There are defect types that cannot be seen in an x-ray image, e.g. delaminations and disbonds. Such defects are virtually invisible to x-rays because they don't change the composition or total amount of materials through which the x-rays travel. When normal radiography fails to produce sufficient contrast, it can be enhanced by the introduction of a contrast medium/a radio-opaque penetrant (e.g. trichloroethane, tetrabromoethane, zinc iodide, silver nitrate or barium sulphate) into the material. This makes defects such as delaminations and disbondings visible in an x-ray image.

Computed tomography (CT)/X-ray tomography (XT) produces 3-dimensional images of objects using x-rays. The scanner circles the object and yields cross-sectional 'slices' through the sample which then make up images. The slice images resulting from the computation show the sample without geometric distortions, making it possible to measure distances between different points in the sample using the images. Such measurements would not be possible with traditional shadowgraphs where points at different distances from the x-ray source would appear with different magnifications.

Thermography works on the principle that when materials/components heated at a suitable rate, heat capacity/heat flow in a material changes by the presence of some types of anomalies. These changes cause localized temperature differences in the material. The technique is a non-contact one and is well suited to detecting disbonds and delaminations. It is most suited to large planar structures or curved components with large radii of curvature. IR cameras are commonly used to detect radiated heat and are controlled by TV video electronics. Liquid crystal coatings and pyroelectric detectors have also been used to detect IR radiation.

Leak testing evaluates the integrity of a vessel, barrier or pipe to contain a fluid or gas.

Shearography/Holography exploits the fact that when a composite is loaded in shear, the surface will deform differently in the presence of near-surface defects. In laser shearography (LS) the specimen is illuminated with laser light when unloaded and under load, and the interference fringe patterns generated by the small variations in strain is detected using an optical interferometer. Types of defects best detected under LS include delaminations, disbonding and impact damage.

The **mechanical impedance** method is similar to the coin-tap test except that the excitation is continuous harmonic rather than impulse. The sensitivities of these techniques decrease as the depth of the flaw increases, therefore, they are better suited to detecting near-surface delaminations.

The **membrane resonance** method is similar to the mechanical impedance method except that it specifically measures local resonant vibration, and the excitation source is non-contact. It works on the principle that the layers above a delamination constitute a membrane, which has a thickness the same as the depth of the specimen where the delamination has occurred. Accordingly at frequencies around the membrane resonance, the vibration response for a given input force-amplitude will be greater at the delamination than in a sound region at the same depth.

4.13 Self-assessment questions

1. Which of the following fibres has excellent compressive properties?
 - a) Glass
 - b) Carbon
 - c) Aramid
2. Which of the following fibres has poor compressive properties?
 - a) Glass
 - b) Carbon
 - c) Aramid

gaiTeye
Challenge the way we run

**EXPERIENCE THE POWER OF
FULL ENGAGEMENT...**

**RUN FASTER.
RUN LONGER..
RUN EASIER...**

**READ MORE & PRE-ORDER TODAY
WWW.GAITEYE.COM**

The advertisement features a runner in a red top and black leggings running on a path. The background is a warm, golden-orange glow. Technical diagrams, including a dotted line and a circular diagram with lines, are overlaid on the runner's feet. A yellow button with a hand cursor icon is located in the bottom right corner of the ad.

3. Describe the mechanical test methods, which are specifically appropriate for continuous fibre reinforced PMCs.
4. Explain, by giving specific examples, how the dynamic mechanical thermal properties of unidirectional fibre reinforced composites are influenced by the fibre direction.
5. A hybrid unidirectional continuous fibre reinforced epoxy resin composite contains 30% by volume graphite fibre and 30% by volume Kevlar 49. Estimate the longitudinal specific modulus of the composite. Express the result in a unit of velocity and indicate its significance. Select the required data from the table below.

Properties of constituent materials

Material	Density, g / cm ³	Tensile modulus, GPa	Tensile strength, MPa
Epoxy resin	1.25	3.5	70
E-glass fibre	2.58	72.5	3450
Graphite-HM fibre	1.9	390	2400
Kevlar 49	1.44	131	3700
Kevlar 149	1.47	186	3400

Answer: $E_c/\rho_c = 105 \times 10^6 \text{ m}^2/\text{sec}^2$.

The square root of E_c/ρ_c is the velocity of sound in the material, in this case in the longitudinal direction.

6. Sports products made from composites offer significant reductions in sports injuries such as “tennis elbow”. What particular property of the material has contributed to this improvement? Express this property in terms of the modulus of rigidity of the material.

Answer: $\tan\delta$.

7. Describe and compare different ways of determining T_g . Why is T_g an important parameter to measure in composites?
8. Compare aluminium alloy tennis racquets with those fabricated from carbon fibre reinforced plastics for player comfort.

Answer: although aluminium racquets are tough and moderately priced, the fibre-plastics composite ones are lighter and offer much better vibration damping that considerably reduces the occurrence of tennis elbow.

9. Briefly describe five different NDT methods for PMCs and compare their suitability for determining the presence of voids.

5 Applications and materials selection

5.1 Applications

Applications of composites, as for materials in general, depend on their technical functionality and processability within the constraints of cost and sustainability, and safety, health & environment (SHE). Composites offer an advantage compared with other materials in that their structures/properties can be tailored. Applications include construction, transportation (road, rail and marine), sports and leisure, electrical and energy as well as aerospace. The subject is covered extensively in the literature, for example, on applications in general (Campbell (2010, p. 18), Van Paepegem (2014) and Toray (2012)), on building & construction (Singleton & Hutchinson 2010), on aircraft applications (Baker et al. (2004, p. 234) and Bombardier 2011), on wind turbine blades (Gurit wind-energy handbook 2014), on vehicles (NHTSA report 2012 and Carpenter 2008), on sports & leisure (Easterling 1993), on bio-medical applications (Hu 2012, p. 111) and on carbon-fibre sensors (Hu 2012, p. 357).

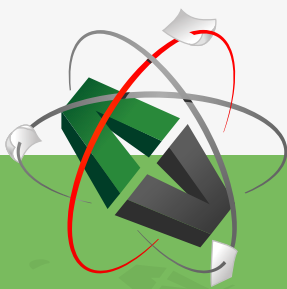
5.1.1 Aerospace

In the early 1970s, composite materials were introduced to airframe structures to increase the performance and life of the airframe. In 1977, the National Aeronautics and Space Administration (NASA) Advanced Composite Structures Program introduced the use of composites in primary structures in commercial aircraft, i.e. the Boeing 737 horizontal stabilizer.

The use of glass-fibre (GF) composites goes back to World War II. At the time, the aircraft industry was reluctant to use glass-fibre composites more widely because of the low stiffness of glass-fibres and the poor strength and toughness of polyester resins, particularly at elevated temperatures. The development of stronger, tougher, and more durable resins, such as epoxies, led to the increased use of E-glass laminates in some aircrafts. For example, virtually the entire airframe, wings, and fuselage of modern gliders are built from GF/epoxy. As described in Baker et al. (2004), “In the 1960s the development of S2-type glass, which has greater stiffness and strength than E-glass, allowed a greater variety of aircraft structures and components to be made. GF/epoxy honeycomb sandwich panels are also used in a variety of components on modern military aircraft, such as the fixed trailing edge on the B-2 bomber.

Another common use of composites with E-glass or quartz fibre reinforcement is in radomes on commercial and fighter aircrafts, in bay- and wing-mounted radomes on supersonic aircraft and missiles, and in the large radar domes on Airborne Early Warning and Control (AEW&C) military aircraft. This is because of the excellent transparency of glass to radar signals. Glass/epoxy is widely used in helicopter components, such as in the spars to the main and tail rotor blades, fuselage body panels, and flooring. Glass fibres are also used in combination with carbon and Kevlar fibres in hybrid composites for a wide variety of aircraft components, such as wing-body fairings, engine pylon fairings, and engine cowlings. Polyesters have been used in composites for cabin interiors; however, in this application, phenolics are now preferred due to their excellent flame resistance.”

This e-book
is made with
SetaPDF



PDF components for **PHP** developers

www.setasign.com



Baker et al. (2004) have also described the carbon fibre-reinforced epoxy resin as the most important polymer-matrix composite for aircraft structures. In spite of the relatively high raw material costs, because of advantages over metals, their usage is increasing. Baker et al. state, “The need for high stiffness to minimize the depth of wings and tail in high performance military aircraft both for aero- elastic (the elastic properties of structures that are subject to aerodynamic pressures) and stealth reasons ensures that all future aircraft will have composite wing and empennage (the tail) skins. The requirement for stealth as well as minimum weight also ensures that most of the fuselage skin will be composite. For radar absorption, leading edges will be made of honeycomb structure with outer composite skins based on non-conducting fibres such as quartz rather than carbon present in the rest of the structure. This skin material allows the radar waves to penetrate into the honeycomb core coated with radar-absorbing material, rather than being reflected back to the receiver.”

Modern improved composite materials and matured processes have encouraged commercial aircraft companies to increase the use of composites in primary and secondary structures. Driven by the demand for fuel-efficient, light-weight, and high-stiffness structures that have fatigue durability and corrosion resistance, recent planes, the Boeing 787 Dreamliner and the Airbus A350, incorporate 50% advanced composites in their primary structures of fuselage and wings, marking a striking milestone in composite usage in commercial aviation. Figure 5.1 shows the use of composites in commercial aircraft applications.

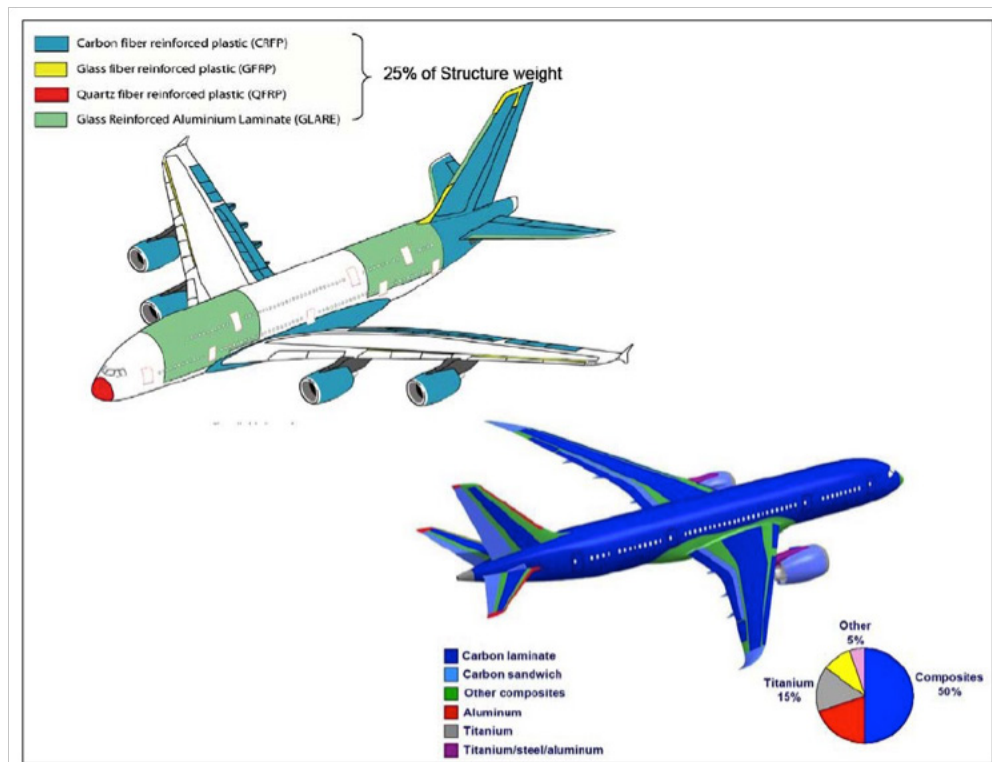


Figure 5.1 Composite materials applications in commercial aircrafts (source: Tomblin & Waruna 2011)

Typical products include composite ducting, structural and non-structural panels, seat shells, lightweight ventilation ducts, etc.

Focusing on composite applications in primary structures of a significant size, the vertical tail-plane of the A310/300 was certified in 1985. A description of this composite part, which can be considered as being the first one ever, with a brief survey of the certification work carried out at that time, was presented by Schulz (1984) at the ICAS 84 symposium.

The A320, with all the control surfaces and the whole tail-plane made out of composite, was certified in 1988, and turned out to be a significant breakthrough in the introduction of such materials in aircraft structures.

With an application now to the wings and the fuselage, the Boeing 787, followed by the Airbus A350 XWB, represents the second major step of this evolution. In both programmes a proportion of advanced composites approaching 50% is now achieved. Figure 5.2 illustrates how this composite ratio evolved over time for commercial aircraft.

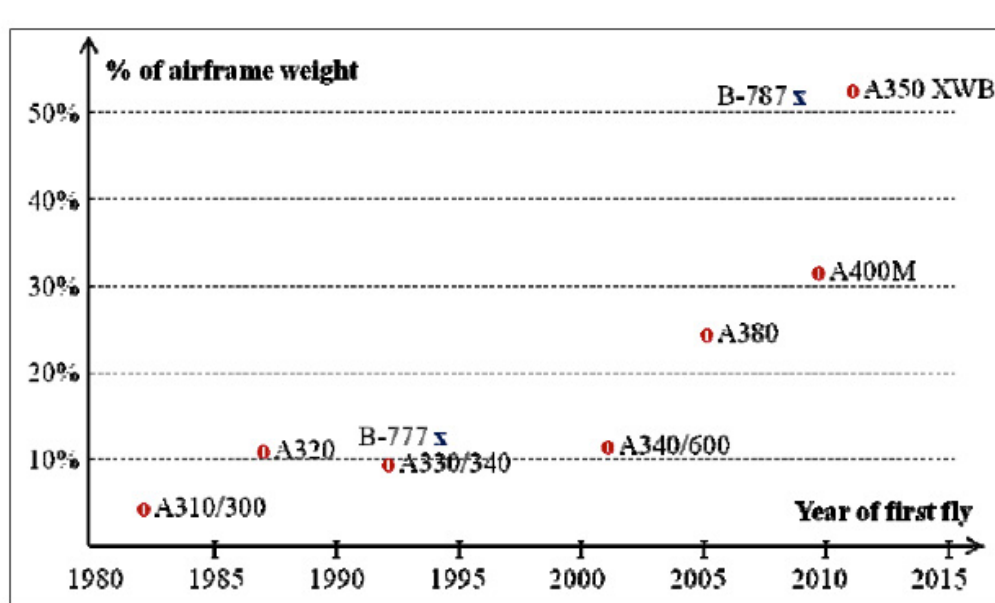


Figure 5.2 Evolution of the composite ratio on commercial aircraft (source: Rouchon 2009)

5.1.2 Wind turbine blades

The increasing demand to reduce the cost of energy generated from the wind drives wind turbine designs towards larger blades. These large structures experience high cycle fatigue and can contain defects from manufacture or be subject to damage-events, so it is desirable that they possess a high degree of damage tolerance to prevent costly failures and to minimise forced maintenance.

Rotor blades are the largest rotating components of a wind turbine. They should last for a minimum of 20 years. During this time they will be subjected to varying wind loads. Thus, they should be designed against different types of damage. The macroscale testing of composite materials for wind turbine rotor blades involves testing of the base materials (usually unidirectional layers), laminates, sandwich core materials, adhesives, gelcoats and interfaces between various layers under both static and cyclic loads. Strength and fatigue characterisation is made by traditional tension, compression and shear testing as well as fracture mechanics testing of interfaces (Brøndsted et al. 2005).

In an overview paper, Sørensen (2009) describes the major trends in the development of new wind turbines as being (a) development of larger size wind turbines, and (b) offshore placement in large wind turbine parks. Combined, the two trends lead to several challenges with respect to rotor blades:

First, the weight of wind turbine rotor blades increases dramatically with increasing blade length. For future blades, the gravitation loads will exceed the aerodynamic loads. Thus, weight savings become of great importance. In the design phase, this can be achieved by better design of structural details and by the use of stronger materials. More accurate design methods are needed and better material testing methods and material models are needed to give a better description of the properties of the materials.

A dark blue advertisement for Rand Merchant Bank. The background features a large, faint, stylized graphic of a lion's head. In the center, the text "YOU THINK. YOU CAN WORK AT RMB" is written in large, white, sans-serif capital letters. In the top right corner, there is a white rectangular box containing the Rand Merchant Bank logo (a lion holding a key) and the text "RAND MERCHANT BANK", "A Division of FirstRand Bank Limited", and "Traditional values. Innovative ideas.".

**YOU THINK.
YOU CAN WORK
AT RMB**

RAND MERCHANT BANK
A Division of FirstRand Bank Limited
Traditional values. Innovative ideas.

Rand Merchant Bank uses good business to create a better world, which is one of the reasons that the country's top talent chooses to work at RMB. For more information visit us at www.rmb.co.za

Thinking that can change your world

Rand Merchant Bank is an Authorised Financial Services Provider



Second, since wind turbine blades are traditionally made of relatively few parts being glued together, it becomes of great importance to ensure high quality uniformity. Blades that have manufacturing defects will be repaired, since large parts are costly and it is therefore very unattractive to discard them.

Third, since offshore wind turbines are difficult and costly to access, it is desirable to reduce the need for manual inspection as much as possible. Sensors that can detect damage in the blades will be built-in, so that blade damage can be detected in time and inspection can be restricted to damaged blades.

Fourth, there must be reliable modelling tools available for modelling of the damage evolution in wind turbine blades, such that it becomes possible to make accurate assessments of the detected damage and thus make knowledge-based decisions regarding whether the blade should be replaced, repaired, or kept in use without being repaired.

Gurit (<http://www.gurit.com/files/documents/spar-brochurev2pdf.pdf>), a supplier of materials to the wind energy market since 1995, have accounted on the lightning protection of wind turbine blades: the main aim of lightning protection is to avoid a lightning arc inside the blade itself, which can overheat the structural laminate, causing permanent damage. Glass fibre blades are typically fitted with metal lightning receptors near the tip and at intervals along the blade, connected by a heavy gauge copper or aluminium cable. Earth connection is provided through the hub, nacelle and the steel tower to the foundation.

As carbon fibre is a conductor of electricity, the traditional protection systems developed for glass-fibre blades need some refinement to protect carbon spar caps. Cured carbon laminates have a conductivity about 1000 times lower than aluminium, therefore given its large cross-sectional area the carbon spar cap can become a preferential route for the lightning current. The conductivity of the carbon is also dependent on the orientation of the fibres; consequently, a lightning arc can be formed within the laminate itself. Diverting the lightning current from the attachment point along the surface to the blade root, using metallic conductors either fixed to the blade surface or inside the blade, is therefore recommended.

Traditional aluminium conductors for the lightning current are not compatible with carbon composites, since galvanic corrosion can occur, where carbon becomes the cathode (passive end) and the aluminium the anode (reactive end) in the presence of an electrolyte (air moisture). However, there are a series of alternatives, for instance copper, since copper is on the passive end of the electrochemical series avoiding ionic flow between carbon, currently being used both in modern aircraft and wind energy industries. Available technologies according to IEC/TR 61400-24 (2002, p. 41) are:

- lightning air termination systems on the blade surface or embedded in the surface
- adhesive metallic tapes and segmented diverter strips
- internal down conductor systems (used in aircraft and most common on rotor blades up to 50 m, i.e. in leading and trailing edges)
- conducting surface materials (aircraft and new generation rotor blades use metal meshes or surface treatments).

In the aircraft industry, lightning protection of glass and carbon fibre composite materials for wings and surfaces exposed to lightning, is achieved by adding conducting material to the outer layers, thereby reducing damage to a small area at the attachment point. The conducting material may be metal sprayed onto the surface, metal coated fibres in the outer layers of the composite material, metal wire woven into the outer layers of the composite material, or meshes of metal placed just beneath the surface (Figure 5.3 shows a composite sandwich test panel with Cu-wire mesh in the surface). Lightning protection of carbon fibre composite wind turbine blades, similarly, has been made with metal mesh placed along the sides of the blades outside the spar caps (see Figure 5.4 for a diagram of a spar cap). Lightning protection of wind turbine blades becomes more challenging with increasing size, particularly offshore where the uppermost blade tip may be 150 m above sea level. The general trend for larger wind turbine-generator rotor blades is to use metal meshes or surface treatments to make the surface conductive, as in the aerospace industry.

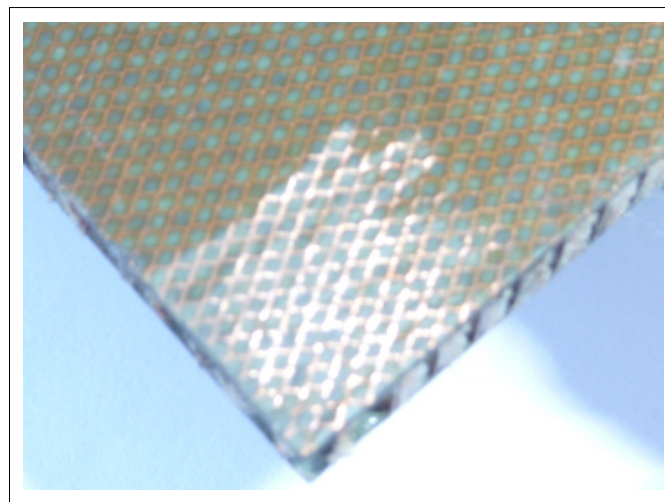


Figure 5.3 A composite-sandwich test panel with Cu-mesh surface. The protective thin coating is scraped off to expose the wire mesh

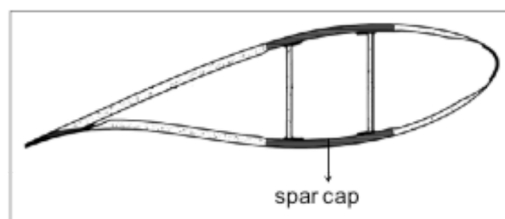


Figure 5.4 A diagram of a spar cap

Alternative material systems to that of thermoset-matrix composites are explored for the production of wind blades; thermoplastics lend themselves to resistance welding and repair methods and are conveniently recyclable at end-of-life. With increased blade lengths, weight reductions can also be achieved with thermoplastic composites. However there are problems associated with the use of thermoplastic composites, Prabhakaran et al. (2011) have reviewed the advantages and disadvantages of thermoplastic composites in the production of wind turbine blades. They have covered thermoplastic material systems such as commingled (PP, PET, PBT and PA6 fibres with glass fibres (GF)), thermoplastic/GF prepregs, and reactive polymer (anionic polyamide 6 (APA6) and cyclic butylene terephthalate (CBT) with GF) systems.

The development of high quality bamboo-based composites has been identified (Brøndsted et al. 2009) as an important alternative towards the use of green materials in low-cost wind turbine applications. The paper also includes tensile and compressive stress-strain behaviour, fatigue life and fracture resistance of the bamboo laminates consisting of hot-pressed layers of bamboo with poplar veneer.



Discover the truth at www.deloitte.ca/careers

Deloitte.

© Deloitte & Touche LLP and affiliated entities.



Click on the ad to read more

The wind energy market is dominated by horizontal axis wind turbines (HAWTs), which work best in open settings, such as offshore or on land in rural areas where the wind is not disturbed by buildings or trees. It is asserted (Brown & Brooks 2009) that vertical axis wind turbines (VAWTs), Figure 5.5, are more suited for built-up urban areas: they have lower wind start-up speeds, can be located nearer to the ground making maintenance easier, work in any wind direction and are relatively quiet. Brown & Brooks have conducted a feasibility study on the use of a one-step vacuum moulded thermoplastic composite sandwich (TPS) material system for a 5 kW vertical axis wind turbine blade, indicating that TPSs offer several advantages including: high fracture toughness and impact tolerance, high fatigue resistance and good specific mechanical properties. In addition, TPSs offer the opportunity for one-step, low cost, clean manufacturing (no styrene emissions), and that they can be recycled at end of life.



Figure 5.5 Vertical axis wind turbine (source: Skyrota LGC)

The proposed blade construction is a sandwich structure with thermoplastic glass reinforced composite skins and a thermoplastic foam core. The skin laminates are manufactured using Twintex™, a commingled woven fabric E-glass/polypropylene material with a 60% fibre weight fraction (see Figure 5.6). The core material is a lightweight polyethylene terephthalate (PET) foam of density 150 kg/m³. The structural response of the sub-scale prototype blade was assessed using a three-point bending test, see Figure 5.7.



Figure 5.6 A roll of Twintex fabric (black yarns are PP)



Figure 5.7 Picture of 3-P bending test setup with a span of 850 mm
(source: Brown & Brooks 2009)

5.1.3 Building and construction

Composites have been used throughout the history of building and construction. Mud and straw were used to make adobe bricks (sun-dried bricks). Lime plaster was traditionally reinforced with straw or animal hair. Wood is a natural fibre reinforced polymer that has always been widely used in construction.

The pultrusion process, producing composite sections/profiles with high concentrations of UD continuous fibre, which enhances stiffness and thermal stability in these materials, has enabled the employment of FRP in building and construction.

A review (Kendall 2008) highlighted that the use of FRP decks in combination with steel structures both for new bridges and to refurbish existing bridges by replacing corroded steel or rotten timber deck enables rapid deck replacement, a reduction in dead load and reduced future maintenance. The benefits of prefabrication include, in some cases, building a complete bridge in the factory before being transported to site for quick and easy installation. While initial costs for an FRP bridge may be slightly higher than a steel equivalent, once the benefits of easier installation and reduced maintenance are taken into account, the total cost will be considerably lower for the FRP option.

A study by Daniel (2003) comparing a number of material options for the construction of pedestrian bridges concluded that:

- structural steel gave the lowest initial cost, with stainless steel the most expensive;
- stainless steel gave the lowest maintenance cost, although it was considered that the predicted maintenance costs for FRP may be very pessimistic;
- combining initial and maintenance costs made steel the cheapest, followed by FRP, aluminium and then stainless steel;
- the environmental analysis of embodied energy put FRP as a clear winner with each other option using more than twice the energy required for FRP; and
- in assessing pollution impacts FRP was again a clear winner.

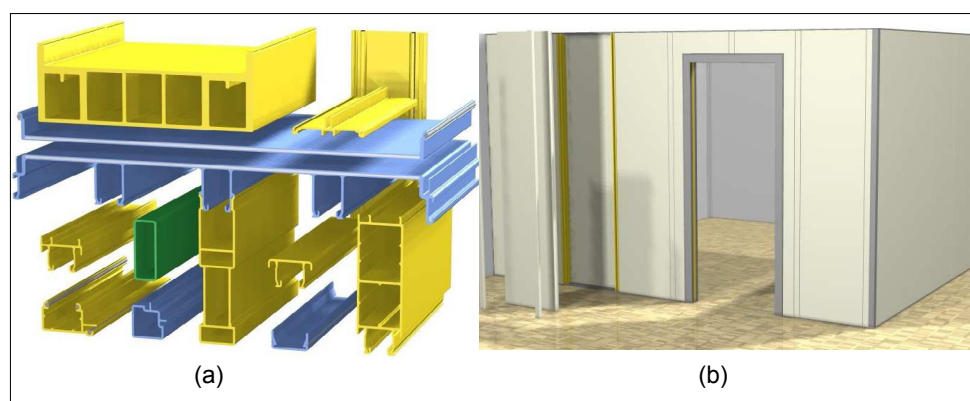
The final material choice was based on ecological factors and the pultruded FGRP sections were used in the installation of the Noordland Footbridge in the Netherlands in 2001.

Many pedestrian bridge projects have been constructed throughout the United States using pultruded composite structural shapes. In the states vulnerable to high seismic activity, concrete bridge columns are being retrofitted with a composite filament winding to increase ductility.

An easy-to-assemble housing suitable for human habitation has been described by Raasch (1998, p. 56). This has a special appeal as emergency housing (especially in natural disaster or military situations), but can also be used to build a wide range of durable, easy-to-assemble structures capable of sheltering from two to 500 people. The system, consists of interlocking pultruded E-glass /isophthalicpolyester modules, is assembled using groove and toggle connectors and adhesives. First into panels; then into wall, floor and roof assemblies; and finally into complete buildings that provide structural integrity without the use of additional framework.

Singleton and Hutchinson (2010) presented details of the Startlink Construction System in cladding for walls and roofs (examples can be seen in Figures 5.8) designed to produce affordable housing. The following key advantages of pultrusions were highlighted:

- resistant to corrosion and attack by insects or fungal growth;
- stable and inert;
- can be fire resistant;
- stronger than steel but only 25% of the weight;
- low thermal transmission; and
- can be delivered to site flat-packed and finished, avoiding all site waste.



Figures 5.8 Startlink (a) pultruded profiles, and (b) interior walls (pultruded panels) (source: Singleton & Hutchinson 2010)

Hobbs (2012) of Gurit in a newsletter describes the Makkah clock tower, the central tower of the Abraj-al Bait development in Makkah, KSA, as the second tallest building in the world standing at 607 m height. The top 200 m of the tower is clad with over 40,000 m² of advanced composite panels, including the largest clocks in the world at 43 m in diameter with 23 m long minute hands.

The newsletter also indicates that Premier Composite Technologies laminated the composite façade on direct CNC cut moulds of polystyrene blocks using a fire retardant laminating binder system designed and supplied by Gurit.

The clock hands presented a particular challenge due to the long slender geometry and wind loading. To meet the wind and geometry challenges, Premier utilized Gurit's carbon fibre prepreg material with foam structural core. The stiffness to weight ratio of the carbon prepreg combined with the mechanical properties and toughness of the structural core enabled the successful construction and operation of the lightweight, yet stiff, clock hands.

**I WANT TO CHANGE DIRECTION,
AND THE WORLD.**

GOT-THE-ENERGY-TO-LEAD.COM

We believe that energy suppliers should be renewable, too. We are therefore looking for enthusiastic new colleagues with plenty of ideas who want to join RWE in changing the world. Visit us online to find out what we are offering and how we are working together to ensure the energy of the future.

RWE
The energy to lead



Prestressing tendons and reinforcement

Fibre composites offer an effective solution for strengthening concrete, bricks or blocks. Three polymer composite materials are commercially available for use as prestressing tendons in concrete (Halliwell 2000, p. 61):

- Polystal is produced by Bayer AG in association with Strabag AG in German. The tendon consists of bundles of bars or rods, each containing E-type glass fibre filaments in an unsaturated polyester resin matrix.
- Parafil is a rope produced by Linear Composites Ltd, UK, which has a core of parallel yarns contained within a polymer sheath. The core yarn can be of many different fibres, but the ones most frequently used are polyester (known as Type A), Kevlar 29 (Type F) and Kevlar 49 (Type G). The lower-modulus polyester ropes are used for guy ropes (a tensioned cable) and some mooring applications. The most suitable rope for use as prestressing tendons is Type G rope, which contains Kevlar 49 as its core yarn. This is the stiffest of the available yarns. Parafil has been used for the repair of structures, and this is likely to be an area in which all non-corroding composite materials are useful. Many distressed structures can be reinstated by prestressing, which closes cracks and restores integrity.
- Arapree is a pretensioning tendon, produced by Enka (part of the worldwide Acordis Group), which is made in the form of pultrusions of the aramid fibre Twaron. The tendons rely on the bond between the concrete and the pultrusion resin. Pretensioned planks have been made with these tendons and the manufacture of railway sleepers has been proposed.

These materials offer the designer of concrete structures corrosion-free tendons, in the form of aramids or glass fibres, which are easier to handle on site because of their light weight. However, these tendons will have to compete with established steel tendon technology by demonstrating their improved long-term durability.

Window frames

Deceuninck have introduced glass fibre-reinforced polyurethane (PU) pultruded profiles, tradenamed Innergy, to fit into PVC windows and door frame chambers as reinforcement/support, see Figure 5.9, instead of aluminium inserts. The result is a new, more efficient system with all the strength and structural reinforcement of aluminium, but with additional benefits such as better thermal insulation. The manufacturers assert that the superior thermal performance of Innergy enables excellent energy savings since it is impermeable to cold or heat, and extremely resistant to condensation, therefore, avoiding staining that can occur with metal reinforcements.



Figure 5.9 Pultruded polyurethane window products (green) (source: Deceuninck brochure 2012)

5.1.4 Sports and leisure

Carbon-fibre composites have been extensively used in the manufacture of tennis racquets, golf clubs, vaulting poles and Formula-1 racing cars, improving performance. This is mainly due to their greater strength, stiffness, toughness, mechanical damping ability and lighter weight compared with the alternative material systems. Carbon fibre (as hybrids with other fibres) reinforced composites continue to successfully replace wood and metal in high-volume components such as fishing rods, tennis racquets, golf clubs, spars/shafts for kayak paddles, windsurfing masts, kites, bicycle handlebars and ski equipment.

A broad coverage of the use of various materials in sports equipment has been presented by Lancashire (2011). The subject is also briefly covered here for some of this equipment.

Tennis racquets

Wooden and metal tennis racquets, with problems of wear, warping and insufficient damping capacity, began to be replaced by polymer-matrix composite racquets from 1970s on. In 1980s, the world market consisted of 55% wood, 30% composite and 15% metal. In 1980 Dunlop developed a unique injection moulding process for producing hollow racquets using 30% by volume short carbon fibre containing polyamide 66 (Haines et al. 1983), which was much less labour intensive than the production methods used for the contemporary racquets made from continuous fibre containing polymer composites. Further information on the manufacturing processes for various types of composite racquets are presented by Lammer & Kotze (2003).

The hollow Dunlop racquet was based on a ‘fusible core’ or ‘lost core’ technique, using a low melting-point metal as the core material. Bismuth (Bi)-tin (Sn) alloy with a melting point of 138°C was employed as the fusible core. The process is also known as “lost-alloy” injection moulding. Clearly the metal core would have to melt at a lower temperature than the plastic material so that it can be melted and run out after the racquet frame was made. The melting point of the metal alloy is some 130°C lower than the melting point of the polymer matrix, therefore, how could the hot plastic material be injected without the metal core melting in the first place?

It was found that at very high injection speeds this was possible because the thermally conductive metal core acted as a heat-sink and remained intact. The core was subsequently melted out in an oil bath at around 150°C and reused. The hollow centre of the racquet is filled with polyurethane foam for mass balance and shock absorption: a low-density PU into the racquet-head and shaft, and a medium-density PU into the handle-end of the frame and under grip. In more recent racquets piezo-electric ceramics are used to provide active damping mechanisms to reduce vibrations.

Figure 5.10 shows a sketch of a short-shot injection moulding to illustrate the melt flow direction, and also an x-ray photograph of a cross-section through the head of the injection-moulded racquet to show the alignment of the carbon fibres. At a racquet frame wall thickness of approximately 2 mm, the short fibres align themselves predominantly in the melt-fill direction, which is fortuitous, rendering the desirable properties of mechanical strength and stiffness.

bookboon.com

Corporate eLibrary

See our Business Solutions for employee learning

[Click here](#)

Management Time Management

Problem solving Self-Confidence Effectiveness

Project Management Goal setting Motivation Coaching

Click on the ad to read more

229

Download free eBooks at bookboon.com

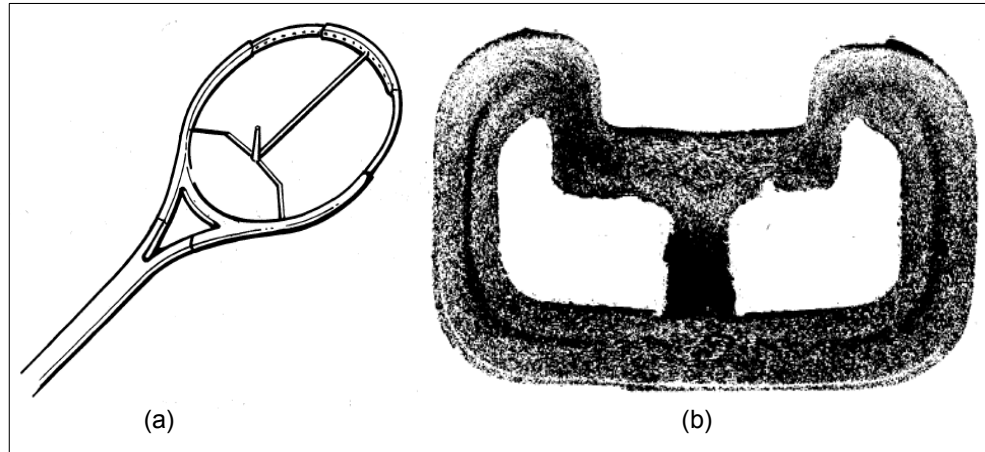


Figure 5.10 Tennis racquet: (a) sketch of a short-shot injection moulding, (b) x-ray photograph of a cross-section through the head of the racquet (showing a predominance of fibre ends) (source: Sang & Aspin)

Modern racquets for other games, such as squash and badminton are also mainly manufactured from polymer-matrix composites.

Pole vaulting

A brief history of the types of poles used in pole vaulting includes:

1900–42 bamboo poles, clearing heights of 4 to 4.77 m

1957 aluminium pole, world record (WR) 4.78 m

1957 steel pole, WR 4.80 m

1961 WR first broken with composite (fibre-glass) pole, 4.83 m.

In the United States, when bamboo became scarce during the Second World War, aluminium and Swedish Steel poles (both hollow) were used during the 1940s and 1950s, despite their heavier weight.

In the early 1960s performances rapidly improved when the relatively rigid poles made from steel or bamboo were superseded by highly flexible poles made of glass fibre or carbon fibre reinforced polymer composites which allowed vaulters to achieve greater heights, see Figure 5.11.

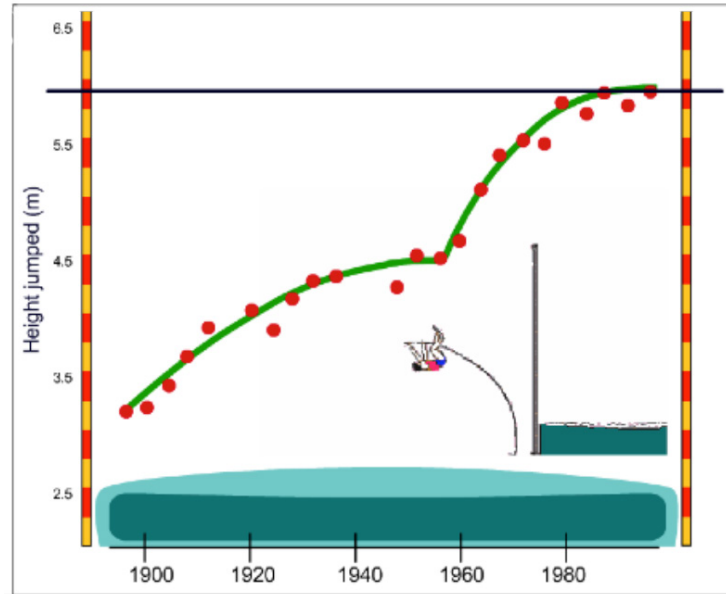


Figure 5.11 Impact of composites on pole vaulting

Pole vaulters benefit from poles produced by wrapping pre-cut sheets of fibreglass that contains resin around a metal pole mandrel, to produce a slightly pre-bent pole that bends more easily under the compression caused by an athlete's take-off. The layers of different fibre arrangements and the amount of fibre used allow the pole to dramatically bend and have the desired length, strength and stiffness. Carbon fibre has been added to the commonly used E-glass and S-glass materials in order to create a pole with greater stiffness and strength and a lighter weight. Figure 5.12 depicts the construction of a composite pole. These poles are substantially lighter, stronger, more flexible and responsive than any other pole used before.

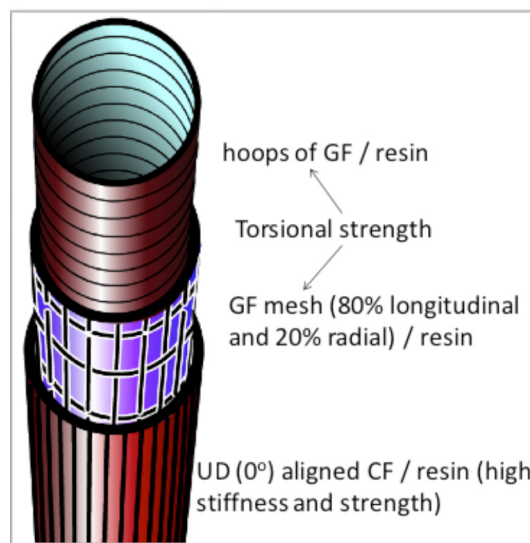


Figure 5.12 Construction of a composite pole

The lighter composite poles enable athletes to have a faster run-up, resulting in a greater take-off speed, giving them more kinetic energy to convert into potential energy and hence height. However, as the equipment is pushed to its limit, failures can occur resulting in potential safety implications. Figure 5.13 shows the fracture surface of a failed pole.

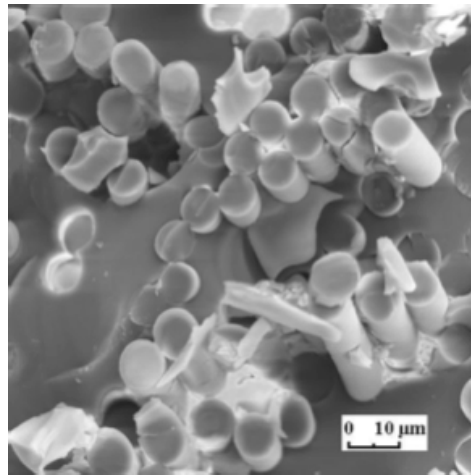


Figure 5.13 The fracture surface of a failed vaulting pole (source: Davis 2010)

Brain power

By 2020, wind could provide one-tenth of our planet's electricity needs. Already today, SKF's innovative know-how is crucial to running a large proportion of the world's wind turbines.

Up to 25 % of the generating costs relate to maintenance. These can be reduced dramatically thanks to our systems for on-line condition monitoring and automatic lubrication. We help make it more economical to create cleaner, cheaper energy out of thin air.

By sharing our experience, expertise, and creativity, industries can boost performance beyond expectations. Therefore we need the best employees who can meet this challenge!

The Power of Knowledge Engineering

Plug into The Power of Knowledge Engineering.
Visit us at www.skf.com/knowledge

SKF

It is said that the advent of composite vaulting poles stemmed from a fibre glass fishing rod (Ware, 1999). A glass-fibre fishing rod manufacturer, Herb Jenks, California, had just built a new deep-sea fishing rod, over 3 m long and 25 mm in diameter. In 1960 Jenks' son, a junior high-school vaulter, borrowed one of these rods for a practice session and surpassed his personal best vault by half a foot (150 mm).

Fibreglass poles, because of their flexibility, enabled development of the 'catapult' technique. A height of 6 m was considered unattainable in pole vaulting, Sergey Bubka, the Ukrainian pole vaulter, cleared this height for the first time in 1985. Bubka continued to break the world record in very small increments 35 times (17 outdoor and 18 indoor), setting his best and final world record with a vault of 6.14 m in 1994. The record held for 21 years until France's Renaud Lavillenie cleared 6.16 metres on 15 February 2014 at the Ukrainian's home city of Donetsk.

Golf clubs

From the early 1930s through the 1970s, the shafts of clubs were made predominantly from steel. Experiments with lighter aluminium shafts were being deemed unsuccessful due to poor torque performance. Steel has good shaft performance but is quite heavy for the average player. In the early 1970s manufacturers introduced golf clubs with shafts made from fibre-reinforced composite materials. Replacing steel with graphite or carbon-fibre reinforced epoxy composite reduced the weight of the club significantly and allowed for the use of longer shafts. A light club can be swung faster than a heavy one, resulting in more club-head speed at impact and, therefore, more distance.

Most woods made today have a boron, carbon or graphite-fibre composite shaft, and titanium, fibre-reinforced epoxy or steel head. Woods are the longest and the most powerful of all the golf clubs.

Bicycles

Chris Boardman won gold and broke the men's individual pursuit world record at the Barcelona Olympic Games in 1992 with an ultra-lightweight full carbon-fibre/epoxy bike designed by Lotus.

Carbon fibre is becoming increasingly popular among bicycle engineers, particularly those working on triathlon or time-trial bicycles. US firms Zyvex Technologies and Enve Composites have partnered to develop a bicycle rim using a carbon nanotube and graphene engineered composite material. Tough, lightweight and easily moulded into highly aerodynamic shapes, the composite materials will become an ever more integral part of racing (IMechE Report, 2012).

IsoTruss lattice structure demonstrates an incredibly high strength-to-weight ratio with a special geometry that uses longitudinal and helically wound members by the filament winding process. The helical (carry transverse shear and torsion loads) and longitudinal (resist all axial and bending loads) members are repeatedly interwoven, yielding a stable configuration. Made from carbon fibre intertwined with Kevlar fibre, the bike's frame, see Figure 5.14, is designed and built at Brigham Young University (BYU, Provo, Utah) and is trademarked as IsoTruss. This is a cage-like structure of open tubular lattice that optimizes the inherent strength of reinforcing pyramids and the isosceles triangles. Hence, the name IsoTruss comes from the "iso" in isosceles, and "truss" comes from the structural feature known as trusses. In three dimensions, the triangles form outward-pointing pyramids along the length of the structure.

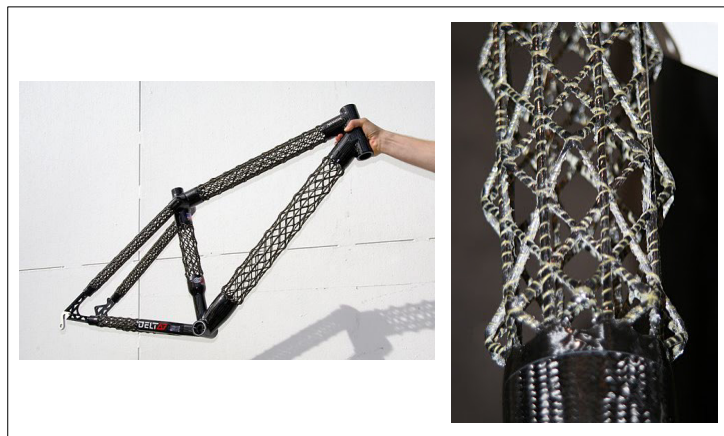


Figure 5.14 IsoTruss open lattice structure bicycle frame (carbon fiber intertwined with Kevlar string)
(source: [Cozy Beehive: IsoTruss Open Lattice Structure for Bicycle Frames](#))

IsoTruss bike frame of Delta 7 Arantix mountain bike weighs approximately 1.2 kg. Figure 5.15 shows weight comparisons of various bicycle frame tubes at equivalent strength. The IsoTruss structure functions like a solid tube with a constant wall thickness, but at a fraction of the weight because so much less material is involved. In bending applications, it is 25% of the weight of an aluminium tube, and 9% of a steel tube, when compared on an equal load basis.

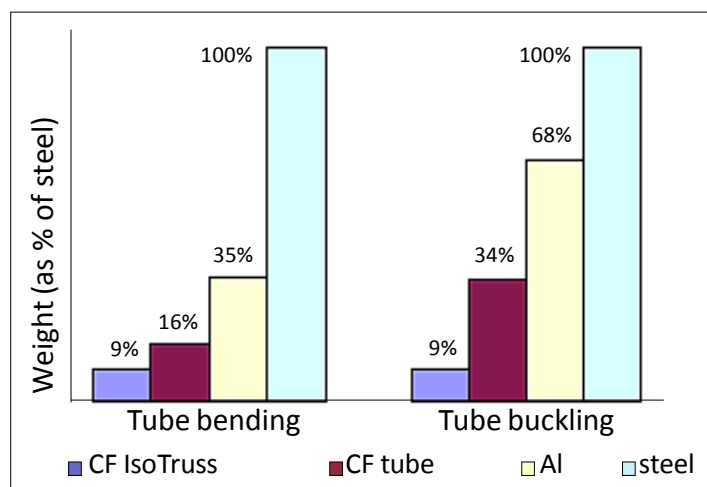


Figure 5.15 Weight comparisons of bicycle frame tubes based on equivalent strength
(source: IsoTruss)

Other examples of the use composites in sports products include canoes, snowboards, skis and surfboards: a Twintex grade of 60/40 by weight glass fibre to PP was selected for the new Robson Brook-16 canoe structure, which measures 488 cm long, has a beam of 99 cm and depth of 48 cm. The combination of Twintex and vacuum bag moulding enables the production of low volume, large thermoplastic composite parts able to meet high mechanical performance and long-life criteria, as well as delivering consistent part quality. This makes it ideal for sport and leisure, niche automotive and marine applications for which high quality is demanded in short production-run parts (NetComposites, 2008).

Composites of sandwich construction (composite skins with a honeycomb core) are used in applications which require high specific stiffness such as snowboards, skis and surfboards.

5.1.5 Bioengineering

Prosthetic foot

The Canadian designer Sebastien Dubois won the BraunPrize 2007 for his design of a **prosthetic foot** which costs only US\$ 8 to produce. The prosthetic foot is made of glass fibre-reinforced composite and is intended to help civilians who are mutilated by landmines and had their lower leg amputated. Glass fibre rather than carbon fibre was used not simply because it is ten times cheaper, but also glass fibre is less rigid but still almost as strong as carbon fibre, so it has a greater elongation at break. It is therefore more reliable, a significant advantage when used in difficult circumstances in remote areas.

With us you can
shape the future.
Every single day.

For more information go to:
www.eon-career.com

Your energy shapes the future.

e.on



Oscar Pistorius, a double amputee runs on well known carbon fibre **blades**. Carbon fibre composites are used to manufacture the foot sections, in order to achieve high strength and stiffness together with relatively low mass. These materials also enable a high degree of design flexibility. Varying the fibre orientation in the foot tailors the bending stiffness of the blade to suit the weight of the athlete.

Surgical implants

Various surgical applications of carbon-fibre reinforced polymer composites have been well covered: Hillock & Howard (2014) have reviewed the subject matter and identified many advantages that CF composites offer, emphasising the reduction in stress shielding of bone, biocompatibility and radiolucency, which quickly brought it to the forefront of successful spine procedures allowing superior monitoring of pathological fractures. Stuart of Invibio Ltd. (2007) in his article on carbon-fibre-reinforced PEEK composite for surgical applications has also indicated that the elastic modulus of the composite closely match the modulus of natural bone while retaining high strength of metals (with high fibre content and by tailoring fibre orientation distribution), good fatigue resistance, extensive biocompatibility and imaging compatibility (compatibility with MRI, CT, and x-ray technologies).

Orthopaedic surgeons have identified **hip implant** stiffness as a factor leading to a condition called “stress shielding”, where a patient’s bone atrophies (bone resorption around the implant) because the applied loads are supported by the more rigid implant and not transferred to the adjacent bone to provide the stimulation needed for natural bone synthesis. Medical device manufacturers and research institutes have addressed this concern with various materials and design approaches: the trend being the replacement of metallic implants, fully or partially, with polymer composites. Work includes the use of both continuous carbon fibre reinforced composites and short carbon fibre reinforced composites. Figure 5.16 shows an implantable-grade PEEK/carbon fibre composite in combination with a metal insert, a unique elastically tailored prosthetic hip, which is capable of withstanding high loads for many millions of cycles.

Carbon-fibre/PEEK composite is very popular, because it is biocompatible and it has very high compressive strength durability and its elastic modulus closely matches that of cortical bone.



Figures 5.16 Implantable-grade PEEK carbon fiber composite in combination with a metal insert has been used to create a unique elastically tailored prosthetic hip (source: Invibio)

Various properties of an injection moulded PEEK hip prosthesis, containing 30% by weight short carbon fibre, were evaluated (Akay & Aslan 1995 and 1996), however, it is not thought that by itself such a moulding will be strong enough to make a suitable hip prosthesis stem. A combination of materials have been more successful, e.g. EPOCH hip implants, which have a cobalt-chromium alloy core (spigot) surrounded by a flexible polymer material with an exterior surface of a titanium fibre mesh that is designed to also encourage bone ingrowth into tiny openings in the mesh. Alternatively implants are coated with hydroxyapatite to provide an active interface to ensure that the bone tissue fuses thoroughly with the surface structure of the implant.

The cervical plate, see Figure 5.17, Invibio's Endolign, is used for the stabilisation of the cervical spine. It is a biocompatible composite material made from pre-impregnated tapes of high levels of continuous fibre reinforced PEEK. The benefits of this plate and screws are said (Netcomposites, 2006) to be:

- excellent fatigue resistance
- low profile (slimmer) plate design with high mechanical strength
- smooth hydrophobic surface to prevent soft tissue attachment
- artefact free imaging procedures (CT and MRI) for accurate and reliable post-operative monitoring
- angle stable screw positioning
- a plate design that supports simple surgical technique.



Figure 5.17 Carbon fibre-reinforced PEEK for cervical plate implant
(source: Netcomposites 2006)

Problems with imaging often relate to difficulties interpreting radiographs taken through casts or fixation devices because the image quality is degraded as a result of absorption or scattering of X-rays. Carbon fibre-reinforced PEEK polymer is one of the most radiolucent of the composite materials.

5.1.6 Transportation: automotive, marine and rail

The transportation industry benefits from lighter materials due to improved energy efficiency. Accordingly, composite materials are increasingly being used in the manufacture of various transportation vehicles.

© 2013 Accenture. All rights reserved.

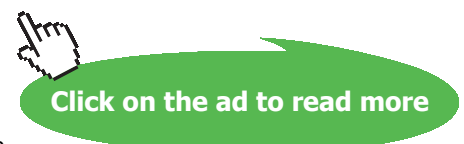
be > your degree

Bring your talent and passion to a global organization at the forefront of business, technology and innovation. Discover how great you can be.

Visit accenture.com/bookboon

Be greater than.
consulting | technology | outsourcing

accenture
High performance. Delivered.



Automotive

“The most environmentally friendly thing you can do for a car that burns gasoline is to make lighter bodies”, Henry Ford.

However, the automotive industry has adopted composites slowly due to their higher costs. Plastics filled with particulates have been used for some time but fibre reinforced composites have only been used in upmarket sports cars, and only recently starting to make meaningful inroads into more traditional cars. On the other hand, composites have been used in racing cars for many years.

Marsh (2003) has stated that “Faced with pressures to produce fuel efficient, low-polluting vehicles, the industry has used fibre reinforced plastic composites to make its products lighter. But producing the composites is energy intensive and polluting, while the durability of conventional composites, often seen as an advantage, is also their Achilles’ heel. Glass, carbon, and aramid fibre reinforced polyester, epoxy, and other similar resins are difficult to recycle and hard to dispose of. They do not degrade naturally and could linger for generations.

Use of thermoplastics offers some relief, as these resins can be thermally recycled to produce new products. But for a more sustainable future and to meet growing regulatory pressures – of which the most pressing is the European Union’s end-of-life vehicles (ELV) directive requiring that, by 2015, all new vehicles should be 95% recyclable (i.e. 85% reuse and/or recycling, with a total recovery of 95%, which includes the combustion of waste materials for energy recovery) – a more complete solution is needed. From present indications, that could turn out to be ‘green’ composites based on fibres and resins derived from plants.”

He has further stated that “A logical starting point is to take recyclable thermoplastic resins (polypropylene, polyethylene, other polyolefins, polyurethane and polyamide are some of those already used in vehicles), and combine them with biodegradable plant-based fibres. Natural fibres have the potential to reduce vehicle weight (up to 40% more compared with glass fibre, which accounts for the majority of automotive composites), while satisfying increasingly stringent environmental criteria. Much less energy is used in growing, harvesting, and preparing natural fibres than in producing glass fibre. The production energy requirement of plant fibres has been estimated as some 4 GJ/t, compared with around 30 GJ/t for glass fibre, which has to be drawn from a melt at several hundred degrees Celsius, using raw materials obtained through energy-intensive mining.

Production of fibres releases CO₂ into the atmosphere, along with NO_x and SO_x gases and dust, this can be a health hazard. Dust and fragments are generated when recycling conventional plastic composites by grinding them down and remain an issue during disposal either to landfill or by incineration. In contrast, the use of natural fibres can minimize harmful pollutants, and their eventual breakdown is environmentally benign.”

Many luxury European car makers, including BMW, Mercedes and Audi have been testing and experimenting with natural fibers like hemp in their productions since the 1990s, when regulations to use recyclable materials forced most European car makers to go greener and make use of fibers such as hemp and kenaf in some form.

The BMW i3, an all-electric car, unveiled in July 2013 weighs about 1200 kg. In order to achieve a lightweight car most of its internal structure and body is made from carbon-fibre reinforced polymer and other low-weight materials, including hemp fibre in the interior, maximizing fuel efficiency and driving range.

TruthOnPot.com (2013) reports, “Weight is essential because the i3 depends entirely on a 22 kWh lithium-ion battery for fuel, which also contributes about 20% of the car’s total mass. The only solution was using a variety of low-weight materials to maximize fuel efficiency and driving range (130–160 km per charge) – hemp being one of them. Like many BMWs before it, the i3 features door panels made of hemp. Mixed together with plastic, hemp helps lower the weight of each panel by approximately 10%”, see Figure 5.18.



Figure 5.18 A BMW door panel made out of hemp. (source: TruthOnPot.com, 2013)

It continues, “But that’s not all. The hemp fibers – which are left exposed – also offer a design element, reports Bloomberg. According to Benoit Jacob, the i3’s designer, the use of natural materials like hemp and kenaf (a plant in the hibiscus family) makes the i3’s interior feel like “a small loft on wheels”.”

The BMW i8 – an electric hybrid supercar is also to incorporate hemp in its body work.

Further applications of natural fibres in various automotive applications are presented in Table 5.1.

Automotive manufacturer	Model and applications
AUDI	A2, A3, A4, A6, A8, Roadster, Coupe Seat backs, side and back door panels, boot lining, hat rack, spare tyre lining
BMW	3, 5, 7 series Door panels, headliner panel, boot lining, seat backs, noise insulation panels
CITROEN	C5 Interior door panelling
FIAT	Punto, Brava, Marea, Alfa Romeo 146, 156
FORD	Mondeo CD 162, Focus
LOTUS	Eco Elise Body panels, spoiler, seats, interior carpets
PEUGEOT	406 Seat backs, parcel shelf
RENAULT	Clio, Twingo Rear parcel shelf
ROVER	2000 and others Insulation, rear storage shelf/panel
SEAT	Door panels, seat backs
TOYOTA	Brevis, Harrier, Celsior, Raum Door panels, seat backs, spare tyre cover
VOLKSWAGEN	Golf, Passat, Bora Door panel, seat back, boot lid finish panel, boot liner
VOLVO	C70, V70 Seat padding, natural foams, cargo floor tray

Table 5.1 Current well-established applications of natural fibres in the automotive industry (source: Suddell 2009)

The MP4-1 was the first fully composite **Formula 1 chassis**, unveiled on 6 March, 1981 by McLaren at British Grand Prix at Silverstone, driving the car the Ulsterman John Watson won the race. Designed as a moulding, see Figures 5.19, rather than the traditional series of flat aluminium/aluminium honeycomb panels mechanically fixed together, the bodywork was a gigantic leap in strength and stiffness that revolutionised racing car design.



Figure 5.19 The first carbon-fibre composite Grand Prix car: (a) monocoque McLaren MP4/1 (1980); (b) McLaren MP4 (MP4/1) competed in the 1981 Formula One Season (sources: Savage 2008, p. 11, and F1Technical.net)

However, the same year at the Italian Grand Prix, Watson lost control of his McLaren at Monza's daunting Lesmo bends and smashed the car into the barriers at 140 mph. He was able to walk away from the debris unscathed. Savage (2008, p. 11) states that, this incident went a long way to removing the doubts in the minds of those unconvinced of the safety of carbon fibre composites under high strain rate loading. In fact, the impact of the energy absorbing properties of composites on the safety of the sport soon became obvious and was accepted by all.

Table 5.2 shows various application examples of the use of glass- and carbon-fibre reinforced polymer composites in various makes of cars to achieve lightweighting, structural stiffness and other associated desirable outcomes.



"I studied English for 16 years but...
...I finally learned to speak it in just six lessons"

Jane, Chinese architect

ENGLISH OUT THERE

Click to hear me talking before and after my unique course download

Application	OEM-model	Composites type	Driver for use of composites	Launch year
Roof Compartment Cover, Trunk Lid	BMW M6 Convertible	GF composites	Weight reduction	2013
Wheel Rims	Daimler Smart's 3rd-Generation Electric Drive	GF composites	Lightweight & Stunning look	2012
Instrument Panel, Inner Door Modules	Land Rover – Evoque	GF composites	Lightweight Fuel economy	2011–12
Engine-mounted Oil-filter Module	Chrysler Pentastar Engines	GF composites	Thermal requirements for cooling-system components	2010–11
Door Module	Faurecia's Jeep Liberty SUV	GF composites	Weight reduction	2010
Air-intake Manifold System	General Motors V6 Engine	GF composites	Weight saving Better acoustic performance	2010
Air-intake Manifold System	Volkswagen Gasoline Engines	GF composites	Weight saving & Better acoustic performance	2009–10
Fluid Filter Module	Daimler AGT-Mercedes	GF composites	38% weight and 16% cost reductions	2009–10
Composite Passenger Cell	BMW i3	CF composites	Lightweight	2013
Car Roof	McLaren MP4-12C Spider	CF composites	Lightweight	2013
Car Roof	BMW M6 Coupe	CF composites	Lightweight	2012
Body Aerodynamics Kit	Callaway Corvette RPO B2K	CF composites	Lightweight	2012
Cabin Frame, Floor Panel, Roof Pillars, Hood, Transmission Tunnel, and Rear Floor	Lexus LFA	CF composites	Lightweight	2012
Body Aerodynamics Kit	Lamborghini Aventador LP700-4 LE-C	CF composites	Lightweight	2012
Front and Rear Bumpers, Bumper Grilles, Side Skirts, and Mirror Covers	Lamborghini Aventador LP700-4	CF composites	Lightweight	2012
Panels on Interior Door	Lamborghini Murcielago SP670-4 SV Twin Turbo	CF composites	Lightweight & Stunning look	2012
Front & Rear Fenders, Trunk Lid and Door Sills	Aston Martin V12 Zagato	CF composites	Lightweight	2012

Table 5.2 Emerging applications will be a driving factor in the growth of composites in the automotive market (source: Kazmierski of Lucintel 2012)

Table 5.3 shows that while not taking into consideration the density of steel, its performance per unit of cost compares well to composites, but when the densities are considered (i.e. when the strength is expressed as the specific strength) the glass fibre composites outperform steel and aluminium; while natural fibre composites perform better still, creating a huge potential to replace competing materials in automotive applications.

Materials	Average amount per car (lbs)	Performance/Price (strength/\$)	Performance/Price (specific strength/\$)
Steel	2000	1.1	0.15
Aluminium	600	0.2	0.08
FRP	77	0.7	0.36
Natural fibre composites	35	1.5	1.15

Table 5.3 Performance-Price comparison of competing materials for automotive applications (source: Kazmierski of Lucintel, 2012)

Marine

Fibreglass has been the common material for recreational boats and yachts for many years. These are mostly randomly oriented glass fibre reinforced polyester composites, giving the structure more uniform material properties. Being fairly cheap, glass fibre can be used in large structures; whereas carbon fibre would be too expensive. Increasingly, however, the carbon fibre is employed in the manufacture of yachts, e.g. VT Mirabella yacht made from CFRP/GRP/polyolefin foam.

Thermoplastic composites are also evaluated for the manufacture of large surface area structures for boats to produce more easily recyclable composites, e.g. Halmatic GFRPP boat. A study by Otheguy et al. (2009) on recycling of an experimental thermoplastic composite boat, built using Twintex T PP 60 woven polypropylene-glass fibre commingled fabric, containing 60 wt.% glass fibre has demonstrated the recyclability of thermoplastic-based composites. In particular they have shown that the hull of a rigid boat, composed of glass/polypropylene laminate along with balsa core material and paint, can be recycled by melt processing into injection mouldable granules which have acceptable properties when processed.

Aramid-fibre composites are also used in boat-building because of their lightweight, strength and toughness.

Fibre-reinforced composites are also used in naval vessels, such as the Swedish Navy stealth ship Visby corvette, see Figure 5.20. It is constructed almost entirely of carbon fibre. It is angular in design (however, avoiding right-angles, which reflect radar right back) to give it a minimal radar signature (or reduced radar cross section). Carbon fibre is also a lot lighter than steel and the Visby, at 600 tonnes, is half the weight of a conventional corvette (a corvette is a fast, lightly armed warship).



Figure 5.20 Swedish Navy Visby stealth corvette: 600 tons – 72 m long – FRP sandwich
(source: Wikipedia 2014)

In Wikipedia (2014), the Visby corvette hull is described as being constructed with a sandwich design consisting of a PVC foam core with a CF and vinyl polyester laminate skin: the composite material as ship hulls provides high strength and rigidity, low weight, good shock resistance, low radar and magnetic signature. Good conductivity and surface flatness means a low radar signature, while good heat insulation lowers the infrared signature and increases survivability in case of fire. The composite sandwich used is also non-magnetic, which lowers the magnetic signature. Composites are also very strong for their relative weight, and less weight means a higher top speed and better maneuverability. The composite weighs roughly 50% less than the steel of equivalent strength.

An advertisement for Duke University's Fuqua School of Business. The background is a light gray with a faint world map. In the top left corner is the Duke University logo: 'DUKE' in a blue box above 'THE FUQUA SCHOOL OF BUSINESS'. The main text reads 'BUSINESS HAPPENS' in large black letters, followed by 'www.fuqua.duke.edu/globalmba' in a smaller font. Below this is an orange button with the text 'Learn More >'. On the right side, there is a circular collage of six diverse people's faces, with the word 'HERE.' in bold black letters in the center of the collage.



Rail

Theengineer (sic) (2014) in its article “Automotive, rail and marine” states, “Weight reduction is a major issue across all areas of the transport sector, not least the rail industry where heavier vehicles use more energy, are costlier to run and are more likely to cause damage to the track than lighter vehicles.

In an effort to address this, a team has developed a lightweight, fully structural, crashworthy cab based on advanced composite sandwich material technology (Carruthers et al. 2011). Conventional rail-vehicle cab structures are typically based on welded steel assemblies, often with a thin non-structural fibre-glass cover and are therefore relatively heavy. They also tend to be very complex, high part-count assemblies with fragmented material usage. This is because they must meet a wide range of demands, including proof loadings, crashworthiness, missile protection, aerodynamics and insulation. Assembly costs are high and there is little in the way of functional integration.

The new prototype composite cab is up to one tonne lighter than conventional structural metallic solutions, made up of 40% fewer parts, and features a modular design that is said to facilitate easy inspection, maintenance and repair.

Life-cycle analysis has estimated that operational savings resulting from each lightweight cab would be in the region of £40,000 over the life of a vehicle. For a fleet of 350 trains, with two cabs per train set, this would provide a total saving of approaching £30m.

Developed as part of the DE-LIGHT Transport European Project, the initiative brought together Newcastle University’s NewRail team, which developed the conceptual and detailed design of the cab, Bombardier Transportation UK, which provided the specification for the cab, and Portuguese composites expert AP&M. The composite cab is based on Bombardier’s new SPACIUM 3.O6 commuter train. The team claims that, with further refinement, it could represent a realistic alternative to SPACIUM’s existing steel-based cab.”

Composite materials supplier Hexel (2008) in their brochure Hexcel’s Composite Materials for the Rail Industry has given wider application details of the use of composites, mainly by way of mouldings from prepregs or prepreg-honeycomb combinations, in the production of the drivers cab, leaf-springs, luggage bins, external doors, ceiling panels and connecting archways for a railway carriage. They have also described how the use of composites in trains, trams and metros leads to rapid construction, high structural stiffness and strength, weight savings, passenger comfort, cost effectiveness, design flexibility and safety.

The use of fire resistant materials is important, particularly in public transportation, and therefore inherently fire resistant polymers, e.g. phenol-formaldehyde resin, should be selected as the matrix for the composite.

Armoured vehicles

Increasingly new materials are being used in the production of armoured plates, particularly for applications designed to reduce the weight of vehicles. In the modern age rapid response is an increasingly important factor and the ability to transport military vehicles by air is increasingly desirable. However, the standard weight of a main battle tank, typically over 60 tonnes, is far too high for most military transports. Smaller tanks at around 20 tonne are conceived using polymer matrix composites (PMCs) instead of steel plates, see Figure 5.21. PMC structures also reduce visibility to radar detection.

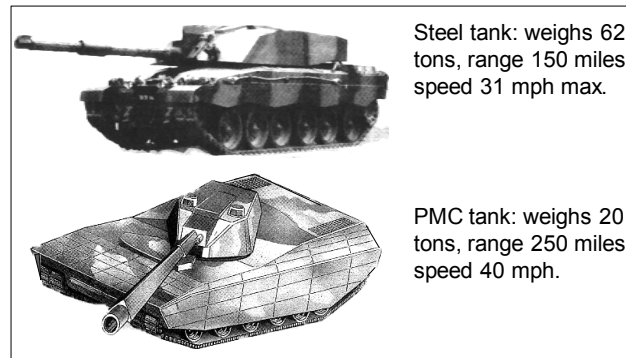


Figure 5.21 PMC tanks are invisible to radar and transportable worldwide by air (Daily Mail, 14 April, 2001)

Other types of armoured vehicles used by both police and military services worldwide also benefit from the use of PMCs, see Figure 5.22.



Figure 5.22 Armoured Land Rovers (CAV-100) with body armour based on S-2 glass fibre panels produced by National Plastics

The use of PMCs in ballistic shields/barriers is detailed by Hogg (2003) and Rojek et al. (2013).

It is outlined that, not least for the reason that there are many different types of projectiles, it is desirable for armour to be based on a multimaterials, multilayer arrangement, with different layers providing specific functionality in the armour. The use of combinations of fibres and novel textile forms may provide further benefits to composite armour systems, either as standalone armour or as part of multi-component armour systems.

The more complex the armour system, the more expensive it becomes to manufacture. In addition to layers of ceramic tiles, composite backing plates, elastomers or aluminium foam core layers, it may be necessary to incorporate separate inner and outer composite layers with improved fire performance, possibly manufactured from phenolic plates. Manufacturing costs increase dramatically, not simply because of the cost of the materials involved but due to the multiple manufacturing stages for separate production and assembly of the various elements.

Manufacturing techniques based on infusion processes are used to integrate different production stages. The infusion process is also compatible with the use of stitched pre-forms for the composite backing plate and can be used to surround and encapsulate the ceramic tiles.

Aramid fibres are characterized by high stiffness, high tensile and flexural strength, as well as fatigue strength. In comparison to other fibres, e.g. glass fibre, Kevlar is distinguished by being less prone to creep rupture even at stress levels up to 70% of tensile strength. However, the problem is its compressive strength, particularly in the case of applications such as ballistic shields, which could be solved by hybrid systems (e.g. with carbon fibre). As far as military applications are concerned, it should be pointed out that these fibres exhibit good resistance to wear and have high toughness, moreover, they are thermally stable and are chemically resistant except to strong organic acids and bases.

Join American online LIGS University!

Interactive Online programs
BBA, MBA, MSc, DBA and PhD

Special Christmas offer:

- ▶ enroll **by December 18th, 2014**
- ▶ **start studying and paying only in 2015**
- ▶ **save up to \$ 1,200** on the tuition!
- ▶ Interactive Online education
- ▶ visit ligsuniversity.com to find out more!

Note: LIGS University is not accredited by any nationally recognized accrediting agency listed by the US Secretary of Education. More info [here](#).



Rojek et al. (2013) have presented a wide coverage of aramid fibres and also UHMWPE fibres, both are known for their toughness and for their use as body armour by the defence industry:

UHMWPE fibres, available under the trade name Dyneema and Spectra, are made with the use of the gel spinning method, an extrusion method with simultaneous one-way stretching, which enables a very high degree of molecular orientation (95%) and crystallinity (85%). The outcome is a greater tensile strength than aramid fibres and lower density. They also have high impact strength, which is important with regard to ballistic shields. Furthermore, they are resistant to humidity, UV radiation, microorganisms and the majority of chemicals. The disadvantage is the relatively low operating temperature. The fibres discussed are combined with epoxy or phenolic matrices to produce composites that are employed in ballistic shields. Phenolic resins are resistant to high temperatures, practically inflammable and emit insignificant amounts of harmful substances during combustion although they turn yellow when exposed to UV radiation. However, the problem is posed by the curing process, which normally requires elevated temperatures. In their work Rojek et al. have employed a low-temperature curing epoxy resin (cured at ambient temperatures) as a matrix that has produced a composite with good resistance to water, weather conditions and chemical media as well as a quite high operating temperature, up to 120°C.

5.1.7 Sensors

Sensors will increasingly be embedded in aircrafts and other critical engineering products such as pressure vessels to continuously monitor the structural integrity. The aim is to obtain information such as the stress, strain, temperature and any damage experienced by the structure.

Carbon fibre as a piezoresistive material (i.e. materials that exhibit a change in resistance when subjected to pressure) can be used in making sensors. This has been described in detail by Horoschenkoff & Christner (2012): carbon fibre sensor (CFS) consists of a single carbon fibre roving with electrically connected endings embedded in a sensor carrier (patch) for electrical insulation. Depending on the requirements of the application different patch types (e.g. glass fibre reinforced plastic (GFRP), polyester film, neat epoxy resin) are used. In terms of mechanical properties GFRP is a particularly suitable patch material. CFSs with a GFRP patch exhibit an improved linearity of the signal due to the supportive effect of the glass fibres to the carbon-sensor fibre especially in the case of compression loading. The manufacturing process of a CFS includes three basic steps: pre-curing of the carbon fibre, preparation of the electrical connection and embedding of the sensor fibre into the sensor carrier. Figure 5.23 shows a CFS with a single layer GFRP patch.

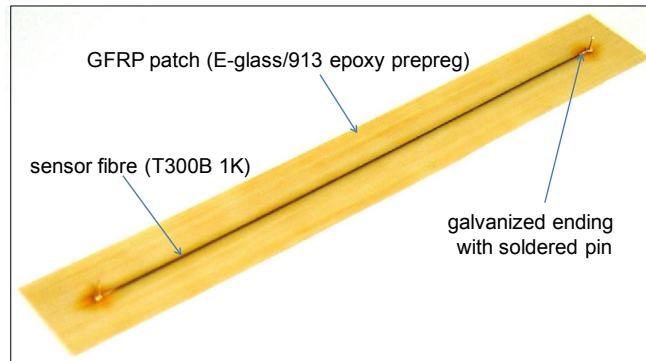


Figure 5.23 Carbon fibre sensor with an ex-Pan sensor fibre and a GFRP patch
(source: Horoschenkoff & Christner 2012)

The pre-curing process is used to stabilize the carbon fibre roving and to align the filaments of the roving. For this purpose the twisted carbon fibre roving (a twist of 20 turns per meter) is impregnated by a low viscosity resin (normally a low viscosity epoxy resin) and cured, under a constant tension force along the roving, at 180°C for 1.5 hours.

Horoschenkoff and Christner cover the electromechanical properties of carbon fibres, including specific resistivity and piezoresistivity; carbon fibre sensor meshes; the use of the CFSs to detect matrix crack initiation and monitor crack growth, and as a sensor system to detect barely visible impact damage in composite laminates.

Their coverage also includes the applications of the CFSs to measure deflection in the carbon fibre reinforced plastics tabletop of a computer tomography (CT) scanner (since CFRP fulfils the X-Ray transparency which is necessary to get the picture quality sufficient for medical diagnosis), and to determine the pressure level and/or monitor degradation processes due to fatigue or overloading of the radial fibre reinforcement in a pressure vessel.

The article in the Engineer by Harris (2014) reports that researchers at the Advanced Technology Centre of BAE Systems have developed a way to cover aircraft panels with an array of tiny sensors that enable the craft to analyse both its own condition and the environment around it in minute detail, see Figure 5.24.

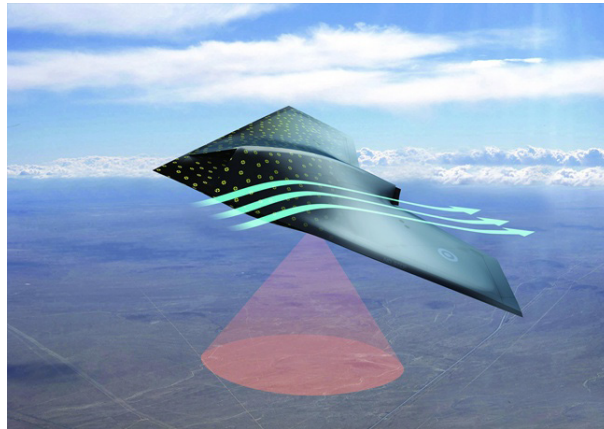


Figure 5.24 Future aircrafts could have “smart skin” to enable them instantly detect damage
(source: Harris 2014)

The company says the wireless sensor packages or “motes”, which could be made to measure a wide range of variables from temperature and wind speed to strain and corrosion, could eventually be shrunk to less than 1 mm³ in size and power themselves using energy-harvesting technology.

An advertisement for the IE Business School Master in Management program. The background is a city street with a man in a green jacket looking to the side. The IE Business School logo is in the top left. A badge in the top right says "#1 EUROPEAN BUSINESS SCHOOL FINANCIAL TIMES 2013". A speech bubble in the middle right says "#gobeyond". The main text reads "MASTER IN MANAGEMENT" and "Because achieving your dreams is your greatest challenge. IE Business School's Master in Management taught in English, Spanish or bilingually, trains young high performance professionals at the beginning of their career through an innovative and stimulating program that will help them reach their full potential." Below this is a list of three bullet points: "Choose your area of specialization.", "Customize your master through the different options offered.", and "Global Immersion Weeks in locations such as Rio de Janeiro, Shanghai or San Francisco." At the bottom, it says "Because you change, we change with you." and provides the website "www.ie.edu/master-management" and email "mim.admissions@ie.edu" along with social media icons for Facebook, Twitter, LinkedIn, YouTube, and Instagram.

ie business school

#1 EUROPEAN BUSINESS SCHOOL
FINANCIAL TIMES 2013

#gobeyond

MASTER IN MANAGEMENT

Because achieving your dreams is your greatest challenge. IE Business School's Master in Management taught in English, Spanish or bilingually, trains young high performance professionals at the beginning of their career through an innovative and stimulating program that will help them reach their full potential.

- Choose your area of specialization.
- Customize your master through the different options offered.
- Global Immersion Weeks in locations such as Rio de Janeiro, Shanghai or San Francisco.

Because you change, we change with you.

www.ie.edu/master-management | mim.admissions@ie.edu | f t in YouTube

Self-Healing Composite Materials

Low energy impact damage to composite structures can be difficult to detect (barely-visible impact damage, BVID) but can result in significant reduction of mechanical properties. Various researchers (Bond (2014), Blaiszik et al. (2010), Pingkarawat et al. (2012), Dry (2005), amongst others) have adopted a nature's/bio-inspired approach to effect damage detection and self-healing in advanced FRP composites. Transportation of functional chemical reagents to the damaged regions is achieved by incorporating hollow fibres, microcapsules and vascular networks into polymer-matrix composites.

Formation of a network in two or three dimensions for transporting of the chemicals for healing through the material represents a problem. Researchers at the Beckman Institute (2014) for Advanced Science and Technology at the University of Illinois have reported a 3D vascular system that allows for high-performance composite materials such as fiberglass to heal autonomously, and repeatedly.

Internal damage in fibre-reinforced composites, materials used in structures of modern airplanes and automobiles, is difficult to detect and nearly impossible to repair by conventional methods. A small, internal crack can quickly develop into irreversible damage from delamination. This remains one of the most significant factors limiting more widespread use of composite materials.

Sottos, White, Moore, and their team at Beckman Institute (2014) created 3D vascular networks (patterns of microchannels filled with 'healing' chemicals) that thread through the composite. The vasculature within the system integrates dual networks that are isolated from one another. Two liquid healing agents (an epoxy resin and hardener) are sequestered in two different microchannel networks. When damage occurs, it ruptures the separate networks of healing agents and allows healing agents to mix and polymerise to form structural glue in the damage zone, autonomously healing the material, over multiple cycles.

Fibre-composite laminates are constructed by weaving and stacking multiple layers of reinforcing fabric, which are then co-infused with a binding polymer resin. Using that same process, the researchers stitched in a sort of fishing line, made from a bio-friendly polymer and coined "sacrificial fibre" within the composite. Once the composite was fabricated, the entire system was heated to melt and evaporate the sacrificial fibres, leaving behind hollow microchannels, which became the vasculature for the self-healing system.

Frost, of Materials World Magazine (2014), reports that inkjet printing and composite materials are being combined to improve the structural integrity of lightweight, self-healing materials by researchers (Hodzic and Smith) at The University of Sheffield. They have developed a process that involves depositing low-viscosity thermoplastic microdroplets onto fibre-reinforced epoxy prepregs, before curing and solidification. These microdroplets form a self-healing agent that is arrested between composite plies, preventing direct contact with neighbouring microdroplets. The material's self-healing properties are activated by external heat to re-fuse the composite layers.

Blaiszik et al. (2010) and Bond (2014) have illustrated different approaches to self-healing, see Figures 5.25:

- a) capsule-based self-healing materials sequester/store the healing agent in discrete capsules until damage triggers rupture and release of the capsule contents.
- b) Vascular self-healing materials sequester the healing agent in a network in the form of capillaries or hollow channels, which may be interconnected one-dimensionally (1D), two-dimensionally (2D), or three-dimensionally (3D), until damage triggers self-healing. After the vasculature is damaged and the first delivery of healing agent occurs, the network may be refilled by an external source or from an undamaged but connected region of the vasculature. This refilling action allows for multiple local healing events.
- c) Intrinsic self-healing materials do not have a sequestered healing agent but possess a latent self-healing functionality that is triggered by damage or by an external stimulus. These materials rely on chain mobility and entanglement, reversible polymerizations, melting of thermoplastic phases, hydrogen bonding, or ionic interactions to initiate self-healing. Because each of these reactions is reversible, multiple healing events are possible.

SMS from your computer
...Sync'd with your Android phone & number

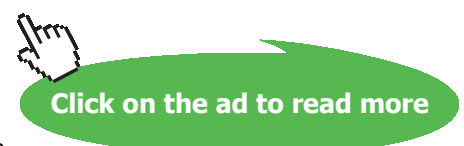
FREE
30 days trial!

Go to
BrowserTexting.com

and start texting from
your computer!

BrowserTexting

The advertisement features a laptop on the left displaying a web interface with a list of contacts and a text message conversation. A blue double-headed arrow connects the laptop screen to an HTC smartphone on the right, which also displays the same text message conversation. The background is a light blue gradient with a dark blue diagonal banner in the top right corner.



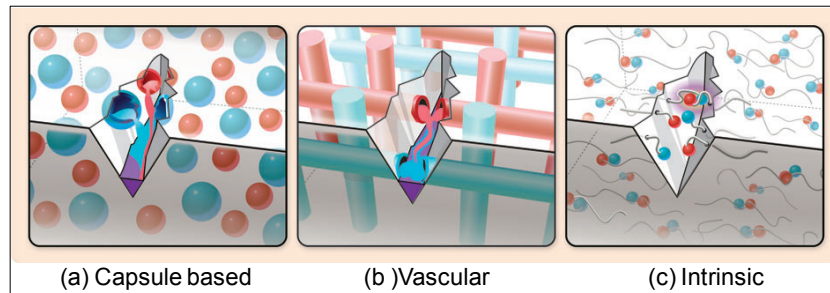


Figure 5.25 Approaches to self-healing include (a) capsule-based, (b) vascular, and (c) intrinsic methods. Each approach differs according to the method by which healing functionality is integrated into the bulk material. Note the shades of red and blue are used in this figure to show a generalized interaction (purple) between two or more species (source: Blaiszik et al. 2010).

Pingkarawat et al. (2012) presents an experimental study into the self-healing repair of delamination cracks in a carbon fibre-epoxy laminate using mendable poly[ethylene-co-(methacrylic acid)] (EMAA) particles or fibres. Their work assesses the delamination crack growth process and the interlaminar toughening mechanisms which result in the self-healing efficiency of epoxy matrix laminates containing EMAA, see Figure 5.26. The study identifies the mechanism responsible for the high recovery in delamination toughness of mendable laminates following self-healing, using EMAA.

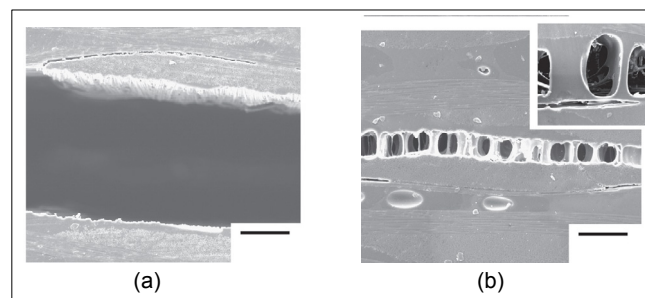
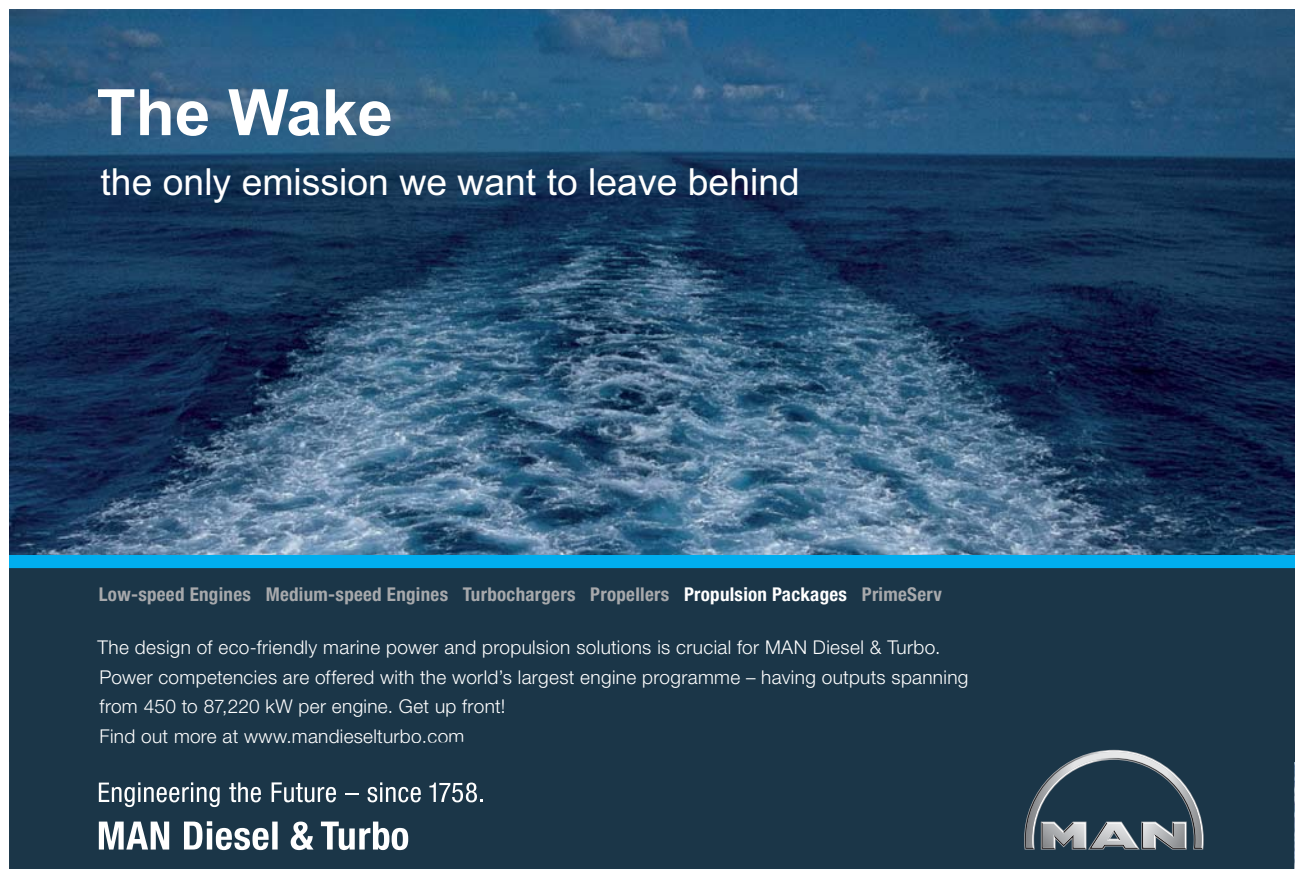


Figure 5.26 Scanning electron microscopy images of the delamination crack in a mendable laminate (a) before self-healing and (b) after self-healing. The inset photograph in (b) shows a higher magnification view of the crack bridging ligaments. Note the absence and presence of crack bridging ligaments of EMAA before and after healing, respectively (source: Pingkarawat et al. 2012)

5.2 Materials selection

The fibre composite approach can provide significant improvements in specific properties (property/density) such as specific strength and stiffness over conventional metal alloys. Additives can also be included in polymers for reasons other than thermo-mechanical property improvements. For example, graphite, PTFE, or molybdenum disulfide are added to polymers as lubricants to lower the coefficient of friction or wear rate in tribological applications such as bearings or slide plates.

The selection process, following the establishment of a product design specification (PDS) and material property profile, involves initial screening that eliminates the candidate materials that don't match the required attributes. Further optimisation is required in order to rank the remaining candidates. This exercise uses material properties or property combinations in order to achieve the best outcome for a given product design. Such property combinations are referred to as **material merit indices** (or performance index). For example, the merit index for a strong and light tension tie-rod is σ_f / ρ and for a stiff and light tension tie-rod is E / ρ . Whereas, the merit indices to select best materials for a stiff and light beam and flat plate in bending are $E^{1/2} / \rho$ and $E^{1/3} / \rho$, respectively. The derivations of the merit indices for stiff and light basic structural elements are shown in the text-box below.

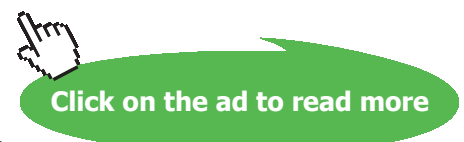


The Wake
the only emission we want to leave behind

Low-speed Engines Medium-speed Engines Turbochargers Propellers Propulsion Packages PrimeServ

The design of eco-friendly marine power and propulsion solutions is crucial for MAN Diesel & Turbo. Power competencies are offered with the world's largest engine programme – having outputs spanning from 450 to 87,220 kW per engine. Get up front!
Find out more at www.mandieselturbo.com

Engineering the Future – since 1758.
MAN Diesel & Turbo



The derivation of a merit index involves expression of an equation for the required attribute; elimination of parameters that are not a property or a fixed quantity, and the remaining properties in the equation produce the merit index.

A cylindrical **tie-rod** of length L is to carry a tensile force F without extending elastically by more than δ , therefore, its stiffness, S , must be at least $S = F / \delta$.

Expressing S in terms of E :

$$E = \sigma / \epsilon = \frac{F/A}{\delta/L}, \text{ therefore, } F = \frac{AE\delta}{L} \text{ and } S = F / \delta = \frac{AE}{L}.$$

The attribute sought is lightness, i.e. minimum mass, m .

$$m = \rho LA \text{ and } S = AE / L$$

where, A is the area of the cross-section, ρ is the density and E is the Young's modulus of the material.

Eliminating the free variable A between the above two equations gives

$$m = SL^2 \left(\frac{\rho}{E} \right)$$

S and L have been specified, therefore, the lightest tie-rod that will provide the stiffness S is that made from the material which gives a minimum value for ρ/E . However, it is more usual to express merit indices in a form for which a maximum is sought (Ashby et al. 2014, p106).

$$\therefore \text{ the merit index for the tie-rod becomes } M = \frac{E}{\rho}$$

Materials with high values of M to be selected.

The merit index for a stiff and light **beam** in bending:

Consider a solid beam of square section, $A = t^2$. It is loaded in 3-point bending over a span of fixed length L with a central force F , under which the elastic deflection must not exceed δ . As before, using the equations for mass and stiffness,

$$m = AL\rho \text{ and } S = cEI / L^3 \text{ under 3-point bending load.}$$

I is the second moment of area of the beam, $I = A^2/12 = t^4/12$, and c a constant.

Substituting for I gives

$$S = \frac{cEA^2}{12L^3}, \text{ therefore, } A^2 = \frac{12SL^3}{cE}$$

Substituting for A in $m = AL\rho$ gives $m = (12SL^3 / c)^{1/2} (L) (\rho / E^{1/2})$,

$$\therefore \text{ the merit index for the beam becomes } M = \frac{E^{1/2}}{\rho}.$$

The merit index for a stiff and light **panel** in bending:

A panel of width w is loaded in 3-point bending over a span of fixed length L with a central force F , under which the elastic deflection must not exceed δ . The thickness t is not fixed and is the free variable.

$$m = AL\rho \text{ and } S = cEI/L^3$$

For a solid panel of thickness t and width w , $I = wt^3/12$

Substituting for I gives

$$S = \frac{cEwt^3}{12L^3}, \text{ therefore, } t^3 = \frac{12SL^3}{cEw} \text{ and } t = \left(\frac{12S}{cEw}\right)^{1/3}L$$

Substituting for t in $m = twL\rho$ gives $m = \left(\frac{12S}{cEw}\right)^{1/3} wL^2\rho$

$$\therefore \text{ the merit index for the panel becomes } M = \frac{E^{1/3}}{\rho}.$$

The aim is to maximise merit indices in material selection. Further information on the material performance index for a stiff and light structural member can be found in Patton et al. (2004) and Farag (2008). Reference has also been made to these specific properties in association with the components of a Formula-1car (Savage 2008, p. 7): specific modulus being a useful indicator for the front-wing pillars loaded in tension, $E^{1/2}/\rho$ for a compression member such as suspension push rod, which is limited by buckling, and $E^{1/3}/\rho$ for a panel loaded in bending such as a rear wing.

Online material property databases such as MatWeb and MatWeb (composites) provide data sheets on thermoplastic and thermoset polymers and their composites. MatWeb (<http://www.matweb.com/reference/composites.aspx>) contains entries for well over 8000 polymers, including both thermoplastics and thermosets, which have been reinforced through the addition of glass fibre, carbon fibre, aramid fibre, wood, or mineral reinforcements. Not all of these are cutting edge products; some merely include inexpensive inorganics such as calcium carbonate or talc as a way of achieving improved dimensional stability in commodity grade plastics such as polypropylene.

Since the vast majority of polymer-based composites are generally processed and sold as polymers, MatWeb has categorized them according to the base resin in their material property data search tools. Some composite fibres and composite core materials are also listed under 'Other Engineering Materials' or in continuous fibre composites in MatWeb database: <http://www.matweb.com/search/MaterialGroupSearch.aspx>.

MatWeb recommends that a good strategy to find the composite material of choice for an application is to pick a category such as polymers, thermoset, e.g. epoxy, and specify a minimum tensile strength or flexural modulus from the property field.

Plots of properties and merit indices against one another are also available in the form of **Bubble Charts** (Ashby, 2005), which employs property charts and enables combinations of properties to be considered in material selection. In property charts a property is plotted against another one on logarithmic scales, which produces fields (bubbles) of property spaces that are occupied by each material class, see Figure 5.27.

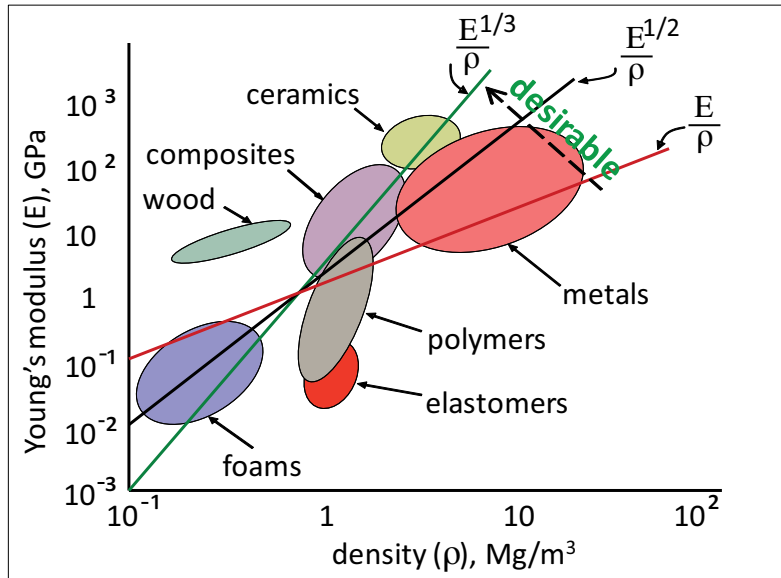


Figure 5.27 E vs. ρ bubble chart for groups of materials for stiff and lightweight design using three material merit indices

TURN TO THE EXPERTS FOR **SUBSCRIBE** CONSULTANCY

Subscribe is one of the leading companies in Europe when it comes to innovation and business development within subscription businesses.

We innovate new subscription business models or improve existing ones. We do business reviews of existing subscription businesses and we develop acquisition and retention strategies.

Learn more at [linkedin.com/company/subscribe](https://www.linkedin.com/company/subscribe) or contact
Managing Director Morten Suhr Hansen at mha@subscribe.dk

SUBSCR**IBE** - to the future



In Figure 5.27, the elastic modulus is plotted against the density on logarithmic scales. The use of log scales enables the inclusion of a wide range of values, representing materials from the very light and flimsy foams to the stiffest and heaviest metals. Similarly, the other combinations of properties may include strength and density, elastic modulus and strength, specific modulus versus specific strength (useful in aerospace applications and for structural purposes), fracture toughness and elastic modulus or strength, thermal conductivity and electrical resistivity or coefficient of linear thermal expansion, strength and maximum service temperature, and strength or Young's modulus and material cost. More recent work also includes evaluation/reduction of environmental concerns/impacts, e.g. embodied energy vs. CO₂ footprint in primary production of various materials (Ghenai 2012), or mechanical properties vs. (embodied energy x density) or (CO₂ footprint x density).

The schematic diagram shown here, Figure 5.27, also illustrates three merit indices to maximise stiffness and lightness for components with different geometries under different modes of loading. The plots of log (E) against log (ρ) for these merit indices produce straight lines, such that the intercepts on the y-axis indicate the values for the material merit indices. This is described below for one of the merit indices. The desirable outcomes are achieved when the candidate materials move the merit-index lines in the direction of the arrow marked “desirable”, i.e. with any one of those three lines, the aim is to move the lines, in parallel, to the left in order to yield a high intercept value, and the materials that fall in the top right-hand corner of the chart are desirable.

For the merit index, $M = E^{1/2} / \rho$, rearranging

$E = (\rho M)^2$, and taking the log gives

$$\log (E) = 2 \log (\rho) + 2 \log (M).$$

A plot of log (E) against log (ρ) produces a straight contour line of slope 2 and y-axis intercept of 2log (M), and therefore as the lines move to the left on the graph a larger intercept and hence a higher value for the merit index results.

5.2.1 Lightweighting

Manufacturing economics and concerns about environmental pollution have combined to put pressure on the designer to rethink the approach to product design, and to consider the entire lifecycle of the product. The two main approaches are lean design (to minimise the total volume of material used) and design for recyclability.

Reduction of waste at source is a simple concept, but one that requires rigorous design appraisal. For example, **over-design** is a common error with plastics parts, which is often related to the design being simply a replication of a previous metal part. Strength and stiffness requirements have been based on the capability of the metal, rather than on an assessment of the true in-service requirements. The designer must ask ‘What is the basis for this requirement?’ and then apply the following design principles:

Optimise wall thickness – an unnecessarily thick wall section requires more material, a longer manufacturing cycle, e.g. longer cooling times for plastics parts and more energy to produce.

Use geometrical features, such as ribbed structures or sandwich/laminate structures instead of thick-walled sections where stiffness is required.

The stiffness of structured components, such as ribbed plates, corrugated panels, sandwich beams can be assessed by using the engineer’s bending theory,

$$\frac{M}{I} = \frac{E}{R}$$

where, M is the bending moment (or the moment of force), I is the second moment of area, E is the elastic modulus of the material, and R is the radius of curvature that forms when the plate is forced to bend. Note that as the deflection of the plate increases, the radius of curvature, R , decreases. Therefore, R becomes an indication of stiffness, such that R is directly proportional to stiffness. Accordingly,

Stiffness $\propto EI$, since from the equation of the bending theory $R = EI / M$.

Also $I = wt^3/12$ for filled rectangular plates, therefore, Stiffness $\propto EI$ or Et^3 .

Placing material as far away as possible from the neutral axis of bending, which increases t , is generally an effective means of increasing I and, thus, stiffness for a given area of plate. Separation of plates can be achieved by using honeycomb or foam cores. However, increases in stiffness may also be achieved by stiffened skin approaches that use ribs and corrugations.

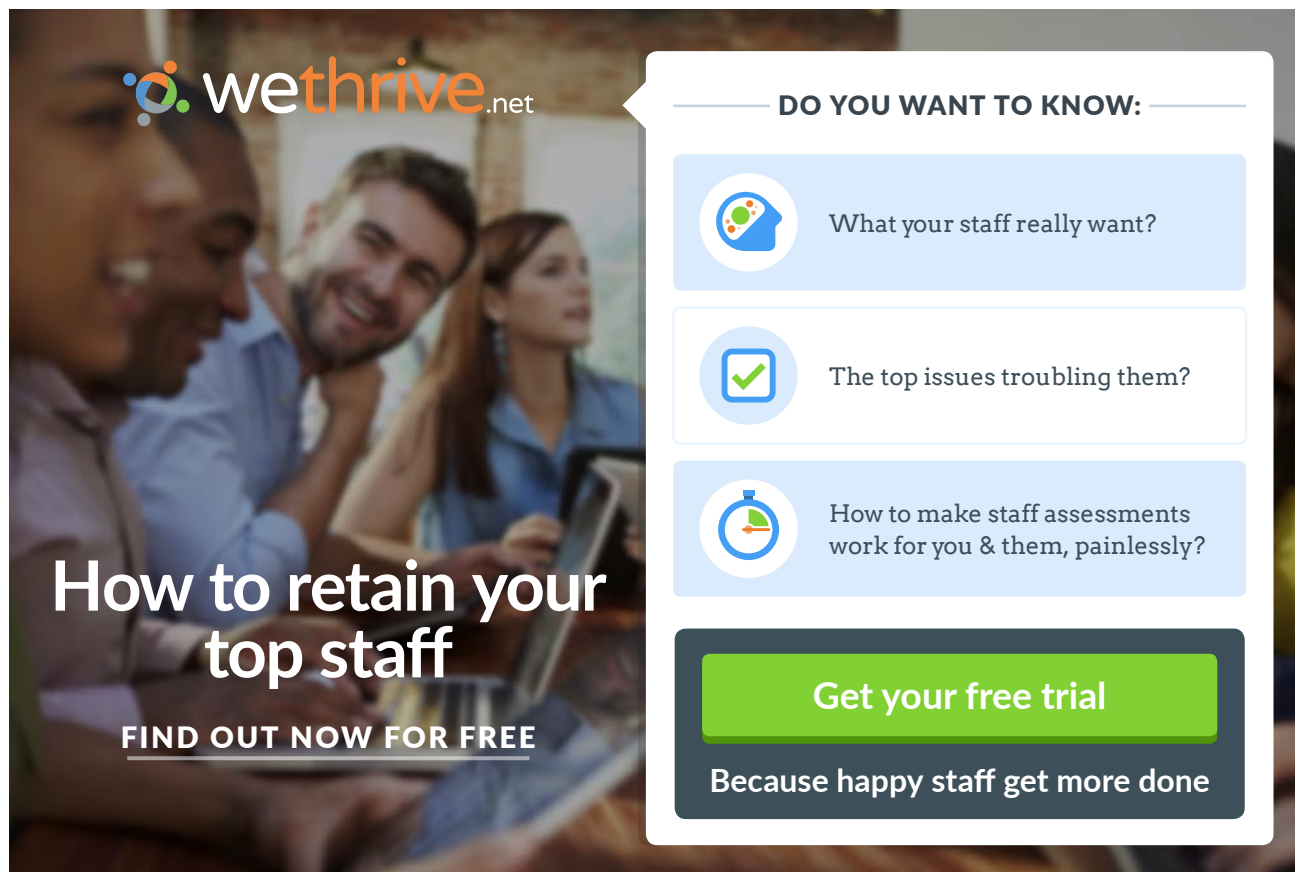
The stiffness of a structure is, therefore, dependent on the elastic modulus of the material and the geometry of the part. Again, the stiffening effect of ribs and corrugations arises from the fact that the geometry results in an increased distance of material from the neutral axis of bending so that the moment of inertia, I , is increased. A stiffening factor may be defined as, $SF = I_{\text{with ribs}} / I_{\text{without ribs}}$.

Henry Ford has been quoted to have said that “the most environmentally friendly thing you can do for a car that burns gasoline is to make **lighter bodies**”. He had hoped to shift from steel to lower weight materials. He had even targeted biocomposites, but progress was halted by World War II.

So (2012) has reported that although attracted initially by environmental benefits, car makers and their suppliers are also asking what added functionality they can get from non-compostable, bio-based materials. One advantage is of course lighter, more cost-effective vehicles. A rule-of-thumb is that 5% less weight means average fuel savings of 3%, according to industry association Plastics Europe.

Advantages of composites compared to steels for automotive and transportation are (Carpenter 2008):

- 1) weight reduction of 20–40 percent,
- 2) styling flexibility in terms of deep drawn panels, which is limited in metal stampings,
- 3) 40–60 percent savings in tooling cost,
- 4) reduced assembly costs and time in part consolidation,
- 5) resistance to corrosion, scratches and dents, and improvement in damping and NVH (noise, vibration and harshness),
- 6) materials and process innovations capable of adding value while providing cost saving, and
- 7) safer structure due to the composite material's higher specific energy absorption (SEA).



wethrive.net

How to retain your top staff

FIND OUT NOW FOR FREE

DO YOU WANT TO KNOW:

- What your staff really want?
- The top issues troubling them?
- How to make staff assessments work for you & them, painlessly?

Get your free trial

Because happy staff get more done

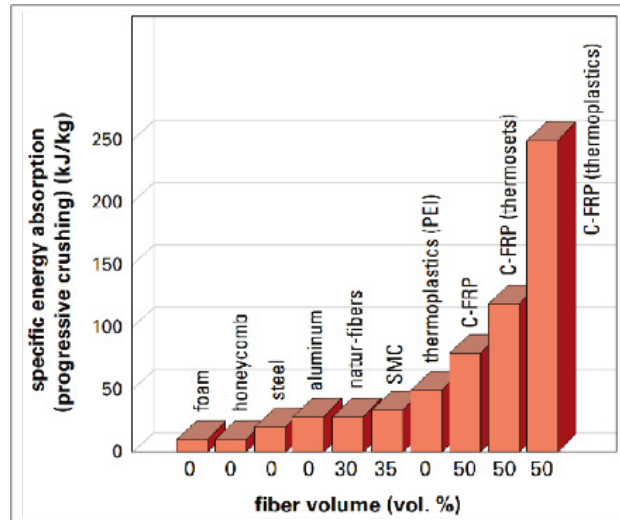


Figure 5.28 Typical values of SEA for some materials (source: Herrman et al. 2002)

Figure 5.28 shows that CF reinforced epoxy resin composite crush cones and similar structures can absorb approximately 120 kJ/kg, and 250 kJ/kg with a thermolpastic marix compared with 20 kJ/kg for steel.

Ford identified four major challenges to high performance and high volume structural polymers in automotive applications:

- improved composite materials must be recyclable,
- carbon fibre must be more affordable,
- robust analytical tools for predicting crash energy absorption including fractures, for determining final shape from manufacturing and under severe loadings and for predicting joint behaviour,
- enhanced component production methods (processing, cycle times), and
- improved vehicle assembly techniques, including faster cycle times, robust coating and painting processes, and effective adhesive joint non destructive evaluation (NDE).

The automotive industry is reducing the weight of its vehicles, largely by adopting lighter weight materials (see Table 5.4) and through vehicle redesign. For example, CF composites offer a 50–70% mass reduction over mild steel (the most used material in vehicles), and GF composites a 25–35% reduction. The US National Institute of Standards and Technology estimates a 10% reduction in mass translates into a fuel savings of 6–7% (ReinforcedPlastics.com, 27 August 2014).

Material	Mass reduction, %
Magnesium	30–70
Carbon fibre composites	50–70
Aluminium & Al-matrix composites	30–60
Titanium	40–45
Glass fibre composites	25–35
Advanced high strength steel	15–25
High strength steel	10–28

Table 5.4 Mass reduction achievable in vehicles with different materials over mild steel (source: Department of Energy)

Car companies aim to exploit every cost-effective opportunity to reduce weight and, with it, fuel consumption. In a 2014 DuPont-sponsored survey with WardsAuto, conducted by Penton Market Research, Kansas, USA, in response to the question “which vehicle area/system is your primary target for lightweighting?” the industry’s focus appears to be powertrains for lightweighting. The breakdown of the response of 900 participants is shown in Table 5.5.

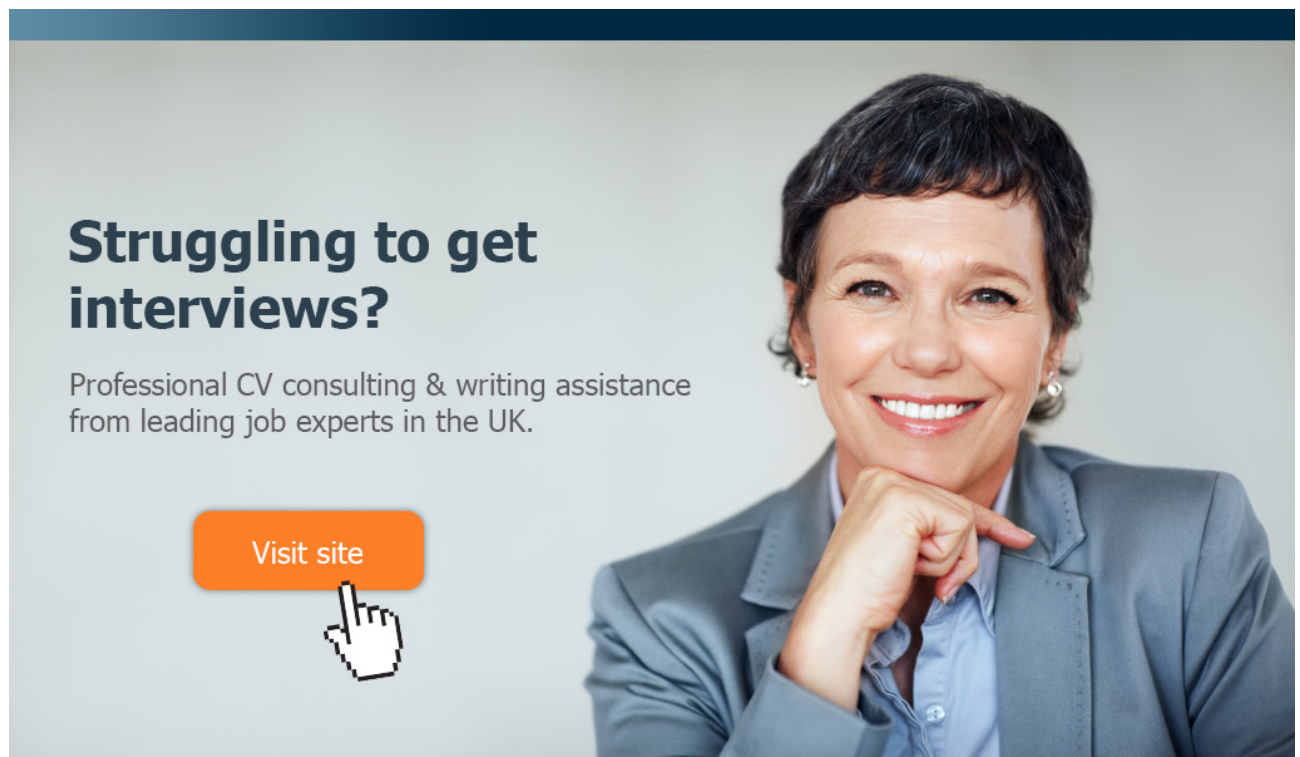
Vehicle part	Level of focus, %
Powertrain (engine & transmission)	24
Chassis (fuel, exhaust & suspension)	12
Body-in-white	11
Body panels	9
Electrical & accessories	9
Interior	7
Tire, rim & wheels	3
Closure panels	1
Glass	1
Other	9
No clear targets	14

Table 5.5 Areas of the vehicle being targeted for lightweighting (Source: 2014 WardsAuto, DuPont Automotive Trends Benchmark Study, conducted by Penton Research)

Savage (2008, p. 14) has covered the use of composites in the construction of Formula 1 cars, stating that “CF composites make up 85% of the volume of Formula 1 cars whilst accounting for less than 25% of its mass. In addition to the chassis there is composite bodywork, cooling ducts for the radiators and brakes, front rear and side crash structures, suspension, gearbox and the steering wheel and column. Some speciality composites are also used. These include carbon-carbon brakes and clutches, and ablatives in and around the exhaust ports.

In addition to obvious weight savings, components such as push rods and wishbones exhibit almost infinite fatigue durability.”

The concept of IsoTruss, see Section 5.1.4, is a good example of achieving lightweight, strength and stiffness by a combination of lightweight material with appropriate geometrical features: a carbon fibre composite tubular 3-D open-truss-structure made up of pyramids formed by isosceles triangles. IsoTruss grid structure provides substantial resistance to local and global column buckling. Figure 5.29 shows a picture of the world’s first road bike frame constructed from carbon fibre and Kevlar crafted into IsoTruss open lattice tube design by mechanically weaving fibre strands around metal rods to create the open lattice structure. The Ascend bicycle frame is reported to weigh 1.8 pounds and is, according to Delta 7, the strongest road bike in its weight class. Figure 5.30 depicts a demonstration of the strength of the IsoTruss tubes.



Struggling to get interviews?

Professional CV consulting & writing assistance from leading job experts in the UK.

Visit site

 Take a short-cut to your next job!
Improve your interview success rate by 70%.

 **TheCVagency**
Visit theagency.co.uk for more info.

 **Click on the ad to read more**



Figure 5.29 Ascend road bike

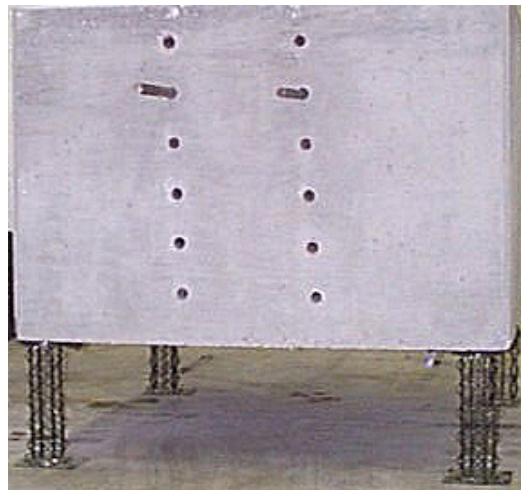


Figure 5.30 Isotrusses together weighing less than 0.5 kg support a reinforced concrete block weighing over 5 ton (source: IsoTruss)

5.2.2 Recycling and Health & Safety

Recycling of polymer-matrix composites have been covered extensively, e.g. Pickering (2006) has reviewed the current status of recycling technologies for thermoset composite materials, the paper by Otheguy, et al. (2009) is on recycling of end-of-life thermoplastic composite boats, Job (2010) has given a summary of R&D on composite recycling, and Halliwell (2006) has examined the end-of-life options for composite waste: recycle, reuse or dispose?

Composite materials are mainly based on thermosetting resin matrices and are difficult to recycle because, unlike thermoplastics, thermosets do not melt. Pickering (2006) has summed up the problems in recycling thermoset composites as follows: “thermosetting polymers are cross linked and cannot be remoulded. Some thermosetting polymers can be converted relatively easily back to their original monomer, such as polyurethane. However, the more common thermosetting resins, such as polyester and epoxy are not practical to depolymerise to their original constituents.” There are other complexities, “composites are often manufactured in combination with other materials. For example there may be foam cores to reduce weight and cost or metal inserts to facilitate fastening onto other components.”

Other problems associated with recycling any material from end-of-life components has also been highlighted, such as the need be able to deal with contamination and the difficulty of collecting, identifying, sorting and separating the scrap material.

The existing technically viable recycling techniques for polymer-matrix composites are shown in Figure 5.31. There are basically three categories of process: those that involve mechanical comminution techniques to reduce the size of the scrap to produce recyclates, chemical decomposition with solvents or supercritical fluids, and those that use thermal processes to break the scrap down into materials and energy. The chemical route, however, constitute an environmental hazard and the resulting chemical mixtures require complex processing to recover useable products.

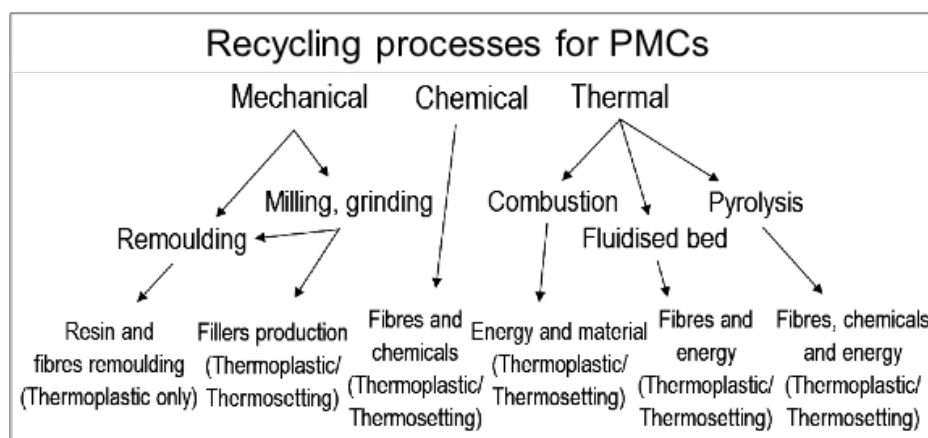


Figure 5.31 Recycling processes for thermoplastic and thermosetting composites (source: Otheguy et al. 2009)

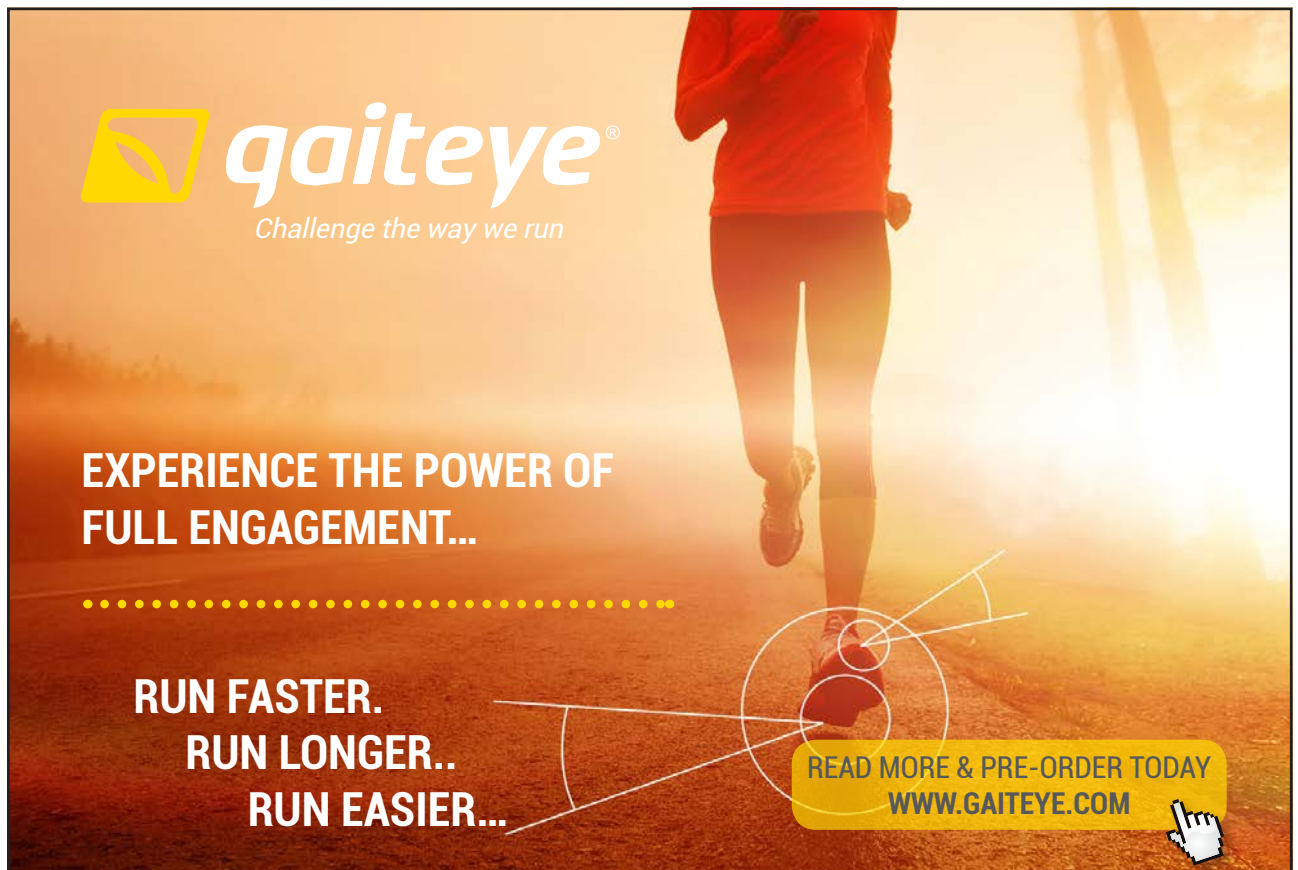
In an alternative classification the quality of the recyclates and the type of recovery is described (Halliwell 2006):

- Primary recycling – conversion of waste into material having properties equivalent to those of the original material
- Secondary recycling – conversion of waste into material having properties inferior to those of the original material
- Tertiary recycling – conversion of waste into chemicals and fuel
- Quaternary recycling – conversion of waste into energy.

The details of these recycling processes can be found in Halliwell (2006), and some excerpts from this reference are included here:

Most tried techniques for **primary and secondary recycling** essentially involve the mixing of some waste material with virgin raw material, which is then processed as if it were all virgin material. Whether the proper designation for the procedure is primary or secondary recycling is a matter of how successful it is. Tertiary recycling refers to chemical decomposition of the polymer, i.e. depolymerisation into useful chemical substances and fuel, while quaternary recycling is synonymous with incineration to recover energy. The technique of incineration without energy utilisation is not really recycling at all, merely a means of reducing waste volume.

From the point of view of material utilisation it is generally preferable to succeed with the highest possible level of recycling, e.g. secondary rather than quaternary recycling. However, from economical and overall resource utilisation perspectives this need not necessarily be the case, since for example secondary recycling may require excessive amounts of energy and other resources (facilities, man power, chemical additives etc.), while quaternary recycling is straightforward and does not require energy or specialised resources.



 **gaiTEYE**[®]
Challenge the way we run

**EXPERIENCE THE POWER OF
FULL ENGAGEMENT...**

.....

**RUN FASTER.
RUN LONGER..
RUN EASIER...**

**READ MORE & PRE-ORDER TODAY
WWW.GAITEYE.COM**

The most attractive recycling option is to recycle waste into material with properties equivalent or at least comparable to those of the original material (as common with metals and glass) since it implies a possibility for an infinite number of recycling circuits. The division between primary and secondary is relative and a question of what extent of property degeneration that one is able to allow while still saying that the properties are equivalent. Common alternative names for primary and secondary recycling are material recovery or mechanical recycling.

Tertiary recycling processes include pyrolysis, supercritical water processing or fluidised-bed processing. Pyrolysis is the heating of waste in the absence of air (oxygen) and is used to separate composite material into its original constituents. The process breaks composites down into gas, oil, fibre and a small amount of carbon. The oil and fibre obtained can both be reprocessed into composites. The operating temperature must be tailored to the type of composite being processed in order to minimise thermal degradation of the fibres recovered.

Supercritical water processing can hydrolyse and decompose composites effectively and cleanly without charring. The process involves heating waste composite in steam at 300 to 500°C resulting in the material being decomposed and partially hydrolysed to phthalic acid, styrene, glass fibre and oil. A supercritical water system for recycling composite waste can be considered if its economics are reasonable. In Japan, a supercritical water processing system has been developed with a generating unit fuelled by mixed waste plastics which are thermally decomposed to generate gas which is in turn used as a fuel to produce supercritical water and electricity.

Fluidised-bed thermal processing for recycling composites results in materials and energy recovery. A fluidised bed is a chamber containing sand which acts like a fluid when suspended in an airstream. The chamber is heated to between 450 and 500°C; too low and the fibres will not be fully cleaned, any higher and the fibres suffer a reduction in strength. Chopped-up composite material is placed in the bed. The resin is evaporated and the fibre is blown by the airstream to a collection point for recovery. Gas enters a secondary combustion chamber for heat recovery leading to clean flue gas and recovered energy.

Quaternary recycling – when composites are combusted with energy recovery, the calorific value will depend on the inorganic content. Although the combustion of composite waste is thought to be cleaner than that of coal, there is still a bulky ash residue. For example, in a typical GRP product 40% is glass, 30% inorganic filler and 30% resin. The glass and the filler do not burn, leaving 70% of the composite as a residue after incineration. It has also been suggested that incinerating composite material with energy recovery results in energy loss (in the region of 400 kJ/kg). Together, these mean that incinerating GRP is not a long-term solution for dealing with this waste stream. Natural-fibre reinforced polymers are thought to be the best type of composites for incineration with energy recovery, as the natural fibres and fillers should burn easily leaving no residue and resulting in no energy losses.

Design considerations:

Designers need to consider the costs of the end-of-life stage of products now – if this is ignored then the eventual costs will be unduly high if legislation changes. Designers must

- make re-use, re-manufacturing and recycling easier for all products: re-using, re-manufacturing or recycling all or part of the product will significantly reduce the eventual costs by reducing raw material use and diverting material away from limited landfill space.
- design the product for re-use in its current form (i.e. without processing) – this can extend the useful life of the product. Future product designs need to incorporate the requirements of subsequent uses, e.g. for packaging and containers, this may mean extra **durability** and the introduction of a re-use system suitable for the market.
- design for product remanufacture or recycling – this needs increased focus on the physical organisation of the product, i.e. the structure and the way in which components and materials are put together. Reducing the number of fastenings and making fastenings easier to undo will help to make the product easier to **disassemble** and recycle.
- design to enable recycling by reducing the number of materials used – single material products are much easier to recycle.
- design to eliminate materials that can be **hazardous** during remanufacturing or make recycling difficult.

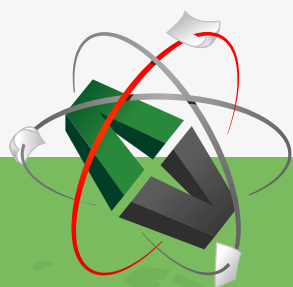
Cleaner design in the future will not be easy but the alternative high end-of-life costs are even less acceptable Halliwell (2006).

Health & safety:

The Occupational Safety & Health Administration (OSHA) of the USA in their technical manual have summed up the potential health hazards associated with the use of advanced composites, see Table 5.6.

Composite component	Organ system target (possible target)	Known (possible) health effect
Resins		
Epoxy resins	Skin, lungs, eyes	Contact and allergic dermatitis, conjunctivitis
Polyurethane resins	Lungs, skin, eyes	Respiratory sensitization, contact dermatitis, conjunctivitis
Phenol formaldehyde	Skin, lungs, eyes	As above (potential carcinogen)
Bismaleimides (BMI)	Skin, lungs, eyes	As above (potential carcinogen)

This e-book
is made with
SetaPDF



PDF components for PHP developers

www.setasign.com



Polyamides	Skin, lungs, eyes	As above (potential carcinogen)
Reinforcing materials		
Aramid fibers	Skin (lungs)	Skin and respiratory irritation, contact dermatitis (chronic interstitial lung disease)
Carbon/graphite fibers	Skin (lungs)	As noted for aramid fibers
Glass fibers (continuous filament)	Skin (lungs)	As noted above
Hardeners and curing agents		
Diaminodiphenylsulfone	–	No known effects with workplace exposure
Methylenedianiline	Liver, skin	Hepatotoxicity, suspect human carcinogen
Other aromatic amines		
Meta-phenylenediamine (MPDA)	Liver, skin (kidney, bladder)	Hepatitis, contact dermatitis (kidney and bladder cancer)
Aliphatic and cyclo-aliphatic amines	Eyes, skin	Severe irritation, contact dermatitis
Polyaminoamide	Eyes, skin	Irritation (sensitization)
Anhydride	Eyes, lungs, skin	Severe eye and skin irritation, respiratory sensitization, contact dermatitis

Table 5.6 Organ system target (source: OSHA 1999)

Further information on the health hazards of the substances indicated in Table 5.6 as well as other associated substances such as dusts and solvents are given in the OSHA Manual. The manual also covers good workplace control measures such as:

Engineering Controls: isolation (e.g. isolated storage, separate process areas, enclosures, closed systems) and local exhaust ventilation are the primary engineering controls found in advanced composites processes.

Work Practice Controls: work practices, as distinguished from engineering controls, involve the way a task is performed. Some fundamental and easily implemented work practices that can be used to minimize exposures when working with advanced composites are:

- good employee training and education;
- following the proper procedures for production, process and control equipment;
- proper use, maintenance, and cleaning of personal protective equipment;
- good personal hygiene program;
- housekeeping;
- periodic inspection and maintenance of production, process and control equipment; and
- good supervision.

Personal Protective Equipment:

- Gloves, protective clothing, and eye protection may frequently be required, especially when working with resins, curing agents, and solvents. Selection of the proper protective materials should be based on permeation data, if available. These types of data are often available for the solvents used, but very little data are available for the resins and curing agents.
- In many advanced composites processes several chemicals or mixtures are involved. There are essentially no permeation data available for chemical mixtures. This means that, in many cases, glove and clothing selection must be a trial and error process.
- Generally, the resins are of a larger molecular size and so are less likely to permeate protective materials than the curing agents and solvents. The aromatic amine curing agents are particularly difficult to protect against. In some advanced composites processes, close hand work and contact is required, and a glove must provide good tactility. Often this type of glove provides the least protection against the resin and curing agent.
- Eye protection can be provided by standard safety glasses with side shields, goggles, or a face shield, as needed.
- Respiratory protection is not required in many advanced composites processes, due to the low vapour pressure of the materials involved. However, respirators may be required where:
 - o airborne solvent levels are high;
 - o dust levels are high (resin mixing, finishing, repair);
 - o large surface areas and significant hand work are involved; and
 - o exotherms are experienced.

Administrative Controls: employee exposures also can be controlled by scheduling operations with the highest exposures at a time when the fewest employees are present.

5.3 Self-assessment questions

1. Huge heights have been cleared by leading pole vaulters; describe the construction of a modern vaulting pole. Make references to performance requirements, design criteria and, therefore, material selection and manufacturing technique.
2. Describe the construction of composite tennis racquets, helicopter rotor blades, snow skis and racing-car cockpits. Relate the performance requirements of these products to their material selection and manufacturing techniques.
3. Why are composite-honeycomb sandwich materials often used in aircraft wing sections?
4. Describe a pultruded composite profile that makes a suitable support for PVC windows and indicate its advantages compared with the widely used mechanical support.
5. What targets are set by the European Union's end-of-life vehicles (ELV) directive for the automotive industry, and what is the industry strategy to meet these targets?

6. What are the advantages of composites compared with steels for automotive and transportation applications?
7. A composite tennis racquet is to be produced by injection moulding; describe the raw material to be used and the details of the production process.
8. Give an account of protection measures taken against lightning strike on aircraft structures.
9. Briefly describe the IsoTruss lattice structure and its application in a product.
10. Briefly describe three different approaches to the construction of self-healing PMCs.
11. Give an account of health & safety and environmental considerations in working with polymer-matrix composites.
12. What are the most significant composite properties in rocket and missile uses?
13. Aluminium in contact with carbon fibre will:
 - a) corrode
 - b) not corrode.
14. Derive a suitable equation for the merit index to select the best materials for a stiff and light beam for use under bending-load conditions. Using this equation and a bubble chart that only shows polymers, composites and metals, illustrate how to select a desirable material.
15. Describe the technically viable recycling techniques for polymer-matrix composites.



The advertisement features a dark blue background with a large, stylized white graphic of a lion's head. The text "YOU THINK. YOU CAN WORK AT RMB" is written in large, white, sans-serif capital letters across the center. In the top right corner, there is a white box containing the Rand Merchant Bank logo (a lion holding a key) and the text "RAND MERCHANT BANK", "A division of FirstRand Bank Limited", and "Traditional values. Innovative ideas."

Rand Merchant Bank uses good business to create a better world, which is one of the reasons that the country's top talent chooses to work at RMB. For more information visit us at www.rmb.co.za

Thinking that can change your world

Rand Merchant Bank is an Authorised Financial Services Provider



Click on the ad to read more

References

Adams, D 2012, 'Impact testing of composite materials', *High-Performance Composites*, May 2012, *CompositesWorld* (<http://www.compositesworld.com/articles/impact-testing-of-composite-materials>).

Adams, DO, et al, 'Development and evaluation of fracture mechanics test methods for sandwich composites' (http://www.niar.wichita.edu/niarworkshops/Portals/0/Utah_Kessler.pdf).

Ahn, S-H & Springer, GS 2000, *Repair of Composite Laminates, Report Number: DOT/FAA/AR-00/46*, US Department of Transportation Federal Aviation Administration (<http://www.tc.faa.gov/its/worldpac/techrpt/ar00-46.pdf>).

Akay & Hanna 1990, 'A comparison of honeycomb-core and foam-core carbon-fibre/epoxy sandwich panels', *Composites*, Vol. 21, No. 4, pp. 325–331.

Akay, M & Barkley, D 1991, 'Fibre orientation and mechanical behaviour in reinforced thermoplastic injection mouldings', *Journal of Materials Science*, 26, pp. 2731–42.

Akay, M & Mun, SKA 1995, 'Bearing strength of autoclave and oven cured Kevlar/epoxy laminates under static and dynamic loading', *Composites*, Vol. 26, No. 6, pp. 451–456.

Akay, M & Spratt, GR 2008, 'Evaluation of thermal ageing of a carbon fibre reinforced bismaleimide', *Composites Science and Technology*, 68, pp. 3081–3086.

Akay, M 1988, 'Relaxation transitions, fracture toughness and post-impact residual capacity of carbon-fibre reinforced composites', *Composites Science and technology*, 33, pp. 1–18.

Akay, M 1990, 'Effects of prepreg ageing and post-cure hygrothermal conditioning on the mechanical behaviour of carbon-fibre/epoxy laminates', *Composites Science and Technology*, 38, pp. 359–370.

Akay, M 1992, 'Bearing strength of as-cured and hygrothermally conditioned carbon-fibre/epoxy composites under static and dynamic loading', *Composites*, Vol. 23, No. 2, pp. 101–108.

Akay, M 1993, 'Aspects of dynamic mechanical analysis in polymeric composites', *Composites Science and Technology*, 47, pp. 419–423.

Akay, M 1994, 'Moisture absorption and its influence on the tensile properties of glass-fibre reinforced polyamide 6,6', *Polymers & Polymer Composites*, Vol. 2, No. 6, pp. 349–354.

Akay, M 2012, *Introduction to polymer science and technology*, Bookboon, Ventus Publishing ApS (<http://bookboon.com/en/introduction-to-polymer-science-and-technology-ebook>).

Akay, M & Aslan, N 1995, 'An estimation of fatigue life for a carbon fibre/poly ether ether ketone hip joint prosthesis', *Proc. Instn. Mech. Engrs., Part H: Jn of Engineering Medicine*, Vol. 209, 93–103.

Akay, M & Aslan, N 1996, 'Numerical and experimental stress analysis of a polymeric composite hip joint prosthesis', *Journal of Biomedical Materials Resaerch*, Vol. 31, 167–182.

Akay, M & Cracknell, JG 1994, 'Epoxy resin-polyethersulphone blends', *Journal of Applied polymer Science*, Vol. 52, 663–688.

Akay, M, Cracknell JG and Farnham, HA 1994, 'Detection of undercure in carbon-fibre/epoxy composites by dynamic mechanical thermal analysis', *Polymers & Polymer Composites*, Vol. 2, No. 5, 317–322.

Akay, M, Kong Ah Mun, S and Stanley, A 1997, 'Influence of moisture on the thermal and mechanical properties of autoclaved and oven-cured Kevlar-49/epoxy laminates', *Composites Science and Technology*, 57, pp. 565–571.



Discover the truth at www.deloitte.ca/careers

Deloitte.

© Deloitte & Touche LLP and affiliated entities.



Click on the ad to read more

Akay, M, O'Regan, DF and Bailey, RS 1995, 'Fracture toughness and impact behaviour of glass-fibre-reinforced polyamide 6,6 injection mouldings', *Composites Science and Technology*, 55, pp. 109–118.

Ashby, MF 2005, *Materials Selection in Mechanical Design*, 3rd edition, Elsevier.

Ashby, MF, Shercliff, H & Cebon, D 2014, *Materials: engineering, science, processing and design*, 3rd edition, Butterworth-Heinemann.

ASTM D 3039 -2008 Standard test method for tensile properties of polymer matrix composite materials.

ASTM D 3479/D 3479M:2012 Standard test method for tension-tension fatigue of polymer matrix composite materials.

ASTM D2344M 00(2006), Standard test method for short-beam strength of polymer matrix composite materials and their laminates.

ASTM D256-10, Standard test methods for determining the Izod pendulum impact resistance of plastics.

ASTM D2583-2007 Standard Test Method for Indentation Hardness of Rigid Plastics by Means of a Barcol Impressor.

ASTM D3418-12e1 Standard test method for transition temperatures and enthalpies of fusion and crystallization of polymers by differential scanning calorimetry.

ASTM D3518M-94(2007), Standard test method for in-plane shear response of polymer matrix composite materials by tensile test of a $\pm 45^\circ$ laminate.

ASTM D3763-06 Standard test method for high speed puncture properties of plastics using load and displacement sensors.

ASTM D4065-12 Standard Practice for Plastics: Dynamic Mechanical Properties: Determination and Report of Procedures.

ASTM D4440-08 Standard Test Method for Plastics: Dynamic Mechanical Properties Melt Rheology.

ASTM D4473-08 Standard Test Method for Plastics: Dynamic Mechanical Properties: Cure Behavior.

ASTM D5229 / D5229M – 12 Standard test method for moisture absorption properties and equilibrium conditioning of polymer matrix composite materials.

ASTM D5279 – 08 Standard Test Method for Plastics: Dynamic Mechanical Properties: In Torsion.

ASTM D5379M-2007, Standard test method for shear properties of composite materials by the V-notched beam method.

ASTM D5528-01 (2007) Standard Test Method for Mode I Interlaminar Fracture Toughness of Unidirectional Fiber-Reinforced Polymer Matrix Composites.

ASTM D5766-11 Standard test method for open-hole tensile strength of polymer matrix composite laminates.

ASTM D5961 (2010) Standard test method for bearing response of polymer matrix composite laminates.

ASTM D6110-10 Standard test method for determining the Charpy impact resistance of notched specimens of plastics.

ASTM D6873 / D6873M-08 Standard practice for bearing fatigue response of polymer matrix composite laminates.

I WANT TO CHANGE DIRECTION,
AND THE WORLD.

GOT-THE-ENERGY-TO-LEAD.COM

We believe that energy suppliers should be renewable, too. We are therefore looking for enthusiastic new colleagues with plenty of ideas who want to join RWE in changing the world. Visit us online to find out what we are offering and how we are working together to ensure the energy of the future.

RWE
The energy to lead



ASTM D7137 (2012) Standard test method for compressive residual strength properties of damaged polymer matrix composite plates.

ASTM D7615 / D7615M-11 Standard practice for open-hole fatigue response of polymer matrix composite laminates.

ASTM E1356-08 Standard test method for assignment of the glass transition temperatures by differential scanning calorimetry.

ASTM E2533-09, Standard guide for nondestructive testing of polymer matrix composites used in aerospace applications.

ASTM E647-13e1 Standard test method for measurement of fatigue crack growth rates.

Avery, J 1998, *Injection Moulding alternatives: a guide for designers and product engineers*, Hanser,

Baker, A, Dutton, S and Kelly, D 2004, *Composite materials for aircraft structures*, 2nd ed., American Institute of Aeronautics and Astronautics, Inc., Reston, Virginia, USA, pp. 289–368. (http://www.barolaaerosports.com/students-corner/barolaaerosports_Composite_Materials_for_Aircraft_Structures_Second_Edition_Aiaa_Education_Series_.pdf).

Barkley, D & Akay, M 1992, 'The design and evaluation of an instrumented impact tester', *Polymer Testing*, 11, pp. 249–270.

Beckman Institute 2014, Repeated self-healing now possible in composite materials (<http://beckman.illinois.edu/news/2014/04/self-healing-composites>).

Beers, D et al. 2001, 'Other high modulus-high tenacity (HM-HT) fibres from linear polymers', Chapter 4 in *High Performance Fibres* (edited by Hearle, JWS), Woodhead Publishing, pp. 93–155 (http://www.ifc.net.au/edit/library_fin_dye_finishing/4.1.04%20M5FIBRE.PDF).

Black, S 2003, *High-Performance Composites*, Posted on: 3/1/2003 (<http://www.compositesworld.com/articles/experienced-aerospace-manufacturer-relies-on-proven-methods>).

Blaiszik, BJ et al. 2010, 'Self-Healing Polymers and Composites', *Annu. Rev. Mater. Res.*, 40:179–211 (<http://autonomic.beckman.illinois.edu/nrs097.pdf>).

Bombardier 2011, 'Bombardier throws down the gauntlet with CSeries airliner', *Reinforcedplastics*, November/December 2011.

- Bond, IP 2014, 'Managing damage & effecting recovery in advanced FRP composites', National Composites Centre, the university of Bristol – Thursday 30th January 2014 (<http://www.bristol.ac.uk/composites/events/2014/ipb-ncc300114.pdf>).
- Brøndsted, P, Holmes, JW, Sørensen, BF and Sun, Z 2009, 'Bamboo based composites for wind turbine blades', *Proceedings of ICCM-17, 27–31 July 2009*, Edinburgh, UK.
- Brøndsted, P, Lilholt, H, and Lystrup, Aa 2005, 'Composite materials for wind power turbine blades', *Annu. Rev. Mater. Res.*, 35, 505-38.
- Brown, KA & Brooks, R 2009, 'Design and analysis of vertical axis thermoplastic composite wind turbine blade', *Proceedings of ICCM-17, 27–31 July 2009*, Edinburgh, UK.
- BS EN ISO 14126:1999, Fibre-reinforced plastic composites. Determination of compressive properties in the in-plane direction.
- BS EN ISO 15310:2005, Reinforced plastics. Determination of the in-plane shear modulus by the plate twist method.
- BS ISO 6721-11:2012 Plastics. Determination of dynamic mechanical properties: Glass transition temperature.
- Bunsell, AR & Renard, J 2005, *Fundamentals of fibre reinforced composite materials*, CRC Press.
- Callister, WD 2007, *Materials science and engineering: an introduction*, 7th edn, Wiley.
- Campbell, FC 2010, *Structural Composite Materials*, ASM International, Ohio, USA.
- Carlile, DR, Leach, DC, Moore, DR and Zahlan, N 1989, 'Mechanical properties of the carbon fiber/ PEEK composite APC-2/AS-4 for structural applications', *Advances in Thermoplastic Matrix Composite Materials*, ASTM STP 1044.
- Carpenter, JA 2008, 'Overview of freedom CAR and its composites crash-energy management work', *The Safety Characterization of Future Plastics and Composite-Intensive Vehicles Workshop*, Cambridge, MA, USA.
- Carpenter, JA 2008, 'Challenges and opportunities for automotive composites', *SPE ACCE*, Troy, MI, USA (http://www.speautomotive.com/SPEA_CD/SPEA2008/pdf/k/K1.pdf).

Carruthers, J, et al. 2011, 'The Design and Prototyping of a Lightweight Crashworthy Rail Vehicle Driver's Cab', *World Congress on Railway Research*, Lille, France, 22–26 May, 2011 (http://www.railway-research.org/IMG/pdf/a3_carruthers_joe-2.pdf).

Chanda, M & Roy, SK 2007, *Plastics Technology Handbook*, 4th edition, CRC Press.

Chelsea Center for Recycling and Economic Development 2000, 'An Investigation of the Potential to Expand the Manufacture of Recycled Wood-Plastic Composite Products in Massachusetts', *Technical Report # 19*, April 2000, University of Massachusetts, Lowell.

Chung, CI 2000, *Extrusion of polymers: theory and practice*, Hanser Publishers, Munich.

Cogswell, FN 1992, *Thermoplastic Aromatic Polymer Composites*, Butterworth-Heinemann, Boston.

Costaa, ML, SFM de Almeidab and Rezendea, MC 2005, 'Hygrothermal effects on dynamic mechanical analysis and fracture behavior of polymeric composites', *Materials Research*, Vol. 8, No. 3, pp. 335–340.

Curtis, PT (Ed) 1988, 'CRAG test methods for the measurement of the engineering properties of fibre reinforced plastics', RAE TR 88012, February 1988, Royal Aerospace Establishment, UK. (<http://www.dtic.mil/cgi-bin/GetTRDoc?AD=ADA201142>).

bookboon.com

Corporate eLibrary

See our Business Solutions for employee learning

Click here

Management Time Management

Problem solving Self-Confidence Effectiveness

Project Management Goal setting Motivation Coaching

Click on the ad to read more

ENG 4793 Module: Non-Destructive Testing (NDT), Georgia Institute of Technology (<http://www-old.me.gatech.edu/jonathan.colton/me4793/ndt.pdf>).

F1Technical.net (<http://www.f1technical.net/f1db/cars/476/mclaren-mp4-1>).

Frag, MM, 2008, 'Quantitative methods of materials substitution: Application to automotive components', *Materials and Design*, 29 (2008), 374–380.

Forest Products Laboratory, Wood-plastic composites (<http://www.fpl.fs.fed.us/documnts/techline/wood-plastic-composites.pdf>).

Franek, F, Badisch, E and Kirchgaßner, M 2009, 'Advanced methods for characterisation of abrasion/erosion resistance of wear protection materials', *FME Transactions*, 37, pp. 61–70 (http://www.mas.bg.ac.rs/istrazivanje/biblioteka/publikacije/Transactions_FME/Volume37/2/02_FFranek.pdf).

Frost, S 2014, 'Self-healing composites inkjet printed', *Materials World Magazine*, 01 Aug 2014 (<http://www.iom3.org/news/inkjet-composites-heal-themselves?c=574>).

Gamstedt, EK & Andersen, SI 2001, 'Fatigue Degradation and Failure of Rotating Composite Structures-Materials Characterisation and Underlying Mechanisms', Risø National Laboratory, Roskilde, Denmark (http://orbit.dtu.dk/fedora/objects/orbit:91229/datastreams/file_7727033/content).

Gardner, DJ & Murdock D, 'Extrusion of wood plastic composites' (<http://entwoodllc.com/PDF/Extrusion%20Paper%2010-11-02.pdf>).

Gardner, DJ, Han, Y and Song W 2008, 'Wood plastic composites technology trends', *Proceedings of the 51st International Convention of Society of Wood Science and Technology*, November 10–12, 2008, Concepción, Chile (<http://www.swst.org/meetings/AM08/proceedings/WS-24.pdf>).

Ghenai, C (editor) 2012, 'Sustainable Development – Energy, Engineering and Technologies-Manufacturing and Environment', *InTech* (<http://cdn.intechopen.com/pdfs-wm/29932.pdf>).

Ghiorse, SR 1993, 'Effect of void contents on the mechanical properties of carbon/ epoxy laminates', *SAMPE Quart.*, 24(2), pp. 54–59.

Giles, HF, Wagner, JR & Mount, EM 2005, *Extrusion: the definitive processing guide and handbook*, William Andrew, Inc., New York.

Gower, MRL, Shaw, RM and Sims, GD 2007, Measurement Good Practice Guide No.101: Good Practice Guide for the Assessment of Damage Tolerance Under Long-Term Loading, National Physical Laboratory, UK. (<http://www.npl.co.uk/publications/The-assessment-of-damage-tolerance-under-long-term-loading>).

Gurit Product Catalogue 2014, GPC-16-0314, (<http://www.gurit.com/files/documents/product-catalogue-2014-emeawebpdf.pdf>).

Gurit wind-energy handbook, 2014 (<http://gurit.fangle.co.uk/wind-energy-handbook-1.aspx>).

Haines et al. 1983, 'The design, development and manufacture of a new and unique tennis racket', *Proc Instn Mech Engrs*, 197B, 71–79.

Halliwell, SM 2000, 'Polymer composites in construction', Building Research Establishment Ltd (http://projects.bre.co.uk/composites/pdf/BR405_short.pdf).

Halliwell, S 2006, 'End of life options for composite waste: Recycle, Reuse or Dispose?' *National Composites Network Best Practice Guide* (<http://www.compositesuk.co.uk/LinkClick.aspx?fileticket=f3y8cNT6pIg%3D&tabid=111&mid=550>).



Brain power

By 2020, wind could provide one-tenth of our planet's electricity needs. Already today, SKF's innovative know-how is crucial to running a large proportion of the world's wind turbines.

Up to 25 % of the generating costs relate to maintenance. These can be reduced dramatically thanks to our systems for on-line condition monitoring and automatic lubrication. We help make it more economical to create cleaner, cheaper energy out of thin air.

By sharing our experience, expertise, and creativity, industries can boost performance beyond expectations. Therefore we need the best employees who can meet this challenge!

The Power of Knowledge Engineering

Plug into The Power of Knowledge Engineering.
Visit us at www.skf.com/knowledge

SKF

Hanawalt, K 2012, 'Wood-Plastics Composites Done Right', *Plastics Technology*, May 2012.

Harris, B 1999, *Engineering composite materials*, The Institute of Materials, London.

Harris B, Reiter H, Adam T, Dickson RF and Fernando G 1990, 'Fatigue behaviour of carbon fibre reinforced plastics', *Composites*, 21 (3), 232–242.

Harris, S 2014, 'BAE uses miniature sensors to give aircraft 'smart skin'', *the Engineer*, 27 August 2014 (<http://www.theengineer.co.uk/aerospace/news/bae-uses-miniature-sensors-to-give-aircraft-smart-skin/1019110.article#ixzz3Buc2Y4G8>).

Herrmann, HG, Mohrdieck, C, and Bjekovic, R 2002, 'Materials for the automotive lightweight design'. *Euromotor: New Advances in Body Engineering: Lightweight material applications, Passive safe*, Aachen, Germany: Institut fur Kraftfahrzeuge.

Hexcel-Qualification Laboratory (2011): http://www.hexcel.com/OurCompany/PlantCertifications/Duxford_GermanischerLloyd.pdf.

Hexcel, April 1999, *Composite repairs, Publication No UTC 102* (http://www.hexcel.com/Resources/DataSheets/Brochure-Data-Sheets/Composite_Repair.pdf).

Hexel (2008), 'Hexcel's Composite Materials for the Rail Industry' (<http://www.hexcel.com/Resources/DataSheets/Brochure-Data-Sheets/Rail.pdf>).

Hexcel (2013), Hexply prepreg technology, Publication No. FGU017c (http://www.hexcel.com/Resources/DataSheets/Brochure-Data-Sheets/Prepreg_Technology.pdf).

Hillock , R & Howard, S 2014, 'Utility of Carbon Fiber Implants in Orthopedic Surgery: Literature Review', *JISRF Reconstructive Review*, Vol. 4, No. 1, March 2014 (http://www.jisrf.org/pdfs/RR_Vol4No1March2014p23-32.pdf).

Hobbs, M 2012, 'Mecca clock tower features Gurit composites', *Reinforced Plastics.com, News*, 23 January 2012 (<http://www.reinforcedplastics.com/view/23390/mecca-clock-tower-features-gurit-composites/>).

Hogg, PJ 2003, 'Composites for Ballistic Applications', *Composites Processing 2003*, CPA, Bromsgrove, U.K. 21st March 2003 (http://compositesuk.co.uk/LinkClick.aspx?fileticket=nc_kfRRu6GY%3D&tabid=105&mid=510).

Horoschenkoff, A & Christner, C 2012, 'Carbon fibre sensor: theory and application', *Composites and their applications*, Hu, N (ed.), InTech, Croatia (http://www.issp.ac.ru/ebooks/books/open/Composites_and_Their_Applications.pdf).

Horoschenkoff, A, & Christner, C 2012, 'Carbon Fibre Sensor: Theory and Application', *inTech* (<http://cdn.intechopen.com/pdfs-wm/38416.pdf>).

Hu, N (editor), 2012, 'Composites and their Applications', In Tech, Croatia (http://www.issp.ac.ru/ebooks/books/open/Composites_and_Their_Applications.pdf).

Hull, 1981, *An introduction to composite materials*, Cambridge University Press, Cambridge, UK.

Humphreys, C 1997, 'Material sciences-part one', Science and Society, a JSPS-UK Research Council Symposium, Pilkington Press, pp. 34–51.

IEC (International Electrotechnical Commission)/TR 61400-24:2002, Technical Report on Wind turbine generator systems – Part 24: Lightning protection (<http://www.eeechina.cn/upload/fck/2011-08-19/634493391466122293.pdf>).

IMechE Report (2012), Sports Engineering: An Unfair Advantage? July 2012.

Intertek Plastics Technology Laboratories (<http://www.ptli.com/testlopedia/tests/DSC-d3417.asp>).

Invibio (<http://www.odtmag.com/articles/2006/05/implantable-plastics-engineering-for-the-long-term>).

ISO 14127:2008, Carbon-fibre-reinforced composites – Determination of the resin, fibre and void contents.

ISO 6603-1:2000. Plastics – Determination of puncture impact behaviour of rigid plastics – **Part 1:** Non-instrumented impact testing.

ISO 6603-2:2000. Plastics – Determination of puncture impact behaviour of rigid plastics – Part 2: Instrumented impact testing.

ISO 527-5 (2009) Plastics – Determination of tensile properties – Part 5: Test conditions for unidirectional fibre-reinforced plastic composites.

ISO 179-1:2010, Plastics – Determination of Charpy impact properties – Part 1: Non-instrumented impact test.

ISO 179-2:1997, Plastics – Determination of Charpy impact properties – Part 2: Instrumented impact test

ISO 180:2000, Plastics – Determination of Izod impact strength.

ISO 15024 (2001) Fibre-reinforced plastic composites – Determination of mode I interlaminar fracture toughness, G_{Ic} , for unidirectionally reinforced materials.

ISO/DIS 15114 (2011) Fibre-reinforced plastic composites – Determination of the mode II fracture resistance for unidirectionally reinforced materials using the calibrated end-loaded split (C-ELS) test and an effective crack length approach.

ISO 18352:2009 Carbon-fibre-reinforced plastics – Determination of compression-after-impact properties at a specified impact-energy level.

ISO 12815:2013 Fibre-reinforced plastic composites – Determination of plain-pin bearing strength.

With us you can
shape the future.
Every single day.

For more information go to:
www.eon-career.com

Your energy shapes the future.

e.on



ISO 13003:2003 Fibre-reinforced plastics – Determination of fatigue properties under cyclic loading conditions.

ISO 11357-1:2009 Plastics – Differential scanning calorimetry (DSC) – Part 1: General principles.

IsoTruss (<http://www.isotruss.com/hsratio.htm>).

Iten Industries: <http://www.itenindustries.com/pultrusion.shtml>.

J&J Mechanic: <http://www.jjmechanic.com/process/pultrusion.htm>.

Job, S 2010, 'Composites recycling' – *Materials KTN Report*, September 2010.

Joyce, P 2003, <http://www.thirdwave.de/3w/tech/armor/carbonfibre.pdf>.

JPS Composite Materials, Anderson, SC, USA, databook (http://jpsglass.com/jps_databook.pdf).

Judd, NCW and Wright, WW 1978, 'Voids and their effects on the mechanical properties of composites – an appraisal', *SAMPE J.*, Vol. 14, Issue 1, pp. 10–14.

Kapadia, A 2007, *Non Destructive Testing of Composites Materials*, National Composites Network, dti (<http://www.compositesuk.co.uk/LinkClick.aspx?fileticket=14Rxzdzdkjw=&>).

Kazmierski, C of Lucintel 2012, 'Growth Opportunities in Global Composites Industry, 2012–2017', *Composites2012, The Composites Exhibition and Convention*, February 21–23, 2012, Mandalay Bay Convention Center, Las Vegas, NV). (<http://www.lucintel.com/lucintel-globalcompositemarketanalysis-acma2012-educationalsession.pdf>).

Kelly 1989, *Concise encyclopedia of composite materials*, Pergamon Press.

Kendall, D 2007, 'Building the future with FRP composites', *Reinforced Plastics*, May 2007. (http://www.imsmarketing.co.uk/nova/imagessept07/May07_building.pdf).

Kendall, D 2008, 'The business case for composites in construction, Reinforced Plastics', July 2008 reporting on *the 7th Annual Conference of the Network Group for Composites in Construction (NGCC)*, held in Farnborough, UK, in May 2008 (<http://www.reinforcedplastics.com/view/2799/the-business-case-for-composites-in-construction/>).

Kopeliovich, D 2012, 'Closed mold fabrication of polymer matrix composites', *SubsTech*, (http://www.substech.com/dokuwiki/doku.php?id=closed_mold_fabrication_of_polymer_matrix_composites).

Kurcz, M, Baser, B, Dittmar, H, Sengbusch, J, & Pfister, H 2004, 'The case for replacing steel with glass-mat thermoplastic composites in spare-wheel well applications', *4th Annual SPE Automotive Composites conference*, Sept 14–15 2004 (http://speautomotive.com/SPEA_CD/SPEA2004/pdf/g/g3.pdf).

Lancashire, RJ 2011, Chemistry and Sport, University of the West Indies, Kingston, Jamaica (<http://wwwchem.uwimona.edu.jm/courses/CHEM2402/Sport/Equipment.html>).

Lammer, H & Kotze, J 2003, *Materials in sport equipment* (editor Jenkins, M), Woodhead Publishing Ltd, Cambridge, England.

Lanzara, G, Yoon, Y, Liu, H, Peng, S and Lee, WI. 2009, 'Carbon nanotube reservoirs for self-healing materials', *Nanotechnology*, Vol. 20, No. 33, Article 335704, 2009.

Linden Industries, Inc: <http://www.lindenindustries.com/>.

Lizotte, A & Cramer, D 2008, 'Evaluation of joining techniques for continuous fibre reinforced thermoplastic composites', *8th Annual Automotive Composites Conference and Exhibition Proceedings, ACCE 2008*, September 16–18, 2008, Troy, Michigan, USA (http://www.speautomotive.com/SPEA_CD/SPEA2008/pdf/j/BJF-07.pdf).

Lucintel Brief, 2011, Opportunities in Natural Fiber Composites, March 2011 (<http://www.lucintel.com/OpportunitiesinNaturalFiberComposites.pdf>).

MakeItFrom.com; *Material properties data base*: <http://www.makeitfrom.com/>.

Mallick. PK (editor) 1997, *Composites Engineering Handbook*, Marcel Dekker, New York.

Mark, JE (editor) 1999, *Polymer data handbook*, Oxford University Press.

Martin Pultrusion: <http://www.martinpultrusion.com/forming.html>.

Mason, K 2004, 'Advances in sizings and surface treatments for carbon fibers', *High-Performance Composites*, March 2004 (<http://www.compositesworld.com/articles/advances-in-sizings-and-surface-treatments-for-carbon-fibers>).

Marsh, G 2003, 'Next step for automotive materials', *materialstoday*, April 2003, pp. 36–43 (http://ac.els-cdn.com/S1369702103004292/1-s2.0-S1369702103004292-main.pdf?_tid=ae4e5fbe-848e-11e4-93b7-00000aab0f26&acdnat=1418671087_7c3317245ab420a648283aa678cc7913).

McConnell, V 2009, 'The making of carbon fiber', *High-Performance Composites*, January 2009 (<http://www.compositesworld.com/articles/the-making-of-carbon-fiber>).

McDaniels, K, Downs, RJ, Meldner, H, Beach, C, Adams, C 2009, 'High Strength-to-Weight Ratio Non-Woven Technical Fabrics for Aerospace Applications', *Cubic Tech Corp., Mesa, Arizona* (<http://www.cubictechnology.com/Technical%20Fabrics%20for%20Aerospace%20Applications.pdf>).

Miodownik, M 2014, *Stuff Matters: The Strange Stories of the Marvellous Materials that Shape Our Man-made World*, Penguin.

Miracle, DB & Donaldson, SL 2001, *Composites (ASM International), ASM Handbook*, Volume 21, pp. 3–17 (http://www.compositcarbonfiberprop.com/carbon_fiber.pdf).

Molded Fiber Glass Companies 2003, Manual on 'designing with fiber reinforced plastics/composites' (http://www.mfgcsc.com/resources/MFG_CSC_FRP_Design_Guide.pdf).

© 2013 Accenture. All rights reserved.

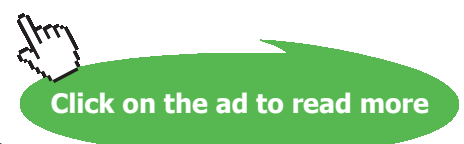
be > your degree

Bring your talent and passion to a global organization at the forefront of business, technology and innovation. Discover how great you can be.

Visit accenture.com/bookboon

Be greater than.
consulting | technology | outsourcing

accenture
High performance. Delivered.



Mwaikambo, LY 2006, 'Review of the history, properties and application of plant fibres', *AJST*, Vol. 7, No. 2, pp. 120–133.

Netcomposites: <http://www.netcomposites.com/guide/laminate-properties/29>.

NetComposites, Interactive Knowledge Base on NDE of Composites
(<http://www.netcomposites.com/ikb/browse/default.asp?ST=1>).

Netcomposites, 2006, 'New Cervical Plate Implant from PEEK Composite' (<http://www.netcomposites.com/news/new-cervical-plate-implant-from-peek-composite/3545>).

NetComposites, 2008, 'Twintex Chosen for Vacuum Bag Moulded Thermoplastic Composite Canoe', publication on 08/04/2008 (<http://www.netcomposites.com/news/twintex-chosen-for-vacuum-bag-moulded-thermoplastic-composite-canoe/4896>).

Netzsch, 'Thermal properties of polymers' (<http://www.netzsch-thermal-analysis.com/en/home.html>).

Nicholson, J W 2006, *The Chemistry of Polymers*, The Royal Society of Chemistry Publication, Cambridge, UK (<http://books.google.co.uk/books?id=FnniJ4MZciQC&pg=PA59&lpg=PA59&dq=chemistry+of+unsaturated+polyesters&source=bl&ots=RoHIcl3YVJ&sig=FBL-losg8gGGRxAAKfsp56VnVdI&hl=en&sa=X&ei=FPa9UMa4KK620QXZ6ICIDQ&ved=0CFMQ6AEwBjgK#v=onepage&q=chemistry%20of%20unsaturated%20polyesters&f=false>).

Nielsen, LE, 1974, *Mechanical Properties of Polymers and Composites*, Marcel Dekker, New York.

OSHA, 1999, Polymer matrix materials: advanced composites, OSHA Technical Manual (OTM) Section III: Chapter 1 (https://www.osha.gov/dts/osta/otm/otm_iii/otm_iii_1.html#t_iii:1_1).

Otheguy, ME, Gibson, AG, Findon, E, Cripps, RM, Mendoza, AO and Castro, MTA 2009, 'Recycling of end-of-life thermoplastic composite boats', *Plastics Rubber and Composites*, Vol. 38, issue: 9–10, pp. 406–411 (<http://www.ncl.ac.uk/newrail/assets/docs/Otheguyetal-Recyclingofend-of-lifethermoplasticcompositeboats.pdf>).

Palucka, T and Bensaude-Vincent, B 2002, 'Composites overview', *History of Recent Science & Technology* (http://authors.library.caltech.edu/5456/1/hrst.mit.edu/hrs/materials/public/composites/Composites_Overview.htm).

Patton R, Li, F and Edwards, KL 2004, 'Causes of weight reduction effects of material substitution on constant stiffness components'. *Thin-Walled Structures*, 42 (2004) 613–637.

Permabond Engineering Adhesives: http://permabond.com/pdf/brochures/PPB_US_022410_PWP.pdf.

Pickering, SJ 2006, 'Recycling technologies for thermoset composite materials – current status', *Composites: Part A* 37 (2006) 1206–1215 (<http://www.tech.plym.ac.uk/sme/mats324/Publications/LCA%20workshop/Pickering%20on%20TS%20recycling.pdf>).

Pingkarawat, K, Wang, CH, Varley, RJ and Mouritz, AP 2012, 'Self-healing of delamination cracks in mendable epoxy matrix laminates using poly[ethylene-co-(methacrylic acid)] thermoplastic', *Composites: Part A* 43 (2012) 1301–1307 (http://ac.els-cdn.com/S1359835X12001030/1-s2.0-S1359835X12001030-main.pdf?_tid=5f83af00-3101-11e4-a67b-00000aabb0f26&acdnat=1409484449_370c02196017979222aa69f89c237c45).

Powell, PC 1994, *Engineering with fibre-polymer laminates*, Kluwer.

Prabhakaran, D, Andersen, RT, Bech, TL, Lilholt, H 2011, 'Thermoplastic composites for future wind turbine blades – pros and cons', *Proceedings of ICCM-18 (The 18th International Conference on Composite Materials)*, 21–26 Aug 2011, Jeju Island, South Korea.

Raasch, JE 1998, 'All-composite construction system provides flexible low-cost shelter', *Composites Technology*, March/April, 1998, pp. 56–58.

Roach, D & Duvall, R, 'Detection of hail impact damage in composite structures at the failure threshold energy',

Rauwendaal, CJ 1981, 'Analysis and experimental evaluation of twin screw extruders', *Polymer Engineering & Science*, Vol, 21, Issue 16, pp. 1092–1100.

Robinson, P & Hodgkinson, JM 2000, 'Interlaminar fracture toughness', *Mechanical testing of advanced fibre composites* (ed. Hodgkinson, JM), Woodhead Publishing Ltd, Cambridge, UK.

Rojek, M, Szymiczek, M, Stabik, J, Mężyk, A, Jamroziak, K, Krzystała, E and Kurowski, J 2013, 'Composite materials with the polymeric matrix applied to ballistic shields', *Archives of Materials Science and Engineering*, 63/1 (2013), 26–35 (http://www.archivesmse.org/vol63_1/6314.pdf).

Rouchon, J 2009, 'Fatigue and damage tolerance evaluation of structures – The composite materials response', *22nd Plantema Memorial Lecture*, National Aerospace Laboratory, NLR-TP-2009-221.

Sandia National Laboratories.

Sang, D & Aspin, K, 'Making a racket', National STEM Centre, SATIS 16–19 unit 99 (<http://www.nationalstemcentre.org.uk/elibrary/resource/987/satis-16-19-units-76-100>).

Savage, G 2008, 'Composite materials technology in Formula 1 motor racing', *Honda Racing F1*, July 2008 (http://speautomotive.com/SPEA_CD/SPEA2008/pdf/k/K3.pdf).

Schemme, M 2008, 'LFT – development status and perspectives', *Plastics, Additives and Compounding*, Vol. 10, Issue 2, pp. 38–43.

Schulz, D 1984, Messerschmitt-Bolkov-Blom GmbH– 'Structural Certification of an Airbus Fin Box in Composite Fibre', *the ICAS 84 symposium*.

Shanmugam, DK, Chen, FL, Siores, E and Brandt, M 2002, 'Comparative study of jetting machining technologies over laser machining technology for cutting composite materials', *Composite Structures* 57, pp. 289–296 (<http://www.worldlasers.com/articles/research/sdarticleii.pdf>).

Sherman, L M 2004, 'Wood-Filled Plastics: they need the right additives for strength, good looks, and long life', *Plastics Technology*, July 2004.



"I studied English for 16 years but...
...I finally learned to speak it in just six lessons"
Jane, Chinese architect

ENGLISH OUT THERE

Click to hear me talking before and after my unique course download

Sims, GD 1999, 'Particular requirements for composites', *Handbook of polymer testing: physical methods*, Brown, R (editor), Marcel Dekker, New York.

Sims GD 2007, 'Review of Composites Standardisation Status and Activities', September 2007, *NCN Guide to Polymer Composites Standards*.

Singleton, MJ & Hutchison, JA 2010, 'The Development of Fibre-Reinforced Polymer (FRP) Composites in Building Construction' (<http://www.compositesuk.co.uk/LinkClick.aspx?fileticket=2tZQmjgn23c%3D&tabid=103&mid=526>).

Skyrota LGC: <http://wintufel.net/skyrota-wind-turbine/>.

Sloan, J 2010, 'Machining carbon composites: Risky business', *High-Performance Composites*, posted on: 4/16/2010 (<http://www.compositesworld.com/articles/machining-carbon-composites-risky-business>).

So, K 2012, 'Automotive giants turn to bioplastics worldwide', *Plastics News, Brussels*, July 31, 2012 (<http://www.plasticsnews.com/article/20120731/NEWS/307319980/automotive-giants-turn-to-bioplastics-worldwide>).

Sørensen, BF 2009, 'Materials and structures for wind turbine rotor blades – an overview', *Proceedings of ICCM-17, 27–31 July 2009*, Edinburgh, UK (<http://www.iccm-central.org/Proceedings/ICCM17proceedings/Themes/Plenaries/P1.3%20Sorensen.pdf>).

Spratt, G 1998, *The Effect of Ageing on the Properties of Bismaleimide Carbon Fibre Composite Materials*, PhD Thesis, University of Ulster Jordanstown, N. Ireland.

SP Systems, Guide to composites, p. 51 (<http://www.bolton.ac.uk/codate/spguidetocomposites.pdf>).

SP Systems 2005 – Composites Engineering Materials: <http://www.carbodydesign.com/pub/4386/sp-systems-guide-to-composites/>.

Stone, DEW and Clark, B 1975, 'Ultrasonic attenuation as a measure of void content in carbon-fiber reinforced plastics', *Non-destructive Testing*, 8 (3), pp. 137–145.

Strong, AB 2006, 'History of Composite Materials-Opportunities and Necessities', Brigham Young University.

- Strong, AB 2008, *Fundamental of Composites Manufacturing: Materials, methods and applications*, 2nd edition, SME, Michigan, USA (http://books.google.co.uk/books?id=aCm9yvodiJcC&pg=PA298&source=gbs_toc_r&cad=4#v=onepage&q&f=false).
- Stuart, G 2007, 'CFR PEEK composite for surgical applications', *Medical Device & Diagnostic Industry*, January 2007 (<http://www.mddionline.com/article/cfr-peek-composite-surgical-applications>).
- Stenzenberger, HD, König P, Herzog M, Romer W, Canning MS and Pierce S 1986, 'Allyl – (propenyl) terminated arylene-ether-sulphone oligomers as co-reactive intermediates for tough bismaleimides', *Proceedings of the 18th International SAMPE Technical conference*, v18, p. 500.
- Stenzenberger HD, Romer W, Herzog M and König P 1988, 'Toughened bismaleimides: modifications with thermoplastics', *Proceedings of the 33rd International SAMPE symposium*, 1988 v33 p. 1546.
- Suddell, B 2009, 'Industrial Fibres: Recent and Current Developments', *Proceedings of the Symposium on Natural Fibres*, pp. 71–82 (<ftp://ftp.fao.org/docrep/fao/011/i0709e/i0709e10.pdf>).
- Summerscales, J & Searle, TJ 2005, 'Low-pressure (vacuum infusion) techniques for moulding large composite structures', *Proc IMechE*, Vol. 219, Part L: *J. Materials: Design and Applications*, pp. 45–58.
- Szekrenyes, A 2005, *Delamination of composite specimens*, PhD thesis, Budapest University of Technology and Economics (http://www.mm.bme.hu/~szeki/files/Phd_Thesis.pdf).
- Tan, L-S 1999, 'Poly(bis maleimide)', *Polymer data handbook* (edited by J.E. Mark), Oxford University Press.
- Theengineer (2014), 'Lightweight crashworthy train cab, Automotive, rail and marine', 27 August 2014 (<http://www.theengineer.co.uk/awards/automotive-rail-and-marine/1005763.article>).
- Thagard, JR, Okoli, OI, and Liang, Z 2004, 'Resin Infusion between Double Flexible Tooling: evaluation of process parameters', *Journal of Reinforced Plastics and Composites*, Vol. 23, No.16.
- Tomblin, J & Waruna, S 2011, 'Determining the fatigue life of composite aircraft structures using life and load-enhancement factors', *Final Report DOT/FAA/AR-10/6*, U.S. Department of Transportation Federal Aviation Administration Air Traffic Organization NextGen & Operations Planning, Office of Research and Technology Development, Washington, DC 20591 (<http://www.tc.faa.gov/its/worldpac/techrpt/ar10-6.pdf>).
- Toray Industries' presentation, 2012, Carbon Fiber Composite Materials (http://www.toray.com/ir/pdf/lib/lib_a136.pdf).

TruthOnPot.com, July 2013 (<http://www.truthonpot.com/2013/07/31/bmws-new-electric-car-sheds-weight-with-hemp/>).

TWI Report (2011) (<http://www.ncn-uk.co.uk/uploads/Joining%20of%20thermoplastic%20composites.pdf>).

Umeco, product data catalogue, 'Introduction to advanced composites and prepreg technology'.

Vaara, P & Leinonen, J 2012, 'Technology Survey on NDT of Carbon-fiber Composites', *Publications of Kemi-Tornio University of Applied Sciences*, Serie B. Reports 8/2012, Kemi, Finland (http://www3.tokem.fi/kirjasto/tiedostot/Vaara_Leinonen_B_8_2012.pdf).

Van Paepegem, W 2014, 'Composites in daily life', *HomMaCom*, (http://www.composites.ugent.be/home_made_composites/composites_in_daily_life.html)

Visconti, IC, Durante, M, Langella, A, and Morano, U 2006, 'Flow front analysis In resin infusion process', *Intelligent Production Machines and Systems* (edited by Pham, DT, Eldukhri, EE and Soroka, AJ): 2nd IPROMS Virtual Conference 3–14 July 2006, Elsevier 2006, Amsterdam, pp. 221–228.

Ware, S 1999, 'Technological progress and the Olympic Games', *Olympic History*, September 1999 (<http://www.isoh.org/articles/67.pdf>).

Weber: http://www.extrudial.com/uploads/media/Weber_EXT_2013_E_screen.pdf.

Wikipedia, 2014, The free encyclopedia (this page was last modified on 28 May 2014) (http://en.wikipedia.org/wiki/Visby-class_corvette).

WRAP, August 2003, Research report on 'wood plastic composites study' – technologies and UK market opportunities' (<http://www.ngcc.org.uk/LinkClick.aspx?fileticket=fbSl6217rKs%3D&tabid=95&mid=478>).

Wyoming Test Fixtures 2000, *Product Catalog* No 106.

Wyoming Test Fixtures (<http://www.wyomingtestfixtures.com/products.html>).

Yang, H, Liu, J, Ji, M and Yang, S 2012, 'Novel Thermoplastic Polyimide Composite Materials', *Thermoplastic- Composite Materials* (edited by Adel El-Sonbati), InTech, pp. 1–10 (http://cdn.intechopen.com/pdfs/32994/InTech-Novel_thermoplastic_polyimide_composite_materials.pdf).

Zhuang, H 1998, 'Synthesis and characterization of aryl phosphine oxide containing thermoplastic polyimides and thermosetting polyimides with controlled reactivity', *PhD thesis*, Virginia Polytechnic Institute and State University (<http://scholar.lib.vt.edu/theses/available/etd-7398-194414/unrestricted/Etd1.pdf>).

Zafeiropoulos NE, Baillie CA, Matthews FL 2001, 'A study of transcrystallinity and its effect on the interface in flax fibre reinforced composite materials', *Composites Part A*, Vol. 32 (Issues 3–4), 525–543 (<http://www.sciencedirect.com/science/article/pii/S1359835X00000580>).

Zhang, S, Minus, ML, Zhu, L, Wong, C-P, Kumar, S 2008, 'Polymer transcrystallinity induced by carbon nanotubes', *Polymer*, 49, 1356-64 (http://www1.coe.neu.edu/~mminus/MINUS_Lab/Publications_files/Polymer_Transcrystallinity%20on%20CNT.pdf).